

Georg-August-Universität Göttingen

INSTITUT FÜR NUMERISCHE UND ANGEWANDTE MATHEMATIK

**Finite Element Methods with Local Projection Stabilization
for Thermally Coupled Incompressible Flow**

Dissertation

zur Erlangung des

mathematisch-naturwissenschaftlichen Doktorgrades

“Doctor rerum naturalium”

an der Georg-August-Universität Göttingen

vorgelegt von

Helene Dallmann

aus

Göttingen

Göttingen 2015

Referent: Prof. Dr. Gert Lube
Korreferent: Prof. Dr. Malte Braack
Tag der mündlichen Prüfung: 07.09.2015

Contents

1. Introduction	1
1.1. Motivation	1
1.2. Outline and Contributions	2
2. Modeling Non-Isothermal Flow in Finite Element Methods	5
2.1. Mathematical Model for Non-Isothermal Flow	5
2.1.1. Navier-Stokes-Fourier Model	5
2.1.2. Oberbeck-Boussinesq Approximation	8
2.1.3. Boundary Conditions	9
2.2. Spatial Discretization	10
2.2.1. Variational Formulation and Ritz Galerkin Method	10
2.2.2. Finite Element Methods	14
2.2.3. Local Projection and Grad-Div Stabilization	17
2.3. Time-Discretization	21
2.3.1. Pressure-Correction Projection Method	22
2.3.2. Segregation Algorithm	24
2.4. Stabilized FEM for the Auxiliary Problems and their Properties	25
2.4.1. Convection-Diffusion Equation	25
2.4.2. Oseen Problem	27
3. Semi-Discrete Analysis for the Oberbeck-Boussinesq Model	31
3.1. Stability of the Semi-Discrete Quantities	31
3.2. Velocity and Temperature Estimates	35
3.2.1. Quasi-Optimal Estimates without LPS-Compatibility Condition	40
3.2.2. Quasi-Optimal Estimates with LPS-Compatibility Condition	55
3.3. Pressure Estimate	65
4. Fully Discrete Analysis	69
4.1. Stability of the Fully Discretized Quantities	71
4.2. Fully Discrete Convergence Results	75
4.2.1. Spatial Discretization of the Continuous Quantities	78
4.2.2. Temporal Discretization of the Space-Discrete Quantities	80

4.2.3. Errors of the Fully Discretized Scheme	95
4.3. Critical Examination of the Required Assumptions	101
5. Numerical Examples	107
5.1. Isothermal Convergence Results: 3D No-Flow Problem	108
5.1.1. Features of the Test Case	108
5.1.2. Numerical Experiments	109
5.2. Isothermal Convergence Results: 2D Couzy Problem	109
5.2.1. Features of the Test Case	110
5.2.2. Numerical Experiments	110
5.3. Non-Isothermal Convergence Results: 2D Traveling Wave	112
5.3.1. Features of the Test Case	112
5.3.2. Numerical Experiments: Spatial Convergence	113
5.3.3. Numerical Experiments: Convergence in Time	116
5.4. Isothermal Laminar Flow: 2D Blasius Boundary Layers	117
5.4.1. Features of the Test Case	117
5.4.2. Numerical Experiments	118
5.5. Non-Isothermal Laminar Flow: 2D Heated Cavity	122
5.5.1. Features of the Test Case	122
5.5.2. Description of Benchmark Quantities	123
5.5.3. Numerical Experiments	124
5.6. Isothermal Turbulent Flow: 3D Taylor–Green Vortex	127
5.6.1. Features of the Test Case	128
5.6.2. Description of Benchmark Quantities	128
5.6.3. Theoretical Justification for the Choice of the LPS SU Parameter	129
5.6.4. Numerical Experiments	130
5.7. Non-Isothermal Flow: 3D Rayleigh–Bénard Convection	133
5.7.1. Features of the Test Case	133
5.7.2. Description of Benchmark Quantities	135
5.7.3. Numerical Experiments	135
6. Discussion and Conclusion	143
6.1. Discussion of the Analytical Results	143
6.2. Discussion of the Numerical Results	147
6.3. Conclusion	149
A. Mathematical Tools and Notation	151
A.1. Notation	151
A.2. Function Spaces	151

A.3. Inequalities and Auxiliary Calculations	154
A.3.1. Useful Inequalities	154
A.3.2. Variants of Gronwall’s Lemma	155
A.3.3. Estimates for the Convective Term	156
A.4. Existence Results	157
B. Appendix: Numerical Examples	159
B.1. Isothermal Convergence Results: 3D No-Flow Problem	159
B.2. Isothermal Convergence Results: 2D Couzy Problem	160
B.3. Non-Isothermal Convergence Results: 2D Traveling Wave	162
B.4. Isothermal Laminar Flow: 2D Blasius Boundary Layers	165
B.5. Non-Isothermal Laminar Flow: 2D Heated Cavity	168
B.6. Isothermal Turbulent Flow: 3D Taylor-Green Vortex	170
B.7. Non-Isothermal Flow: 3D Rayleigh–Bénard Convection	171
Bibliography	173

1. Introduction

1.1. Motivation

The investigation of incompressible flow is a key branch in fluid mechanics. Its mathematical description is based on the Navier-Stokes equations.

The field of computational fluid dynamics (CFD) aims to predict the behavior of flow reliably and faces the difficulty to solve a resulting system of partial differential equations. The development of mathematical models and efficient as well as accurate algorithms is subject to research. The incompressibility constraint couples the velocity and pressure calculation and thus leads to high computational cost.

In addition, the aspect of accurate approximate solutions is an important, yet complicated issue. The challenge is to find a discretization that captures the physically correct macroscopic behavior of the flow. Discretizations using the finite element method (FEM) suffer from spurious oscillations in the numerical solution that arise for example due to dominating convection, internal shear or near boundary layers. Depending on the finite element spaces, poor mass conservation and a violation of the discrete inf-sup stability of the velocity and pressure ansatz spaces can occur. If the latter condition is harmed, the mixed problem becomes singular and (pressure) stabilization techniques have to be used to overcome this. Inf-sup stable elements are not afflicted by this need.

Especially in the case of small diffusion, numerical unphysical instabilities lead to inaccuracy of the method. By mesh refinement, these oscillations can be removed but the resulting computational cost is often not feasible, even while the computing power is ever-expanding nowadays.

In the last decades, various stabilization techniques have been proposed that are supposed to eliminate over- and undershooting. These methods are applied mostly to convection-diffusion type problems, the Stokes equations or the Oseen problem and show positive effects in numerical experiments. In spite of the massive amount of work put into this, there is no method that is an “allrounder” in the sense that it is accurate, efficient and robust with respect to different problems and applications.

Non-isothermal incompressible flow can be modeled by the Oberbeck-Boussinesq approximation if only small temperature differences occur. This model consists of a momentum equation and a Fourier equation governing the velocity and temperature, respectively.

Both equations are coupled through a convection term in the Fourier equation and a reaction term in the momentum equation. Therefore, the problems occurring when the Navier-Stokes equations are solved numerically also arise for the Oberbeck-Boussinesq model.

1.2. Outline and Contributions

It is an important issue of this thesis that the numerical solution of incompressible non-isothermal flow problems is theoretically and empirically justified. Therefore, we introduce a profound model and perform numerical analysis. The model is tested for various numerical examples.

Chapter 2 covers all main steps to establish a fully discrete model that can be implemented and investigated numerically. The underlying mathematical model of our simulations is the Oberbeck-Boussinesq approximation, that is the singular limit of the more general Navier-Stokes-Fourier model for heat driven flow. It is therefore suited to model incompressible flow with small temperature differences. The model is deduced in Section 2.1 and characteristic quantities are defined. As a spatial discretization approach, the finite element method is introduced in Section 2.2, which is one of the most widely used techniques in computational fluid mechanics. It yields an approximate solution of the variational formulation of the problem. Here, important spaces and notations are fixed. Moreover, the usage of grad-div and local projection stabilization (LPS) methods in the literature is reviewed briefly. We adapt this method to the Oberbeck-Boussinesq model. Section 2.3 is dedicated to the time-discretization of the model. We use a method called pressure-correction projection method, which incorporates a backward differentiation formula of second order. Segregation methods are based on an idea by Chorin [Cho69] and Temam [Tem69] and reduce the computational cost since the calculation of pressure and velocity is decoupled. We formulate this method for the Oberbeck-Boussinesq model and sketch the steps in the algorithm for solving the fully discrete scheme. As a preliminary study for the problem of interest, we review the state of research dealing with stabilization of the convection-diffusion-reaction and Oseen equations, see Section 2.4. We also recall results we originally published in [DAL15] about the Oseen problem.

In Chapter 3, we study the semi-discrete problem closely. We extend the analysis from our publications [DAL15] for the Oseen problem and [ADL15] for the Navier-Stokes equations to the thermally coupled setting. We prove stability of the semi-discrete solutions of the stabilized Oberbeck-Boussinesq model and pursue two approaches regarding a priori error estimates. The first variant relies on the discrete inf-sup stability of the velocity and pressure ansatz spaces and the existence of a local interpolation operator preserving the divergence. Secondly, an interpolation operator with additional orthogonality properties is

taken advantage of. By a result of [MST07], this operator exists if a certain compatibility condition between the approximation and projection spaces for velocity and temperature holds. The applicability of the proposed methods is discussed; in particular, possible finite element settings are reviewed. The design of stabilization parameters is studied. The results rely on relatively mild regularity assumptions for the continuous solutions. Also, the convective terms are treated carefully in order to circumvent an exponential deterioration of the error in the limit of vanishing diffusion. Furthermore, a pressure estimate is given using the discrete inf-sup stability.

The fully discretized scheme is treated analytically in Chapter 4. In Section 4.1, we show the stability of the fully discrete solutions of the stabilized Oberbeck-Boussinesq model. Convergence in space and time is proved in Section 4.2 for the stabilized Navier-Stokes equations. The proof utilizes the semi-discrete results from Chapter 3 and combines it with an estimate of the error between the semi-discrete (continuous in time, discretized in space) and fully discrete velocity. The choice of stabilization parameters is addressed. This analysis of the Navier-Stokes equations was published in [AD15], where we present two strategies: In addition to the one performed in this thesis, we also follow the ansatz to discretize in time first and in space afterwards. Both approaches suffer from the artificial introduction of a semi-discrete velocity (either in space or in time). This leads to regularity assumptions for this additional quantity and further restrictions on parameters. For the proofs, we make use of the discrete Gronwall Lemma. The convective terms then lead to an unfeasible restriction of the time step size as $\Delta t \sim \nu^3$ in order to ensure applicability of the Gronwall Lemma. Therefore, we give a critical assessment of the requirement of the proof, see Section 4.3.

The subsequent Chapter 5 is devoted to the numerical simulation of incompressible isothermal and non-isothermal flow. First, we validate the theoretical convergence results with respect to the mesh width and the time step size (Sections 5.1, 5.2, 5.3). The influence of grad-div and LPS stabilization on the spatial and temporal errors is studied for the parameter range suggested by the analysis. Sections 5.4, 5.5, 5.6 and 5.7 are concerned with more realistic flow. The stabilization variants are applied and their performance evaluated via suitable benchmarks. Laminar as well as transient or even turbulent flow examples are simulated. Moreover, it is tested if grad-div and LPS stabilization can act as an implicit turbulence model.

For the simulations, we take advantage of the C++-FEM package `deal.II`, see [BHK07, BHH⁺15], which provides tools for finite element methods. A highly parallel CFD solver for the time dependent Navier-Stokes problem was developed by D. Arndt from Göttingen. It is part of this thesis to extend the implementation to the non-isothermal case. The implementation of a special finite element space, namely the bubble enrichment (see Section 2.2.2), is joint work with D. Arndt.

2. Modeling Non-Isothermal Flow in Finite Element Methods

In this chapter, we introduce a mathematical description of non-isothermal flow and outline the steps towards a fully discrete model that can be considered numerically.

The main issues here are to introduce the Navier-Stokes-Fourier model and the special case of the Oberbeck-Boussinesq model that is valid for incompressible flow and small temperature differences. In order to obtain a discretized description, we consider spatial discretization via the finite element method (FEM) and roughly review time-discretization techniques. Afterwards, properties and results for auxiliary equations are cited.

2.1. Mathematical Model for Non-Isothermal Flow

There are several approaches in mathematical fluid mechanics for modeling flow. One of these is the phenomenological theory of continuum fluid mechanics, where the macroscopic behavior of the fluid is described. It is based on the assumption that the fluid can be modeled as a continuum. A homogeneous fluid in a domain $\Omega \subset \mathbb{R}^d$, $d \in \{2, 3\}$, is described by state variables such as density, fluid velocity and temperature. The time evolution in an interval $(0, T) \subset \mathbb{R}$ is described by partial differential equations. These can be derived by taking balance laws into account.

This short introduction follows the derivations in [FN09a] and [L ow11].

2.1.1. Navier-Stokes-Fourier Model

We assume that the fluid can be described by the following variables.

- (a) Domain $\Omega \subset \mathbb{R}^d$, $d \in \{2, 3\}$, occupied by the fluid,
- (b) mass density $\varrho = \varrho(t, \mathbf{x})$, a non-negative measurable function for $(t, \mathbf{x}) \in (0, T) \times \Omega$,
- (c) velocity $\mathbf{u} = \mathbf{u}(t, \mathbf{x})$, a vector field for $(t, \mathbf{x}) \in (0, T) \times \Omega$,
- (d) temperature $\vartheta = \vartheta(t, \mathbf{x})$, a positive measurable function for $(t, \mathbf{x}) \in (0, T) \times \Omega$ (measured in the Kelvin scale),
- (e) pressure $p = p(\varrho, \vartheta)$, specific internal energy $e = e(\varrho, \vartheta)$ and specific entropy $s = s(\varrho, \vartheta)$,

- (f) stress tensor $\mathbb{T} = \{T_{ij}\}_{i,j=1}^d$ describing the force per unit surface that a fluid part adjoining a surface element imposes on a fluid part on the other side to the same surface element,
- (g) flux of the internal energy \mathbf{q} , which is a vector field,
- (h) volume force acting on the fluid $\mathbf{f} = \mathbf{f}(t, \mathbf{x})$ for $(t, \mathbf{x}) \in (0, T) \times \Omega$,
- (i) rate of production of internal energy $Q = Q(t, \mathbf{x})$ for $(t, \mathbf{x}) \in (0, T) \times \Omega$.

The quantities $(\varrho, \mathbf{u}, \vartheta)$ characterize the current state and motion of the fluid at time t and are called state variables. The other quantities depend on these state variables by fixed relations.

There are important parameters which characterize the behavior of the flow:

	SI unit	Name
ϱ	$kg \cdot m^{-3}$	Density
μ	$kg \cdot m^{-1} \cdot s^{-1}$	Dynamic viscosity
$\nu = \mu/\varrho$	$m^2 \cdot s^{-1}$	Kinematic viscosity
k	$W \cdot m^{-1} \cdot K^{-1}$	Thermal conductivity
c_p	$J \cdot kg^{-1} \cdot K^{-1}$	Specific heat capacity
$\alpha = k/(\varrho c_p)$	$m^2 \cdot s^{-1}$	Thermal diffusivity
β	K^{-1}	Coefficient of thermal expansion
\mathbf{g}	$m^2 \cdot s^{-1}$	Gravitational force
L_{ref}	m	Characteristic length
U_{ref}	$m \cdot s^{-1}$	Characteristic velocity
T_{ref}	s	Characteristic time
$\Delta\theta_{\text{ref}}$	K	Characteristic temperature difference

Among others, these parameters can be combined to dimensionless variables, that are often used for a classification of the flow.

With the characteristic reference values for time T_{ref} , length L_{ref} , density ϱ_{ref} , temperature ϑ_{ref} , velocity U_{ref} and the composed quantities p_{ref} , e_{ref} , μ_{ref} , ζ_{ref} , k_{ref} and source terms f_{ref} , Q_{ref} , we can define the dimensionless variables Sr , Ma , Re , Fr , Pe , Hr (see [FN09a]):

Sr	$L_{\text{ref}}/(T_{\text{ref}}U_{\text{ref}})$	Strouhal number,
Ma	$U_{\text{ref}}/\sqrt{p_{\text{ref}}/\varrho_{\text{ref}}}$	Mach number,
Re	$\varrho_{\text{ref}}U_{\text{ref}}L_{\text{ref}}/\mu_{\text{ref}}$	Reynolds number,
Fr	$U_{\text{ref}}/\sqrt{L_{\text{ref}}f_{\text{ref}}}$	Froude number,
Pe	$p_{\text{ref}}L_{\text{ref}}U_{\text{ref}}/(\vartheta_{\text{ref}}k_{\text{ref}})$	Péclet number,
Hr	$\varrho_{\text{ref}}Q_{\text{ref}}L_{\text{ref}}/(p_{\text{ref}}U_{\text{ref}})$	Heat release parameter.

The Strouhal number Sr describes the relation between the characteristic time scale T_{ref} and the convection time scale $L_{\text{ref}}/U_{\text{ref}}$. The occurring velocity is compared to the speed of sound via the Mach number. The ratio between convective and diffusive forces is represented by the Reynolds numbers Re . The Froude number describes how large the inertial forces are compared to external forces. Pe is defined as the ratio of the advection rate to the diffusion rate at length scale L_{ref} .

Definition 2.1.1 (Dimensionless quantities).

We define the Prandtl number Pr , the Grashof number Gr and the Rayleigh number Ra as follows:

$$Pr = \frac{\nu}{\alpha}, \quad Gr = \frac{|\mathbf{g}|\beta\Delta\theta_{\text{ref}}L_{\text{ref}}^3}{\nu^2}, \quad Ra = Gr Pr = \frac{|\mathbf{g}|\beta\Delta\theta_{\text{ref}}L_{\text{ref}}^3}{\nu\alpha}.$$

By Stokes' law, it holds

$$\mathbb{T} = \mathbb{S} - p\mathbb{I}$$

with the viscous stress tensor \mathbb{S} . For Newtonian fluids, it is given by

$$\mathbb{S} = \mu(\vartheta) \left(\nabla \mathbf{u} + (\nabla \mathbf{u})^T - \frac{2}{3} \nabla \cdot \mathbf{u} \mathbb{I} \right) + \zeta(\vartheta) \nabla \cdot \mathbf{u} \mathbb{I}$$

with dynamic viscosity $\mu(\vartheta)$, bulk viscosity $\zeta(\vartheta)$ and the identity matrix \mathbb{I} . The internal energy flux \mathbf{q} is determined by the thermal conductivity $k(\vartheta)$ by

$$\mathbf{q} = -k(\vartheta) \nabla \vartheta.$$

The rate of energy production σ is defined as

$$\sigma = \frac{1}{\vartheta} \left(\frac{Ma^2}{Re} \mathbb{S} \cdot \nabla \mathbf{u} - \frac{1}{Pe} \frac{\mathbf{q} \cdot \nabla \vartheta}{\vartheta} \right).$$

Let D denote the differential with respect to ϱ and ϑ . So by the second law of thermodynamics, the Gibbs' equation holds:

$$\vartheta Ds(\varrho, \vartheta) = De(\varrho, \vartheta) + p(\varrho, \vartheta) D \left(\frac{1}{\varrho} \right).$$

The Navier-Stokes-Fourier equations governing the behavior of the fluid result from physical principles, namely mass conservation, balance of linear momentum as well as the total

energy and entropy balance. Scaling by characteristic variables yields the dimensionless model for $(t, \mathbf{x}) \in (0, T) \times \Omega$:

$$\begin{aligned}
Sr \partial_t \varrho + \nabla \cdot (\varrho \mathbf{u}) &= 0, \\
Sr \partial_t (\varrho \mathbf{u}) + \nabla \cdot (\varrho \mathbf{u} \otimes \mathbf{u}) + \frac{1}{Ma^2} \nabla p(\varrho, \vartheta) &= \frac{1}{Re} \nabla \cdot \mathbb{S} - \frac{1}{Fr^2} \varrho \mathbf{f}, \\
Sr \partial_t (\varrho s(\varrho, \vartheta)) + \nabla \cdot (\varrho s(\varrho, \vartheta) \mathbf{u}) + \frac{1}{Pe} \nabla \cdot \left(\frac{\mathbf{q}}{\vartheta} \right) &= \sigma + Hr \varrho \frac{Q}{\vartheta}, \\
Sr \partial_t \int_{\Omega} \left(\frac{Ma^2}{2} \varrho |\mathbf{u}|^2 + \varrho e(\varrho, \vartheta) \right) dx &= \int_{\Omega} \left(\frac{Ma^2}{Fr^2} \varrho \mathbf{f} \cdot \mathbf{u} + Hr \rho Q \right) dx.
\end{aligned} \tag{2.1}$$

2.1.2. Oberbeck-Boussinesq Approximation

The Navier-Stokes-Fourier equations (2.1) are a general mathematical model for non-isothermal flow.

In many applications, the Mach number is small, as the fluid velocity is small compared with the speed of sound. This means that no shocks occur and the acoustic waves have negligible influence on the flow. In the limit $Ma \rightarrow 0$, the pressure tends to a constant, whereas the speed of sound tends to infinity. If additionally the temperature differences are small, incompressibility $\nabla \cdot \mathbf{u} = 0$ follows from mass conservation. The so-called Oberbeck-Boussinesq model approximates the Navier-Stokes-Fourier equations for a simultaneously small Froude number $Fr \approx \sqrt{Ma}$. This can be obtained by a formal asymptotic expansion. Often the volume force \mathbf{f} can be written as a gradient of a scalar potential $F = F(\mathbf{x})$:

$$\mathbf{f} = \nabla F.$$

If we write $Ma =: \varepsilon$, $Fr = \sqrt{\varepsilon}$ and assume that all of the other dimensionless characteristics are of order $\mathcal{O}(1)$, we can expand the quantities ϱ , \mathbf{u} and ϑ around $\bar{\varrho}$, \mathbf{U} , $\bar{\vartheta}$ as a series of ε . Neglecting higher order terms of ε , we can derive the Oberbeck-Boussinesq approximation:

$$\begin{aligned}
\bar{\varrho}(\partial_t \mathbf{U} + \nabla \cdot (\mathbf{U} \otimes \mathbf{U})) + \nabla P &= \nabla \cdot \mathbb{S} - r \nabla F, \\
\nabla \cdot \mathbf{U} &= 0, \\
\bar{\varrho} c_p(\bar{\varrho}, \bar{\vartheta})(\partial_t \theta + \nabla \cdot (\theta \mathbf{U})) - \nabla \cdot (k(\bar{\vartheta}) \nabla \theta) &= 0.
\end{aligned} \tag{2.2}$$

These are equations for the incompressible velocity \mathbf{U} , the temperature θ and the pressure P . Note that θ describes the difference to the mean temperature $\bar{\vartheta}$ and P is a Lagrange multiplier for the divergence free condition, which does not coincide with the thermodynamic pressure. Due to the incompressibility of \mathbf{U} , we have

$$\mathbb{S} = \mu(\bar{\vartheta}) \left(\nabla \mathbf{U} + (\nabla \mathbf{U})^T \right).$$

In (2.2), the specific heat capacity at constant pressure c_p and the thermal conductivity k are taken at constant density $\bar{\rho}$ and constant temperature $\bar{\vartheta}$. Moreover, the temperature dependent reduced density $r = r(\theta)$ appears in the momentum equation; it arises as a linearization of the density around the mean temperature $\bar{\vartheta}$. It fulfills

$$r + \bar{\rho}\bar{\beta}(\theta - \bar{\vartheta}) = 0$$

with the coefficient of thermal expansion $\bar{\beta}$. We draw the reader's attention to the fact that the force term $\bar{\rho}\bar{\beta}\bar{\vartheta}\nabla F$ can be incorporated in the pressure and does not influence the velocity field.

The Oberbeck-Boussinesq system is considered in [Obe79] in order to model the flow of diluted gases due to temperature differences. As it is shown in [FN09b], the asymptotic limit for the general Navier–Stokes–Fourier system is the Oberbeck–Boussinesq system as both Mach and Froude numbers tend to zero.

2.1.3. Boundary Conditions

In the following section, we present some possibilities to equip the Navier-Stokes-Fourier model (2.1) or the Oberbeck-Boussinesq equations (2.2) on a bounded domain Ω with boundary conditions on $\partial\Omega$. These are also shown in [Löw11].

Let \mathbf{n} denote the outer unit normal vector at the boundary. If the system is completely isolated, we set

$$\mathbf{u} \cdot \mathbf{n}|_{\partial\Omega} = 0, \quad \mathbb{S}\mathbf{n} \times \mathbf{n}|_{\partial\Omega} = 0, \quad \mathbf{q} \cdot \mathbf{n}|_{\partial\Omega} = 0. \quad (2.3)$$

The fluid does not leave the domain, there is no heat transfer in wall-normal direction and no static friction influences the flow. In this case, no boundary layers occur near the walls.

A more realistic situation is created if there is a (homogeneous) Dirichlet condition on a part of the boundary $\Gamma_0 \subset \partial\Omega$; so the velocity is set to zero on Γ_0 . The temperature at the wall can be prescribed via Dirichlet conditions or a fixed heat transfer can be imposed:

$$\mathbf{u}|_{\Gamma_0} = 0, \quad \theta|_{\Gamma_0} = \theta_{wall} \quad \text{or} \quad \mathbf{q} \cdot \mathbf{n}|_{\Gamma_0} = q_{wall}. \quad (2.4)$$

These so-called no-slip conditions can lead to thin boundary layers for small viscosity. If only a part of the physical domain is simulated, there are artificial boundaries. Typically, these are boundaries describing inflow or outflow:

$$\Gamma_- := \{\mathbf{x} \in \partial\Omega \mid \mathbf{u} \cdot \mathbf{n} < 0\}, \quad \Gamma_+ := \{\mathbf{x} \in \partial\Omega \mid \mathbf{u} \cdot \mathbf{n} > 0\}.$$

In case of inflow, we can prescribe

$$\mathbf{u}|_{\Gamma_-} = \mathbf{u}_{in}, \quad \theta|_{\Gamma_-} = \theta_{in}. \quad (2.5)$$

At outflow boundaries it is desired to impose conditions that do not influence the outflow. An often considered possibility is called “do-nothing” boundary condition (see [Gre91], for instance)

$$(\nu \nabla \mathbf{u} - p \mathbb{I}) \cdot \mathbf{n}|_{\Gamma_+} = 0, \quad \mathbf{q} \cdot \mathbf{n}|_{\Gamma_+} = 0. \quad (2.6)$$

2.2. Spatial Discretization

There are several methods available to perform a discretization in space. We pursue the ansatz of finite elements, which are introduced in Section 2.2.2. Finite element methods (FEM) are special Ritz Galerkin methods and approximate the weak solution of the differential equation.

Also, finite difference methods (FDM), finite volume methods (FVM) and spectral methods can be used for discretizing in space. We refer the reader to [RST08] and [QV08] for details.

2.2.1. Variational Formulation and Ritz Galerkin Method

From now on, we consider the simplified time-dependent Navier-Stokes-Fourier model with Oberbeck-Boussinesq approximation and homogeneous Dirichlet data. We call this the Oberbeck-Boussinesq equations:

$$\begin{aligned} \partial_t \mathbf{u} - \nu \Delta \mathbf{u} + (\mathbf{u} \cdot \nabla) \mathbf{u} + \nabla p + \beta \theta \mathbf{g} &= \mathbf{f}_u && \text{in } (0, T) \times \Omega, \\ \nabla \cdot \mathbf{u} &= 0 && \text{in } (0, T) \times \Omega, \\ \partial_t \theta - \alpha \Delta \theta + (\mathbf{u} \cdot \nabla) \theta &= f_\theta && \text{in } (0, T) \times \Omega, \\ \mathbf{u} = \mathbf{0}, \theta &= 0 && \text{in } (0, T) \times \partial\Omega, \\ \mathbf{u}(0, \cdot) &= \mathbf{u}_0(\cdot), \theta(0, \cdot) = \theta_0(\cdot) && \text{in } \Omega \end{aligned} \quad (2.7)$$

in a bounded polyhedral Lipschitz domain $\Omega \subset \mathbb{R}^d$, $d \in \{2, 3\}$, with boundary $\partial\Omega$. Here $\mathbf{u}: [0, T] \times \Omega \rightarrow \mathbb{R}^d$, $p: [0, T] \times \Omega \rightarrow \mathbb{R}$ and $\theta: [0, T] \times \Omega \rightarrow \mathbb{R}$ denote the unknown velocity, pressure and temperature fields for given viscosity $\nu > 0$, thermal diffusivity $\alpha > 0$, thermal expansion coefficient $\beta > 0$ and external forces $\mathbf{f}_u \in L^2(0, T; [L^2(\Omega)]^d) \cap C(0, T; [L^2(\Omega)]^d)$, $f_\theta \in L^2(0, T; L^2(\Omega)) \cap C(0, T; L^2(\Omega))$, gravitation $\mathbf{g} \in L^\infty(0, T; [L^\infty(\Omega)]^d)$ and initial data $\mathbf{u}_0 \in [L^2(\Omega)]^d$, $\theta_0 \in L^2(\Omega)$.

In order to guarantee well-posedness of the variational formulation, we define suitable function spaces. Let

$$\mathbf{V} := [W_0^{1,2}(\Omega)]^d, \quad Q := L_*^2(\Omega) := \left\{ q \in L^2(\Omega) \mid \int_{\Omega} q \, dx = 0 \right\}, \quad \Theta := W_0^{1,2}(\Omega). \quad (2.8)$$

The variational formulation of (2.7) can be derived by multiplication with respective test functions and integration over the domain Ω . Integration by parts and taking the homogeneous Dirichlet boundary conditions into account yield the variational formulation. Note that the test functions do not depend on time. The variational formulation for fixed time $t \in (0, T)$ reads:

Find $(\mathbf{u}(t), p(t), \theta(t)) \in \mathbf{V} \times Q \times \Theta$ such that it holds for all $(\mathbf{v}, q, \psi) \in \mathbf{V} \times Q \times \Theta$

$$\begin{aligned} (\partial_t \mathbf{u}(t), \mathbf{v}) + (\nu \nabla \mathbf{u}(t), \nabla \mathbf{v}) + c_u(\mathbf{u}(t); \mathbf{u}(t), \mathbf{v}) \\ - (p(t), \nabla \cdot \mathbf{v}) + (\beta \theta(t) \mathbf{g}, \mathbf{v}) = (\mathbf{f}_u(t), \mathbf{v}), \end{aligned} \quad (2.9)$$

$$(\nabla \cdot \mathbf{u}(t), q) = 0,$$

$$(\partial_t \theta(t), \psi) + (\alpha \nabla \theta(t), \nabla \psi) + c_\theta(\mathbf{u}(t); \theta(t), \psi) = (f_\theta(t), \psi) \quad (2.10)$$

with

$$\begin{aligned} c_u(\mathbf{w}; \mathbf{u}, \mathbf{v}) &:= \frac{1}{2} [((\mathbf{w} \cdot \nabla) \mathbf{u}, \mathbf{v}) - ((\mathbf{w} \cdot \nabla) \mathbf{v}, \mathbf{u})], \\ c_\theta(\mathbf{w}; \theta, \psi) &:= \frac{1}{2} [((\mathbf{w} \cdot \nabla) \theta, \psi) - ((\mathbf{w} \cdot \nabla) \psi, \theta)]. \end{aligned}$$

The skew-symmetric form of the convective terms c_u, c_θ is chosen for conservation purposes (in the discretized problem). Note that it holds $c_u(\mathbf{w}; \mathbf{u}, \mathbf{v}) = ((\mathbf{w} \cdot \nabla) \mathbf{u}, \mathbf{v})$ for solenoidal \mathbf{w} (for c_θ analogously). In the following, we omit the dependence on t .

The so-called (continuous) inf-sup condition

$$\exists \beta_c < 0: \quad \inf_{q \in Q \setminus \{0\}} \sup_{\mathbf{v} \in \mathbf{V} \setminus \{0\}} \frac{(q, \nabla \cdot \mathbf{v})}{\|q\|_Q \|\mathbf{v}\|_{\mathbf{V}}} \geq \beta_c \quad (2.11)$$

has important consequences. Uniqueness of the pressure p in (2.9) is guaranteed by (2.11), see [Bab73, Bre74]. We point out that the inf-sup condition is fulfilled for the spaces $\mathbf{V} \times Q = [W_0^{1,2}(\Omega)]^d \times L_*^2(\Omega)$, which we consider throughout this thesis. Due to the closed range theorem, the space

$$\mathbf{V}^{div} := \{ \mathbf{v} \in \mathbf{V} \mid (q, \nabla \cdot \mathbf{v}) = 0 \quad \forall q \in Q \} \quad (2.12)$$

does not only consist of $\mathbf{0}$. So we can look for weakly solenoidal solutions $\mathbf{u} \in \mathbf{V}^{div}$. If (2.9) is tested with solenoidal test functions as well, all pressure terms can be eliminated.

The pressure p can be recovered via the inf-sup condition afterwards.

The underlying idea of Ritz Galerkin methods is to approximate the solution spaces \mathbf{V} , Q , Θ by finite dimensional conforming subspaces $\mathbf{V}_h \subset \mathbf{V}$, $Q_h \subset Q$, $\Theta_h \subset \Theta$. The dimensions of \mathbf{V}_h , Q_h and Θ_h tend to infinity for decreasing discretization parameter $h \rightarrow 0$; they are dense in the respective spaces. Then the discretized variational formulation reads:

Find $(\mathbf{u}_h(t), p_h(t), \theta_h(t)) \in \mathbf{V}_h \times Q_h \times \Theta_h$ such that

$$\begin{aligned} (\partial_t \mathbf{u}_h, \mathbf{v}_h) + (\nu \nabla \mathbf{u}_h, \nabla \mathbf{v}_h) + c_u(\mathbf{u}_h; \mathbf{u}_h, \mathbf{v}_h) \\ - (p_h, \nabla \cdot \mathbf{v}_h) + (\beta \theta_h \mathbf{g}, \mathbf{v}_h) = (\mathbf{f}_u, \mathbf{v}_h), \end{aligned} \quad (2.13)$$

$$(\nabla \cdot \mathbf{u}_h, q_h) = 0,$$

$$(\partial_t \theta_h, \psi_h) + (\alpha \nabla \theta_h, \nabla \psi_h) + c_\theta(\mathbf{u}_h; \theta_h, \psi_h) = (f_\theta, \psi_h) \quad (2.14)$$

for any $t \in (0, T)$ and test functions $\mathbf{v}_h \in \mathbf{V}_h$, $q_h \in Q_h$, $\psi_h \in \Theta_h$. With the notation $n_V := \dim(\mathbf{V}_h)$, $n_Q := \dim(Q_h)$, $n_\Theta := \dim(\Theta_h)$, we can pick bases according to

$$\begin{aligned} \mathbf{V}_h &= \text{span}\{\mathbf{v}_i \mid i = 1, \dots, n_V\}, & Q_h &= \text{span}\{q_j \mid j = 1, \dots, n_Q\}, \\ \Theta_h &= \text{span}\{\psi_k \mid k = 1, \dots, n_\Theta\}. \end{aligned}$$

If we use the basis representation

$$\mathbf{u}_h = \sum_{i=1}^{n_V} u_i \mathbf{v}_i, \quad p_h = \sum_{j=1}^{n_Q} p_j q_j, \quad \theta_h = \sum_{k=1}^{n_\Theta} \theta_k \psi_k$$

and denote the coefficient vectors again with $u_h \in \mathbb{R}^{n_V}$, $p_h \in \mathbb{R}^{n_Q}$, $\theta_h \in \mathbb{R}^{n_\Theta}$, we can formulate an equivalent nonlinear system of finitely many equations for (2.13)-(2.14) as follows: Let

$$\begin{aligned} M_u &:= [(\mathbf{v}_j, \mathbf{v}_i)]_{i,j} \in \mathbb{R}^{n_V \times n_V}, & M_\theta &:= [(\psi_j, \psi_i)]_{i,j} \in \mathbb{R}^{n_\Theta \times n_\Theta}, \\ B &:= [(\nabla \cdot \mathbf{v}_i, q_j)]_{i,j} \in \mathbb{R}^{n_V \times n_Q}, & G &:= [(\beta \psi_j \mathbf{g}, \mathbf{v}_i)]_{i,j} \in \mathbb{R}^{n_V \times n_\Theta}, \\ A_u(w) &:= [(\nu \nabla \mathbf{v}_j, \nabla \mathbf{v}_i) + c_u(w, \mathbf{v}_j, \mathbf{v}_i)]_{i,j} \in \mathbb{R}^{n_V \times n_V}, \\ A_\theta(\mathbf{w}) &:= [(\alpha \nabla \psi_j, \nabla \psi_i) + c_\theta(\mathbf{w}, \psi_j, \psi_i)]_{i,j} \in \mathbb{R}^{n_\Theta \times n_\Theta}, \\ F_u(t) &:= [(\mathbf{f}_u(t), \mathbf{v}_i)]_i \in \mathbb{R}^{n_V}, & F_\theta(t) &:= [(f_\theta(t), \psi_j)]_j \in \mathbb{R}^{n_\Theta}. \end{aligned}$$

The equivalent problem is:

Find $(u_h, p_h, \theta_h) : (0, T) \rightarrow \mathbb{R}^{n_v} \times \mathbb{R}^{n_Q} \times \mathbb{R}^{n_\theta}$ such that

$$\begin{pmatrix} M_u & 0 & 0 \\ 0 & 0 & 0 \\ 0 & 0 & M_\theta \end{pmatrix} \begin{pmatrix} u'_h(t) \\ p'_h(t) \\ \theta'_h(t) \end{pmatrix} = \begin{pmatrix} F_u(t) \\ 0 \\ F_\theta(t) \end{pmatrix} - \begin{pmatrix} A_u(u_h(t)) & B & G \\ B^T & 0 & 0 \\ 0 & 0 & A_\theta(u_h(t)) \end{pmatrix} \begin{pmatrix} u_h(t) \\ p_h(t) \\ \theta_h(t) \end{pmatrix}. \quad (2.15)$$

The respective initial conditions are obtained by projecting the continuous initial conditions onto the discrete ansatz spaces.

We impose a discrete inf-sup condition for \mathbf{V}_h and Q_h throughout this thesis:

Assumption 2.2.1 (Discrete inf-sup stability).

Let $\mathbf{V}_h \subset \mathbf{V}$ and $Q_h \subset Q$ be FE spaces satisfying a discrete inf-sup-condition

$$\inf_{q_h \in Q_h \setminus \{0\}} \sup_{\mathbf{v}_h \in \mathbf{V}_h \setminus \{0\}} \frac{(\nabla \cdot \mathbf{v}_h, q_h)}{\|\nabla \mathbf{v}_h\|_0 \|q_h\|_0} \geq \beta_h > 0 \quad (2.16)$$

with a constant β_h independent of h .

Note that even for conforming discrete ansatz spaces, the continuous inf-sup condition (2.11) does not imply the discrete one (2.16). If discrete ansatz spaces are used that are not inf-sup stable, the mixed problem (2.15) becomes singular. In order to circumvent this, we only use inf-sup stable elements. For instance, the well known Taylor-Hood elements fulfill Assumption 2.2.1, see [BP79]. We introduce them below and use them frequently during our numerical experiments.

Under the discrete inf-sup condition, we can define the non-trivial space of weakly solenoidal functions

$$\mathbf{V}_h^{div} := \{\mathbf{v}_h \in \mathbf{V}_h \mid (q_h, \nabla \cdot \mathbf{v}_h) = 0 \forall q_h \in Q_h\} \neq \{0\}. \quad (2.17)$$

We point out that this space is not conforming in the sense that

$$\mathbf{V}_h^{div} \not\subset \mathbf{V}^{div}.$$

In general, this leads to poor mass conservation $\|\nabla \cdot \mathbf{u}_h\|_0 \neq 0$. Because of $1 \in Q_h$, at least global mass conservation $\int_\Omega \nabla \cdot \mathbf{u}_h(\mathbf{x}) d\mathbf{x} = 0$ holds if a continuous discrete pressure space is used.

2.2.2. Finite Element Methods

In this section, we introduce the concept of Finite Element Methods (FEM) and define special elements that are important in the following chapters. For details and analytical results regarding FEM, we refer the reader to [GR12, BS08, ESW14], for example.

Finite element methods are a special case of Ritz Galerkin methods, which have the following properties. The domain is divided into fragments of simpler geometry, namely into finitely many elements of finite size. The approximate solution is represented as a linear combination of finitely many ansatz functions and is inserted into the differential equation. The ansatz and test functions are defined piecewise (locally) on the subdomains, where certain matching conditions guarantee conformity of the method. Considering also initial and boundary conditions leads to a large, finite dimensional system of equations that can be solved numerically.

Definition 2.2.2 (Finite element).

A finite element (FE) in \mathbb{R}^d is a triple (T, P_T, Σ_T) , where $T \subset \mathbb{R}^d$ is a closed subset with $\text{int}(T) \neq \emptyset$ and Lipschitz-continuous boundary and $P_T \subset \{\varphi: T \rightarrow \mathbb{R}\}$ is a finite m -dimensional space of ansatz functions. The set of degrees of freedom Σ_T consists of m linearly independent linear forms ψ_i acting on P_T , such that each $p \in P_T$ is well-defined by the values of the m elements of Σ_T :

$$\forall \{\alpha_i\}_{i=1}^m \subset \mathbb{R}^m \quad \exists! p \in P_T: \quad \psi_i(p) = \alpha_i, \quad i = 1, \dots, m.$$

A basis $\{\phi_j\}_{j=1}^m \subset P_T$ is called nodal basis if $\psi_i(\phi_j) = \delta_{ij}$.

Let Ω be a bounded polyhedral domain. Consider a non-overlapping subdivision \mathcal{T}_h of Ω into finitely many polyhedral cells $T_i \in \mathcal{T}_h$, $i = 1, \dots, n_T < \infty$.

Definition 2.2.3 (Admissible triangulation).

A subdivision $\mathcal{T}_h = \{T_i\}_{i=1}^{n_T}$ of Ω is called admissible if $\bar{\Omega} = \bigcup_{i=1}^{n_T} T_i$ and if the intersection of two different closed subdomains T_i and T_j is either empty, exactly one common surface (if $d = 3$), exactly one whole common edge (if $d \geq 2$) or exactly one common point (if $d \geq 1$).

Definition 2.2.4 (Shape regular and quasi-uniform triangulations).

The diameter h_T of a cell $T \in \mathcal{T}_h$ is defined by the diameter of the smallest ball B_T^{in} such that $T \subset B_T^{in}$. A family $\{\mathcal{T}_h\}$ of triangulations is called shape regular if there exists $c > 0$ such that for all \mathcal{T}_h in this family:

$$\max_{T \in \mathcal{T}_h} \frac{h_T^d}{|T|} \leq c,$$

where $|T| := \int_T 1 \, d\mathbf{x}$ is the measure of T in \mathbb{R}^d . A shape regular family $\{\mathcal{T}_h\}$ is called quasi-uniform if, additionally, for all \mathcal{T}_h holds

$$\frac{\max_{T \in \mathcal{T}_h} |T|}{\min_{T \in \mathcal{T}_h} |T|} \leq \rho$$

with a fixed $\rho > 0$.

Let us introduce simplicial and quadrilateral elements as well as enriched finite element spaces.

Definition 2.2.5 (Simplicial and quadrilateral finite elements).

Denote by $\hat{T} \subset \mathbb{R}^d$ the reference element. Let $\alpha \in \mathbb{N}_0^d$ be a multiindex and $\mathbf{x}^\alpha := \prod_{i=1}^d x_i^{\alpha_i}$ for $\mathbf{x} \in \mathbb{R}^d$. Then the spaces

$$\begin{aligned} \mathbb{P}_k(\hat{T}) &:= \text{span} \left\{ \hat{T} \rightarrow \mathbb{R}, \mathbf{x} \mapsto \mathbf{x}^\alpha \mid \alpha \in \mathbb{N}_0^d, \sum_{i=1}^d \alpha_i \leq k \right\}, \\ \mathbb{Q}_k(\hat{T}) &:= \text{span} \left\{ \hat{T} \rightarrow \mathbb{R}, \mathbf{x} \mapsto \mathbf{x}^\alpha \mid \alpha \in \mathbb{N}_0^d, \max_{1 \leq i \leq d} \{\alpha_i\} \leq k \right\} \end{aligned}$$

define the spaces of triangular (simplicial) and rectangular (quadrilateral/hexahedral) finite elements.

In case of simplicial or quadrilateral elements, \hat{T} is the unit simplex or cube in \mathbb{R}^d . Moreover, we set

$$\mathbb{R}_k(\hat{T}) := \begin{cases} \mathbb{P}_k(\hat{T}) & \text{on simplices } \hat{T}, \\ \mathbb{Q}_k(\hat{T}) & \text{on quadrilaterals/hexahedra } \hat{T}. \end{cases}$$

Now, we need the notion of barycentric coordinates for the reference simplex \hat{T} in \mathbb{R}^d . Because \hat{T} is convex, we can write it as the convex hull of its vertices $\{\mathbf{p}^i\}_{i=0}^d$:

$$\hat{T} = \left\{ \hat{\mathbf{x}} = \sum_{i=0}^d \hat{\lambda}_i \mathbf{p}^i \in \mathbb{R}^d : \hat{\lambda}_i \geq 0, \sum_{i=0}^d \hat{\lambda}_i = 1 \right\}. \quad (2.18)$$

This representation yields a parametrization of \hat{T} : The coordinates $\hat{\lambda}_i$ with $i = 0, \dots, d$ in (2.18) are called barycentric coordinates.

Definition 2.2.6 (Bubble-enriched spaces).

We call $b_{\hat{T}} := \prod_{i=0}^d \hat{\lambda}_i \in \hat{\mathbb{P}}_{d+1}$ a polynomial bubble function on the reference simplex \hat{T}

with barycentric coordinates $\hat{\lambda}_i$. Denote by $\psi(\hat{\mathbf{x}}) := \prod_{i=1}^d (1 - \hat{x}_i^2)$ a d -quadratic bubble function on the reference cube. Then we define bubble-enriched spaces as

$$\mathbb{P}_k^+(\hat{T}) := \mathbb{P}_k(\hat{T}) + b_{\hat{T}} \cdot \mathbb{P}_{k-2}(\hat{T}), \quad \mathbb{Q}_k^+(\hat{T}) := \mathbb{Q}_k(\hat{T}) + \psi \cdot \text{span}\{\hat{x}_i^{k-1}, i = 1, \dots, d\}.$$

We note that $\mathbb{Q}_k^+(\hat{T})$ has exactly d basis functions more than $\mathbb{Q}_k(\hat{T})$ and introduce the abbreviation

$$\mathbb{R}_k^+(\hat{T}) := \begin{cases} \mathbb{P}_k^+(\hat{T}) & \text{on simplices } \hat{T}, \\ \mathbb{Q}_k^+(\hat{T}) & \text{on quadrilaterals/hexahedra } \hat{T}. \end{cases}$$

We are interested in so-called mapped finite elements, that are constructed as transformations from the reference element. Denote by $F_T: \hat{T} \rightarrow T$ the reference mapping. For simplices T , F_T is affine and bijective. In case of quadrilaterals/hexahedra, F_T is a multilinear mapping from \hat{T} to arbitrary quadrilaterals/hexahedra. Henceforth, we require that F_T is bijective and its Jacobian is bounded for a family of triangulations according to

$$\exists c_1, c_2 > 0: \quad c_1 h_T^d \leq |\det DF_T(\hat{\mathbf{x}})| \leq c_2 h_T^d \quad \forall \hat{\mathbf{x}} \in \hat{T} \quad (2.19)$$

with constants $c_1, c_2 > 0$ independent of the cell diameter h_T .

Definition 2.2.7 (Mapped finite elements).

The Lagrangian mapped finite elements are given by

$$\begin{aligned} Y_{h,-k} &:= \{v_h \in L^2(\Omega) : v_h|_T \circ F_T \in \mathbb{R}_k(\hat{T}) \forall T \in \mathcal{T}_h\}, & Y_{h,k} &:= Y_{h,-k} \cap W^{1,2}(\Omega), \\ Y_{h,-k}^+ &:= \{v_h \in L^2(\Omega) : v_h|_T \circ F_T \in \mathbb{R}_k^+(\hat{T}) \forall T \in \mathcal{T}_h\}, & Y_{h,k}^+ &:= Y_{h,-k}^+ \cap W^{1,2}(\Omega). \end{aligned}$$

We deploy this definition to construct ansatz spaces for the discrete quantities. Let k_u be the polynomial degree for the discrete velocity, k_p for the discrete pressure and k_θ for the discrete temperature spaces. We often consider

$$\mathbf{V}_h = [Y_{h,k_u}^{(+)}]^d \cap \mathbf{V}, \quad Q_h = Y_{h,\pm k_p} \cap Q, \quad \Theta_h = Y_{h,k_\theta}^{(+)} \cap \Theta$$

without or with bubble-enrichment, where the latter is indicated by the superscript $+$. For convenience, we also write $\mathbf{V}_h = \mathbb{R}_{k_u}^{(+)}$, $Q_h = \mathbb{R}_{\pm k_p}$, $\Theta_h = \mathbb{R}_{k_\theta}^{(+)}$. The triple of ansatz spaces for velocity, pressure and temperature is often denoted by $\mathbb{R}_{k_u}^{(+)} \wedge \mathbb{R}_{\pm k_p} \wedge \mathbb{R}_{k_\theta}^{(+)}$.

Remark 2.2.8. We point out that $\mathbf{u}_h|_T \in [W^{1,\infty}(T)]^d$ for all $\mathbf{u}_h \in \mathbf{V}_h = [Y_{h,k_u}^{(+)}]^d \cap \mathbf{V}$. This is due to the FE framework we introduced: $\mathbf{u}_h|_T \circ F_T$ is a smooth function on the reference cell for all $T \in \mathcal{T}_h$. In addition, the reference mapping F_T is bijective and affine or multi-linear.

2.2.3. Local Projection and Grad-Div Stabilization

The Ritz Galerkin scheme (2.13)-(2.14) is prone to suffering from instabilities occurring in the numerical solution. This might be due to dominating advection or by a violation of the discrete inf-sup condition (2.16). Many stabilization techniques have been proposed in order to cope with these spurious oscillations. Besides, instabilities in the discrete velocity can occur due to a poor mass conservation of the velocity-pressure ansatz spaces at high Reynolds numbers, see [Lin09]. For instance, this becomes relevant for conforming mixed finite element methods.

For the steady Navier-Stokes equations or related auxiliary problems as the Oseen model, the widely used residual-based stabilization (RBS) methods add consistent stabilization terms to the variational formulation in the sense that the additional terms vanish for the exact strong solution. RBS methods penalize the residual of the differential equation. The non-symmetric form of the stabilization terms and the occurrence of second order derivatives in the residual are drawbacks regarding the efficiency of this method. An overview about RBS methods and other stabilization techniques for can be found in [RST08].

A common way is a combination of pressure-stabilizing / Petrov-Galerkin (PSPG) and Streamline-Upwind Petrov-Galerkin (SUPG) for advection together with a stabilization of the divergence constraint (grad-div). This technique is studied, for example, in [LR06a]. The SUPG method relies on testing the residual with the streamline derivative and was introduced in [BH82], PSPG was considered in [JS86, HFB86].

The so-called grad-div stabilization is an additional element-wise stabilization of the divergence constraint. It enhances the discrete mass conservation and reduces the effect of the pressure error on the velocity error (cf. [GLOS05, CELR11]). In case of advection dominated flow, it plays an important role for robustness.

Due to the mentioned drawbacks of RBS methods, other stabilization techniques are considered in the literature. [BBJL07] gives an overview over different stabilization techniques, discusses the residual-based SUPG/PSPG method and presents a symmetric stabilization technique that is related to variational multiscale (VMS) methods introduced by [HMJ00] (see also [BB06]). The key idea of VMS methods is a separation of scales into large scales, small resolved scales and small unresolved scales. VMS methods model the influence of the unresolved scales on the resolved scales, where it is often assumed that the unresolved scales only influence the small resolved scales. Only parts of the residual are used. Therefore, the consistency of the method is not guaranteed. Instead, an approximate Galerkin orthogonality holds. So convergence rates of (quasi-)optimal order can be shown. Note that many stabilization techniques can be interpreted as VMS methods.

Similar to VMS methods, local projection based stabilization (LPS) methods rely on the idea to separate the discrete function spaces into small resolved and large resolved scales and to add stabilization terms only on the small scales. The stabilization terms can be

interpreted as models for the influence of the unresolved scales that act on the smallest resolved scales. This method has the interesting features of adding solely symmetric terms to the formulation and avoiding the computation of second derivatives of the basis functions. The work of [MST07] provides a special interpolation operator, that is important for the numerical analysis of the LPS method. In [LRL08], a unified numerical analysis for finite element discretizations of the Oseen problem using the LPS method is given. Equal-order and inf-sup stable velocity-pressure ansatz spaces are taken into account. The LPS method considered in [BBJL07] stabilizes the pressure as well as the convective terms and is thus applicable to equal-order elements for velocity and pressure (for these elements, the discrete inf-sup condition does not hold). In [BL09], several analytical results for finite element methods for incompressible flow problems with local projection stabilization are discussed.

Since local projection and grad-div stabilization have proven useful for a large variety of flow problems, we want to apply them to the Oberbeck-Boussinesq model (2.7). It is a common procedure to transfer models introduced for e.g. the Navier-Stokes problem to non-isothermal flow. For example, in [LL12], a projection-based variational multiscale method is applied to large-eddy simulation of the Oberbeck-Boussinesq model.

Let us formulate the Oberbeck-Boussinesq model with streamline-upwind local projection stabilization (LPS SU) and grad-div stabilization. Since both velocity and temperature are considered in the advection-dominated regime, we want to add LPS in order to stabilize both quantities. We assume inf-sup stable discrete velocity and pressure, hence, no stabilization for the pressure is applied.

From now on, $\{\mathcal{T}_h\}$ is an admissible and shape-regular family of triangulations into d -simplices, quadrilaterals ($d = 2$) or hexahedra ($d = 3$). Let $\{\mathcal{M}_h\}$ and $\{\mathcal{L}_h\}$ be families of shape-regular macro decompositions of Ω for velocity and temperature. They represent the coarse scales in velocity and temperature. In [MST07] and later in [KL09], two approaches are mentioned for choosing the space of large scales. In the so-called two-level approach, the large scales are defined by using a coarse mesh. The coarse mesh \mathcal{M}_h is constructed such that each macro-element $M \in \mathcal{M}_h$ is the union of one or more neighboring elements $T \in \mathcal{T}_h$. So \mathcal{M}_h arises by coarsening of the original mesh \mathcal{T}_h or, equivalently, \mathcal{T}_h is derived from \mathcal{M}_h by barycentric refinement of d -simplices or regular (dyadic) refinement of quadrilaterals and hexahedra. In the one-level LPS-approach, the coarse scales can be represented via a lower order finite elements space on \mathcal{T}_h . Another way is to enrich the fine spaces. We can use the same abstract framework by setting $\mathcal{M}_h = \mathcal{T}_h$. \mathcal{L}_h is constructed analogously for the temperature.

Throughout this thesis, we suppose that the following assumption holds true.

Assumption 2.2.9 (Fine and coarse triangulations).

Let $\{\mathcal{T}_h\}$, $\{\mathcal{M}_h\}$, $\{\mathcal{L}_h\}$ be admissible and shape-regular families of non-overlapping triangulations into d -simplices, quadrilaterals ($d = 2$) or hexahedra ($d = 3$). The so-called macro elements $M \in \mathcal{M}_h$, $L \in \mathcal{L}_h$ denote the union of one or more neighboring cells $T \in \mathcal{T}_h$: There is $n_{\mathcal{T}_h} < \infty$ such that all M and L are formed as a conjunction of at most $n_{\mathcal{T}_h}$ cells $T \in \mathcal{T}_h$. Denote by h_T , h_M and h_L the diameters of cells $T \in \mathcal{T}_h$, $M \in \mathcal{M}_h$ and $L \in \mathcal{L}_h$, respectively. In addition, we require that there are constants $C_1, C_2 > 0$ such that

$$h_T \leq h_M \leq C_1 h_T, \quad h_T \leq h_L \leq C_2 h_T \quad \forall T \subset M, T \subset L, M \in \mathcal{M}_h, L \in \mathcal{L}_h.$$

Denote by $F_T: \hat{T} \rightarrow T$ the reference mapping. We require that F_T is bijective and its Jacobian is bounded for $\{\mathcal{T}_h\}$ according to

$$\exists c_1, c_2 > 0: \quad c_1 h_T^d \leq |\det DF_T(\hat{\mathbf{x}})| \leq c_2 h_T^d \quad \forall \hat{\mathbf{x}} \in \hat{T} \quad (2.20)$$

with constants $c_1, c_2 > 0$ independent of the cell diameter h_T .

Obviously, this is true for one-level methods. In case of two-level methods, it holds for barycentric or regular refinement (cf. [MT14]).

Definition 2.2.10 (Fine and coarse finite element spaces).

We denote by $Y_h^u, Y_h^\theta \subset H^1(\Omega) \cap L^\infty(\Omega)$ finite element spaces of functions that are continuous on \mathcal{T}_h . We consider the conforming finite element spaces

$$\mathbf{V}_h = [Y_h^u]^d \cap \mathbf{V}, \quad Q_h \subset Y_h^p \cap Q, \quad \Theta_h = Y_h^\theta \cap \Theta$$

for velocity, pressure and temperature, where Y_h^p is a finite element space of continuous or discontinuous functions on \mathcal{T}_h . Moreover, let $\mathbf{D}_{\mathcal{M}_h}^u \subset [L^\infty(\Omega)]^d$, $D_{\mathcal{L}_h}^\theta \subset L^\infty(\Omega)$ denote discontinuous finite element spaces on \mathcal{M}_h for \mathbf{u}_h and on \mathcal{L}_h for θ_h , respectively. We set

$$\mathbf{D}_M^u = \{\mathbf{v}_h|_M: \mathbf{v}_h \in \mathbf{D}_{\mathcal{M}_h}^u\}, \quad D_L^\theta = \{\psi_h|_L: \psi_h \in D_{\mathcal{L}_h}^\theta\}.$$

In the following, we often write for combinations of finite element spaces

$$(\mathbf{V}_h / \mathbf{D}_{\mathcal{M}_h}^u) \wedge Q_h \wedge (\Theta_h / D_{\mathcal{L}_h}^\theta), \quad \text{or} \quad (\mathbf{V}_h / \mathbf{D}_M^u) \wedge Q_h \wedge (\Theta_h / D_L^\theta).$$

If no LPS is applied, we omit the respective coarse space in the above notation.

Definition 2.2.11 (Fluctuation operators).

For $M \in \mathcal{M}_h$ and $L \in \mathcal{L}_h$, let $\pi_M^u: [L^2(M)]^d \rightarrow \mathbf{D}_M^u$, $\pi_L^\theta: L^2(L) \rightarrow D_L^\theta$ be the orthogonal

L^2 -projections onto the respective macro spaces. The so-called fluctuation operators are defined by

$$\begin{aligned}\kappa_M^u &: [L^2(M)]^d \rightarrow [L^2(M)]^d, & \kappa_L^\theta &: L^2(L) \rightarrow L^2(L), \\ \kappa_M^u &:= Id - \pi_M^u, & \kappa_L^\theta &:= Id - \pi_L^\theta.\end{aligned}$$

\mathcal{E}_h is defined as the set of inner element faces $E \notin \partial\Omega$ of \mathcal{T}_h . We denote by h_E the diameter of the face $E \in \mathcal{E}_h$. For two cells T_E and T'_E shared by E , let \mathbf{n}_E be the unit normal vector pointing from T_E into T'_E . For piecewise smooth functions w_h , we denote by $[w_h]_E := (w_h|_{T_E})|_E - (w_h|_{T'_E})|_E$ the jump over the face E . Note that this is unique up to a sign.

Let $\mathbf{u}_h \in \mathbf{V}_h$. For all macro elements $M \in \mathcal{M}_h$ and $L \in \mathcal{L}_h$, we denote the element-wise averaged streamline directions by $\mathbf{u}_M \in \mathbb{R}^d$, $\mathbf{u}_L \in \mathbb{R}^d$. For instance, we can choose

$$\mathbf{u}_M := \frac{1}{|M|} \int_M \mathbf{u}_h(\mathbf{x}) \, d\mathbf{x}, \quad \mathbf{u}_L := \frac{1}{|L|} \int_L \mathbf{u}_h(\mathbf{x}) \, d\mathbf{x}.$$

The semi-discrete stabilized Oberbeck-Boussinesq model reads:

Find $(\mathbf{u}_h, p_h, \theta_h): (0, T) \rightarrow \mathbf{V}_h \times Q_h \times \Theta_h$ such that for all $(\mathbf{v}_h, q_h, \psi_h) \in \mathbf{V}_h \times Q_h \times \Theta_h$:

$$\begin{aligned}(\partial_t \mathbf{u}_h, \mathbf{v}_h) + (\nu \nabla \mathbf{u}_h, \nabla \mathbf{v}_h) + c_u(\mathbf{u}_h; \mathbf{u}_h, \mathbf{v}_h) - (p_h, \nabla \cdot \mathbf{v}_h) + (\nabla \cdot \mathbf{u}_h, q_h) \\ + (\beta \mathbf{g} \theta_h, \mathbf{v}_h) + s_u(\mathbf{u}_h; \mathbf{u}_h, \mathbf{v}_h) + t_h(\mathbf{u}_h; \mathbf{u}_h, \mathbf{v}_h) + i_h(p_h, q_h) = (\mathbf{f}_u, \mathbf{v}_h),\end{aligned} \quad (2.21)$$

$$(\partial_t \theta_h, \psi_h) + (\alpha \nabla \theta_h, \nabla \psi_h) + c_\theta(\mathbf{u}_h; \theta_h, \psi_h) + s_\theta(\mathbf{u}_h; \theta_h, \psi_h) = (f_\theta, \psi_h) \quad (2.22)$$

with the streamline-upwind (SUPG)-type stabilizations s_u , s_θ , the grad-div stabilization t_h and the pressure jump stabilization i_h according to

$$\begin{aligned}s_u(\mathbf{w}_h; \mathbf{u}, \mathbf{v}) &:= \sum_{M \in \mathcal{M}_h} \tau_M^u(\mathbf{w}_M) (\kappa_M^u((\mathbf{w}_M \cdot \nabla) \mathbf{u}), \kappa_M^u((\mathbf{w}_M \cdot \nabla) \mathbf{v}))_M, \\ s_\theta(\mathbf{w}_h; \theta, \psi) &:= \sum_{L \in \mathcal{L}_h} \tau_L^\theta(\mathbf{w}_L) (\kappa_L^\theta((\mathbf{w}_L \cdot \nabla) \theta), \kappa_L^\theta((\mathbf{w}_L \cdot \nabla) \psi))_L, \\ t_h(\mathbf{w}_h; \mathbf{u}, \mathbf{v}) &:= \sum_{M \in \mathcal{M}_h} \gamma_M(\mathbf{w}_M) (\nabla \cdot \mathbf{u}, \nabla \cdot \mathbf{v})_M, \\ i_h(p, q) &:= \sum_{E \in \mathcal{E}_h} \phi_E([p]_E, [q]_E)_E\end{aligned}$$

with non-negative stabilization parameters τ_M^u , τ_L^θ , γ_M , ϕ_E . Note that the pressure stabilization takes care of pressure jumps in case a discontinuous ansatz space Q_h is chosen. The set of stabilization parameters $\tau_M^u(\mathbf{u}_h)$, $\tau_L^\theta(\mathbf{u}_h)$, $\gamma_M(\mathbf{u}_h)$, and ϕ_E has to be determined later on.

Taking the discrete inf-sup stability from Assumption 2.2.1 into account, we can look for weakly solenoidal solutions $\mathbf{u}_h \in \mathbf{V}_h^{div}$ and reformulate the stabilized Oberbeck-Boussinesq model (2.21)-(2.22) as follows:

Find $(\mathbf{u}_h, p_h, \theta_h): (0, T) \rightarrow \mathbf{V}_h^{div} \times Q_h \times \Theta_h$ such that for all $(\mathbf{v}_h, q_h, \psi_h) \in \mathbf{V}_h \times Q_h \times \Theta_h$:

$$\begin{aligned} & (\partial_t \mathbf{u}_h, \mathbf{v}_h) + (\nu \nabla \mathbf{u}_h, \nabla \mathbf{v}_h) + c_u(\mathbf{u}_h; \mathbf{u}_h, \mathbf{v}_h) - (p_h, \nabla \cdot \mathbf{v}_h) + (\beta \mathbf{g} \theta_h, \mathbf{v}_h) \\ & \quad + s_u(\mathbf{u}_h; \mathbf{u}_h, \mathbf{v}_h) + t_h(\mathbf{u}_h; \mathbf{u}_h, \mathbf{v}_h) + i_h(p_h, q_h) = (\mathbf{f}_u, \mathbf{v}_h), \\ & (\partial_t \theta_h, \psi_h) + (\alpha \nabla \theta_h, \nabla \psi_h) + c_\theta(\mathbf{u}_h; \theta_h, \psi_h) + s_\theta(\mathbf{u}_h; \theta_h, \psi_h) = (f_\theta, \psi_h). \end{aligned}$$

We utilize this formulation later for the analysis.

2.3. Time-Discretization

In the previous section, we introduced a spatial discretization of the Oberbeck-Boussinesq model using finite elements. The resulting initial value problem (2.15) has to be discretized in time in order to solve the equations numerically. For an introduction to different methods, we refer to [HNW93].

Consider a finite partition of the time interval $0 = t_0 < t_1 < \dots < t_N = T$, where we want to compute the solution at. The time step sizes are $\Delta t_n := t_n - t_{n-1}$. In case of an equidistant partition, we write $\Delta t := \Delta t_n$ for all $1 \leq n \leq N$.

The initial value problem can be formulated as a differential equation with an algebraic constraint. We seek for a solution $y_n = (u_h, p_h, \theta_h)(t_n)$ at each time step t_n , $1 \leq n \leq N$. The challenge is to find a time-discretization scheme such that the constraint is fulfilled simultaneously. There are one-step methods where only the previous value y_{n-1} is used for the calculation of y_n . In contrast, multi-step methods take the last k values y_{n-i} ($i = 1, \dots, k$) into account.

Different schemes based on a discretization of the coupled system (2.15) are presented in [L ow11]. It is discussed that the incompressibility constraint is not guaranteed in general if an explicit scheme is used. If the differential equation with constraint is treated with an implicit scheme, a coupled system of nonlinear equations has to be solved in each time step.

In order to reduce the computational cost, we consider a splitting algorithm which we introduce below. This constitutes a major difference to the algorithm used in [L ow11] - from an implementation point of view as well as for the analytical consideration of the fully discrete algorithm.

2.3.1. Pressure-Correction Projection Method

For the discretization in time, we use a splitting method called (rotational or standard incremental) pressure-correction projection method, which is based on the backward differentiation formula of second order (BDF2).

Projection methods were introduced by Chorin [Cho69] and Temam [Tem69] in order to remove the coupling of \mathbf{u} and p through the incompressibility constraint. The basic idea is to split the problem into several steps, such that the pressure and velocity calculations are decoupled.

Different pressure segregation methods are considered in [Bad06] and an overview is given in [GMS06]. Guermond discusses the fractional step incremental projection method in [Gue99] for the unstabilized Navier-Stokes equations with BDF2 time-discretization. Shen presents analysis for a different second order time-discretization scheme in [She96]. The rotational pressure-correction projection method is proposed by [TMVDV96] and incorporates a divergence correction in order to prevent some numerical boundary layers. Applied to the linear Stokes problem, this modified method is considered in [GS04].

An equidistant discretization in time with constant time step size $\Delta t > 0$ is assumed henceforth. Let $N := T/\Delta t \in \mathbb{N}$ and $t_n := n\Delta t$, $n \leq N$. Recall the continuous ansatz spaces $\mathbf{V} \times Q \times \Theta = [H_0^1(\Omega)]^d \times L_*^2(\Omega) \times H_0^1(\Omega)$ and the discrete finite dimensional finite element spaces from Section 2.2 satisfying

$$\begin{aligned} \mathbf{V}_h &\subset \mathbf{V} && \text{for the velocity,} \\ Q_h &\subset [Q \cap W^{1,2}(\Omega)] \subset L_*^2(\Omega) && \text{for the pressure,} \\ \Theta_h &\subset \Theta && \text{for the temperature.} \end{aligned}$$

Besides, we consider (due to the discrete inf-sup condition, Assumption 2.2.1)

$$\mathbf{V}_h^{div} := \{\mathbf{v}_h \in \mathbf{V}_h \mid (q_h, \nabla \cdot \mathbf{v}_h) = 0 \forall q_h \in Q_h\} \neq \{\mathbf{0}\}$$

and introduce the finite dimensional space \mathbf{Y}_h according to

$$\mathbf{Y}_h := \mathbf{V}_h^{div} \oplus \nabla Q_h. \quad (2.23)$$

Let P_B be the L^2 -orthogonal projector into a space $\mathbf{B} \subset [L^2(\Omega)]^d$, such that $(\mathbf{u} - P_B \mathbf{u}, \mathbf{v}) = 0$ holds for all $\mathbf{u} \in [L^2(\Omega)]^d$ and $\mathbf{v} \in \mathbf{B}$. We define the operator D_t to abbreviate the discrete time derivative by

$$D_t \mathbf{u}^n := \frac{3\mathbf{u}^n - 4\mathbf{u}^{n-1} + \mathbf{u}^{n-2}}{2\Delta t}. \quad (2.24)$$

In each time step t_n , we solve the momentum equation for a velocity $\tilde{\mathbf{u}}_{ht}^n \in \mathbf{V}_h$, that is not necessarily in \mathbf{V}_h^{div} . In order to fulfill the incompressibility condition, $\tilde{\mathbf{u}}_{ht}^n$ is projected onto the space of weakly solenoidal functions in a second step. The resulting velocity is denoted \mathbf{u}_{ht}^n .

The fully discretized and stabilized scheme reads in weak formulation:

Find $\tilde{\mathbf{u}}_{ht}^n \in \mathbf{V}_h$ such that for all $\mathbf{v}_h \in \mathbf{V}_h$:

$$\begin{aligned} \left(\frac{3\tilde{\mathbf{u}}_{ht}^n - 4\mathbf{u}_{ht}^{n-1} + \mathbf{u}_{ht}^{n-2}}{2\Delta t}, \mathbf{v}_h \right) + \nu(\nabla \tilde{\mathbf{u}}_{ht}^n, \nabla \mathbf{v}_h) + c_u(\tilde{\mathbf{u}}_{ht}^n; \tilde{\mathbf{u}}_{ht}^n, \mathbf{v}_h) + t_h(\tilde{\mathbf{u}}_{ht}^n; \tilde{\mathbf{u}}_{ht}^n, \mathbf{v}_h) \\ + s_u(\tilde{\mathbf{u}}_{ht}^n; \tilde{\mathbf{u}}_{ht}^n, \mathbf{v}_h) - (p_{ht}^{n-1}, \nabla \cdot \mathbf{v}_h) + \beta(\mathbf{g}(t_n)\theta_{ht}^{n*}, \mathbf{v}_h) = (\mathbf{f}_u(t_n), \mathbf{v}_h), \\ \tilde{\mathbf{u}}_{ht}^n|_{\partial\Omega} = 0, \end{aligned} \quad (2.25)$$

where $\theta_{ht}^{n*} := 2\theta_{ht}^{n-1} - \theta_{ht}^{n-2}$ is an extrapolation of second order of the temperature θ_{ht}^n .

Find $\mathbf{u}_{ht}^n \in \mathbf{V}_h^{div}$ and $p_{ht}^n \in Q_h$ such that for all $\mathbf{y}_h \in \mathbf{Y}_h$ and $q_h \in Q_h$:

$$\begin{aligned} \left(\frac{3\mathbf{u}_{ht}^n - 3\tilde{\mathbf{u}}_{ht}^n}{2\Delta t} + \nabla(p_{ht}^n - p_{ht}^{n-1} + \chi^{\text{rot}}\pi_{Q_h}(\nu\nabla \cdot \tilde{\mathbf{u}}_{ht}^n)), \mathbf{y}_h \right) + i_h(p_{ht}^n, q_h) = 0, \\ (\nabla \cdot \mathbf{u}_{ht}^n, q_h) = 0, \\ \mathbf{u}_{ht}^n|_{\partial\Omega} = 0. \end{aligned} \quad (2.26)$$

Here, $\chi^{\text{rot}} \in \{0, 1\}$ and π_{Q_h} denotes the L^2 -projection into the pressure space Q_h . The case $\chi^{\text{rot}} = 0$ describes the incremental scheme, that is analyzed in Chapter 4, and $\chi^{\text{rot}} = 1$ the scheme with rotational correction. The latter is used in our algorithm.

For the temperature equation, we search for $\theta_{ht}^n \in \Theta_h$ such that for all $\psi_h \in \Theta_h$

$$\begin{aligned} (D_t\theta_{ht}^n, \psi_h) + \alpha(\nabla\theta_{ht}^n, \nabla\psi_h) + c_\theta(\tilde{\mathbf{u}}_{ht}^n; \theta_{ht}^n, \psi_h) + s_\theta(\tilde{\mathbf{u}}_{ht}^n; \theta_{ht}^n, \psi_h) = (f_\theta(t_n), \psi_h), \\ \theta_{ht}^n|_{\partial\Omega} = 0. \end{aligned} \quad (2.27)$$

We call (2.25) the advection-diffusion step, (2.26) the projection step and (2.27) the temperature step. Indeed, (2.26) causes \mathbf{u}_{ht}^n to be the L^2 -orthogonal projection $P_{div}\tilde{\mathbf{u}}_{ht}^n$ of $\tilde{\mathbf{u}}_{ht}^n$ into \mathbf{V}_h^{div} , since it holds for all $\mathbf{w}_h \in \mathbf{V}_h^{div}$ (due to the projection step with $q_h = 0$):

$$(\tilde{\mathbf{u}}_{ht}^n - \mathbf{u}_{ht}^n, \mathbf{w}_h) = (\nabla(p_{ht}^n - p_{ht}^{n-1} + \chi^{\text{rot}}\pi_p(\nu\nabla \cdot \tilde{\mathbf{u}}_{ht}^n)), \mathbf{w}_h) = 0 \quad \Rightarrow \quad \mathbf{u}_{ht}^n = P_{div}\tilde{\mathbf{u}}_{ht}^n.$$

Remark 2.3.1. For the first time step, we use a BDF1 instead of the BDF2 scheme. In particular, the advection-diffusion, projection and temperature steps in the fully discretized setting read

Find $\tilde{\mathbf{u}}_{ht}^1 \in \mathbf{V}_h$ such that for all $\mathbf{v}_h \in \mathbf{V}_h$:

$$\begin{aligned} & \left(\frac{\tilde{\mathbf{u}}_{ht}^1 - \mathbf{u}_{ht}^0}{\Delta t}, \mathbf{v}_h \right) + \nu(\nabla \tilde{\mathbf{u}}_{ht}^1, \nabla \mathbf{v}_h) + c_u(\tilde{\mathbf{u}}_{ht}^1; \tilde{\mathbf{u}}_{ht}^1, \mathbf{v}_h) + t_h(\tilde{\mathbf{u}}_{ht}^1; \tilde{\mathbf{u}}_{ht}^1, \mathbf{v}_h) \\ & + s_u(\tilde{\mathbf{u}}_{ht}^1; \tilde{\mathbf{u}}_{ht}^1, \mathbf{v}_h) - (p_{ht}^0, \nabla \cdot \mathbf{v}_h) + \beta(\mathbf{g}(t_1)\theta_{ht}^0, \mathbf{v}_h) = (\mathbf{f}_u(t_1), \mathbf{v}_h). \end{aligned}$$

Find $\mathbf{u}_{ht}^1 \in \mathbf{V}_h^{div}$ and $p_{ht}^1 \in Q_h$ such that for all $\mathbf{y}_h \in \mathbf{Y}_h$ and $q_h \in Q_h$:

$$\left(\frac{\mathbf{u}_{ht}^1 - \tilde{\mathbf{u}}_{ht}^1}{\Delta t} + \nabla(p_{ht}^1 - p_{ht}^0 + \chi^{\text{rot}}\pi_p \nabla \cdot \tilde{\mathbf{u}}_{ht}^1), \mathbf{y}_h \right) + i_h(p_{ht}^1, q_h) = 0.$$

Find $\theta_{ht}^1 \in \Theta_h$ such that for all $\psi_h \in \Theta_h$:

$$\left(\frac{\theta_{ht}^1 - \theta_{ht}^0}{\Delta t}, \psi_h \right) + \alpha(\nabla \theta_{ht}^1, \nabla \psi_h) + c_\theta(\tilde{\mathbf{u}}_{ht}^1; \theta_{ht}^1, \psi_h) + s_\theta(\tilde{\mathbf{u}}_{ht}^1; \theta_{ht}^1, \psi_h) = (f_\theta(t_1), \psi_h).$$

The initial values are projections of the continuous initial data.

2.3.2. Segregation Algorithm

In our algorithm, we just want to solve for $\tilde{\mathbf{u}}_{ht}^n$. If we assume that test functions from \mathbf{V}_h are allowed in the projection step (2.26), we can eliminate the weakly solenoidal field \mathbf{u}_{ht}^n , replace (2.25) by the equation

$$\begin{aligned} & (D_t \tilde{\mathbf{u}}_{ht}^n, \mathbf{v}_h) + \nu(\nabla \tilde{\mathbf{u}}_{ht}^n, \nabla \mathbf{v}_h) + c(\tilde{\mathbf{u}}_{ht}^n; \tilde{\mathbf{u}}_{ht}^n, \mathbf{v}_h) + t_h(\tilde{\mathbf{u}}_{ht}^n; \tilde{\mathbf{u}}_{ht}^n, \mathbf{v}_h) + s_h(\tilde{\mathbf{u}}_{ht}^n; \tilde{\mathbf{u}}_{ht}^n, \mathbf{v}_h) \\ & + \beta(\mathbf{g}(t_n)\theta_{ht}^{n*}, \mathbf{v}_h) = (\mathbf{f}_u(t_n), \mathbf{v}_h) + \left(p_{ht}^{n-1} + \frac{4}{3}(p_{ht}^{n-1} - p_{ht}^{n-2} + \chi^{\text{rot}}\pi_{Q_h}(\nu \nabla \cdot \tilde{\mathbf{u}}_{ht}^{n-1})) \right. \\ & \quad \left. - \frac{1}{3}(p_{ht}^{n-2} - p_{ht}^{n-3} + \chi^{\text{rot}}\pi_{Q_h}(\nu \nabla \cdot \tilde{\mathbf{u}}_{ht}^{n-2})), \nabla \cdot \mathbf{v}_h \right) \quad (2.28) \end{aligned}$$

and solve a Poisson problem for the pressure p_{ht}^n instead of equation (2.26):

$$\begin{aligned} & (\nabla(p_{ht}^n - p_{ht}^{n-1} + \chi^{\text{rot}}\pi_{Q_h}(\nu \nabla \cdot \tilde{\mathbf{u}}_{ht}^n)), \nabla q_h) + i_h(p_{ht}^n, q_h) = \left(\frac{3\nabla \cdot \tilde{\mathbf{u}}_{ht}^n}{2\Delta t}, q_h \right), \\ & (\mathbf{n} \cdot \nabla p_{ht}^n)|_{\partial\Omega} = 0. \quad (2.29) \end{aligned}$$

Then \mathbf{u}_{ht}^n can be recovered according to

$$\mathbf{u}_{ht}^n = \tilde{\mathbf{u}}_{ht}^n - \nabla(p_{ht}^n - p_{ht}^{n-1} + \chi^{\text{rot}}\pi_{Q_h}(\nu \nabla \cdot \tilde{\mathbf{u}}_{ht}^n)).$$

We use this approach in our implementation. The issue of equivalence of the problems (2.25)-(2.26) and (2.28)-(2.29) is discussed by Guermond in [Gue96] for a first order un-stabilized projection scheme.

2.4. Stabilized FEM for the Auxiliary Problems and their Properties

The Oberbeck-Boussinesq model consists of a momentum equation for the velocity and a Fourier part for the temperature. The convection-diffusion-reaction equation serves as an auxiliary model for the latter. The Oseen model is a linearization of the Navier-Stokes equations and is therefore suited for a preparatory study. In fact, many techniques of numerical analysis translate from the Navier-Stokes (and the Oseen) model to the Oberbeck-Boussinesq model. In this section, we review some stabilization techniques for finite element methods applied to these auxiliary problems.

2.4.1. Convection-Diffusion Equation

In the following, we examine the steady convection-diffusion-reaction problem as an auxiliary problem for the Fourier equation in the Oberbeck-Boussinesq model

$$-\varepsilon\Delta u + \mathbf{b} \cdot \nabla u + cu = f \quad \text{in } \Omega, \quad u = u_b \quad \text{in } \partial\Omega. \quad (2.30)$$

Here, $\varepsilon > 0$ is a constant and $\mathbf{b} \in [W^{1,\infty}(\Omega)]^d$, $c \in L^\infty(\Omega)$, $f \in L^2(\Omega)$, $u_b \in H^{1/2}(\partial\Omega)$. Consider the space $V := H^1(\Omega)$. Define the bilinear form a and the linear form f as

$$a(v, w) := \varepsilon(\nabla v, \nabla w) + (\mathbf{b} \cdot \nabla v + cu, w), \quad f(v) := (f, v) \quad (2.31)$$

for $v, w \in V$. Then the variational formulation reads:

$$\begin{aligned} \text{Find } u \in V \text{ such that } \quad a(u, v) &= (f, v) \quad \forall v \in V \\ u|_{\partial\Omega} &= u_b. \end{aligned} \quad (2.32)$$

Due to the Lax-Milgram Lemma [A.4.1](#), there exists a unique weak solution $u \in V$ of [\(2.32\)](#) if the linear form f is continuous and the bilinear form a is V -elliptic and continuous. In order to obtain the ellipticity condition, it is usually assumed that there is $\sigma_0 > 0$ such that

$$c - \frac{1}{2}\nabla \cdot \mathbf{b} \geq \sigma_0 \quad \text{a.e. in } \Omega. \quad (2.33)$$

This limits the applicability of the uniqueness result since in many problems the convective velocity \mathbf{b} is solenoidal and there are no reaction type terms, resulting in $\sigma_0 = 0$. This is also the case for the Oberbeck-Boussinesq model. Optimal convergence results rely on [\(2.33\)](#) with $\sigma_0 > 0$, although numerical tests show that a violation of this condition does not necessarily lead to a deterioration of the errors.

The solution of convection-dominated convection-diffusion-reaction problems with finite element methods is subject to ongoing research. Since the unstabilized Galerkin formulation is not stable if implemented, stabilization is needed in order to increase accuracy and robustness of the method. It is a standard procedure in the finite element context to add terms to (2.32) providing artificial diffusion in order to improve stability. We refer to [RST08] for an overview over different methods applied to the convection-diffusion-reaction problem.

Galerkin least-squares methods (for example SUPG) can be applied to the problem. [BR94] and [FNS98] point out that the enrichment of the finite element space is equivalent to stabilization of streamline diffusion type in certain settings. A different approach is considered in [BH04]: A continuous interior penalty (CIP) technique, which was originally proposed by [DD76], penalizes gradient jumps across element boundaries. Also, a nonlinear term adding diffusion on the element edges in the tangential direction is introduced in order to guarantee monotonicity. It is shown that the method is stable in the hyperbolic limit of vanishing diffusion and optimal a priori error estimates are presented. The local projection stabilization we considered in Section 2.2.3 has also been applied to convection-diffusion equations, for instance by [KL09] or [GT10].

The above techniques manage to reduce most of the numerical instabilities and oscillations. However, they do not fully eliminate over- and undershoots of approximate solutions along discontinuities, shocks or sharp layers.

As a remedy, several so-called Spurious Oscillations at Layers Diminishing (SOLD) methods were proposed. SOLD methods add a shock-capturing term to the stabilized formulation, see [LR06b], for instance. Often this term depends on the discrete solution in a nonlinear way and is designed to eliminate oscillations at shocks without diminishing the accuracy in smooth regions. For an overview, we refer to the studies in [JK07, JK08]. In particular, there are SOLD methods that add diffusion in crosswind direction and manage to reduce the oscillations considerably. In [KLR02], a shock-capturing term of the form

$$\sum_{T \in \mathcal{T}_h} \tau_T(w) \left(\frac{\mathbf{b}^\perp \cdot \nabla u}{|\mathbf{b}|}, \frac{\mathbf{b}^\perp \cdot \nabla v}{|\mathbf{b}|} \right)_T + \sum_{T \in \mathcal{T}_h} \tau_T^{SL}(w) \left(\frac{\mathbf{b} \cdot \nabla u}{|\mathbf{b}|}, \frac{\mathbf{b} \cdot \nabla v}{|\mathbf{b}|} \right)_T$$

is considered, that adds artificial diffusion in crosswind and streamline directions \mathbf{b}^\perp and \mathbf{b} , respectively. The parameters τ_T, τ_T^{SL} are chosen in a consistent way. The authors show existence of discrete solutions as well as error estimates. The idea of SOLD methods is seized in [BJK13] and is combined with the LPS ansatz for convection-diffusion-reaction equations. Due to our notation from Section 2.2.3, the stabilized Galerkin formulation reads:

$$a(u_h, v_h) + s_h(u_h, v_h) + d_h(u_h; u_h, v_h) = (f, v_h),$$

where

$$\begin{aligned} s_h(u, v) &= \sum_{M \in \mathcal{M}_h} \tau_M (\kappa_M(\mathbf{b}_M \cdot \nabla u), \kappa_M(\mathbf{b}_M \cdot \nabla v))_M, \\ d_h(w; u, v) &= \sum_{M \in \mathcal{M}_h} \tau_M^{sold}(w) (\kappa_M(P_M \nabla u), \kappa_M(P_M \nabla v))_M \end{aligned} \quad (2.34)$$

and $P_M: \mathbb{R}^d \rightarrow \mathbb{R}^d$ is the projection onto the crosswind direction of \mathbf{b}_M :

$$P_M = \begin{cases} \mathbb{I} - \frac{\mathbf{b}_M \otimes \mathbf{b}_M}{|\mathbf{b}_M|^2} & \text{if } \mathbf{b}_M \neq 0, \\ 0 & \text{if } \mathbf{b}_M = 0. \end{cases} \quad (2.35)$$

Depending on the choice of stabilization parameters τ_M and τ_M^{sold} , this method allows to prove existence of a unique solution even if the condition (2.33) with $\sigma_0 > 0$ is not satisfied. A study in [ACF⁺11] investigates the performance of different techniques for convection-dominated convection–diffusion equations. Among others the SUPG method, a SOLD finite element method, a CIP stabilization, a discontinuous Galerkin finite element method, and a total variation diminishing finite element method (FEM-TVD) are investigated. It becomes obvious that a method that preserves sharp layers while avoiding spurious oscillations is still an open problem.

2.4.2. Oseen Problem

Consider the linear steady Oseen problem in a bounded, polyhedral domain $\Omega \subset \mathbb{R}^d$, $d \in \{2, 3\}$ with solenoidal \mathbf{b} . This serves as a preliminary study of the Navier-Stokes equations with $\mathbf{b} = \mathbf{u}$. If the Navier-Stokes equations are semi-discretized in time first by an implicit scheme and the nonlinearity is handled using fixed point iterations, we obtain a sequence of auxiliary Oseen-type equations in each iteration:

$$\begin{aligned} -\nu \Delta \mathbf{u} + (\mathbf{b} \cdot \nabla) \mathbf{u} + \sigma \mathbf{u} + \nabla p &= \mathbf{f} && \text{in } (0, T) \times \Omega, \\ \nabla \cdot \mathbf{u} &= 0 && \text{in } (0, T) \times \Omega. \end{aligned} \quad (2.36)$$

When the variational formulation of (2.36) is solved, numerical instabilities have to be taken care of. These occur due to dominating convection $0 < \nu \ll \|\mathbf{b}\|_\infty$ or due to the violation of the discrete inf-sup condition (2.16). In addition, poor mass conservation of the discrete velocity-pressure ansatz spaces can cause instabilities at high Reynolds numbers; [Lin09] examines a physically relevant example. As mentioned in Section 2.2.3, several stabilization variants have been studied. We emphasize that additional grad-div stabilization enhances the discrete mass conservation. [GLOS05] considers the combination of SUPG and grad-div stabilization (for the incompressible Navier–Stokes problem).

In [OLHL09], grad–div stabilization is examined as a subgrid pressure model in the framework of variational multiscale methods for the Stokes and Oseen problem. The cases of inf–sup stable and equal-order elements of velocity and pressure are taken into account. Furthermore, the techniques we listed for the convection-diffusion-reaction problem can be applied to the Oseen model. We also mention non-conforming methods like the discontinuous Galerkin method (see e.g. [CKS04]).

Different stabilized FE methods on isotropic meshes for the Oseen problem (2.36) are examined in [BBJL07]: The residual-based SUPG/PSPG method and symmetric stabilization techniques (in particular the LPS method) are compared. The issue of parameter design is addressed. All presented methods handle the dominating advection in a different way. They share the need of pressure stabilization if equal-order finite element spaces for velocity and pressure are applied. This is due to the violation of the discrete inf-sup condition.

Local projection stabilization in combination with equal-order and inf-sup stable elements are considered in [LRL08]. Stabilization terms for fluctuations of the streamline derivative $\mathbf{b} \cdot \nabla \mathbf{u}_h$, divergence $\nabla \cdot \mathbf{u}_h$ and pressure gradient ∇p_h as

$$\sum_{M \in \mathcal{M}_h} \left(\tau_M^u (\kappa_M^u (\mathbf{b} \cdot \nabla \mathbf{u}_h), \kappa_M^u (\mathbf{b} \cdot \nabla \mathbf{v}_h))_M + \gamma_M (\kappa_M^p (\nabla \cdot \mathbf{u}_h), \kappa_M^p (\nabla \cdot \mathbf{v}_h))_M \right. \\ \left. + \tau_M^u (\kappa_M^u (\nabla p_h), \kappa_M^u (\nabla q_h))_M \right) \quad (2.37)$$

are introduced. The a priori analysis on isotropic meshes gives comparable results to the classical RBS method, but suggests a simpler parameter design. The convergence properties of different LPS variants, including the one-level and the two-level approaches, are studied by [KT13].

In [MST07], the LPS method (2.37) is analyzed for the stationary Oseen problem (2.36), where an additional compatibility condition between the approximation and projection velocity ansatz spaces $\mathbf{Y}_{h,k_u}(M) = [Y_{h,k_u}]^d|_M$ and \mathbf{D}_M^u is assumed:

$$\exists \beta_u > 0: \quad \inf_{\mathbf{w}_h \in \mathbf{D}_M^u} \sup_{\mathbf{v}_h \in \mathbf{Y}_{h,k_u}(M)} \frac{(\mathbf{v}_h, \mathbf{w}_h)_M}{\|\mathbf{v}_h\|_{0,M} \|\mathbf{w}_h\|_{0,M}} \geq \beta_u. \quad (2.38)$$

It is shown that this requirement gives rise to an interpolation operator with additional orthogonality properties. Thus, stability and a priori error bounds of optimal order can be established. Furthermore, suitable simplicial and quadrilateral ansatz spaces are suggested that fulfill (2.38). In the paper [MT14], the authors provide an overview regarding stabilized finite element methods for the Oseen problem, in particular, in the case of local

projection stabilization methods for inf-sup stable finite element methods with $k_p = k_u - 1$. A unified representation according to

$$\sum_{M \in \mathcal{M}_h} \left(\tau_M^u(\kappa_M^u(\mathbf{b}_M \cdot \nabla \mathbf{u}_h), \kappa_M^u(\mathbf{b}_M \cdot \nabla \mathbf{v}_h))_M + \gamma_M(\kappa_M^p(\nabla \cdot \mathbf{u}_h), \kappa_M^p(\nabla \cdot \mathbf{v}_h))_M \right) \quad (2.39)$$

(without pressure stabilization) leads to an overview over suitable ansatz spaces including parameter design.

In our paper [DAL15], we consider the linear time-dependent Oseen problem

$$\begin{aligned} \partial_t \mathbf{u} - \nu \Delta \mathbf{u} + (\mathbf{b} \cdot \nabla) \mathbf{u} + \nabla p &= \mathbf{f} && \text{in } (0, T) \times \Omega, \\ \nabla \cdot \mathbf{u} &= 0 && \text{in } (0, T) \times \Omega \end{aligned} \quad (2.40)$$

together with LPS SU and grad-div stabilization. Inf-sup stable velocity-pressure FE pairs are chosen. We consider two settings of LPS spaces: The first ansatz makes use of the discrete inf-sup condition. From [GS03], the existence of a quasi-local interpolation operator $j_u: \mathbf{V}^{div} \rightarrow \mathbf{V}_h^{div}$ preserving the discrete divergence is guaranteed. We obtain a method of quasi-optimal order $k_u = k_p + 1$ provided that

$$Re_M := \frac{h_M \|\mathbf{b}\|_{L^\infty(M)}}{\nu} \leq \frac{1}{\sqrt{\nu}},$$

which gives a restriction on the local mesh width h_M . This method is applicable to almost all combinations of approximation and projection spaces $\mathbf{Y}_{h, k_u}(M)$ and \mathbf{D}_M^u . Secondly, we seize the idea to assume (2.38). This restricts not only the range of possible fine and coarse velocity ansatz spaces, but also for the pressure ansatz space. Indeed, both ansatzes prove to be beneficial for the fully coupled Oberbeck-Boussinesq model, see Section 3. We also tried the addition of crosswind stabilization (2.34), but numerical tests did not indicate an improvement (the results are not shown in [DAL15]). Therefore, we do not pursue this technique further in this thesis. We emphasize the positive effect of additional element-wise stabilization of the divergence constraint, which becomes apparent also in the numerical experiments. The grad-div stabilization improves the robustness in case of $0 < \nu \ll 1$.

Recent results from [dFGAJN15] for the time-dependent Oseen problem (2.40) reinforce the benefits and stabilizing effects of grad-div stabilization for inf-sup stable mixed finite elements. The authors show that the Galerkin approximations can be stabilized by adding only grad-div stabilization. Robust error estimates with respect to small viscosities are obtained if the solution is sufficiently smooth.

3. Semi-Discrete Analysis for the Oberbeck-Boussinesq Model

In this chapter, we analyze the semi-discrete Oberbeck-Boussinesq problem, i.e., discrete in space but continuous in time. Stability and convergence of the semi-discrete quantities are proven under certain conditions we introduce below.

From now on and throughout this thesis, we suppose that the discrete inf-sup condition (Assumptions 2.2.1) and Assumption 2.2.9 for the fine and coarse triangulations hold. Recall that the stabilized Oberbeck-Boussinesq model (2.21)-(2.22) can be reformulated using the discrete inf-sup stability from Assumption 2.2.1 for these ansatz spaces.

Find $(\mathbf{u}_h, p_h, \theta_h): (0, T) \rightarrow \mathbf{V}_h^{div} \times Q_h \times \Theta_h$ such that for all $(\mathbf{v}_h, q_h, \psi_h) \in \mathbf{V}_h \times Q_h \times \Theta_h$:

$$\begin{aligned} (\partial_t \mathbf{u}_h, \mathbf{v}_h) + (\nu \nabla \mathbf{u}_h, \nabla \mathbf{v}_h) + c_u(\mathbf{u}_h; \mathbf{u}_h, \mathbf{v}_h) - (p_h, \nabla \cdot \mathbf{v}_h) + (\beta \mathbf{g} \theta_h, \mathbf{v}_h) \\ + s_u(\mathbf{u}_h; \mathbf{u}_h, \mathbf{v}_h) + t_h(\mathbf{u}_h; \mathbf{u}_h, \mathbf{v}_h) + i_h(p_h, q_h) = (\mathbf{f}_u, \mathbf{v}_h), \end{aligned} \quad (3.1)$$

$$(\partial_t \theta_h, \psi_h) + (\alpha \nabla \theta_h, \nabla \psi_h) + c_\theta(\mathbf{u}_h; \theta_h, \psi_h) + s_\theta(\mathbf{u}_h; \theta_h, \psi_h) = (f_\theta, \psi_h) \quad (3.2)$$

with $\mathbf{f}_u \in L^2(0, T; [L^2(\Omega)]^d) \cap C(0, T; [L^2(\Omega)]^d)$, $f_\theta \in L^2(0, T; L^2(\Omega)) \cap C(0, T; L^2(\Omega))$, $\mathbf{g} \in L^\infty(0, T; [L^\infty(\Omega)]^d)$ and cell-wise constant $\mathbf{u}_M, \mathbf{u}_L \in \mathbb{R}^d$. Let the initial data be given as suitable interpolations of the continuous initial values in the respective finite element spaces as

$$\mathbf{u}_h(0) = j_u \mathbf{u}_0 =: \mathbf{u}_{h,0} \in \mathbf{V}_h \subset [L^2(\Omega)]^d, \quad \theta_h(0) = j_\theta \theta_0 =: \theta_{h,0} \in \Theta_h \subset L^2(\Omega),$$

where $(j_u, j_\theta): \mathbf{V} \times \Theta \rightarrow \mathbf{V}_h \times \Theta_h$ denote interpolation operators. We remark that for solenoidal \mathbf{u}_0 , we can find an interpolation operator j_u such that $\mathbf{u}_{h,0} \in \mathbf{V}_h^{div}$ (cf. [GS03]). This formulation allows us to estimate the velocity separately in a first step and obtain an upper bound for the pressure error afterwards via the discrete inf-sup condition.

3.1. Stability of the Semi-Discrete Quantities

We address the question regarding the existence of a semi-discrete solution of (3.1)-(3.2). This is obtained via a stability result for $\mathbf{u}_h \in \mathbf{V}_h^{div}$ and $\theta_h \in \Theta_h$; it yields control over

the kinetic energy and dissipation introduced by fluctuations. The definition of the mesh-dependent expressions below is motivated by symmetric testing in (3.1)-(3.2).

Definition 3.1.1.

For $(\mathbf{v}, q) \in \mathbf{V} \times Q$ and $\theta \in \Theta$, we define

$$\begin{aligned} |||(\mathbf{v}, q)|||_{LPS}^2 &:= \nu \|\nabla \mathbf{v}\|_0^2 + s_u(\mathbf{u}_h; \mathbf{v}, \mathbf{v}) + t_h(\mathbf{u}_h; \mathbf{v}, \mathbf{v}) + i_h(q, q), \\ [[\theta]]_{LPS}^2 &:= \alpha \|\nabla \theta\|_0^2 + s_\theta(\mathbf{u}_h; \theta, \theta). \end{aligned}$$

We also write $|||\mathbf{v}_h|||_{LPS} := |||(\mathbf{v}_h, 0)|||_{LPS}$ and introduce

$$\begin{aligned} \|(\mathbf{v}, q)\|_{L^2(0,T;LPS)}^2 &:= \int_0^T |||(\mathbf{v}, q)(t)|||_{LPS}^2 dt, & \|\mathbf{v}\|_{L^2(0,T;LPS)}^2 &:= \int_0^T |||\mathbf{v}(t)|||_{LPS}^2 dt, \\ \|\theta\|_{L^2(0,T;LPS)}^2 &:= \int_0^T [[\theta(t)]]_{LPS}^2 dt. \end{aligned}$$

The following result states the desired stability.

Theorem 3.1.2 (Stability of velocity and temperature).

Assume $(\mathbf{u}_h, p_h, \theta_h) \in \mathbf{V}_h^{div} \times Q_h \times \Theta_h$ is a solution of (3.1)-(3.2) with initial data $\mathbf{u}_{h,0} \in [L^2(\Omega)]^d$, $\theta_{h,0} \in L^2(\Omega)$. For $0 \leq t \leq T$, we obtain

$$\begin{aligned} \|\theta_h\|_{L^\infty(0,t;L^2(\Omega))} &\leq \|\theta_{h,0}\|_0 + \|f_\theta\|_{L^1(0,t;L^2(\Omega))} =: C_\theta(T, \theta_{h,0}, f_\theta), \\ \|\mathbf{u}_h\|_{L^\infty(0,t;L^2(\Omega))} &\leq \|\mathbf{u}_{h,0}\|_0 + \|\mathbf{f}_u\|_{L^1(0,t;L^2(\Omega))} \\ &\quad + \beta \|\mathbf{g}\|_{L^1(0,t;L^\infty(\Omega))} \left(\|\theta_{h,0}\|_0 + \|f_\theta\|_{L^1(0,t;L^2(\Omega))} \right) \\ &=: C_u(T, \mathbf{u}_{h,0}, \theta_{h,0}, \mathbf{f}_u, f_\theta), \\ \|\theta_h\|_{L^2(0,t;LPS)} &\leq C_\theta(T, \theta_{h,0}, f_\theta), \\ \|\mathbf{u}_h\|_{L^2(0,t;LPS)} &\leq \|(\mathbf{u}_h, p_h)\|_{L^2(0,t;LPS)} \leq C_u(T, \mathbf{u}_{h,0}, \theta_{h,0}, \mathbf{f}_u, f_\theta). \end{aligned}$$

Proof. Let us start with the first claim for the temperature. Testing with $\psi_h = \theta_h \in \Theta_h$ in (3.2) gives

$$\frac{1}{2} \frac{d}{dt} \|\theta_h\|_0^2 + [[\theta_h]]_{LPS}^2 = (\partial_t \theta_h, \theta_h) + (\alpha \nabla \theta_h, \nabla \theta_h) + s_\theta(\mathbf{u}_h; \theta_h, \theta_h) = (f_\theta, \theta_h). \quad (3.3)$$

Due to $s_\theta(\mathbf{u}_h; \theta_h, \theta_h) \geq 0$, it follows

$$\|\theta_h\|_0 \frac{d}{dt} \|\theta_h\|_0 = \frac{1}{2} \frac{d}{dt} \|\theta_h\|_0^2 \leq \|f_\theta\|_0 \|\theta_h\|_0 \quad \Rightarrow \quad \frac{d}{dt} \|\theta_h\|_0 \leq \|f_\theta\|_0.$$

Integration in time leads to

$$\|\theta_h(t)\|_0 \leq \|\theta_{h,0}\|_0 + \|f_\theta\|_{L^1(0,T;L^2(\Omega))} = C_\theta(T, \theta_{h,0}, f_\theta). \quad (3.4)$$

For the velocity, we test with $(\mathbf{u}_h, p_h) \in \mathbf{V}_h^{div} \times Q_h$ in (3.1)

$$\begin{aligned} \frac{1}{2} \frac{d}{dt} \|\mathbf{u}_h\|_0^2 + \|(\mathbf{u}_h, p_h)\|_{LPS}^2 &= (\partial_t \mathbf{u}_h, \mathbf{u}_h) + (\nu \nabla \mathbf{u}_h, \nabla \mathbf{u}_h) + s_u(\mathbf{u}_h; \mathbf{u}_h, \mathbf{u}_h) \\ &+ t_h(\mathbf{u}_h; \mathbf{u}_h, \mathbf{u}_h) + i_h(p_h, p_h) = (\mathbf{f}_u - \beta \mathbf{g} \theta_h, \mathbf{u}_h). \end{aligned} \quad (3.5)$$

We obtain

$$\|\mathbf{u}_h\|_0 \frac{d}{dt} \|\mathbf{u}_h\|_0 = \frac{1}{2} \frac{d}{dt} \|\mathbf{u}_h\|_0^2 \leq (\|\mathbf{f}_u\|_0 + \beta \|\mathbf{g}\|_\infty \|\theta_h\|_0) \|\mathbf{u}_h\|_0.$$

Hence, $\frac{d}{dt} \|\mathbf{u}_h\|_0 \leq \|\mathbf{f}_u\|_0 + \beta \|\mathbf{g}\|_\infty \|\theta_h\|_0$. Integration in time and using stability of the temperature (3.4) give:

$$\begin{aligned} \|\mathbf{u}_h(t)\|_0 &\leq \|\mathbf{u}_{h,0}\|_0 + \|\mathbf{f}_u\|_{L^1(0,t;L^2(\Omega))} + \beta \|\mathbf{g}\|_{L^1(0,t;L^\infty(\Omega))} \|\theta_h\|_{L^\infty(0,t;L^2(\Omega))} \\ &\leq \|\mathbf{u}_{h,0}\|_0 + \|\mathbf{f}_u\|_{L^1(0,T;L^2(\Omega))} + \beta \|\mathbf{g}\|_{L^1(0,T;L^\infty(\Omega))} \left(\|\theta_{h,0}\|_0 + \|f_\theta\|_{L^1(0,T;L^2(\Omega))} \right) \\ &= C_u(T, \mathbf{u}_{h,0}, \theta_{h,0}, \mathbf{f}_u, f_\theta) \end{aligned} \quad (3.6)$$

for all $t \in [0, T]$. In order to estimate the diffusive and stabilization terms, we go back to (3.3), integrate in time and apply (3.4):

$$\begin{aligned} \int_0^t \|[\theta_h(\tau)]\|_{LPS}^2 d\tau &\leq \int_0^t \|f_\theta(\tau)\|_0 \|\theta_h(\tau)\|_0 d\tau + \frac{1}{2} \|\theta_{h,0}\|_0^2 \\ &\leq \|\theta_h\|_{L^\infty(0,t;L^2(\Omega))} \|f_\theta\|_{L^1(0,t;L^2(\Omega))} + \frac{1}{2} \|\theta_{h,0}\|_0^2 \leq C_\theta(T, \theta_{h,0}, f_\theta)^2. \end{aligned}$$

The analogous procedure for \mathbf{u}_h and p_h , starting from (3.5) and using (3.6), yields:

$$\begin{aligned} \int_0^t \|(\mathbf{u}_h, p_h)(\tau)\|_{LPS}^2 d\tau &\leq \int_0^t \|\mathbf{f}_u(\tau) - \beta \mathbf{g} \theta_h(\tau)\|_0 \|\mathbf{u}_h(\tau)\|_0 d\tau + \frac{1}{2} \|\mathbf{u}_{h,0}\|_0^2 \\ &\leq \|\mathbf{u}_h\|_{L^\infty(0,t;L^2(\Omega))} \left(\|\mathbf{f}_u\|_{L^1(0,t;L^2(\Omega))} + \beta \|\mathbf{g}\|_{L^1(0,t;L^\infty(\Omega))} \|\theta_h\|_{L^\infty(0,t;L^2(\Omega))} \right) + \frac{1}{2} \|\mathbf{u}_{h,0}\|_0^2 \\ &\leq C_u(T, \mathbf{u}_{h,0}, \theta_{h,0}, \mathbf{f}_u, f_\theta)^2. \end{aligned}$$

□

Now, we can prove an existence result for the semi-discrete quantities.

Corollary 3.1.3 (Existence of solutions and stability of the pressure).

There exists a semi-discrete solution $(\mathbf{u}_h, p_h, \theta_h): [0, T] \rightarrow \mathbf{V}_h^{div} \times Q_h \times \Theta_h$ of problem

(3.1)-(3.2) with initial data $\mathbf{u}_{h,0} \in \mathbf{V}_h^{div}$, $\theta_{h,0} \in \Theta_h$. Additionally, we require $\mathbf{u}_h \in W^{1,1}(0, T; [L^2(\Omega)]^d)$. For $0 \leq t \leq T$, we obtain

$$\begin{aligned} \beta_h \|p_h\|_{L^1(0,t;L^2(\Omega))} &\leq \|\mathbf{f}_u\|_{L^1(0,t;L^2(\Omega))} + \|\partial_t \mathbf{u}_h\|_{L^1(0,t;L^2(\Omega))} \\ &+ C_u(T, \mathbf{u}_{h,0}, \theta_{h,0}, \mathbf{f}_u, f_\theta) \int_0^t \left(\sqrt{\nu} + \max_{M \in \mathcal{M}_h} \left\{ \sqrt{\tau_M^u} |\mathbf{u}_M| + \sqrt{\gamma_M} \right\} \right) d\tau \\ &+ \frac{C}{\nu} C_u(T, \mathbf{u}_{h,0}, \theta_{h,0}, \mathbf{f}_u, f_\theta)^2 + \beta \|\mathbf{g}\|_{L^1(0,t;L^\infty(\Omega))} C_\theta(T, \theta_{h,0}, f_\theta). \end{aligned}$$

Proof. Consider the semi-discrete initial value problem:

Find $(\mathbf{u}_h, \theta_h) : [0, T] \rightarrow \mathbf{V}_h^{div} \times \Theta_h$ such that

$$\begin{aligned} (\partial_t \mathbf{u}_h, \mathbf{v}_h) &= (\mathbf{f}_u, \mathbf{v}_h) - (\nu \nabla \mathbf{u}_h, \nabla \mathbf{v}_h) - c_u(\mathbf{u}_h; \mathbf{u}_h, \mathbf{v}_h) - (\beta \mathbf{g} \theta_h, \mathbf{v}_h) \\ &\quad - s_u(\mathbf{u}_h; \mathbf{u}_h, \mathbf{v}_h) - t_h(\mathbf{u}_h; \mathbf{u}_h, \mathbf{v}_h), \\ (\partial_t \theta_h, \psi_h) &= (f_\theta, \psi_h) - (\alpha \nabla \theta_h, \nabla \psi_h) - c_\theta(\mathbf{u}_h; \theta_h, \psi_h) - s_\theta(\mathbf{u}_h; \theta_h, \psi_h) \end{aligned} \quad (3.7)$$

for $(\mathbf{v}_h, \psi_h) \in \mathbf{V}_h^{div} \times \Theta_h$, with initial conditions

$$\mathbf{u}_h(0) = \mathbf{u}_{h,0} \in \mathbf{V}_h^{div}, \quad \theta_h(0) = \theta_{h,0} \in \Theta_h.$$

\mathbf{V}_h^{div} and Θ_h are finite dimensional Banach spaces and the right-hand side of (3.7) depends continuously on $(t, \mathbf{u}_h, \theta_h) \in [0, T] \times \mathbf{V}_h^{div} \times \Theta_h$. As a consequence of Theorem 3.1.2, each (potential) solution of (3.7) is bounded on $[0, T]$. This implies boundedness of the right-hand side in $[0, T] \times \mathbf{V}_h^{div} \times \Theta_h$. Then the generalized Peano theorem A.4.2 is applicable and yields the local existence of a solution of (3.7). This solution can be extended to $[0, T]$. Furthermore, the closed range theorem yields that due to the discrete inf-sup stability, a solution (\mathbf{u}_h, θ_h) of (3.7) gives rise to $p_h \in Q_h$ such that $(\mathbf{u}_h, p_h, \theta_h)$ solves the Oberbeck-Boussinesq problem (3.1)-(3.2).

Due to the discrete inf-sup condition from Assumption 2.2.1, it is a standard result (see e.g. [BS08]) that for all $p_h \in Q_h$, there exists a unique $\mathbf{v}_h \in \mathbf{V}_h$ with

$$\nabla \cdot \mathbf{v}_h = -p_h, \quad \|\nabla \mathbf{v}_h\|_0 \leq \frac{1}{\beta_h} \|p_h\|_0. \quad (3.8)$$

Testing with $(\mathbf{v}_h, 0) \in \mathbf{V}_h \times Q_h$ in (3.1), we obtain

$$\begin{aligned} \beta_h \|\nabla \mathbf{v}_h\|_0 \|p_h\|_0 &\leq \|p_h\|_0^2 = -(p_h, \nabla \cdot \mathbf{v}_h) = (\mathbf{f}_u, \mathbf{v}_h) - (\partial_t \mathbf{u}_h, \mathbf{v}_h) - (\nu \nabla \mathbf{u}_h, \nabla \mathbf{v}_h) \\ &\quad - c_u(\mathbf{u}_h; \mathbf{u}_h, \mathbf{v}_h) - (\beta \mathbf{g} \theta_h, \mathbf{v}_h) - s_u(\mathbf{u}_h; \mathbf{u}_h, \mathbf{v}_h) - t_h(\mathbf{u}_h; \mathbf{u}_h, \mathbf{v}_h) \\ &\leq \|\nabla \mathbf{v}_h\|_0 \left(\|\mathbf{f}_u\|_{-1} + \|\partial_t \mathbf{u}_h\|_{-1} + \nu \|\nabla \mathbf{u}_h\|_0 + C \|\nabla \mathbf{u}_h\|_0^2 + \beta \|\mathbf{g}\|_\infty \|\theta_h\|_{-1} \right) \end{aligned}$$

$$\begin{aligned}
& + \|\mathbf{u}_h\|_{LPS} \max_{M \in \mathcal{M}_h} \left\{ \sqrt{\tau_M^u} |\mathbf{u}_M| \right\} + \sum_{M \in \mathcal{M}_h} \gamma_M \|\nabla \cdot \mathbf{u}_h\|_{0,M} \\
& \leq \|\nabla \mathbf{v}_h\|_0 \left(\|\mathbf{f}_u\|_{-1} + \|\partial_t \mathbf{u}_h\|_{-1} + \sqrt{\nu} \|\mathbf{u}_h\|_{LPS} + \frac{C}{\nu} \|\mathbf{u}_h\|_{LPS}^2 + \beta \|\mathbf{g}\|_\infty \|\theta_h\|_{-1} \right. \\
& \left. + \|\mathbf{u}_h\|_{LPS} \max_{M \in \mathcal{M}_h} \left\{ \sqrt{\tau_M^u} |\mathbf{u}_M| \right\} + \max_{M \in \mathcal{M}_h} \sqrt{\gamma_M} \|\mathbf{u}_h\|_{LPS} \right),
\end{aligned}$$

where we used standard estimates for the convective term and that

$$\begin{aligned}
s_u(\mathbf{u}_h; \mathbf{u}_h, \mathbf{v}_h) & \leq s_u(\mathbf{u}_h; \mathbf{u}_h, \mathbf{u}_h)^{1/2} s_u(\mathbf{u}_h; \mathbf{v}_h, \mathbf{v}_h)^{1/2} \\
& \leq \|\mathbf{u}_h\|_{LPS} \max_{M \in \mathcal{M}_h} \left\{ \sqrt{\tau_M^u} |\mathbf{u}_M| \right\} \|\nabla \mathbf{v}_h\|_0.
\end{aligned}$$

By integration in time and using the Cauchy-Schwarz inequality, we have for all $0 \leq t \leq T$

$$\begin{aligned}
\beta_h \|p_h\|_{L^1(0,t;L^2(\Omega))} & \leq \|\mathbf{f}_u\|_{L^1(0,t;L^2(\Omega))} + \|\partial_t \mathbf{u}_h\|_{L^1(0,t;L^2(\Omega))} \\
& + \|\mathbf{u}_h\|_{L^2(0,t;LPS)} \int_0^t \sqrt{\nu} d\tau + \frac{C}{\nu} \|\mathbf{u}_h\|_{L^2(0,t;LPS)}^2 + \beta \|\mathbf{g}\|_{L^1(0,t;L^\infty(\Omega))} \|\theta_h\|_{L^\infty(0,t;L^2(\Omega))} \\
& + \|\mathbf{u}_h\|_{L^2(0,t;LPS)} \int_0^t \max_{M \in \mathcal{M}_h} \left\{ \sqrt{\tau_M^u} |\mathbf{u}_M| \right\} d\tau + \|\mathbf{u}_h\|_{L^2(0,t;LPS)} \int_0^t \max_{M \in \mathcal{M}_h} \sqrt{\gamma_M} d\tau.
\end{aligned}$$

Because of the stability of \mathbf{u}_h and θ_h from Theorem 3.1.2, it holds for all $0 \leq t \leq T$

$$\begin{aligned}
\beta_h \|p_h\|_{L^1(0,t;L^2(\Omega))} & \leq \|\mathbf{f}_u\|_{L^1(0,t;L^2(\Omega))} + \|\partial_t \mathbf{u}_h\|_{L^1(0,t;L^2(\Omega))} \\
& + C_u(t, \mathbf{u}_{h,0}, \theta_{h,0}, \mathbf{f}_u, f_\theta) \int_0^t \left(\sqrt{\nu} + \max_{M \in \mathcal{M}_h} \left\{ \sqrt{\tau_M^u} |\mathbf{u}_M| + \sqrt{\gamma_M} \right\} \right) d\tau \\
& + \frac{C}{\nu} C_u(t, \mathbf{u}_{h,0}, \theta_{h,0}, \mathbf{f}_u, f_\theta)^2 + \beta \|\mathbf{g}\|_{L^1(0,t;L^\infty(\Omega))} C_\theta(t, \theta_{h,0}, f_\theta).
\end{aligned}$$

Finally, this estimate ensures existence and uniqueness of the discrete pressure. \square

Remark 3.1.4. If we assume Lipschitz continuity of the right-hand side of problem (3.7), the Picard-Lindelöf Theorem yields uniqueness of the solution.

3.2. Velocity and Temperature Estimates

In this section, we derive quasi-optimal error estimates in the finite element setting introduced in Section 2.2.3. In particular, let the Assumptions 2.2.1 and 2.2.9 hold. We use similar techniques as in our publications [DAL15] and [ADL15] for the time-dependent Oseen and Navier-Stokes problems.

For the analysis, we introduce a decomposition of the error into a discretization and a consistency error.

Definition 3.2.1 (Error decomposition).

Let $(j_u, j_p, j_\theta): \mathbf{V} \times Q \times \Theta \rightarrow \mathbf{V}_h \times Q_h \times \Theta_h$ denote interpolation operators. We introduce

$$\begin{aligned} \xi_{u,h} &:= \mathbf{u} - \mathbf{u}_h, & \xi_{p,h} &:= p - p_h, & \xi_{\theta,h} &:= \theta - \theta_h, \\ \eta_{u,h} &:= \mathbf{u} - j_u \mathbf{u}, & \eta_{p,h} &:= p - j_p p, & \eta_{\theta,h} &:= \theta - j_\theta \theta, \\ \mathbf{e}_{u,h} &:= j_u \mathbf{u} - \mathbf{u}_h, & e_{p,h} &:= j_p p - p_h, & e_{\theta,h} &:= j_\theta \theta - \theta_h. \end{aligned} \quad (3.9)$$

Indeed, the semi-discrete errors are decomposed as $\xi_{u,h} = \eta_{u,h} + \mathbf{e}_{u,h}$, $\xi_{p,h} = \eta_{p,h} + e_{p,h}$ and $\xi_{\theta,h} = \eta_{\theta,h} + e_{\theta,h}$. Furthermore, we need the following assumptions.

Assumption 3.2.2 (Interpolation operators).

Assume that for integers $k_u \geq 1$, $k_p \geq 1$, $k_\theta \geq 1$, there are bounded linear interpolation operators $j_u: \mathbf{V} \rightarrow \mathbf{V}_h$ and $j_p: Q \rightarrow Q_h$ such that for all $M \in \mathcal{M}_h$, for all $\mathbf{w} \in \mathbf{V} \cap [W^{l_u,2}(\Omega)]^d$ with $1 \leq l_u \leq k_u + 1$:

$$\|\mathbf{w} - j_u \mathbf{w}\|_{0,M} + h_M \|\nabla(\mathbf{w} - j_u \mathbf{w})\|_{0,M} \leq Ch_M^{l_u} \|\mathbf{w}\|_{W^{l_u,2}(\omega_M)} \quad (3.10)$$

and for all $q \in Q \cap W^{l_p,2}(\Omega)$ with $1 \leq l_p \leq k_p + 1$:

$$\|q - j_p q\|_{0,M} + h_M \|\nabla(q - j_p q)\|_{0,M} \leq Ch_M^{l_p} \|q\|_{W^{l_p,2}(\omega_M)} \quad (3.11)$$

on a suitable patch $\omega_M \supseteq M$. Let for all $M \in \mathcal{M}_h$

$$\|\mathbf{v} - j_u \mathbf{v}\|_{\infty,M} \leq Ch_M |\mathbf{v}|_{W^{1,\infty}(\omega_M)} \quad \forall \mathbf{v} \in [W^{1,\infty}(\Omega)]^d. \quad (3.12)$$

There is also a bounded linear interpolation operator $j_\theta: \Theta \rightarrow \Theta_h$ such that for all $L \in \mathcal{L}_h$ and for all $\psi \in \Theta \cap W^{l_\theta,2}(\Omega)$ with $1 \leq l_\theta \leq k_\theta + 1$:

$$\|\psi - j_\theta \psi\|_{0,L} + h_L \|\nabla(\psi - j_\theta \psi)\|_{0,L} \leq Ch_L^{l_\theta} \|\psi\|_{W^{l_\theta,2}(\omega_L)} \quad (3.13)$$

on a suitable patch $\omega_L \supseteq L$. In addition, assume for all $L \in \mathcal{L}_h$, $M \in \mathcal{M}_h$

$$\begin{aligned} \|\psi - j_\theta \psi\|_{\infty,L} &\leq Ch_L |\psi|_{W^{1,\infty}(\omega_L)} & \forall \psi &\in W^{1,\infty}(\Omega), \\ \|\psi - j_\theta \psi\|_{\infty,M} &\leq Ch_M |\psi|_{W^{1,\infty}(\omega_M)} & \forall \psi &\in W^{1,\infty}(\Omega). \end{aligned} \quad (3.14)$$

These properties are well considered; see the book of [Cia02], for example, where the approximation of functions in Sobolev spaces by finite element spaces is discussed. In [SZ90], a Lagrange type interpolation operator is constructed with the desired properties. The last property (3.14) for j_θ holds due to the fact that all $M \in \mathcal{M}_h$ and $L \in \mathcal{L}_h$ are formed as a conjunction of at most $n_{\mathcal{T}_h} < \infty$ cells $T \in \mathcal{T}_h$. So if the interpolator is

constructed such that the above estimates hold true on all $T \in \mathcal{T}_h$, the same localized estimates hold on $M \in \mathcal{M}_h$ and $L \in \mathcal{L}_h$.

We point out that due to [GS03], there exists a quasi-local interpolation operator that preserves the discrete divergence and has the above properties.

Assumption 3.2.3 (Properties of the fluctuation operators).

Assume that for given integers $k_u, k_\theta \geq 1$, there are $s_u \in \{0, \dots, k_u\}$ and $s_\theta \in \{0, \dots, k_\theta\}$ such that the fluctuation operators $\kappa_M^u = Id - \pi_M^u$ and $\kappa_L^\theta = Id - \pi_L^\theta$ provide the following approximation properties: There is $C > 0$ such that for $\mathbf{w} \in [W^{l,2}(M)]^d$ with $M \in \mathcal{M}_h$, $l = 0, \dots, s_u$ and for $\psi \in W^{r,2}(L)$ with $L \in \mathcal{L}_h$, $r = 0, \dots, s_\theta$, it holds

$$\|\kappa_M^u \mathbf{w}\|_{0,M} \leq Ch_M^l \|\mathbf{w}\|_{W^{l,2}(M)}, \quad \|\kappa_L^\theta \psi\|_{0,L} \leq Ch_L^r \|\psi\|_{W^{r,2}(L)}.$$

Note that this is a property of the coarse spaces \mathbf{D}_M^u and D_L^θ and is always true for $s_u = s_\theta = 0$. It is also satisfied, for example, if $\mathbb{P}_{s_u-1} \subset \mathbf{D}_M^u$ and $\mathbb{P}_{s_\theta-1} \subset D_L^\theta$, as it is argued in [MST07].

Assumption 3.2.4 (Local inverse inequality).

Let the FE spaces $[Y_h^u]^d$ for the velocity and Y_h^θ for the temperature satisfy the local inverse inequalities

$$\begin{aligned} \|\nabla \mathbf{w}_h\|_{0,M} &\leq Ch_M^{-1} \|\mathbf{w}_h\|_{0,M} \quad \forall \mathbf{w}_h \in [Y_h^u]^d, \quad M \in \mathcal{M}_h, \\ \|\nabla \psi_h\|_{0,L} &\leq Ch_L^{-1} \|\psi_h\|_{0,L} \quad \forall \psi_h \in Y_h^\theta, \quad L \in \mathcal{L}_h. \end{aligned}$$

This condition holds true for shape-regular subdivisions of Ω and Lagrangian finite element spaces from Definition 2.2.7. A proof can be found in [Bra07].

Assumption 3.2.5 (Streamline directions).

Let $\mathbf{u}_h \in \mathbf{V}_h \cap [W^{1,\infty}(\Omega)]^d$. For all macro elements $M \in \mathcal{M}_h$ and $L \in \mathcal{L}_h$, let the element-wise averaged streamline directions $\mathbf{u}_M \in \mathbb{R}^d$, $\mathbf{u}_L \in \mathbb{R}^d$ be such that

$$\begin{aligned} \|\mathbf{u}_M\| &\leq C \|\mathbf{u}_h\|_{\infty,M}, & \|\mathbf{u}_h - \mathbf{u}_M\|_{\infty,M} &\leq Ch_M \|\mathbf{u}_h\|_{W^{1,\infty}(M)}, \\ \|\mathbf{u}_L\| &\leq C \|\mathbf{u}_h\|_{\infty,L}, & \|\mathbf{u}_h - \mathbf{u}_L\|_{\infty,L} &\leq Ch_L \|\mathbf{u}_h\|_{W^{1,\infty}(L)} \end{aligned}$$

with $C > 0$ independent of h_M, h_L .

One possible definition satisfying Assumption 3.2.5 is

$$\mathbf{u}_M := \frac{1}{|M|} \int_M \mathbf{u}_h(\mathbf{x}) \, d\mathbf{x}, \quad \mathbf{u}_L := \frac{1}{|L|} \int_L \mathbf{u}_h(\mathbf{x}) \, d\mathbf{x}. \quad (3.15)$$

For the error analysis in Section 3.2.2, we need the following requirement.

Assumption 3.2.6 (Interpolators with orthogonality property).

Assume that for integers $k_u, k_\theta \geq 1$, the following holds: Let $M \in \mathcal{M}_h, L \in \mathcal{L}_h$. There are interpolation operators i_u, i_θ satisfying $i_u: \mathbf{V} \rightarrow \mathbf{V}_h$ such that for $1 \leq l_u \leq k_u + 1$

$$(\mathbf{v} - i_u \mathbf{v}, \mathbf{w}_h)_M = 0 \quad \forall \mathbf{w}_h \in \mathbf{D}_M^u \quad \forall \mathbf{v} \in \mathbf{V}, \quad (3.16)$$

$$\|\mathbf{v} - i_u \mathbf{v}\|_{0,M} + h_M |\mathbf{v} - i_u \mathbf{v}|_{W^{1,2}(M)} \leq Ch_M^{l_u} \|\mathbf{v}\|_{W^{l_u,2}(\omega_M)} \quad \forall \mathbf{v} \in \mathbf{V} \cap [W^{l_u,2}(\Omega)]^d, \quad (3.17)$$

$$\|\mathbf{v} - i_u \mathbf{v}\|_{\infty,M} \leq Ch_M |\mathbf{v}|_{W^{1,\infty}(\omega_M)} \quad \forall \mathbf{v} \in [W^{1,\infty}(\Omega)]^d \quad (3.18)$$

and $i_\theta: \Theta \rightarrow \Theta_h$ such that for $1 \leq l_\theta \leq k_\theta + 1$

$$(\psi - i_\theta \psi, \phi_h)_L = 0 \quad \forall \phi_h \in D_L^\theta \quad \forall \psi \in \Theta, \quad (3.19)$$

$$\|\psi - i_\theta \psi\|_{0,L} + h_L |\psi - i_\theta \psi|_{W^{1,2}(L)} \leq Ch_L^{l_\theta} \|\psi\|_{W^{l_\theta,2}(\omega_L)} \quad \forall \psi \in \Theta \cap W^{l_\theta,2}(\Omega), \quad (3.20)$$

$$\|\psi - i_\theta \psi\|_{\infty,M} \leq Ch_M |\psi|_{W^{1,\infty}(\omega_M)} \quad \forall \psi \in W^{1,\infty}(\Omega) \quad (3.21)$$

with suitable patches $\omega_M \supseteq M, \omega_L \supseteq L$.

Such interpolation operators exist, if the following so-called LPS compatibility condition holds.

Lemma 3.2.7 (LPS compatibility condition).

Let $M \in \mathcal{M}_h, L \in \mathcal{L}_h$. Consider Lagrangian finite element spaces Y_h^u for the velocity and Y_h^θ for the temperature of piecewise polynomial functions, where the degrees are (at least) $k_u \geq 1$ and $k_\theta \geq 1$, respectively. Denote $\mathbf{Y}_h^u(M) := \{\mathbf{v}_h|_M: \mathbf{v}_h \in [Y_h^u]^d, \mathbf{v}_h = \mathbf{0} \text{ on } \Omega \setminus M\}$ and $Y_h^\theta(L) := \{\theta_h|_L: \theta_h \in [Y_h^\theta]^d, \theta_h = 0 \text{ on } \Omega \setminus L\}$. If the Assumptions 3.2.2, 3.2.4 and the conditions

$$\exists \beta_u > 0: \quad \inf_{\mathbf{w}_h \in \mathbf{D}_M^u} \sup_{\mathbf{v}_h \in \mathbf{Y}_h^u(M)} \frac{(\mathbf{v}_h, \mathbf{w}_h)_M}{\|\mathbf{v}_h\|_{0,M} \|\mathbf{w}_h\|_{0,M}} \geq \beta_u, \quad (3.22)$$

$$\exists \beta_\theta > 0: \quad \inf_{\psi_h \in D_L^\theta} \sup_{\theta_h \in Y_h^\theta(L)} \frac{(\theta_h, \psi_h)_L}{\|\theta_h\|_{0,L} \|\psi_h\|_{0,L}} \geq \beta_\theta \quad (3.23)$$

hold, then there are interpolation operators i_u and i_θ satisfying Assumption 3.2.6.

Proof. In [MST07], from the condition (3.22), an interpolation operator $i_u: \mathbf{V} \rightarrow \mathbf{V}_h$ is constructed with the properties (3.16), (3.17): Let

$$\mathbf{W}_h(M) := \{\mathbf{v}_h \in \mathbf{Y}_h^u(M): (\mathbf{v}_h, \mathbf{w}_h) = 0 \quad \forall \mathbf{w}_h \in \mathbf{D}_M^u\} \subset \mathbf{Y}_h^u(M)$$

and $\mathbf{W}_h(M)^\perp$ the L^2 -orthogonal complement of $\mathbf{W}_h(M)$ in $\mathbf{Y}_h^u(M)$. Consider the interpolation operator j_u given by Assumption 3.2.2. As it is shown in [MST07], for each $\mathbf{v} \in [H^1(\Omega)]^d$, there exists a unique $\mathbf{z}_h(\mathbf{v}) \in \mathbf{W}_h(M)^\perp$ such that

$$(\mathbf{z}_h(\mathbf{v}), \mathbf{w}_h)_M = (\mathbf{v} - j_u \mathbf{v}, \mathbf{w}_h)_M \quad \forall \mathbf{w}_h \in \mathbf{D}_M^u, \quad (3.24)$$

$$\|\mathbf{z}_h(\mathbf{v})\|_{0,M} \leq \frac{1}{\beta_u} \|\mathbf{v} - j_u \mathbf{v}\|_{0,M}, \quad (3.25)$$

since (3.22) holds. Define $i_u \mathbf{v}|_M := j_u \mathbf{v}|_M + \mathbf{z}_h(\mathbf{v})$ for all $M \in \mathcal{M}_h$. This gives rise to an interpolation operator $i_u: [H^1(\Omega)]^d \rightarrow [Y_h^u]^d$ satisfying for all $M \in \mathcal{M}_h$

$$\begin{aligned} \|\mathbf{v} - i_u \mathbf{v}\|_{0,M} &\leq \left(1 + \frac{1}{\beta_u}\right) \|\mathbf{v} - j_u \mathbf{v}\|_{0,M} \\ &\leq Ch_M^l \|\mathbf{v}\|_{W^{l,2}(\omega_M)} \quad \forall \mathbf{v} \in [W^{l,2}(\Omega)]^d, \quad 1 \leq l \leq k_u + 1. \end{aligned}$$

The orthogonality (3.16) follows from (3.24). The approximation property in the H^1 -semi-norm can be established via the inverse inequality from Assumption 3.2.4 applied to (3.25) and the triangle inequality. Hence, (3.17) is shown.

The fact that i_u fulfills (3.18) can be understood by transformation on the reference element \hat{T} . For $T \in \mathcal{T}_h$, let $\hat{\mathbf{z}}_h(\mathbf{v}) := \mathbf{z}_h(\mathbf{v}) \circ F_T$ denote the transformation of $\mathbf{z}_h(\mathbf{v})|_T$ onto \hat{T} via the bijective reference mapping $F_T: \hat{T} \rightarrow T$. Moreover, we use finite element spaces such that

$$c_1 h_T^d \leq |\det DF_T(\hat{\mathbf{x}})| \leq c_2 h_T^d \quad \forall \hat{\mathbf{x}} \in \hat{T}$$

with constants $c_1, c_2 > 0$ independent of the cell diameter h_T . Since $[Y_h^u]^d$ is finite dimensional, all norms on this space are equivalent. So we have for all $T \in \mathcal{T}_h$

$$\|\mathbf{z}_h(\mathbf{v})\|_{\infty,T} \leq \|\hat{\mathbf{z}}_h(\mathbf{v})\|_{\infty,\hat{T}} \leq c \|\hat{\mathbf{z}}_h(\mathbf{v})\|_{0,\hat{T}} \leq Ch_T^{-d/2} \|\mathbf{z}_h(\mathbf{v})\|_{0,T}$$

with $c > 0$ independent of h_T . With this, the properties of the fine and coarse triangulations from Assumption 2.2.9, (3.25) and the properties of j_u by Assumption 3.2.2, we have for all $\mathbf{v} \in [W^{1,\infty}(\Omega)]^d$:

$$\begin{aligned} \|\mathbf{v} - i_u \mathbf{v}\|_{\infty,M} &\leq \|\mathbf{v} - j_u \mathbf{v}\|_{\infty,M} + \|\mathbf{z}_h(\mathbf{v})\|_{\infty,M} \leq \|\mathbf{v} - j_u \mathbf{v}\|_{\infty,M} + Ch_M^{-d/2} \|\mathbf{z}_h(\mathbf{v})\|_{0,M} \\ &\leq \|\mathbf{v} - j_u \mathbf{v}\|_{\infty,M} + Ch_M^{-d/2} \|\mathbf{v} - j_u \mathbf{v}\|_{0,M} \leq C \|\mathbf{v} - j_u \mathbf{v}\|_{\infty,M} \\ &\leq Ch_M |\mathbf{v}|_{W^{1,\infty}(\omega_M)} \end{aligned}$$

for all $M \in \mathcal{M}_h$. The analogous construction yields the claim for i_θ . \square

3.2.1. Quasi-Optimal Estimates without LPS-Compatibility Condition

In order to prove semi-discrete error estimates, we have to bound the difference of the convective terms for velocity and temperature. We move this into the lemma below. The following mesh-dependent quantities are useful:

Definition 3.2.8 (Local Reynolds and Péclet numbers).

For $M \in \mathcal{M}_h$, $L \in \mathcal{L}_h$ and $\mathbf{u}_h \in L^\infty(\Omega)$, we introduce the local Reynolds number Re_M and the local Péclet number Pe_L as

$$Re_M := \frac{\|\mathbf{u}_h\|_{\infty, M} h_M}{\nu}, \quad Pe_L := \frac{\|\mathbf{u}_h\|_{\infty, L} h_L}{\alpha}.$$

Since we are interested in suitable choices of stabilization parameters, none of the used constants $C > 0$ depends on any of the problem parameters, h_M , h_L or the (continuous or discrete) solution in the following.

Lemma 3.2.9 (Convective terms without compatibility condition).

Let $\varepsilon > 0$ and $(\mathbf{u}, p, \theta) \in \mathbf{V}^{div} \times Q \times \Theta$, $(\mathbf{u}_h, p_h, \theta_h) \in \mathbf{V}_h^{div} \times Q_h \times \Theta_h$ be solutions of (2.9)-(2.10) and (3.1)-(3.2) satisfying $\mathbf{u} \in [W^{1,\infty}(\Omega)]^d$, $\theta \in W^{1,\infty}(\Omega)$. If Assumption 3.2.2 holds, we can estimate the difference of the convective terms in the momentum equation

$$\begin{aligned} & c_u(\mathbf{u}; \mathbf{u}, \mathbf{e}_{u,h}) - c_u(\mathbf{u}_h; \mathbf{u}_h, \mathbf{e}_{u,h}) \\ & \leq \frac{1}{4\varepsilon} \sum_{M \in \mathcal{M}_h} \frac{1 + \nu Re_M^2}{h_M^2} \|\boldsymbol{\eta}_{u,h}\|_{0,M}^2 + 3\varepsilon \|\boldsymbol{\eta}_{u,h}\|_{LPS}^2 + 4\varepsilon \|\mathbf{e}_{u,h}\|_{LPS}^2 \\ & + \left[|\mathbf{u}|_{W^{1,\infty}(\Omega)} + \varepsilon \max_{M \in \mathcal{M}_h} \{h_M^2 |\mathbf{u}|_{W^{1,\infty}(M)}^2\} + \frac{C}{\varepsilon} \max_{M \in \mathcal{M}_h} \left\{ \frac{h_M^2}{\gamma_M} |\mathbf{u}|_{W^{1,\infty}(M)}^2 \right\} \right. \\ & \left. + \frac{C}{\varepsilon} \max_{M \in \mathcal{M}_h} \{\gamma_M^{-1} \|\mathbf{u}\|_{\infty, M}^2\} \right] \|\mathbf{e}_{u,h}\|_0^2 \end{aligned}$$

with C independent of h_M , h_L , ε , the problem parameters and the solutions. The difference of the convective terms in the Fourier equation can be bounded as

$$\begin{aligned} & c_\theta(\mathbf{u}; \theta, \mathbf{e}_{\theta,h}) - c_\theta(\mathbf{u}_h; \theta_h, \mathbf{e}_{\theta,h}) \\ & \leq \frac{1}{4\varepsilon} \sum_{M \in \mathcal{M}_h} \frac{1}{h_M^2} \|\boldsymbol{\eta}_{u,h}\|_{0,M}^2 + 3\varepsilon \|\boldsymbol{\eta}_{u,h}\|_{LPS}^2 + 3\varepsilon \|\mathbf{e}_{u,h}\|_{LPS}^2 + 7\varepsilon \|\mathbf{e}_{\theta,h}\|_{LPS}^2 \\ & + \frac{1}{28\varepsilon} \sum_{L \in \mathcal{L}_h} \frac{\alpha Pe_L^2}{h_L^2} \|\boldsymbol{\eta}_{\theta,h}\|_{0,L}^2 + \frac{1}{2} |\theta|_{W^{1,\infty}(\Omega)} \|\mathbf{e}_{u,h}\|_0^2 + \|\mathbf{e}_{\theta,h}\|_0^2 \left(\frac{1}{2} |\theta|_{W^{1,\infty}(\Omega)} \right. \\ & \left. + \varepsilon \max_{M \in \mathcal{M}_h} \{h_M^2 |\theta|_{W^{1,\infty}(M)}^2\} + \frac{C}{\varepsilon} \max_{M \in \mathcal{M}_h} \left\{ \frac{h_M^2}{\gamma_M} |\theta|_{W^{1,\infty}(M)}^2 \right\} + \frac{C}{\varepsilon} \max_{M \in \mathcal{M}_h} \{\gamma_M^{-1} \|\theta\|_{\infty, M}^2\} \right) \end{aligned}$$

with $C > 0$ independent of the problem parameters, h_M , h_L and the solutions.

Proof. In this proof, we perform similar estimates for velocity and temperature. Therefore, we present every step for the velocity and a shortened version for the temperature directly afterwards.

Due to the result from [GS03], the existence of a quasi-local interpolation operator preserving the discrete divergence is guaranteed from Assumptions 2.2.1 and 3.2.2. We denote this operator by $j_u: \mathbf{V}^{div} \rightarrow \mathbf{V}_h^{div}$. It has the approximation properties (3.10) and (3.12). For j_θ , we choose the interpolation operator provided by Assumption 3.2.2. With the splitting $\boldsymbol{\eta}_{u,h} + \mathbf{e}_{u,h} = (\mathbf{u} - j_u \mathbf{u}) + (j_u \mathbf{u} - \mathbf{u}_h)$ from Definition 3.2.1 and integration by parts, we calculate

$$\begin{aligned} c_u(\mathbf{u}_h; \mathbf{u}_h, \mathbf{e}_{u,h}) &= \frac{1}{2}(\mathbf{u}_h \cdot \nabla \mathbf{u}_h, \mathbf{e}_{u,h}) - \frac{1}{2}(\mathbf{u}_h \cdot \nabla \mathbf{e}_{u,h}, \mathbf{u}_h) \\ &= \frac{1}{2}(\mathbf{u}_h \cdot \nabla \mathbf{u}_h, \mathbf{e}_{u,h}) + \frac{1}{2}(\mathbf{u}_h \cdot \nabla \mathbf{e}_{u,h}, \mathbf{e}_{u,h}) - \frac{1}{2}(\mathbf{u}_h \cdot \nabla \mathbf{e}_{u,h}, j_u \mathbf{u}) \\ &= (\mathbf{u}_h \cdot \nabla j_u \mathbf{u}, \mathbf{e}_{u,h}) + \frac{1}{2}((\nabla \cdot \mathbf{u}_h) j_u \mathbf{u}, \mathbf{e}_{u,h}). \end{aligned}$$

Together with an analogous reformulation for the temperature terms, this yields

$$\begin{aligned} c_u(\mathbf{u}; \mathbf{u}, \mathbf{e}_{u,h}) - c_u(\mathbf{u}_h; \mathbf{u}_h, \mathbf{e}_{u,h}) &= \underbrace{((\mathbf{u} - \mathbf{u}_h) \cdot \nabla \mathbf{u}, \mathbf{e}_{u,h})}_{=: T_1^u} + \underbrace{(\mathbf{u}_h \cdot \nabla (\mathbf{u} - j_u \mathbf{u}), \mathbf{e}_{u,h})}_{=: T_2^u} - \underbrace{\frac{1}{2}((\nabla \cdot \mathbf{u}_h) j_u \mathbf{u}, \mathbf{e}_{u,h})}_{=: T_3^u}, \\ c_\theta(\mathbf{u}; \theta, e_{\theta,h}) - c_\theta(\mathbf{u}_h; \theta_h, e_{\theta,h}) &= \underbrace{((\mathbf{u} - \mathbf{u}_h) \cdot \nabla \theta, e_{\theta,h})}_{=: T_1^\theta} + \underbrace{(\mathbf{u}_h \cdot \nabla (\theta - j_\theta \theta), e_{\theta,h})}_{=: T_2^\theta} - \underbrace{\frac{1}{2}((\nabla \cdot \mathbf{u}_h) j_\theta \theta, e_{\theta,h})}_{=: T_3^\theta}. \end{aligned}$$

Now, we bound each term separately. Using Young's inequality with $\varepsilon > 0$, we calculate:

$$\begin{aligned} T_1^u &\leq \sum_{M \in \mathcal{M}_h} \|\nabla \mathbf{u}\|_{\infty, M} \left(\|\mathbf{e}_{u,h}\|_{0, M}^2 + \|\boldsymbol{\eta}_{u,h}\|_{0, M} \|\mathbf{e}_{u,h}\|_{0, M} \right) \\ &= |\mathbf{u}|_{W^{1, \infty}(\Omega)} \|\mathbf{e}_{u,h}\|_0^2 + \sum_{M \in \mathcal{M}_h} \frac{1}{h_M} |\mathbf{u}|_{W^{1, \infty}(M)} \|\boldsymbol{\eta}_{u,h}\|_{0, M} h_M \|\mathbf{e}_{u,h}\|_{0, M} \\ &\leq \frac{1}{4\varepsilon} \sum_{M \in \mathcal{M}_h} \frac{1}{h_M^2} \|\boldsymbol{\eta}_{u,h}\|_{0, M}^2 + \left(|\mathbf{u}|_{W^{1, \infty}(\Omega)} + \varepsilon \max_{M \in \mathcal{M}_h} \{h_M^2 |\mathbf{u}|_{W^{1, \infty}(M)}\} \right) \|\mathbf{e}_{u,h}\|_0^2 \quad (3.26) \end{aligned}$$

and for the temperature:

$$T_1^\theta \leq \sum_{M \in \mathcal{M}_h} \|\nabla \theta\|_{\infty, M} \|e_{\theta,h}\|_{0, M} \left(\|\mathbf{e}_{u,h}\|_{0, M} + \|\boldsymbol{\eta}_{u,h}\|_{0, M} \right)$$

$$\begin{aligned}
&= |\theta|_{W^{1,\infty}(\Omega)} \|e_{u,h}\|_0 \|e_{\theta,h}\|_0 + \sum_{M \in \mathcal{M}_h} \frac{1}{h_M} |\theta|_{W^{1,\infty}(M)} \|\boldsymbol{\eta}_{u,h}\|_{0,M} h_M \|e_{\theta,h}\|_{0,M} \\
&\leq \frac{1}{4\varepsilon} \sum_{M \in \mathcal{M}_h} \frac{1}{h_M^2} \|\boldsymbol{\eta}_{u,h}\|_{0,M}^2 + \varepsilon \max_{M \in \mathcal{M}_h} \{h_M^2 |\theta|_{W^{1,\infty}(M)}^2\} \|e_{\theta,h}\|_0^2 \\
&+ \frac{1}{2} |\theta|_{W^{1,\infty}(\Omega)} \|e_{\theta,h}\|_0^2 + \frac{1}{2} |\theta|_{W^{1,\infty}(\Omega)} \|e_{u,h}\|_0^2. \tag{3.27}
\end{aligned}$$

For the terms T_2^u and T_2^θ , we have via integration by parts

$$\begin{aligned}
T_2^u &= (\mathbf{u}_h \cdot \nabla \boldsymbol{\eta}_{u,h}, \mathbf{e}_{u,h}) = -(\mathbf{u}_h \cdot \nabla \mathbf{e}_{u,h}, \boldsymbol{\eta}_{u,h}) - ((\nabla \cdot \mathbf{u}_h) \mathbf{e}_{u,h}, \boldsymbol{\eta}_{u,h}) =: T_{21}^u + T_{22}^u, \\
T_2^\theta &= (\mathbf{u}_h \cdot \nabla \eta_{\theta,h}, e_{\theta,h}) = -(\mathbf{u}_h \cdot \nabla e_{\theta,h}, \eta_{\theta,h}) - ((\nabla \cdot \mathbf{u}_h) e_{\theta,h}, \eta_{\theta,h}) =: T_{21}^\theta + T_{22}^\theta.
\end{aligned}$$

Term T_{21}^u is the most critical one. Note that $\mathbf{u}_h|_M \in [L^\infty(M)]^d$ and $\mathbf{u}_h|_L \in [L^\infty(L)]^d$. This is due to the definition of the finite element spaces. We calculate using the local Reynolds number $Re_M = \|\mathbf{u}_h\|_{\infty,M} h_M / \nu$ from Definition 3.2.8 and Young's inequality:

$$\begin{aligned}
T_{21}^u &= -(\mathbf{u}_h \cdot \nabla \mathbf{e}_{u,h}, \boldsymbol{\eta}_{u,h}) \leq \sum_{M \in \mathcal{M}_h} \|\mathbf{u}_h\|_{\infty,M} \|\nabla \mathbf{e}_{u,h}\|_{0,M} \|\boldsymbol{\eta}_{u,h}\|_{0,M} \\
&\leq \sqrt{\nu} \|\nabla \mathbf{e}_{u,h}\|_0 \left(\sum_{M \in \mathcal{M}_h} \nu \frac{\|\mathbf{u}_h\|_{\infty,M}^2 h_M^2}{\nu^2} h_M^{-2} \|\boldsymbol{\eta}_{u,h}\|_{0,M}^2 \right)^{1/2} \\
&\leq \varepsilon \|e_{u,h}\|_{LPS}^2 + \frac{1}{4\varepsilon} \sum_{M \in \mathcal{M}_h} \nu Re_M^2 h_M^{-2} \|\boldsymbol{\eta}_{u,h}\|_{0,M}^2. \tag{3.28}
\end{aligned}$$

With the local Péclet number $Pe_L = \|\mathbf{u}_h\|_{\infty,L} h_L / \alpha$ and Young's inequality, we bound T_{21}^θ as:

$$T_{21}^\theta = -(\mathbf{u}_h \cdot \nabla e_{\theta,h}, \eta_{\theta,h}) \leq 7\varepsilon \|e_{\theta,h}\|_{LPS}^2 + \frac{1}{28\varepsilon} \sum_{L \in \mathcal{L}_h} \alpha Pe_L^2 h_L^{-2} \|\eta_{\theta,h}\|_{0,L}^2. \tag{3.29}$$

Using $(\nabla \cdot \mathbf{u}, q) = 0$ for all $q \in L^2(\Omega)$, Assumption 3.2.2 and Young's inequality with $\varepsilon > 0$, we obtain

$$\begin{aligned}
T_{22}^u &= -((\nabla \cdot \mathbf{u}_h) \boldsymbol{\eta}_{u,h}, \mathbf{e}_{u,h}) = ((\nabla \cdot (\boldsymbol{\eta}_{u,h} + \mathbf{e}_{u,h})) \boldsymbol{\eta}_{u,h}, \mathbf{e}_{u,h}) \\
&\leq \sum_{M \in \mathcal{M}_h} \|\boldsymbol{\eta}_{u,h}\|_{\infty,M} \left(\|\nabla \cdot \mathbf{e}_{u,h}\|_{0,M} + \|\nabla \cdot \boldsymbol{\eta}_{u,h}\|_{0,M} \right) \|\mathbf{e}_{u,h}\|_{0,M} \\
&\leq \sum_{M \in \mathcal{M}_h} \frac{Ch_M}{\sqrt{\gamma_M}} |\mathbf{u}|_{W^{1,\infty}(M)} \sqrt{\gamma_M} \left(\|\nabla \cdot \mathbf{e}_{u,h}\|_{0,M} + \|\nabla \cdot \boldsymbol{\eta}_{u,h}\|_{0,M} \right) \|\mathbf{e}_{u,h}\|_{0,M} \\
&\leq \varepsilon \|\boldsymbol{\eta}_{u,h}\|_{LPS}^2 + \varepsilon \|e_{u,h}\|_{LPS}^2 + \frac{C}{\varepsilon} \max_{M \in \mathcal{M}_h} \left\{ \frac{h_M^2}{\gamma_M} |\mathbf{u}|_{W^{1,\infty}(M)}^2 \right\} \|e_{u,h}\|_0^2 \tag{3.30}
\end{aligned}$$

and in a similar fashion

$$\begin{aligned}
T_{22}^\theta &= -((\nabla \cdot \mathbf{u}_h)e_{\theta,h}, \eta_{\theta,h}) = ((\nabla \cdot (\boldsymbol{\eta}_{u,h} + \mathbf{e}_{u,h}))\eta_{\theta,h}, e_{\theta,h}) \\
&\leq \sum_{M \in \mathcal{M}_h} \|\eta_{\theta,h}\|_{\infty, M} \left(\|\nabla \cdot \mathbf{e}_{u,h}\|_{0, M} + \|\nabla \cdot \boldsymbol{\eta}_{u,h}\|_{0, M} \right) \|e_{\theta,h}\|_{0, M} \\
&\leq \varepsilon \|\boldsymbol{\eta}_{u,h}\|_{LPS}^2 + \varepsilon \|\mathbf{e}_{u,h}\|_{LPS}^2 + \frac{C}{\varepsilon} \max_{M \in \mathcal{M}_h} \left\{ \frac{h_M^2}{\gamma_M} |\theta|_{W^{1,\infty}(M)}^2 \right\} \|e_{\theta,h}\|_0^2. \tag{3.31}
\end{aligned}$$

Utilizing the splitting according to Definition 3.2.1, we have

$$\begin{aligned}
T_3^u &= -\frac{1}{2}((\nabla \cdot \mathbf{u}_h)j_u \mathbf{u}, \mathbf{e}_{u,h}) = \frac{1}{2}((\nabla \cdot \mathbf{u}_h)\boldsymbol{\eta}_{u,h}, \mathbf{e}_{u,h}) - \frac{1}{2}((\nabla \cdot \mathbf{u}_h)\mathbf{u}, \mathbf{e}_{u,h}) = T_{31}^u + T_{32}^u, \\
T_3^\theta &= -\frac{1}{2}((\nabla \cdot \mathbf{u}_h)j_\theta \theta, e_{\theta,h}) = \frac{1}{2}((\nabla \cdot \mathbf{u}_h)\eta_{\theta,h}, e_{\theta,h}) - \frac{1}{2}((\nabla \cdot \mathbf{u}_h)\theta, e_{\theta,h}) = T_{31}^\theta + T_{32}^\theta.
\end{aligned}$$

We exploit $T_{31}^u = -\frac{1}{2}T_{22}^u$, $T_{31}^\theta = -\frac{1}{2}T_{22}^\theta$ and estimate as in (3.30) and (3.31):

$$|T_{31}^u| \leq \varepsilon \|\boldsymbol{\eta}_{u,h}\|_{LPS}^2 + \varepsilon \|\mathbf{e}_{u,h}\|_{LPS}^2 + \frac{C}{\varepsilon} \max_{M \in \mathcal{M}_h} \left\{ \frac{h_M^2}{\gamma_M} |\mathbf{u}|_{W^{1,\infty}(M)}^2 \right\} \|\mathbf{e}_{u,h}\|_0^2, \tag{3.32}$$

$$|T_{31}^\theta| \leq \varepsilon \|\boldsymbol{\eta}_{u,h}\|_{LPS}^2 + \varepsilon \|\mathbf{e}_{u,h}\|_{LPS}^2 + \frac{C}{\varepsilon} \max_{M \in \mathcal{M}_h} \left\{ \frac{h_M^2}{\gamma_M} |\theta|_{W^{1,\infty}(M)}^2 \right\} \|e_{\theta,h}\|_0^2. \tag{3.33}$$

For the terms T_{32}^u and T_{32}^θ , we use that $(\nabla \cdot \mathbf{u}, q) = 0$ for all $q \in L^2(\Omega)$ and Young's inequality:

$$\begin{aligned}
|T_{32}^u| &= \frac{1}{2}|(\nabla \cdot \mathbf{u}_h, \mathbf{u} \cdot \mathbf{e}_{u,h})| = \frac{1}{2}|(\nabla \cdot (-\boldsymbol{\eta}_{u,h} - \mathbf{e}_{u,h} + \mathbf{u}), \mathbf{u} \cdot \mathbf{e}_{u,h})| \\
&\leq \frac{1}{2}|(\nabla \cdot \boldsymbol{\eta}_{u,h}, \mathbf{u} \cdot \mathbf{e}_{u,h})| + \frac{1}{2}|(\nabla \cdot \mathbf{e}_{u,h}, \mathbf{u} \cdot \mathbf{e}_{u,h})| \\
&\leq \frac{1}{2} \sum_{M \in \mathcal{M}_h} \left(\|\mathbf{u}\|_{\infty, M} \sqrt{\gamma_M} \|\nabla \cdot \boldsymbol{\eta}_{u,h}\|_{0, M} \frac{1}{\sqrt{\gamma_M}} \|\mathbf{e}_{u,h}\|_{0, M} \right. \\
&\quad \left. + \|\mathbf{u}\|_{\infty, M} \sqrt{\gamma_M} \|\nabla \cdot \mathbf{e}_{u,h}\|_{0, M} \frac{1}{\sqrt{\gamma_M}} \|\mathbf{e}_{u,h}\|_{0, M} \right) \\
&\leq \varepsilon \|\boldsymbol{\eta}_{u,h}\|_{LPS}^2 + \varepsilon \|\mathbf{e}_{u,h}\|_{LPS}^2 + \frac{C}{\varepsilon} \max_{M \in \mathcal{M}_h} \{ \gamma_M^{-1} \|\mathbf{u}\|_{\infty, M}^2 \} \|\mathbf{e}_{u,h}\|_0^2, \tag{3.34}
\end{aligned}$$

$$\begin{aligned}
|T_{32}^\theta| &= \frac{1}{2}|(\nabla \cdot \mathbf{u}_h, \theta \cdot e_{\theta,h})| \leq \frac{1}{2}|(\nabla \cdot \boldsymbol{\eta}_{u,h}, \theta \cdot e_{\theta,h})| + \frac{1}{2}|(\nabla \cdot \mathbf{e}_{u,h}, \theta \cdot e_{\theta,h})| \\
&\leq \frac{1}{2} \sum_{M \in \mathcal{M}_h} \left(\|\theta\|_{\infty, M} \|\nabla \cdot \boldsymbol{\eta}_{u,h}\|_{0, M} \|e_{\theta,h}\|_{0, M} + \|\theta\|_{\infty, M} \|\nabla \cdot \mathbf{e}_{u,h}\|_{0, M} \|e_{\theta,h}\|_{0, M} \right) \\
&\leq \varepsilon \|\boldsymbol{\eta}_{u,h}\|_{LPS}^2 + \varepsilon \|\mathbf{e}_{u,h}\|_{LPS}^2 + \frac{C}{\varepsilon} \max_{M \in \mathcal{M}_h} \{ \gamma_M^{-1} \|\theta\|_{\infty, M}^2 \} \|e_{\theta,h}\|_0^2. \tag{3.35}
\end{aligned}$$

Combining the above bounds (3.26)-(3.35) for velocity and temperature separately yields the claim. \square

Remark 3.2.10. The local quantities Re_M and Pe_M on the right-hand side blow up for very small ν and α . If we additionally require Assumption 3.2.4 in Lemma 3.2.9, we can conduct a different estimate of the critical term T_{21}^u (and similarly for T_{21}^θ):

$$\begin{aligned} T_{21}^u &= -(\mathbf{u}_h \cdot \nabla \mathbf{e}_{u,h}, \boldsymbol{\eta}_{u,h}) \leq \sum_{M \in \mathcal{M}_h} \|\mathbf{u}_h\|_{\infty, M} \|\nabla \mathbf{e}_{u,h}\|_{0, M} \|\boldsymbol{\eta}_{u,h}\|_{0, M} \\ &\leq C \sum_{M \in \mathcal{M}_h} \|\mathbf{u}_h\|_{\infty, M} \|\mathbf{e}_{u,h}\|_{0, M} h_M^{-1} \|\boldsymbol{\eta}_{u,h}\|_{0, M} \\ &\leq \|\mathbf{u}_h\|_{\infty}^2 \|\mathbf{e}_{u,h}\|_0^2 + C \sum_{M \in \mathcal{M}_h} h_M^{-2} \|\boldsymbol{\eta}_{u,h}\|_{0, M}^2. \end{aligned}$$

We require to fulfill the conditions stated below.

Assumption 3.2.11 (Parameter bounds).

Assume that for all $M \in \mathcal{M}_h$, $E \in \mathcal{E}_h$ and $L \in \mathcal{L}_h$:

$$\begin{aligned} \tau_M^u(\mathbf{u}_M) &\geq 0, \quad \gamma_M(\mathbf{u}_M) \geq 0, \quad \phi_E \geq 0, \quad \tau_L^\theta(\mathbf{u}_L) \geq 0, \\ \max_{M \in \mathcal{M}_h} \gamma_M(\mathbf{u}_M) &\in L^\infty(0, T), \quad \max_{M \in \mathcal{M}_h} \gamma_M(\mathbf{u}_M)^{-1} \in L^\infty(0, T), \quad \max_{E \in \mathcal{E}_h} \phi_E \in L^\infty(0, T), \\ \max_{M \in \mathcal{M}_h} \tau_M^u(\mathbf{u}_M) |\mathbf{u}_M|^2 &\in L^\infty(0, T), \quad \max_{L \in \mathcal{L}_h} \tau_L^\theta(\mathbf{u}_L) |\mathbf{u}_L|^2 \in L^\infty(0, T), \\ \max_{M \in \mathcal{M}_h} Re_M &\in L^\infty(0, T), \quad \max_{L \in \mathcal{L}_h} Pe_L \in L^\infty(0, T). \end{aligned}$$

These considerations give rise to the following quasi-optimal semi-discrete error estimate for the LPS-model (3.1)-(3.2).

Theorem 3.2.12 (Error estimate without compatibility condition).

Let $(\mathbf{u}, p, \theta): [0, T] \rightarrow \mathbf{V}^{div} \times Q \times \Theta$, $(\mathbf{u}_h, p_h, \theta_h): [0, T] \rightarrow \mathbf{V}_h^{div} \times Q_h \times \Theta_h$ be solutions of (2.9)-(2.10) and (3.1)-(3.2) satisfying

$$\begin{aligned} \mathbf{u} &\in L^\infty(0, T; [W^{1,\infty}(\Omega)]^d), \quad \theta \in L^\infty(0, T; W^{1,\infty}(\Omega)), \quad p \in L^2(0, T; Q \cap C(\Omega)), \\ \partial_t \mathbf{u} &\in L^2(0, T; [L^2(\Omega)]^d), \quad \partial_t \theta \in L^2(0, T; L^2(\Omega)). \end{aligned}$$

Let Assumptions 3.2.2, and 3.2.11 be valid and $\mathbf{u}_h(0) = j_u \mathbf{u}_0$, $\theta_h(0) = j_\theta \theta_0$. We obtain for $\mathbf{e}_{u,h} = j_u \mathbf{u} - \mathbf{u}_h$, $e_{p,h} = j_p p - p_h$, $e_{\theta,h} = j_\theta \theta - \theta_h$ of the LPS-method (3.1)-(3.2) for all $0 \leq t \leq T$:

$$\begin{aligned} &\|\mathbf{e}_{u,h}\|_{L^\infty(0,t; L^2(\Omega))}^2 + \|e_{\theta,h}\|_{L^\infty(0,t; L^2(\Omega))}^2 + \int_0^t \left(\|(\mathbf{e}_{u,h}, e_{p,h})(\tau)\|_{LPS}^2 + \|e_{\theta,h}(\tau)\|_{LPS}^2 \right) d\tau \\ &\leq C \int_0^t e^{C_{G,h}(\mathbf{u}, \theta)(t-\tau)} \left\{ \sum_{M \in \mathcal{M}_h} \left[(\nu + \tau_M^u |\mathbf{u}_M|^2 + \gamma_M d) \|\nabla \boldsymbol{\eta}_{u,h}(\tau)\|_{0, M}^2 \right. \right. \\ &\quad \left. \left. + (1 + \nu Re_M^2) h_M^{-2} \|\boldsymbol{\eta}_{u,h}(\tau)\|_{0, M}^2 + \|\partial_t \boldsymbol{\eta}_{u,h}(\tau)\|_{0, M}^2 + \tau_M^u |\mathbf{u}_M|^2 \|\kappa_M^u(\nabla \mathbf{u})(\tau)\|_{0, M}^2 \right] \right\} \end{aligned}$$

$$\begin{aligned}
& + \min\left(\frac{d}{\nu}, \frac{1}{\gamma_M}\right) \|\eta_{p,h}(\tau)\|_{0,M}^2 + \sum_{E \in \mathcal{E}_h} \phi_E \|\eta_{p,h}(\tau)\|_{E,0,E}^2 \\
& + \sum_{L \in \mathcal{L}_h} \left[\|\partial_t \eta_{\theta,h}(\tau)\|_0^2 + \left(\frac{\alpha P e_L^2}{h_L^2} + \beta \|\mathbf{g}\|_{\infty,L} \right) \|\eta_{\theta,h}(\tau)\|_{0,L}^2 \right. \\
& \left. + (\alpha + \tau_L^\theta |\mathbf{u}_L|^2) \|\nabla \eta_{\theta,h}(\tau)\|_{0,L}^2 + \tau_L^\theta |\mathbf{u}_L|^2 \|\kappa_L^\theta (\nabla \theta)(\tau)\|_{0,L}^2 \right] d\tau
\end{aligned}$$

with $(\boldsymbol{\eta}_{u,h}, \eta_{p,h}, \eta_{\theta,h}) = (\mathbf{u} - j_u \mathbf{u}, p - j_p p, \theta - j_\theta \theta)$, the local Reynolds number $Re_M = h_M \|\mathbf{u}_h\|_{\infty,M} / \nu$, the local Péclet number $Pe_L = \|\mathbf{u}_h\|_{\infty,L} h_L / \alpha$ and the Gronwall constant

$$\begin{aligned}
C_{G,h}(\mathbf{u}, \theta) &= 1 + \beta \|\mathbf{g}\|_{\infty} + |\mathbf{u}|_{W^{1,\infty}(\Omega)} + |\theta|_{W^{1,\infty}(\Omega)} \\
&+ \max_{M \in \mathcal{M}_h} \{h_M^2 |\mathbf{u}|_{W^{1,\infty}(M)}^2\} + \max_{M \in \mathcal{M}_h} \left\{ \frac{h_M^2}{\gamma_M} |\mathbf{u}|_{W^{1,\infty}(M)}^2 \right\} + \max_{M \in \mathcal{M}_h} \{\gamma_M^{-1} \|\mathbf{u}\|_{\infty,M}^2\} \\
&+ \max_{M \in \mathcal{M}_h} \{h_M^2 |\theta|_{W^{1,\infty}(M)}^2\} + \max_{M \in \mathcal{M}_h} \left\{ \frac{h_M^2}{\gamma_M} |\theta|_{W^{1,\infty}(M)}^2 \right\} + \max_{M \in \mathcal{M}_h} \{\gamma_M^{-1} \|\theta\|_{\infty,M}^2\}.
\end{aligned}$$

Proof. We choose the same interpolation operators $j_u: \mathbf{V}^{div} \rightarrow \mathbf{V}_h^{div}$ and $j_\theta: \Theta \rightarrow \Theta_h$ as in Lemma 3.2.9. For the pressure, we use the interpolation operator $j_p: Q \rightarrow Q_h$ from Assumption 3.2.2.

Subtracting (3.1) from (2.9), testing with $(\mathbf{v}_h, q_h) = (\mathbf{e}_{u,h}, e_{p,h}) \in \mathbf{V}_h^{div} \times Q_h$ and using Definition 3.2.1 lead to an error equation for the velocity:

$$\begin{aligned}
0 &= (\partial_t (\mathbf{u} - \mathbf{u}_h), \mathbf{e}_{u,h}) + (\nu \nabla (\mathbf{u} - \mathbf{u}_h), \nabla \mathbf{e}_{u,h}) - (p - p_h, \nabla \cdot \mathbf{e}_{u,h}) + c_u(\mathbf{u}; \mathbf{u}, \mathbf{e}_{u,h}) \\
&- c_u(\mathbf{u}_h; \mathbf{u}_h, \mathbf{e}_{u,h}) - s_u(\mathbf{u}_h; \mathbf{u}_h, \mathbf{e}_{u,h}) - t_h(\mathbf{u}_h; \mathbf{u}_h, \mathbf{e}_{u,h}) - i_h(p_h, e_{p,h}) \\
&+ (\beta \mathbf{g}(\theta - \theta_h), \mathbf{e}_{u,h}) \\
&= (\partial_t \boldsymbol{\eta}_{u,h}, \mathbf{e}_{u,h}) + (\partial_t \mathbf{e}_{u,h}, \mathbf{e}_{u,h}) + (\nu \nabla \boldsymbol{\eta}_{u,h}, \nabla \mathbf{e}_{u,h}) + (\nu \nabla \mathbf{e}_{u,h}, \nabla \mathbf{e}_{u,h}) - (\eta_{p,h}, \nabla \cdot \mathbf{e}_{u,h}) \\
&+ c_u(\mathbf{u}; \mathbf{u}, \mathbf{e}_{u,h}) - c_u(\mathbf{u}_h; \mathbf{u}_h, \mathbf{e}_{u,h}) + s_u(\mathbf{u}_h; \mathbf{e}_{u,h}, \mathbf{e}_{u,h}) + s_u(\mathbf{u}_h; \boldsymbol{\eta}_{u,h}, \mathbf{e}_{u,h}) \\
&- s_u(\mathbf{u}_h; \mathbf{u}, \mathbf{e}_{u,h}) + t_h(\mathbf{u}_h; \mathbf{e}_{u,h}, \mathbf{e}_{u,h}) - t_h(\mathbf{u}_h; j_u \mathbf{u}, \mathbf{e}_{u,h}) \\
&+ i_h(e_{p,h}, e_{p,h}) - i_h(j_p p, e_{p,h}) + \beta(\mathbf{g}e_{\theta,h}, \mathbf{e}_{u,h}) + \beta(\mathbf{g}\eta_{\theta,h}, \mathbf{e}_{u,h}),
\end{aligned}$$

where we used $(e_{p,h}, \nabla \cdot \mathbf{e}_{u,h}) = 0$ due to $\mathbf{e}_{u,h} \in \mathbf{V}_h^{div}$. With the definition of $||| \cdot |||_{LPS}$, the fact that $(\nabla \cdot \mathbf{u}, q) = 0$ for all $q \in L^2(\Omega)$ and continuity of p , this implies

$$\begin{aligned}
& \frac{1}{2} \partial_t \|\mathbf{e}_{u,h}\|_0^2 + |||(\mathbf{e}_{u,h}, e_{p,h})|||_{LPS}^2 \\
&= -(\partial_t \boldsymbol{\eta}_{u,h}, \mathbf{e}_{u,h}) - \nu(\nabla \boldsymbol{\eta}_{u,h}, \nabla \mathbf{e}_{u,h}) + (\eta_{p,h}, \nabla \cdot \mathbf{e}_{u,h}) + c_u(\mathbf{u}_h; \mathbf{u}_h, \mathbf{e}_{u,h}) - c_u(\mathbf{u}; \mathbf{u}, \mathbf{e}_{u,h}) \\
&- s_u(\mathbf{u}_h; \boldsymbol{\eta}_{u,h}, \mathbf{e}_{u,h}) - t_h(\mathbf{u}_h; \boldsymbol{\eta}_{u,h}, \mathbf{e}_{u,h}) - i_h(\eta_{p,h}, e_{p,h}) \\
&+ s_u(\mathbf{u}_h; \mathbf{u}, \mathbf{e}_{u,h}) - \beta(\mathbf{g}e_{\theta,h}, \mathbf{e}_{u,h}) - \beta(\mathbf{g}\eta_{\theta,h}, \mathbf{e}_{u,h}).
\end{aligned}$$

The right-hand side terms are bounded as:

$$\begin{aligned}
-(\partial_t \boldsymbol{\eta}_{u,h}, \mathbf{e}_{u,h}) &\leq \|\partial_t \boldsymbol{\eta}_{u,h}\|_0 \|\mathbf{e}_{u,h}\|_0 \leq \frac{1}{4} \|\partial_t \boldsymbol{\eta}_{u,h}\|_0^2 + \|\mathbf{e}_{u,h}\|_0^2, \\
-\nu (\nabla \boldsymbol{\eta}_{u,h}, \nabla \mathbf{e}_{u,h}) &\leq \sqrt{\nu} \|\nabla \boldsymbol{\eta}_{u,h}\|_0 \|\mathbf{e}_{u,h}\|_{LPS}, \\
(\eta_{p,h}, \nabla \cdot \mathbf{e}_{u,h}) &\leq \left(\sum_{M \in \mathcal{M}_h} \min\left(\frac{d}{\nu}, \frac{1}{\gamma_M}\right) \|\eta_{p,h}\|_{0,M}^2 \right)^{1/2} \|\mathbf{e}_{u,h}\|_{LPS}, \\
-s_u(\mathbf{u}_h; \boldsymbol{\eta}_{u,h}, \mathbf{e}_{u,h}) &\leq \left(\sum_{M \in \mathcal{M}_h} \tau_M^u |\mathbf{u}_M|^2 \|\nabla \boldsymbol{\eta}_{u,h}\|_{0,M}^2 \right)^{1/2} \|\mathbf{e}_{u,h}\|_{LPS}, \\
-t_h(\mathbf{u}_h; \boldsymbol{\eta}_{u,h}, \mathbf{e}_{u,h}) &\leq \left(\sum_{M \in \mathcal{M}_h} \gamma_M d \|\nabla \boldsymbol{\eta}_{u,h}\|_{0,M}^2 \right)^{1/2} \|\mathbf{e}_{u,h}\|_{LPS}, \\
-i_h(\eta_{p,h}, e_{p,h}) &\leq \left(\sum_{E \in \mathcal{E}_h} \phi_E \|\eta_{p,h}\|_{0,E}^2 \right)^{1/2} \left(\sum_{E \in \mathcal{E}_h} \phi_E \|e_{p,h}\|_{0,E}^2 \right)^{1/2}, \\
s_u(\mathbf{u}_h; \mathbf{u}, \mathbf{e}_{u,h}) &\leq \left(\sum_{M \in \mathcal{M}_h} \tau_M^u |\mathbf{u}_M|^2 \|\kappa_M^u(\nabla \mathbf{u})\|_{0,M}^2 \right)^{1/2} \|\mathbf{e}_{u,h}\|_{LPS}, \\
|\beta(\mathbf{g}e_{\theta,h}, \mathbf{e}_{u,h}) + \beta(\mathbf{g}\eta_{\theta,h}, \mathbf{e}_{u,h})| &\leq \beta \|\mathbf{g}\|_\infty (\|e_{\theta,h}\|_0 + \|\eta_{\theta,h}\|_0) \|\mathbf{e}_{u,h}\|_0 \\
&\leq \beta \|\mathbf{g}\|_\infty \left(\|e_{\theta,h}\|_0^2 + \frac{1}{4} \|\mathbf{e}_{u,h}\|_0^2 + \frac{1}{3} \|\eta_{\theta,h}\|_0^2 + \frac{3}{4} \|\mathbf{e}_{u,h}\|_0^2 \right) \\
&= \beta \|\mathbf{g}\|_\infty \left(\|e_{\theta,h}\|_0^2 + \|\mathbf{e}_{u,h}\|_0^2 \right) + \frac{\beta \|\mathbf{g}\|_\infty}{3} \|\eta_{\theta,h}\|_0^2.
\end{aligned}$$

Due to $\|\mathbf{e}_{u,h}\|_{LPS} \leq \|(\mathbf{e}_{u,h}, e_{p,h})\|_{LPS}$, this implies

$$\begin{aligned}
&\frac{1}{2} \partial_t \|\mathbf{e}_{u,h}\|_0^2 + \|(\mathbf{e}_{u,h}, e_{p,h})\|_{LPS}^2 \\
&\leq \frac{1}{4} \|\partial_t \boldsymbol{\eta}_{u,h}\|_0^2 + \|\mathbf{e}_{u,h}\|_0^2 + c_u(\mathbf{u}_h; \mathbf{u}_h, \mathbf{e}_{u,h}) - c_u(\mathbf{u}; \mathbf{u}, \mathbf{e}_{u,h}) \\
&+ \|(\mathbf{e}_{u,h}, e_{p,h})\|_{LPS} \left[\sqrt{\nu} \|\nabla \boldsymbol{\eta}_{u,h}\|_0 + \left(\sum_{M \in \mathcal{M}_h} \tau_M^u |\mathbf{u}_M|^2 \|\nabla \boldsymbol{\eta}_{u,h}\|_{0,M}^2 \right)^{1/2} \right. \\
&+ \left. \left(\sum_{M \in \mathcal{M}_h} \gamma_M d \|\nabla \boldsymbol{\eta}_{u,h}\|_{0,M}^2 \right)^{1/2} + \left(\sum_{M \in \mathcal{M}_h} \min\left(\frac{d}{\nu}, \frac{1}{\gamma_M}\right) \|\eta_{p,h}\|_{0,M}^2 \right)^{1/2} \right. \\
&+ \left. \left(\sum_{M \in \mathcal{M}_h} \tau_M^u |\mathbf{u}_M|^2 \|\kappa_M^u(\nabla \mathbf{u})\|_{0,M}^2 \right)^{1/2} + \left. \left(\sum_{E \in \mathcal{E}_h} \phi_E \|\eta_{p,h}\|_{0,E}^2 \right)^{1/2} \right] \\
&+ \beta \|\mathbf{g}\|_\infty \left(\|e_{\theta,h}\|_0^2 + \|\mathbf{e}_{u,h}\|_0^2 \right) + \frac{\beta \|\mathbf{g}\|_\infty}{3} \|\eta_{\theta,h}\|_0^2
\end{aligned}$$

and thus via Young's inequality

$$\begin{aligned}
&\frac{1}{2} \partial_t \|\mathbf{e}_{u,h}\|_0^2 + (1 - 2\varepsilon) \|(\mathbf{e}_{u,h}, e_{p,h})\|_{LPS}^2 \\
&\leq \frac{1}{4} \|\partial_t \boldsymbol{\eta}_{u,h}\|_0^2 + \|\mathbf{e}_{u,h}\|_0^2 + [c_u(\mathbf{u}_h; \mathbf{u}_h, \mathbf{e}_{u,h}) - c_u(\mathbf{u}; \mathbf{u}, \mathbf{e}_{u,h})]
\end{aligned}$$

$$\begin{aligned}
& + \frac{3}{4\varepsilon} \sum_{M \in \mathcal{M}_h} \left[(\nu + \tau_M^u |\mathbf{u}_M|^2 + \gamma_M d) \|\nabla \boldsymbol{\eta}_{u,h}\|_{0,M}^2 + \min\left(\frac{d}{\nu}, \frac{1}{\gamma_M}\right) \|\eta_{p,h}\|_{0,M}^2 \right. \\
& + \left. \tau_M^u |\mathbf{u}_M|^2 \|\kappa_M^u (\nabla \mathbf{u})\|_{0,M}^2 \right] + \frac{3}{4\varepsilon} \sum_{E \in \mathcal{E}_h} \phi_E \|\eta_{p,h}\|_{0,E}^2 \\
& + \beta \|\mathbf{g}\|_\infty \left(\|e_{\theta,h}\|_0^2 + \|\mathbf{e}_{u,h}\|_0^2 \right) + \frac{\beta \|\mathbf{g}\|_\infty}{3} \|\eta_{\theta,h}\|_0^2. \tag{3.36}
\end{aligned}$$

Lemma 3.2.9 yields for the convective terms:

$$\begin{aligned}
& c_u(\mathbf{u}; \mathbf{u}, \mathbf{e}_{u,h}) - c_u(\mathbf{u}_h; \mathbf{u}_h, \mathbf{e}_{u,h}) \\
& \leq \frac{1}{4\varepsilon} \sum_{M \in \mathcal{M}_h} \frac{1 + \nu Re_M^2}{h_M^2} \|\boldsymbol{\eta}_{u,h}\|_{0,M}^2 + 3\varepsilon \|\boldsymbol{\eta}_{u,h}\|_{LPS}^2 + 4\varepsilon \|\mathbf{e}_{u,h}\|_{LPS}^2 \\
& + \left[|\mathbf{u}|_{W^{1,\infty}(\Omega)} + \varepsilon \max_{M \in \mathcal{M}_h} \{h_M^2 |\mathbf{u}|_{W^{1,\infty}(M)}^2\} + \frac{C}{\varepsilon} \max_{M \in \mathcal{M}_h} \left\{ \frac{h_M^2}{\gamma_M} |\mathbf{u}|_{W^{1,\infty}(M)}^2 \right\} \right. \\
& \left. + \frac{C}{\varepsilon} \max_{M \in \mathcal{M}_h} \{\gamma_M^{-1} \|\mathbf{u}\|_{\infty,M}^2\} \right] \|\mathbf{e}_{u,h}\|_0^2.
\end{aligned}$$

We incorporate this into (3.36) and obtain with a constant C independent of the problem parameters, h_M , h_L , the solutions and ε

$$\begin{aligned}
& \frac{1}{2} \partial_t \|\mathbf{e}_{u,h}\|_0^2 + (1 - 6\varepsilon) \|(\mathbf{e}_{u,h}, e_{p,h})\|_{LPS}^2 \\
& \leq \frac{1}{4} \|\partial_t \boldsymbol{\eta}_{u,h}\|_0^2 + \frac{C}{\varepsilon} \sum_{M \in \mathcal{M}_h} \frac{1 + \nu Re_M^2}{h_M^2} \|\boldsymbol{\eta}_{u,h}\|_{0,M}^2 + \left[1 + \beta \|\mathbf{g}\|_\infty \right. \\
& + \left. |\mathbf{u}|_{W^{1,\infty}(\Omega)} + \varepsilon \max_{M \in \mathcal{M}_h} \{h_M^2 |\mathbf{u}|_{W^{1,\infty}(M)}^2\} + \frac{C}{\varepsilon} \max_{M \in \mathcal{M}_h} \left\{ \frac{h_M^2}{\gamma_M} |\mathbf{u}|_{W^{1,\infty}(M)}^2 \right\} \right. \\
& + \left. \frac{C}{\varepsilon} \max_{M \in \mathcal{M}_h} \{\gamma_M^{-1} \|\mathbf{u}\|_{\infty,M}^2\} \right] \|\mathbf{e}_{u,h}\|_0^2 + \frac{C}{\varepsilon} \sum_{M \in \mathcal{M}_h} \left[(\nu + \tau_M^u |\mathbf{u}_M|^2 + \gamma_M d) \|\nabla \boldsymbol{\eta}_{u,h}\|_{0,M}^2 \right. \\
& + \left. \min\left(\frac{d}{\nu}, \frac{1}{\gamma_M}\right) \|\eta_{p,h}\|_{0,M}^2 + \tau_M^u |\mathbf{u}_M|^2 \|\kappa_M^u (\nabla \mathbf{u})\|_{0,M}^2 \right] + \frac{C}{\varepsilon} \sum_{E \in \mathcal{E}_h} \phi_E \|\eta_{p,h}\|_{0,E}^2 \\
& + \beta \|\mathbf{g}\|_\infty \|e_{\theta,h}\|_0^2 + C \beta \|\mathbf{g}\|_\infty \|\eta_{\theta,h}\|_0^2. \tag{3.37}
\end{aligned}$$

Now, subtracting (3.2) from (2.10) with $\psi_h = e_{\theta,h} \in \Theta_h$ as a test function leads to an error equation for the temperature:

$$\begin{aligned}
0 & = (\partial_t(\theta - \theta_h), e_{\theta,h}) + (\alpha \nabla(\theta - \theta_h), \nabla e_{\theta,h}) + c_\theta(\mathbf{u}; \theta, e_{\theta,h}) \\
& - c_\theta(\mathbf{u}_h; \theta_h, e_{\theta,h}) - s_\theta(\mathbf{u}_h; \theta_h, e_{\theta,h}) \\
& = (\partial_t \eta_{\theta,h}, e_{\theta,h}) + (\partial_t e_{\theta,h}, e_{\theta,h}) + (\alpha \nabla \eta_{\theta,h}, \nabla e_{\theta,h}) + (\alpha \nabla e_{\theta,h}, \nabla e_{\theta,h}) \\
& + c_\theta(\mathbf{u}; \theta, e_{\theta,h}) - c_\theta(\mathbf{u}_h; \theta_h, e_{\theta,h}) + s_\theta(\mathbf{u}_h; e_{\theta,h}, e_{\theta,h}) - s_\theta(\mathbf{u}_h; j_\theta \theta, e_{\theta,h}).
\end{aligned}$$

We utilize the definition of $[\cdot]_{LPS}$ and calculate

$$\begin{aligned} \frac{1}{2}\partial_t \|e_{\theta,h}\|_0^2 + [e_{\theta,h}]_{LPS}^2 &= -(\partial_t \eta_{\theta,h}, e_{\theta,h}) - \alpha(\nabla \eta_{\theta,h}, \nabla e_{\theta,h}) \\ &\quad + c_\theta(\mathbf{u}_h; \theta_h, e_{\theta,h}) - c_\theta(\mathbf{u}; \theta, e_{\theta,h}) - s_\theta(\mathbf{u}_h; \eta_{\theta,h}, e_{\theta,h}) + s_\theta(\mathbf{u}_h; \theta, e_{\theta,h}). \end{aligned}$$

In a similar way as for the velocity terms, we estimate:

$$\begin{aligned} -(\partial_t \eta_{\theta,h}, e_{\theta,h}) &\leq \|\partial_t \eta_{\theta,h}\|_0 \|e_{\theta,h}\|_0 \leq \frac{1}{4} \|\partial_t \eta_{\theta,h}\|_0^2 + \|e_{\theta,h}\|_0^2, \\ -\alpha(\nabla \eta_{\theta,h}, \nabla e_{\theta,h}) &\leq \sqrt{\alpha} \|\nabla \eta_{\theta,h}\|_0 [e_{\theta,h}]_{LPS}, \\ -s_\theta(\mathbf{u}_h; \eta_{\theta,h}, e_{\theta,h}) &\leq \left(\sum_{L \in \mathcal{L}_h} \tau_L^\theta |\mathbf{u}_L|^2 \|\nabla \eta_{\theta,h}\|_{0,L}^2 \right)^{1/2} [e_{\theta,h}]_{LPS}, \\ s_\theta(\mathbf{u}_h; \theta, e_{\theta,h}) &\leq \left(\sum_{L \in \mathcal{L}_h} \tau_L^\theta |\mathbf{u}_L|^2 \|\kappa_L^\theta(\nabla \theta)\|_{0,L}^2 \right)^{1/2} [e_{\theta,h}]_{LPS}. \end{aligned}$$

With Young's inequality, we have

$$\begin{aligned} &\frac{1}{2}\partial_t \|e_{\theta,h}\|_0^2 + (1 - 2\varepsilon)[e_{\theta,h}]_{LPS}^2 \\ &\leq \frac{1}{4} \|\partial_t \eta_{\theta,h}\|_0^2 + \|e_{\theta,h}\|_0^2 + c_\theta(\mathbf{u}_h; \theta_h, e_{\theta,h}) - c_\theta(\mathbf{u}; \theta, e_{\theta,h}) \\ &\quad + \frac{3}{8\varepsilon} \sum_{L \in \mathcal{L}_h} \left[(\alpha + \tau_L^\theta |\mathbf{u}_L|^2) \|\nabla \eta_{\theta,h}\|_{0,L}^2 + \tau_L^\theta |\mathbf{u}_L|^2 \|\kappa_L^\theta(\nabla \theta)\|_{0,L}^2 \right]. \end{aligned} \quad (3.38)$$

Due to Lemma 3.2.9, the difference of the convective terms in the Fourier equation can be bounded by:

$$\begin{aligned} &c_\theta(\mathbf{u}; \theta, e_{\theta,h}) - c_\theta(\mathbf{u}_h; \theta_h, e_{\theta,h}) \\ &\leq \frac{1}{4\varepsilon} \sum_{M \in \mathcal{M}_h} \frac{1}{h_M^2} \|\boldsymbol{\eta}_{u,h}\|_{0,M}^2 + 3\varepsilon \|\boldsymbol{\eta}_{u,h}\|_{LPS}^2 + 3\varepsilon \|\mathbf{e}_{u,h}\|_{LPS}^2 + 7\varepsilon [e_{\theta,h}]_{LPS}^2 \\ &\quad + \frac{1}{28\varepsilon} \sum_{L \in \mathcal{L}_h} \frac{\alpha P e_L^2}{h_L^2} \|\eta_{\theta,h}\|_{0,L}^2 + \frac{1}{2} \|\theta\|_{W^{1,\infty}(\Omega)} \|\mathbf{e}_{u,h}\|_0^2 + \|e_{\theta,h}\|_0^2 \left(\frac{1}{2} \|\theta\|_{W^{1,\infty}(\Omega)} \right. \\ &\quad \left. + \varepsilon \max_{M \in \mathcal{M}_h} \{h_M^2 |\theta|_{W^{1,\infty}(M)}^2\} + \frac{C}{\varepsilon} \max_{M \in \mathcal{M}_h} \left\{ \frac{h_M^2}{\gamma_M} |\theta|_{W^{1,\infty}(M)}^2 \right\} + \frac{C}{\varepsilon} \max_{M \in \mathcal{M}_h} \{ \gamma_M^{-1} \|\theta\|_{\infty,M}^2 \} \right). \end{aligned} \quad (3.39)$$

The combination of (3.38) and (3.39) with a constant C independent of the problem parameters, h_M , h_L , the solutions and ε gives

$$\frac{1}{2}\partial_t \|e_{\theta,h}\|_0^2 + (1 - 9\varepsilon)[e_{\theta,h}]_{LPS}^2 \leq \frac{1}{4} \|\partial_t \eta_{\theta,h}\|_0^2 + \frac{C}{\varepsilon} \sum_{L \in \mathcal{L}_h} \frac{\alpha P e_L^2}{h_L^2} \|\eta_{\theta,h}\|_{0,L}^2$$

$$\begin{aligned}
& + \frac{C}{\varepsilon} \sum_{M \in \mathcal{M}_h} \frac{1}{h_M^2} \|\boldsymbol{\eta}_{u,h}\|_{0,M}^2 + 3\varepsilon \|\boldsymbol{\eta}_{u,h}\|_{LPS}^2 + 3\varepsilon \|\mathbf{e}_{u,h}\|_{LPS}^2 + \frac{1}{2} |\theta|_{W^{1,\infty}(\Omega)} \|\mathbf{e}_{u,h}\|_0^2 \\
& + \left[1 + \frac{1}{2} |\theta|_{W^{1,\infty}(\Omega)} + \varepsilon \max_{M \in \mathcal{M}_h} \{h_M^2 |\theta|_{W^{1,\infty}(M)}^2\} \right. \\
& + \left. \frac{C}{\varepsilon} \max_{M \in \mathcal{M}_h} \left\{ \frac{h_M^2}{\gamma_M} |\theta|_{W^{1,\infty}(M)}^2 \right\} + \frac{C}{\varepsilon} \max_{M \in \mathcal{M}_h} \{ \gamma_M^{-1} \|\theta\|_{\infty,M}^2 \} \right] \|e_{\theta,h}\|_0^2 \\
& + \frac{C}{\varepsilon} \sum_{L \in \mathcal{L}_h} \left[(\alpha + \tau_L^\theta |\mathbf{u}_L|^2) \|\nabla \eta_{\theta,h}\|_{0,L}^2 + \tau_L^\theta |\mathbf{u}_L|^2 \|\kappa_L^\theta(\nabla \theta)\|_{0,L}^2 \right]. \tag{3.40}
\end{aligned}$$

Note that

$$\|\boldsymbol{\eta}_{u,h}\|_{LPS}^2 \leq \sum_{M \in \mathcal{M}_h} (\nu + \tau_M^u |\mathbf{u}_M|^2 + \gamma_M d) \|\nabla \boldsymbol{\eta}_{u,h}\|_{0,M}^2.$$

Adding (3.37) and (3.40) results in

$$\begin{aligned}
& \frac{1}{2} \partial_t \|\mathbf{e}_{u,h}\|_0^2 + (1 - 9\varepsilon) \|\mathbf{e}_{u,h}, e_{p,h}\|_{LPS}^2 + \frac{1}{2} \partial_t \|e_{\theta,h}\|_0^2 + (1 - 9\varepsilon) \|e_{\theta,h}\|_{LPS}^2 \\
& \leq \frac{1}{4} \|\partial_t \boldsymbol{\eta}_{u,h}\|_0^2 + \frac{1}{4} \|\partial_t \eta_{\theta,h}\|_0^2 + \frac{C}{\varepsilon} \sum_{M \in \mathcal{M}_h} \frac{2 + \nu Re_M^2}{h_M^2} \|\boldsymbol{\eta}_{u,h}\|_{0,M}^2 \\
& + \left[1 + \beta \|\mathbf{g}\|_\infty + |\mathbf{u}|_{W^{1,\infty}(\Omega)} + \varepsilon \max_{M \in \mathcal{M}_h} \{h_M^2 |\mathbf{u}|_{W^{1,\infty}(M)}^2\} + \frac{C}{\varepsilon} \max_{M \in \mathcal{M}_h} \left\{ \frac{h_M^2}{\gamma_M} |\mathbf{u}|_{W^{1,\infty}(M)}^2 \right\} \right. \\
& + \left. \frac{C}{\varepsilon} \max_{M \in \mathcal{M}_h} \{ \gamma_M^{-1} \|\mathbf{u}\|_{\infty,M}^2 \} + \frac{1}{2} |\theta|_{W^{1,\infty}(\Omega)} \right] \|\mathbf{e}_{u,h}\|_0^2 \\
& + \left(\frac{C}{\varepsilon} + C\varepsilon \right) \sum_{M \in \mathcal{M}_h} (\nu + \tau_M^u |\mathbf{u}_M|^2 + \gamma_M d) \|\nabla \boldsymbol{\eta}_{u,h}\|_{0,M}^2 \\
& + \frac{C}{\varepsilon} \sum_{M \in \mathcal{M}_h} \left[\min \left(\frac{d}{\nu}, \frac{1}{\gamma_M} \right) \|\eta_{p,h}\|_{0,M}^2 + \tau_M^u |\mathbf{u}_M|^2 \|\kappa_M^u(\nabla \mathbf{u})\|_{0,M}^2 \right] \\
& + \frac{C}{\varepsilon} \sum_{E \in \mathcal{E}_h} \phi_E \|\eta_{p,h}\|_{E}^2 + \sum_{L \in \mathcal{L}_h} \left(\frac{C \alpha P e_L^2}{\varepsilon h_L^2} + C\beta \|\mathbf{g}\|_{\infty,L} \right) \|\eta_{\theta,h}\|_{0,L}^2 \\
& + \left[1 + \frac{1}{2} |\theta|_{W^{1,\infty}(\Omega)} + \beta \|\mathbf{g}\|_\infty + \varepsilon \max_{M \in \mathcal{M}_h} \{h_M^2 |\theta|_{W^{1,\infty}(M)}^2\} \right. \\
& + \left. \frac{C}{\varepsilon} \max_{M \in \mathcal{M}_h} \left\{ \frac{h_M^2}{\gamma_M} |\theta|_{W^{1,\infty}(M)}^2 \right\} + \frac{C}{\varepsilon} \max_{M \in \mathcal{M}_h} \{ \gamma_M^{-1} \|\theta\|_{\infty,M}^2 \} \right] \|e_{\theta,h}\|_0^2 \\
& + \frac{C}{\varepsilon} \sum_{L \in \mathcal{L}_h} \left[(\alpha + \tau_L^\theta |\mathbf{u}_L|^2) \|\nabla \eta_{\theta,h}\|_{0,L}^2 + \tau_L^\theta |\mathbf{u}_L|^2 \|\kappa_L^\theta(\nabla \theta)\|_{0,L}^2 \right].
\end{aligned}$$

We choose $\varepsilon = \frac{1}{18}$ and get (where \lesssim indicates that the left-hand side is smaller or equal than a generic constant times the right-hand side)

$$\partial_t \|\mathbf{e}_{u,h}\|_0^2 + \|\mathbf{e}_{u,h}, e_{p,h}\|_{LPS}^2 + \partial_t \|e_{\theta,h}\|_0^2 + \|e_{\theta,h}\|_{LPS}^2$$

$$\begin{aligned}
&\lesssim \|\partial_t \boldsymbol{\eta}_{u,h}\|_0^2 + \|\partial_t \eta_{\theta,h}\|_0^2 + \sum_{M \in \mathcal{M}_h} \frac{1 + \nu Re_M^2}{h_M^2} \|\boldsymbol{\eta}_{u,h}\|_{0,M}^2 \\
&+ \left[1 + \beta \|\mathbf{g}\|_\infty + |\mathbf{u}|_{W^{1,\infty}(\Omega)} + \max_{M \in \mathcal{M}_h} \{h_M^2 |\mathbf{u}|_{W^{1,\infty}(M)}^2\} + \max_{M \in \mathcal{M}_h} \left\{ \frac{h_M^2}{\gamma_M} |\mathbf{u}|_{W^{1,\infty}(M)}^2 \right\} \right. \\
&+ \max_{M \in \mathcal{M}_h} \{ \gamma_M^{-1} \|\mathbf{u}\|_{\infty,M}^2 \} + |\theta|_{W^{1,\infty}(\Omega)} \left. \right] \|\mathbf{e}_{u,h}\|_0^2 \\
&+ \sum_{M \in \mathcal{M}_h} (\nu + \tau_M^u |\mathbf{u}_M|^2 + \gamma_M d) \|\nabla \boldsymbol{\eta}_{u,h}\|_{0,M}^2 \\
&+ \sum_{M \in \mathcal{M}_h} \left[\min\left(\frac{d}{\nu}, \frac{1}{\gamma_M}\right) \|\eta_{p,h}\|_{0,M}^2 + \tau_M^u |\mathbf{u}_M|^2 \|\kappa_M^u(\nabla \mathbf{u})\|_{0,M}^2 \right] \\
&+ \sum_{E \in \mathcal{E}_h} \phi_E \|\llbracket \eta_{p,h} \rrbracket_E\|_{0,E}^2 + \sum_{L \in \mathcal{L}_h} \left(\frac{\alpha P e_L^2}{h_L^2} + \beta \|\mathbf{g}\|_{\infty,L} \right) \|\eta_{\theta,h}\|_{0,L}^2 \\
&+ \left[1 + |\theta|_{W^{1,\infty}(\Omega)} + \beta \|\mathbf{g}\|_\infty + \max_{M \in \mathcal{M}_h} \{h_M^2 |\theta|_{W^{1,\infty}(M)}^2\} \right. \\
&+ \max_{M \in \mathcal{M}_h} \left\{ \frac{h_M^2}{\gamma_M} |\theta|_{W^{1,\infty}(M)}^2 \right\} + \max_{M \in \mathcal{M}_h} \{ \gamma_M^{-1} \|\theta\|_{\infty,M}^2 \} \left. \right] \|e_{\theta,h}\|_0^2 \\
&+ \sum_{L \in \mathcal{L}_h} \left[(\alpha + \tau_L^\theta |\mathbf{u}_L|^2) \|\nabla \eta_{\theta,h}\|_{0,L}^2 + \tau_L^\theta |\mathbf{u}_L|^2 \|\kappa_L^\theta(\nabla \theta)\|_{0,L}^2 \right].
\end{aligned}$$

We require that all the terms on the right-hand side are integrable in time. This holds due to the regularity assumptions on \mathbf{u} and θ , Assumption 3.2.11, $\mathbf{g} \in L^\infty(0, T; [L^\infty(\Omega)]^d)$ and the fact that the fluctuation operators are bounded. Application of Gronwall's Lemma A.3.5 for $\|(\mathbf{e}_{u,h}, e_{\theta,h})\|_0^2 := \|\mathbf{e}_{u,h}\|_0^2 + \|e_{\theta,h}\|_0^2$ with the Gronwall constant

$$\begin{aligned}
C_{G,h}(\mathbf{u}, \theta) &= 1 + \beta \|\mathbf{g}\|_\infty + |\mathbf{u}|_{W^{1,\infty}(\Omega)} + |\theta|_{W^{1,\infty}(\Omega)} \\
&+ \max_{M \in \mathcal{M}_h} \{h_M^2 |\mathbf{u}|_{W^{1,\infty}(M)}^2\} + \max_{M \in \mathcal{M}_h} \left\{ \frac{h_M^2}{\gamma_M} |\mathbf{u}|_{W^{1,\infty}(M)}^2 \right\} + \max_{M \in \mathcal{M}_h} \{ \gamma_M^{-1} \|\mathbf{u}\|_{\infty,M}^2 \} \\
&+ \max_{M \in \mathcal{M}_h} \{h_M^2 |\theta|_{W^{1,\infty}(M)}^2\} + \max_{M \in \mathcal{M}_h} \left\{ \frac{h_M^2}{\gamma_M} |\theta|_{W^{1,\infty}(M)}^2 \right\} + \max_{M \in \mathcal{M}_h} \{ \gamma_M^{-1} \|\theta\|_{\infty,M}^2 \}
\end{aligned}$$

gives the claim since the initial error $(\mathbf{e}_{u,h}, e_{\theta,h})(0)$ vanishes. \square

Corollary 3.2.13 (Method of quasi-optimal order).

Consider a solution $(\mathbf{u}, p, \theta): [0, T] \rightarrow \mathbf{V}^{div} \times Q \times \Theta$ of (2.9)-(2.10) satisfying

$$\begin{aligned}
\mathbf{u} &\in L^\infty(0, T; [W^{1,\infty}(\Omega)]^d) \cap L^2(0, T; [W^{k_u+1,2}(\Omega)]^d), \\
\partial_t \mathbf{u} &\in L^2(0, T; [W^{k_u,2}(\Omega)]^d), \quad p \in L^2(0, T; W^{k_p+1,2}(\Omega) \cap C(\Omega)), \\
\theta &\in L^\infty(0, T; W^{1,\infty}(\Omega)) \cap L^2(0, T; W^{k_\theta+1,2}(\Omega)), \\
\partial_t \theta &\in L^2(0, T; W^{k_\theta,2}(\Omega))
\end{aligned}$$

and a solution $(\mathbf{u}_h, p_h, \theta_h): [0, T] \rightarrow \mathbf{V}_h^{div} \times Q_h \times \Theta_h$ of (3.1)-(3.2). Let Assumptions 3.2.2, 3.2.3 and 3.2.11 be valid as well as $\mathbf{u}_h(0) = j_u \mathbf{u}_0$, $\theta_h(0) = j_\theta \theta_0$ hold. For $0 \leq t \leq T$, we obtain the a priori estimate for the semi-discrete error $\xi_{u,h} = \mathbf{u} - \mathbf{u}_h$, $\xi_{p,h} = p - p_h$, $\xi_{\theta,h} = \theta - \theta_h$:

$$\begin{aligned}
& \|\xi_{u,h}\|_{L^\infty(0,t;L^2(\Omega))}^2 + \|\xi_{\theta,h}\|_{L^\infty(0,t;L^2(\Omega))}^2 + \int_0^t \left(\|(\xi_{u,h}, \xi_{p,h})(\tau)\|_{LPS}^2 + \|[\xi_{\theta,h}(\tau)]\|_{LPS}^2 \right) d\tau \\
& \leq C \int_0^t e^{C_{G,h}(\mathbf{u},\theta)(t-\tau)} \left\{ \sum_{M \in \mathcal{M}_h} h_M^{2k_u} \left[(1 + \nu Re_M^2 + \nu + \tau_M^u |\mathbf{u}_M|^2 + \gamma_M d) \|\mathbf{u}(\tau)\|_{W^{k_u+1,2}(\omega_M)}^2 \right. \right. \\
& \quad \left. \left. + \|\partial_t \mathbf{u}(\tau)\|_{W^{k_u,2}(\omega_M)}^2 + \tau_M^u |\mathbf{u}_M|^2 h_M^{2(s_u-k_u)} \|\mathbf{u}(\tau)\|_{W^{s_u+1,2}(\omega_M)}^2 \right] \right. \\
& \quad \left. + \sum_{M \in \mathcal{M}_h} h_M^{2(k_p+1)} \left[\min\left(\frac{d}{\nu}, \frac{1}{\gamma_M}\right) + \max_{T \subset M, E \in \partial T} \left\{ \frac{\phi_E}{h_T} \right\} \right] \|p(\tau)\|_{W^{k_p+1,2}(\omega_M)}^2 \right. \\
& \quad \left. + \sum_{L \in \mathcal{L}_h} h_L^{2k_\theta} \left[\|\partial_t \theta(\tau)\|_{W^{k_\theta,2}(\omega_L)}^2 + \left(\alpha Pe_L^2 + h_L^2 \beta \|\mathbf{g}\|_{\infty,L} + \alpha + \tau_L^\theta |\mathbf{u}_L|^2 \right) \|\theta(\tau)\|_{W^{k_\theta+1,2}(\omega_L)}^2 \right. \right. \\
& \quad \left. \left. + \tau_L^\theta |\mathbf{u}_L|^2 h_L^{2(s_\theta-k_\theta)} \|\theta(\tau)\|_{W^{s_\theta+1,2}(\omega_L)}^2 \right] \right\} d\tau \tag{3.41}
\end{aligned}$$

with the local Reynolds number $Re_M = h_M \|\mathbf{u}_h\|_{\infty,M} / \nu$, the local Péclet number $Pe_L = \|\mathbf{u}_h\|_{\infty,L} h_L / \alpha$, $s_u \in \{0, \dots, k_u\}$, $s_\theta \in \{0, \dots, k_\theta\}$ and the Gronwall constant

$$\begin{aligned}
C_{G,h}(\mathbf{u}, \theta) &= 1 + \beta \|\mathbf{g}\|_\infty + |\mathbf{u}|_{W^{1,\infty}(\Omega)} + |\theta|_{W^{1,\infty}(\Omega)} \\
& \quad + \max_{M \in \mathcal{M}_h} \{h_M^2 |\mathbf{u}|_{W^{1,\infty}(M)}^2\} + \max_{M \in \mathcal{M}_h} \left\{ \frac{h_M^2}{\gamma_M} |\mathbf{u}|_{W^{1,\infty}(M)}^2 \right\} + \max_{M \in \mathcal{M}_h} \{\gamma_M^{-1} \|\mathbf{u}\|_{\infty,M}^2\} \\
& \quad + \max_{M \in \mathcal{M}_h} \{h_M^2 |\theta|_{W^{1,\infty}(M)}^2\} + \max_{M \in \mathcal{M}_h} \left\{ \frac{h_M^2}{\gamma_M} |\theta|_{W^{1,\infty}(M)}^2 \right\} + \max_{M \in \mathcal{M}_h} \{\gamma_M^{-1} \|\theta\|_{\infty,M}^2\}. \tag{3.42}
\end{aligned}$$

Proof. We split the semi-discrete error as

$$\xi_{u,h} = \boldsymbol{\eta}_{u,h} + \mathbf{e}_{u,h}, \quad \xi_{\theta,h} = \eta_{\theta,h} + e_{\theta,h}, \quad \xi_{p,h} = \eta_{p,h} + e_{p,h}$$

and use the triangle inequality in order to estimate the approximation and consistency errors separately. The interpolation results in $\mathbf{V}_h^{div} \times Q_h \times \Theta_h$, according to Assumption 3.2.2, are applied to Theorem 3.2.12. Further, we take advantage of the approximation properties of the fluctuation operators from Assumption 3.2.3 with $s_u \in \{0, \dots, k_u\}$, $s_\theta \in \{0, \dots, k_\theta\}$. This provides a bound for the consistency error in the following way for all $0 \leq \tau \leq t \leq T$

$$\sum_{M \in \mathcal{M}_h} (\nu + \tau_M^u |\mathbf{u}_M|^2 + d\gamma_M) \|\nabla \boldsymbol{\eta}_{u,h}(\tau)\|_{0,M}^2$$

$$\begin{aligned}
& + \sum_{M \in \mathcal{M}_h} (1 + \nu R e_M^2) h_M^{-2} \|\boldsymbol{\eta}_{u,h}(\tau)\|_{0,M}^2 + \sum_{M \in \mathcal{M}_h} \min\left(\frac{d}{\nu}, \frac{1}{\gamma_M}\right) \|\eta_{p,h}(\tau)\|_{0,M}^2 \\
& + \sum_{L \in \mathcal{L}_h} \left(\frac{\alpha P e_L^2}{h_L^2} + \beta \|\mathbf{g}\|_{\infty,L} \right) \|\eta_{\theta,h}(\tau)\|_{0,L}^2 + (\alpha + \tau_L^\theta |\mathbf{u}_L|^2) \|\nabla \eta_{\theta,h}(\tau)\|_{0,L}^2 \\
& \leq C \sum_{M \in \mathcal{M}_h} h_M^{2k_u} (1 + \nu R e_M^2 + \tau_M^u |\mathbf{u}_M|^2 + d \gamma_M) \|\mathbf{u}(\tau)\|_{W^{k_u+1,2}(\omega_M)}^2 \\
& + C \sum_{M \in \mathcal{M}_h} h_M^{2(k_p+1)} \min\left(\frac{d}{\nu}, \frac{1}{\gamma_M}\right) \|p(\tau)\|_{W^{k_p+1,2}(\omega_M)}^2 \\
& + \sum_{L \in \mathcal{L}_h} h_L^{2k_\theta} (\alpha P e_L^2 + h_L^2 \beta \|\mathbf{g}\|_{\infty,L} + \alpha + \tau_L^\theta |\mathbf{u}_L|^2) \|\theta(\tau)\|_{W^{k_\theta+1,2}(\omega_L)}^2.
\end{aligned}$$

Furthermore, it holds

$$\begin{aligned}
\|\partial_t \boldsymbol{\eta}_{u,h}(\tau)\|_0^2 & \leq C \sum_{M \in \mathcal{M}_h} h_M^{2k_u} \|\partial_t \mathbf{u}(\tau)\|_{W^{k_u,2}(\omega_M)}^2, \\
\tau_M^u |\mathbf{u}_M|^2 \|\kappa_M^u (\nabla \mathbf{u}(\tau))\|_{0,M}^2 & \leq C \sum_{M \in \mathcal{M}_h} \tau_M^u |\mathbf{u}_M|^2 h_M^{2s_u} \|\mathbf{u}\|_{W^{s_u+1,2}(\omega_M)}^2, \\
\|\partial_t \eta_{\theta,h}(\tau)\|_0^2 & \leq C \sum_{L \in \mathcal{L}_h} h_L^{2k_\theta} \|\partial_t \theta(\tau)\|_{W^{k_\theta,2}(\omega_L)}^2, \\
\tau_L^\theta |\mathbf{u}_L|^2 \|\kappa_L^\theta (\nabla \theta(\tau))\|_{0,L}^2 & \leq C \sum_{L \in \mathcal{L}_h} \tau_L^\theta |\mathbf{u}_L|^2 h_L^{2s_\theta} \|\theta(\tau)\|_{W^{s_\theta+1,2}(\omega_L)}^2.
\end{aligned}$$

For the pressure jump term, we utilize the trace inequality [A.3.3](#):

$$\begin{aligned}
\sum_{E \in \mathcal{E}_h} \phi_E \|\llbracket \eta_{p,h}(\tau) \rrbracket_E\|_{0,E}^2 & \leq \sum_{M \in \mathcal{M}_h} \sum_{T \subset M} \sum_{E \in \partial T} \phi_E \|\llbracket \eta_{p,h}(\tau) \rrbracket_E\|_{0,E}^2 \\
& \leq C_{tr} \sum_{M \in \mathcal{M}_h} \sum_{T \subset M} \max_{E \in \partial T} \phi_E (h_T^{-1} \|\eta_{p,h}(\tau)\|_{0,T}^2 + h_T \|\nabla \eta_{p,h}(\tau)\|_{0,T}^2) \\
& \leq C \sum_{M \in \mathcal{M}_h} \max_{T \subset M, E \in \partial T} \left\{ \frac{\phi_E}{h_T} \right\} h_M^{2(k_p+1)} \|p(\tau)\|_{W^{k_p+1,2}(\omega_M)}^2,
\end{aligned}$$

where we applied $h_T \leq h_M \leq Ch_T$ and the approximation property of $j_p p$ due to Assumption [3.2.2](#). For the interpolation errors, we exploit the approximation properties from Assumption [3.2.2](#):

$$\begin{aligned}
\|\boldsymbol{\eta}_{u,h}(\tau)\|_0^2 & \leq C \sum_{M \in \mathcal{M}_h} h_M^{2(k_u+1)} \|\mathbf{u}(\tau)\|_{W^{k_u+1,2}(\omega_M)}^2, \\
\|\eta_{\theta,h}(\tau)\|_0^2 & \leq C \sum_{L \in \mathcal{L}_h} h_L^{2(k_\theta+1)} \|\theta(\tau)\|_{W^{k_\theta+1,2}(\omega_L)}^2, \\
\|(\boldsymbol{\eta}_{u,h}, \eta_{p,h})(\tau)\|_{LPS}^2 & \leq \sum_{M \in \mathcal{M}_h} (\nu + \tau_M^u |\mathbf{u}_M|^2 + \gamma_M d) \|\nabla \boldsymbol{\eta}_{u,h}(\tau)\|_{0,M}^2 + \sum_{E \in \mathcal{E}_h} \phi_E \|\llbracket \eta_{p,h} \rrbracket_E\|_{0,E}^2
\end{aligned}$$

$$\begin{aligned}
&\leq C \sum_{M \in \mathcal{M}_h} h_M^{2k_u} (\nu + \tau_M^u |\mathbf{u}_M|^2 + \gamma_M d) \|\mathbf{u}(\tau)\|_{W^{k_u+1,2}(\omega_M)}^2 \\
&+ C \sum_{M \in \mathcal{M}_h} \max_{T \subset M, E \in \partial T} \left\{ \frac{\phi_E}{h_T} \right\} h_M^{2(k_p+1)} \|p(\tau)\|_{W^{k_p+1,2}(\omega_M)}^2, \\
\|[\eta_{\theta,h}(\tau)]\|_{LPS}^2 &\leq \sum_{L \in \mathcal{L}_h} (\alpha + \tau_L^\theta |\mathbf{u}_L|^2) \|\nabla \eta_{\theta,h}\|_{0,M}^2 \\
&\leq C \sum_{L \in \mathcal{L}_h} h_L^{2k_\theta} (\alpha + \tau_L^\theta |\mathbf{u}_L|^2) \|\theta(\tau)\|_{W^{k_\theta+1,2}(\omega_L)}^2.
\end{aligned}$$

The combination gives the claim. \square

In the convection dominated regime, the error estimate (3.41) does not blow up for the limit of vanishing ν or α if for all $M \in \mathcal{M}_h$ and $L \in \mathcal{L}_h$

$$Re_M = \frac{h_M \|\mathbf{u}_h\|_{\infty,M}}{\nu} \leq \frac{1}{\sqrt{\nu}} \quad \text{and} \quad Pe_L = \frac{h_L \|\mathbf{u}_h\|_{\infty,L}}{\alpha} \leq \frac{1}{\sqrt{\alpha}}. \quad (3.43)$$

Thus, we obtain a method of order $k := \min\{k_u, k_p + 1, k_\theta\}$ provided that $Re_M \leq C/\sqrt{\nu}$ and $Pe_L \leq C/\sqrt{\alpha}$. This gives a restriction on the local mesh widths h_M and h_L . It is in agreement with our findings for the Oseen equation (cf. [DAL15]) and is less restrictive than the usual condition $Re_M := h_M \|\mathbf{b}\|_{\infty,M}/\nu \leq C$ for the Galerkin method applied to advection-diffusion problems where \mathbf{b} is a stationary velocity field. An alternative stability estimate is given in [MST07] for the stationary Oseen problem which requires the global (and thus more restrictive) condition $Re_\Omega := \frac{\|\mathbf{b}\|_{\infty} C_P}{\nu} \leq \frac{1}{\sqrt{\nu}}$. The restriction (3.43) can be avoided: We refer to Remark 3.2.10 where an alternative estimate for the convective term is given, provided that Assumption 3.2.4 holds. This bears the disadvantage of a Gronwall constant depending on $\|\mathbf{u}_h\|_{\infty}^2$ and thus on the discrete velocity.

Now, we address the question of suitable settings and choices of stabilization parameters for our analysis. The presented approach is applicable to many combinations of ansatz spaces. The interpolation property from Assumption 3.2.2 and the discrete inf-sup condition (Assumption 2.2.1) hold for our finite element setting of Lagrangian elements

$$\mathbf{V}_h = \mathbb{R}_{k_u}^{(+)}, \quad Q_h = \mathbb{R}_{\pm(k_u-1)}, \quad \Theta_h = \mathbb{R}_{k_\theta}^{(+)}$$

from Definition 2.2.7 with $k_u \geq 2$, $k_\theta \geq 2$. In [MT14] (Table 1 and 2), fine and coarse discrete ansatz spaces are presented that fulfill the approximation property of the fluctuation operators (Assumption 3.2.3). We summarize possible variants of the triples $(\mathbf{V}_h/D_M^u) \wedge Q_h \wedge (\Theta_h/D_L^\theta)$ with $s_u \in \{1, \dots, k_u\}$, $s_\theta \in \{1, \dots, k_\theta\}$.

- One-level methods:

$$\begin{aligned}
&(\mathbb{P}_{k_u}/\mathbb{P}_{s_u-1}) \wedge \mathbb{P}_{k_u-1} \wedge (\mathbb{P}_{k_\theta}/\mathbb{P}_{s_\theta-1}), & (\mathbb{Q}_{k_u}/\mathbb{Q}_{s_u-1}) \wedge \mathbb{Q}_{k_u-1} \wedge (\mathbb{Q}_{k_\theta}/\mathbb{Q}_{s_\theta-1}), \\
&(\mathbb{P}_{k_u}^+/\mathbb{P}_{s_u-1}) \wedge \mathbb{P}_{-(k_u-1)} \wedge (\mathbb{P}_{k_\theta}^+/\mathbb{P}_{s_\theta-1}), & (\mathbb{Q}_{k_u}/\mathbb{P}_{s_u-1}) \wedge \mathbb{P}_{-(k_u-1)} \wedge (\mathbb{Q}_{k_\theta}/\mathbb{P}_{s_\theta-1}).
\end{aligned}$$

- Two-level methods (for the construction of the coarse space, see [MST07, MT14]):

$$\begin{aligned} & (\mathbb{P}_{k_u}/\mathbb{P}_{s_u-1}) \wedge \mathbb{P}_{k_u-1} \wedge (\mathbb{P}_{k_\theta}/\mathbb{P}_{s_\theta-1}), & (\mathbb{Q}_{k_u}/\mathbb{Q}_{s_u-1}) \wedge \mathbb{Q}_{k_u-1} \wedge (\mathbb{Q}_{k_\theta}/\mathbb{Q}_{s_\theta-1}), \\ & (\mathbb{P}_{k_u}^+/\mathbb{P}_{s_u-1}) \wedge \mathbb{P}_{-(k_u-1)} \wedge (\mathbb{P}_{k_\theta}^+/\mathbb{P}_{s_\theta-1}), & (\mathbb{Q}_{k_u}/\mathbb{P}_{s_u-1}) \wedge \mathbb{P}_{-(k_u-1)} \wedge (\mathbb{Q}_{k_\theta}/\mathbb{P}_{s_\theta-1}). \end{aligned}$$

With the mesh restriction (3.43), these possibilities result in a parameter choice as

$$\begin{aligned} \gamma_M &= \gamma_0, \quad 0 \leq \phi_E \leq \phi_0 h_T, \\ 0 \leq \tau_M^u(\mathbf{u}_M) &\leq \tau_0^u \frac{h_M^{2(k_u-s_u)}}{|\mathbf{u}_M|^2}, \quad 0 \leq \tau_L^\theta(\mathbf{u}_L) \leq \tau_0^\theta \frac{h_L^{2(k_\theta-s_\theta)}}{|\mathbf{u}_L|^2} \end{aligned} \quad (3.44)$$

for $M \in \mathcal{M}_h$ and $L \in \mathcal{L}_h$, where $\gamma_0, \phi_0, \tau_0^u, \tau_0^\theta = \mathcal{O}(1)$ denote non-negative tuning constants. With the parameter choice (3.44), Assumption 3.2.11 is satisfied. In these possible settings, we can apply Theorem 3.2.12 and Corollary 3.2.13. We point out that in order to get an optimal rate k in (3.41), one might want to choose

$$k := k_u = k_\theta = k_p + 1.$$

A choice of grad-div and LPS SU parameters as in (3.44) balances the terms in the upper bound of the semi-discrete error (3.41). In addition, the Gronwall constant (3.42) does not blow up for small ν if $\gamma_M > 0$. An h -independent γ_M (or at least $\gamma_M \geq Ch$) also diminishes the growth of the Gronwall constant with $\|\mathbf{u}\|_{W^{1,\infty}(\Omega)}$ and $|\theta|_{W^{1,\infty}(\Omega)}$ and is therefore favorable. In case of $\mathbf{u}_M = \mathbf{0}$, we set $\tau_M^u(\mathbf{u}_M) = 0$ and $\tau_L^\theta(\mathbf{u}_L) = 0$ if $\mathbf{u}_L = \mathbf{0}$ as the whole LPS term vanishes. The pressure jump stabilization may be set to zero; in particular, it vanishes for a continuous discrete pressure ansatz space. For discontinuous p_h , the term i_h on the left-hand side gives additional control over the pressure jumps over cells.

For the discussion below, we write $k := k_u = k_\theta = k_p + 1$. In [MT14], a similar bound for the Oseen problem is proposed: $\tau_M^u |\mathbf{b}_M|^2 \leq Ch_M^{k-s_u}$ and $\gamma_M \sim 1$. The design of the grad-div parameter set $\{\gamma_M\}_M$ is still an open problem, see e.g. [JJLR13] for the Stokes problem. An equilibration argument in our analysis (3.41) suggests

$$\gamma_M \sim \max \left(0; \frac{\|p\|_{W^{k,2}(M)}}{\|\mathbf{u}\|_{W^{k+1,2}(M)}} - \nu \right). \quad (3.45)$$

Indeed, in different flow examples, the choice (3.45) yields distinct γ_M : In case of flow with $\mathbf{f}_u \equiv \mathbf{0}$, $(\mathbf{u} \cdot \nabla)\mathbf{u} = \partial_t \mathbf{u} = \mathbf{0}$ and $-\nu \Delta \mathbf{u} + \nabla p = \mathbf{0}$ (Poiseuille flow), we would choose $\gamma_M = 0$, as $\|p\|_{W^{k,2}(\Omega)} / \|\mathbf{u}\|_{W^{k+1,2}(\Omega)} \sim \nu$. For the Taylor-Green vortex with $\mathbf{f}_u \equiv \mathbf{0}$, one has $\partial_t \mathbf{u} - \nu \Delta \mathbf{u} = \mathbf{0}$ and $(\mathbf{u} \cdot \nabla)\mathbf{u} + \nabla p = 0$, thus leading to $\|p\|_{W^{k,2}(\Omega)} / \|\mathbf{u}\|_{W^{k+1,2}(\Omega)} \sim 1$. If ν is small, $\gamma_M \sim 1$ follows. Unfortunately, (3.45) is not a viable choice for γ_M in practice. Especially in the advection dominated case, grad-div stabilization with $\gamma_M > \nu$ has a regularizing effect. Furthermore, $\gamma_M > \nu$ is essential for the independence of the Gronwall

constant $C_{G,h}(\mathbf{u}, \theta)$ of ν . Corollary 3.2.13 and the above discussion clarify that $\gamma_M = \mathcal{O}(1)$ is a reasonable compromise. Our numerical tests also confirm this.

3.2.2. Quasi-Optimal Estimates with LPS-Compatibility Condition

The restrictions $Re_M \leq \nu^{-1/2}$, $Pe_L \leq \alpha^{-1/2}$ in (3.43) stem from the estimate of the convective terms (Lemma 3.2.9) in the analysis of Theorem 3.2.12. Taking Assumption 3.2.6 into account, we can circumvent this. As this represents a compatibility condition between the fine and coarse discrete spaces \mathbf{V}_h/D_M^u and Θ_h/D_L^θ , the number of possible ansatz spaces is limited. Moreover, the interpolation operator $i_u: \mathbf{V} \rightarrow \mathbf{V}_h$ for the velocity does not map to \mathbf{V}_h^{div} in general. Consequently, in addition to the analysis of Theorem 3.2.12, a mixed velocity-pressure term has to be handled. As a first step, we prove a preparatory lemma for the convective terms.

Lemma 3.2.14 (Convective terms with compatibility condition).

Let $\varepsilon > 0$ and Assumptions 3.2.2, 3.2.4, 3.2.5, 3.2.6 hold. Consider solutions $(\mathbf{u}, p, \theta) \in \mathbf{V}^{div} \times Q \times \Theta$, $(\mathbf{u}_h, p_h, \theta_h) \in \mathbf{V}_h^{div} \times Q_h \times \Theta_h$ of (2.9)-(2.10) and (3.1)-(3.2) satisfying $\mathbf{u} \in [W^{1,\infty}(\Omega)]^d$, $\theta \in W^{1,\infty}(\Omega)$, $\mathbf{u}_h \in [W^{1,\infty}(\Omega)]^d$. Let $C > 0$ be a generic constant. For the difference of the convective terms in the momentum equation, we have

$$\begin{aligned} c_u(\mathbf{u}; \mathbf{u}, \mathbf{e}_{u,h}) - c_u(\mathbf{u}_h; \mathbf{u}_h, \mathbf{e}_{u,h}) &\leq \frac{1}{4\varepsilon} \sum_{M \in \mathcal{M}_h} \left(\frac{1}{h_M^2} + \frac{2}{\tau_M^u} \right) \|\boldsymbol{\eta}_{u,h}\|_{0,M}^2 \\ &\quad + 3\varepsilon \|\boldsymbol{\eta}_{u,h}\|_{LPS}^2 + 4\varepsilon \|\mathbf{e}_{u,h}\|_{LPS}^2 \\ &\quad + \left[|\mathbf{u}|_{W^{1,\infty}(\Omega)} + \varepsilon \max_{M \in \mathcal{M}_h} \{h_M^2 |\mathbf{u}|_{W^{1,\infty}(M)}^2\} + \frac{C}{\varepsilon} \max_{M \in \mathcal{M}_h} \left\{ \frac{h_M^2}{\gamma_M} |\mathbf{u}|_{W^{1,\infty}(M)}^2 \right\} \right. \\ &\quad \left. + \frac{C}{\varepsilon} \max_{M \in \mathcal{M}_h} \{\gamma_M^{-1} \|\mathbf{u}\|_{\infty,M}^2\} + C\varepsilon \max_{M \in \mathcal{M}_h} \{\tau_M^u |\mathbf{u}_h|_{W^{1,\infty}(M)}^2\} \right] \|\mathbf{e}_{u,h}\|_0^2. \end{aligned}$$

The difference of the convective terms in the Fourier equation can be bounded as

$$\begin{aligned} c_\theta(\mathbf{u}; \theta, e_{\theta,h}) - c_\theta(\mathbf{u}_h; \theta_h, e_{\theta,h}) &\leq \frac{1}{4\varepsilon} \sum_{M \in \mathcal{M}_h} \frac{1}{h_M^2} \|\boldsymbol{\eta}_{u,h}\|_{0,M}^2 + \frac{C}{\varepsilon} \sum_{L \in \mathcal{L}_h} \frac{1}{\tau_L^\theta} \|\eta_{\theta,h}\|_{0,L}^2 \\ &\quad + 3\varepsilon \|\boldsymbol{\eta}_{u,h}\|_{LPS}^2 + 3\varepsilon \|\mathbf{e}_{u,h}\|_{LPS}^2 + 7\varepsilon |e_{\theta,h}|_{LPS}^2 \\ &\quad + \frac{1}{2} |\theta|_{W^{1,\infty}(\Omega)} \|e_{u,h}\|_0^2 + \|e_{\theta,h}\|_0^2 \left(\frac{1}{2} |\theta|_{W^{1,\infty}(\Omega)} + C\varepsilon \max_{L \in \mathcal{L}_h} \{\tau_L^\theta |\mathbf{u}_h|_{W^{1,\infty}(L)}^2\} \right. \\ &\quad \left. + \varepsilon \max_{M \in \mathcal{M}_h} \{h_M^2 |\theta|_{W^{1,\infty}(M)}^2\} + \frac{C}{\varepsilon} \max_{M \in \mathcal{M}_h} \left\{ \frac{h_M^2}{\gamma_M} |\theta|_{W^{1,\infty}(M)}^2 \right\} + \frac{C}{\varepsilon} \max_{M \in \mathcal{M}_h} \{\gamma_M^{-1} \|\theta\|_{\infty,M}^2\} \right). \end{aligned}$$

Proof. We choose the interpolation operators provided by Assumption 3.2.6 and rename $j_u := i_u: \mathbf{V} \rightarrow \mathbf{V}_h$ and $j_\theta := i_\theta: \Theta \rightarrow \Theta_h$. These interpolators satisfy the usual approximation properties as required in Assumption 3.2.2. Therefore, all the estimates of the proof of Lemma 3.2.9 remain valid, but we modify the terms T_{21}^u, T_{21}^θ . Assumption 3.2.6 provides the orthogonality of j_u on \mathbf{D}_M^u and j_θ on D_L^θ , hence

$$\begin{aligned} T_{21}^u &= -(\mathbf{u}_h \cdot \nabla e_{u,h}, \boldsymbol{\eta}_{u,h}) = \sum_{M \in \mathcal{M}_h} ((\mathbf{u}_M - \mathbf{u}_h) \cdot \nabla e_{u,h}, \boldsymbol{\eta}_{u,h}) - \sum_{M \in \mathcal{M}_h} (\mathbf{u}_M \cdot \nabla e_{u,h}, \boldsymbol{\eta}_{u,h}) \\ &= \underbrace{\sum_{M \in \mathcal{M}_h} ((\mathbf{u}_M - \mathbf{u}_h) \cdot \nabla e_{u,h}, \boldsymbol{\eta}_{u,h})_M}_{T_{211}^u} - \underbrace{\sum_{M \in \mathcal{M}_h} (\mathbf{u}_M \cdot \nabla e_{u,h} - \pi_M^u(\mathbf{u}_M \cdot \nabla e_{u,h}), \boldsymbol{\eta}_{u,h})_M}_{T_{212}^u}, \\ T_{21}^\theta &= -(\mathbf{u}_h \cdot \nabla e_{\theta,h}, \eta_{\theta,h}) = \sum_{L \in \mathcal{L}_h} ((\mathbf{u}_L - \mathbf{u}_h) \cdot \nabla e_{\theta,h}, \eta_{\theta,h})_{0,L} - \sum_{L \in \mathcal{L}_h} (\mathbf{u}_L \cdot \nabla e_{\theta,h}, \eta_{\theta,h})_{0,L} \\ &= \underbrace{\sum_{L \in \mathcal{L}_h} ((\mathbf{u}_L - \mathbf{u}_h) \cdot \nabla e_{\theta,h}, \eta_{\theta,h})_{0,L}}_{T_{211}^\theta} - \underbrace{\sum_{L \in \mathcal{L}_h} (\mathbf{u}_L \cdot \nabla e_{\theta,h} - \pi_L^\theta(\mathbf{u}_L \cdot \nabla e_{\theta,h}), \eta_{\theta,h})_{0,L}}_{T_{212}^\theta}. \end{aligned}$$

Using the inverse inequalities from Assumption 3.2.4 for discrete velocity and temperature ansatz spaces, Young's inequality and Assumption 3.2.5 for the streamline direction yields:

$$\begin{aligned} T_{211}^u &\leq \sum_{M \in \mathcal{M}_h} ((\mathbf{u}_M - \mathbf{u}_h) \cdot \nabla e_{u,h}, \boldsymbol{\eta}_{u,h})_M \leq \sum_{M \in \mathcal{M}_h} \|\nabla e_{u,h}\|_{0,M} \|\mathbf{u}_M - \mathbf{u}_h\|_{\infty,M} \|\boldsymbol{\eta}_{u,h}\|_{0,M} \\ &\leq C \sum_{M \in \mathcal{M}_h} \frac{\|\mathbf{u}_M - \mathbf{u}_h\|_{\infty,M}}{h_M} \|e_{u,h}\|_{0,M} \|\boldsymbol{\eta}_{u,h}\|_{0,M} \\ &\leq C \left(\sum_{M \in \mathcal{M}_h} \frac{\|\mathbf{u}_M - \mathbf{u}_h\|_{\infty,M}^2 \tau_M^u}{h_M^2} \|e_{u,h}\|_{0,M}^2 \right)^{1/2} \left(\sum_{M \in \mathcal{M}_h} \frac{1}{\tau_M^u} \|\boldsymbol{\eta}_{u,h}\|_{0,M}^2 \right)^{1/2} \\ &\leq \frac{1}{4\varepsilon} \sum_{M \in \mathcal{M}_h} \frac{1}{\tau_M^u} \|\boldsymbol{\eta}_{u,h}\|_{0,M}^2 + C\varepsilon \max_{M \in \mathcal{M}_h} \left(\frac{\tau_M^u}{h_M^2} \|\mathbf{u}_M - \mathbf{u}_h\|_{\infty,M}^2 \right) \|e_{u,h}\|_0^2 \\ &\leq \frac{1}{4\varepsilon} \sum_{M \in \mathcal{M}_h} \frac{1}{\tau_M^u} \|\boldsymbol{\eta}_{u,h}\|_{0,M}^2 + C\varepsilon \max_{M \in \mathcal{M}_h} \left(\tau_M^u |\mathbf{u}_h|_{W^{1,\infty}(M)}^2 \right) \|e_{u,h}\|_0^2, \\ T_{211}^\theta &\leq \sum_{L \in \mathcal{L}_h} ((\mathbf{u}_L - \mathbf{u}_h) \cdot \nabla e_{\theta,h}, \eta_{\theta,h})_L \leq \sum_{L \in \mathcal{L}_h} \|\nabla e_{\theta,h}\|_{0,L} \|\mathbf{u}_L - \mathbf{u}_h\|_{\infty,L} \|\eta_{\theta,h}\|_{0,L} \\ &\leq \frac{1}{4\varepsilon} \sum_{L \in \mathcal{L}_h} \frac{1}{\tau_L^\theta} \|\eta_{\theta,h}\|_{0,L}^2 + C\varepsilon \max_{L \in \mathcal{L}_h} \left(\frac{\tau_L^\theta}{h_L^2} \|\mathbf{u}_L - \mathbf{u}_h\|_{\infty,L}^2 \right) \|e_{\theta,h}\|_0^2 \\ &\leq \frac{1}{4\varepsilon} \sum_{L \in \mathcal{L}_h} \frac{1}{\tau_L^\theta} \|\eta_{\theta,h}\|_{0,L}^2 + C\varepsilon \max_{L \in \mathcal{L}_h} \left(\tau_L^\theta |\mathbf{u}_h|_{W^{1,\infty}(L)}^2 \right) \|e_{\theta,h}\|_0^2. \end{aligned}$$

For the terms T_{212}^u and T_{212}^θ , we have with the definition of the fluctuation operators and Young's inequality

$$\begin{aligned} T_{212}^u &= \sum_{M \in \mathcal{M}_h} (\kappa_M^u(\mathbf{u}_M \cdot \nabla \mathbf{e}_{u,h}), \boldsymbol{\eta}_{u,h})_M \leq \varepsilon \|\mathbf{e}_{u,h}\|_{LPS}^2 + \frac{1}{4\varepsilon} \sum_{M \in \mathcal{M}_h} \frac{1}{\tau_M^u} \|\boldsymbol{\eta}_{u,h}\|_{0,M}^2, \\ T_{212}^\theta &= \sum_{L \in \mathcal{L}_h} (\kappa_L^\theta(\mathbf{u}_L \cdot \nabla e_{\theta,h}), \eta_{\theta,h})_{0,L} \leq 7\varepsilon \|e_{\theta,h}\|_{LPS}^2 + \frac{1}{28\varepsilon} \sum_{L \in \mathcal{L}_h} \frac{1}{\tau_L^\theta} \|\eta_{\theta,h}\|_{0,L}^2. \end{aligned}$$

In summary, we obtain

$$\begin{aligned} &c_u(\mathbf{u}; \mathbf{u}, \mathbf{e}_{u,h}) - c_u(\mathbf{u}_h; \mathbf{u}_h, \mathbf{e}_{u,h}) \\ &\leq \frac{1}{4\varepsilon} \sum_{M \in \mathcal{M}_h} \left(\frac{1}{h_M^2} + \frac{2}{\tau_M^u} \right) \|\boldsymbol{\eta}_{u,h}\|_{0,M}^2 + 3\varepsilon \|\boldsymbol{\eta}_{u,h}\|_{LPS}^2 + 4\varepsilon \|\mathbf{e}_{u,h}\|_{LPS}^2 \\ &\quad + \left[|\mathbf{u}|_{W^{1,\infty}(\Omega)} + \varepsilon \max_{M \in \mathcal{M}_h} \{h_M^2 |\mathbf{u}|_{W^{1,\infty}(M)}^2\} + \frac{C}{\varepsilon} \max_{M \in \mathcal{M}_h} \left\{ \frac{h_M^2}{\gamma_M} |\mathbf{u}|_{W^{1,\infty}(M)}^2 \right\} \right. \\ &\quad \left. + \frac{C}{\varepsilon} \max_{M \in \mathcal{M}_h} \{\gamma_M^{-1} \|\mathbf{u}\|_{\infty,M}^2\} + C\varepsilon \max_{M \in \mathcal{M}_h} \{\tau_M^u |\mathbf{u}_h|_{W^{1,\infty}(M)}^2\} \right] \|\mathbf{e}_{u,h}\|_0^2, \\ &c_\theta(\mathbf{u}; \theta, e_{\theta,h}) - c_\theta(\mathbf{u}_h; \theta_h, e_{\theta,h}) \\ &\leq \frac{1}{4\varepsilon} \sum_{M \in \mathcal{M}_h} \frac{1}{h_M^2} \|\boldsymbol{\eta}_{u,h}\|_{0,M}^2 + \frac{C}{\varepsilon} \sum_{L \in \mathcal{L}_h} \frac{1}{\tau_L^\theta} \|\eta_{\theta,h}\|_{0,L}^2 \\ &\quad + 3\varepsilon \|\boldsymbol{\eta}_{u,h}\|_{LPS}^2 + 3\varepsilon \|\mathbf{e}_{u,h}\|_{LPS}^2 + 7\varepsilon \|e_{\theta,h}\|_{LPS}^2 \\ &\quad + \frac{1}{2} |\theta|_{W^{1,\infty}(\Omega)} \|\mathbf{e}_{u,h}\|_0^2 + \|e_{\theta,h}\|_0^2 \left(\frac{1}{2} |\theta|_{W^{1,\infty}(\Omega)} + C\varepsilon \max_{L \in \mathcal{L}_h} \{\tau_L^\theta |\mathbf{u}_h|_{W^{1,\infty}(L)}^2\} \right. \\ &\quad \left. + \varepsilon \max_{M \in \mathcal{M}_h} \{h_M^2 |\theta|_{W^{1,\infty}(M)}^2\} + \frac{C}{\varepsilon} \max_{M \in \mathcal{M}_h} \left\{ \frac{h_M^2}{\gamma_M} |\theta|_{W^{1,\infty}(M)}^2 \right\} + \frac{C}{\varepsilon} \max_{M \in \mathcal{M}_h} \{\gamma_M^{-1} \|\theta\|_{\infty,M}^2\} \right). \end{aligned}$$

□

In order to improve the estimates from Section 3.2.1, we make use of this lemma and the following additional assumption on the parameter bounds.

Assumption 3.2.15 (Parameter bounds).

Assume that for all $M \in \mathcal{M}_h$, $E \in \mathcal{E}_h$ and $L \in \mathcal{L}_h$:

$$\begin{aligned} &\tau_M^u(\mathbf{u}_M) \geq 0, \quad \gamma_M(\mathbf{u}_M) \geq 0, \quad \phi_E \geq 0, \quad \tau_L^\theta(\mathbf{u}_L) \geq 0, \\ &\max_{M \in \mathcal{M}_h} \gamma_M(\mathbf{u}_M) \in L^\infty(0, T), \quad \max_{M \in \mathcal{M}_h} \gamma_M(\mathbf{u}_M)^{-1} \in L^\infty(0, T), \\ &\max_{E \in \mathcal{E}_h} \phi_E \in L^\infty(0, T), \quad \max_{E \in \mathcal{E}_h} \phi_E^{-1} \in L^\infty(0, T), \\ &\max_{M \in \mathcal{M}_h} \tau_M^u(\mathbf{u}_M) |\mathbf{u}_M|^2 \in L^\infty(0, T), \quad \max_{L \in \mathcal{L}_h} \tau_L^\theta(\mathbf{u}_L) |\mathbf{u}_L|^2 \in L^\infty(0, T), \end{aligned}$$

$$\begin{aligned} \max_{M \in \mathcal{M}_h} h_M^2 \tau_M^u (\mathbf{u}_M)^{-1} &\in L^\infty(0, T), & \max_{L \in \mathcal{L}_h} h_L^2 \tau_L^\theta (\mathbf{u}_L)^{-1} &\in L^\infty(0, T), \\ \max_{M \in \mathcal{M}_h} \tau_M^u |\mathbf{u}_h|_{W^{1,\infty}(M)}^2 &\in L^\infty(0, T), & \max_{L \in \mathcal{L}_h} \tau_L^\theta |\mathbf{u}_h|_{W^{1,\infty}(L)}^2 &\in L^\infty(0, T). \end{aligned}$$

Theorem 3.2.16 (Error estimate with compatibility condition).

We consider solutions $(\mathbf{u}, p, \theta): [0, T] \rightarrow \mathbf{V}^{div} \times Q \times \Theta$ and $(\mathbf{u}_h, p_h, \theta_h): [0, T] \rightarrow \mathbf{V}_h^{div} \times Q_h \times \Theta_h$ of (2.9)-(2.10) and (3.1)-(3.2) with the following regularity properties

$$\begin{aligned} \mathbf{u} &\in L^\infty(0, T; [W^{1,\infty}(\Omega)]^d), & \theta &\in L^\infty(0, T; W^{1,\infty}(\Omega)), & p &\in L^2(0, T; Q \cap C(\Omega)), \\ \partial_t \mathbf{u} &\in L^2(0, T; [L^2(\Omega)]^d), & \partial_t \theta &\in L^2(0, T; L^2(\Omega)), & \mathbf{u}_h(t) &\in [W^{1,\infty}(\Omega)]^d \quad \forall t \in [0, T]. \end{aligned}$$

Let Assumptions 3.2.2, 3.2.4, 3.2.5, 3.2.6 and 3.2.15 be valid. Moreover, assume $\nabla Q_h|_M \subset \mathbf{D}_M^u$ for all $M \in \mathcal{M}_h$ and $\mathbf{u}_h(0) = j_u \mathbf{u}_0$, $\theta_h(0) = j_\theta \theta_0$. Then for $0 \leq t \leq T$, we obtain the error estimate

$$\begin{aligned} &\|e_{u,h}\|_{L^\infty(0,t;L^2(\Omega))}^2 + \|e_{\theta,h}\|_{L^\infty(0,t;L^2(\Omega))}^2 + \int_0^t \left(\|(\mathbf{e}_{u,h}, e_{p,h})(\tau)\|_{LPS}^2 + \|[e_{\theta,h}(\tau)]\|_{LPS}^2 \right) d\tau \\ &\leq C \int_0^t e^{C'_{G,h}(\mathbf{u}, \theta, \mathbf{u}_h)(t-\tau)} \left\{ \sum_{M \in \mathcal{M}_h} \left[(\nu + \tau_M^u |\mathbf{u}_M|^2 + \gamma_M d) \|\nabla \boldsymbol{\eta}_{u,h}(\tau)\|_{0,M}^2 \right. \right. \\ &\quad + \left. \left(\frac{1}{h_M^2} + \frac{1}{\tau_M^u} \right) \|\boldsymbol{\eta}_{u,h}(\tau)\|_{0,M}^2 + \min\left(\frac{d}{\nu}, \frac{1}{\gamma_M}\right) \|\eta_{p,h}(\tau)\|_{0,M}^2 \right. \\ &\quad + \left. \|\partial_t \boldsymbol{\eta}_{u,h}(\tau)\|_{0,M}^2 + \tau_M^u |\mathbf{u}_M|^2 \|\kappa_M^u(\nabla \mathbf{u})(\tau)\|_{0,M}^2 \right] \\ &\quad + \sum_{E \in \mathcal{E}_h} \left[\phi_E \|\eta_{p,h}(\tau)\|_{E}^2 + \chi_{disc}(Q_h) \frac{1}{\phi_E} \|\boldsymbol{\eta}_{u,h}(\tau) \cdot \mathbf{n}_E\|_{0,E}^2 \right] \\ &\quad + \sum_{L \in \mathcal{L}_h} \left[(\alpha + \tau_L^\theta |\mathbf{u}_L|^2) \|\nabla \eta_{\theta,h}(\tau)\|_{0,L}^2 + \left(\frac{1}{\tau_L^\theta} + \beta \|\mathbf{g}\|_{\infty,L} \right) \|\eta_{\theta,h}(\tau)\|_{0,L}^2 \right. \\ &\quad \left. + \tau_L^\theta |\mathbf{u}_L|^2 \|\kappa_L^\theta(\nabla \theta)(\tau)\|_{0,L}^2 + \|\partial_t \eta_{\theta,h}(\tau)\|_{0,L}^2 \right] \left. \right\} d\tau \end{aligned}$$

with $(\boldsymbol{\eta}_{u,h}, \eta_{p,h}, \eta_{\theta,h}) = (\mathbf{u} - j_u \mathbf{u}_h, p - j_p p_h, \theta - j_\theta \theta_h)$, $\chi_{disc}(Q_h) \in \{0, 1\}$ (vanishing if Q_h is continuous and $\chi_{disc}(Q_h) = 1$ if Q_h is discontinuous) and Gronwall constant

$$\begin{aligned} C'_G(\mathbf{u}, \theta, \mathbf{u}_h) &= 1 + \beta \|\mathbf{g}\|_\infty + |\mathbf{u}|_{W^{1,\infty}(\Omega)} + |\theta|_{W^{1,\infty}(\Omega)} \\ &\quad + \max_{M \in \mathcal{M}_h} \{h_M^2 |\mathbf{u}|_{W^{1,\infty}(M)}^2\} + \max_{M \in \mathcal{M}_h} \left\{ \frac{h_M^2}{\gamma_M} |\mathbf{u}|_{W^{1,\infty}(M)}^2 \right\} + \max_{M \in \mathcal{M}_h} \{\gamma_M^{-1} \|\mathbf{u}\|_{\infty,M}^2\} \\ &\quad + \max_{M \in \mathcal{M}_h} \{h_M^2 |\theta|_{W^{1,\infty}(M)}^2\} + \max_{M \in \mathcal{M}_h} \left\{ \frac{h_M^2}{\gamma_M} |\theta|_{W^{1,\infty}(M)}^2 \right\} + \max_{M \in \mathcal{M}_h} \{\gamma_M^{-1} \|\theta\|_{\infty,M}^2\} \\ &\quad + \max_{M \in \mathcal{M}_h} \left\{ \tau_M^u |\mathbf{u}_h|_{W^{1,\infty}(M)}^2 \right\} + \max_{L \in \mathcal{L}_h} \left\{ \tau_L^\theta |\mathbf{u}_h|_{W^{1,\infty}(L)}^2 \right\}. \end{aligned}$$

Proof. Consider the interpolation operators $j_u := i_u$ and $j_\theta := i_\theta$ from Assumption 3.2.6 as in the previous Lemma 3.2.14. For the pressure, choose the interpolation operator j_p from Assumption 3.2.2. They have the usual approximation properties as stated in Assumption 3.2.2. We modify the proof of Theorem 3.2.12 in the sense that the estimate for the convective terms from Lemma 3.2.14 is taken advantage of. Note that $\mathbf{e}_{u,h}$ is no longer weakly solenoidal.

Subtracting (3.1) from (2.9), testing with $(\mathbf{v}_h, q_h) = (\mathbf{e}_{u,h}, e_{p,h}) \in \mathbf{V}_h \times Q_h$ and using Definition 3.2.1 lead to the error equation for the velocity according to:

$$\begin{aligned} & \frac{1}{2} \partial_t \|\mathbf{e}_{u,h}\|_0^2 + \|(\mathbf{e}_{u,h}, e_{p,h})\|_{LPS}^2 \\ &= -(\partial_t \boldsymbol{\eta}_{u,h}, \mathbf{e}_{u,h}) - \nu (\nabla \boldsymbol{\eta}_{u,h}, \nabla \mathbf{e}_{u,h}) + (\eta_{p,h}, \nabla \cdot \mathbf{e}_{u,h}) - (e_{p,h}, \nabla \cdot \boldsymbol{\eta}_{u,h}) + c_u(\mathbf{u}_h; \mathbf{u}_h, \mathbf{e}_{u,h}) \\ & \quad - c_u(\mathbf{u}; \mathbf{u}, \mathbf{e}_{u,h}) - s_u(\mathbf{u}_h; \boldsymbol{\eta}_{u,h}, \mathbf{e}_{u,h}) - i_h(\eta_{p,h}, e_{p,h}) - t_h(\mathbf{u}_h; \boldsymbol{\eta}_{u,h}, \mathbf{e}_{u,h}) + s_u(\mathbf{u}_h; \mathbf{u}, \mathbf{e}_{u,h}) \\ & \quad - \beta(\mathbf{g}e_{\theta,h}, \mathbf{e}_{u,h}) - \beta(\mathbf{g}\eta_{\theta,h}, \mathbf{e}_{u,h}). \end{aligned}$$

We use the bounds for the right-hand side as in the proof of Theorem 3.2.12 except for the convective terms and an additional mixed term. This mixed term $-(e_{p,h}, \nabla \cdot \boldsymbol{\eta}_{u,h})$ does not vanish in general. Since $\nabla Q_h|_M \subset \mathbf{D}_M^u$ for all $M \in \mathcal{M}_h$, Lemma 3.2.7 yields $(\nabla e_{p,h}, \boldsymbol{\eta}_{u,h})_M = 0$ for all $M \in \mathcal{M}_h$. Integration by parts gives with normal vectors \mathbf{n}_E on edges E

$$\begin{aligned} -(e_{p,h}, \nabla \cdot \boldsymbol{\eta}_{u,h}) &= (\nabla e_{p,h}, \boldsymbol{\eta}_{u,h}) - \sum_{E \in \mathcal{E}_h} ([e_{p,h}]_E, \boldsymbol{\eta}_{u,h} \cdot \mathbf{n}_E)_E \\ &= - \sum_{E \in \mathcal{E}_h} ([e_{p,h}]_E, \boldsymbol{\eta}_{u,h} \cdot \mathbf{n}_E)_E. \end{aligned}$$

In case of continuous discrete pressure, we have $[e_{p,h}]_E = 0$ and thus $(e_{p,h}, \nabla \cdot \boldsymbol{\eta}_{u,h}) = 0$. For discontinuous discrete pressure, we take advantage of the stabilization term i_h :

$$\begin{aligned} - \sum_{E \in \mathcal{E}_h} ([e_{p,h}]_{0,E}, \boldsymbol{\eta}_{u,h} \cdot \mathbf{n}_E)_E &\leq \left(\sum_{E \in \mathcal{E}_h} \frac{1}{\phi_E} \|\boldsymbol{\eta}_{u,h} \cdot \mathbf{n}_E\|_{0,E}^2 \right)^{1/2} \|(\mathbf{e}_{u,h}, e_{p,h})\|_{LPS} \\ &\leq \frac{1}{4\varepsilon} \sum_{E \in \mathcal{E}_h} \frac{1}{\phi_E} \|\boldsymbol{\eta}_{u,h} \cdot \mathbf{n}_E\|_{0,E}^2 + \varepsilon \|(\mathbf{e}_{u,h}, e_{p,h})\|_{LPS}^2. \end{aligned}$$

Due to Assumption 3.2.6, Lemma 3.2.14 provides a refined estimate of the convective error term in the momentum equation:

$$\begin{aligned} & c_u(\mathbf{u}; \mathbf{u}, \mathbf{e}_{u,h}) - c_u(\mathbf{u}_h; \mathbf{u}_h, \mathbf{e}_{u,h}) \\ & \leq \frac{1}{4\varepsilon} \sum_{M \in \mathcal{M}_h} \left(\frac{1}{h_M^2} + \frac{2}{\tau_M^u} \right) \|\boldsymbol{\eta}_{u,h}\|_{0,M}^2 + 3\varepsilon \|(\boldsymbol{\eta}_{u,h})\|_{LPS}^2 + 4\varepsilon \|(\mathbf{e}_{u,h})\|_{LPS}^2 \end{aligned}$$

$$\begin{aligned}
& + \left[|\mathbf{u}|_{W^{1,\infty}(\Omega)} + \varepsilon \max_{M \in \mathcal{M}_h} \{h_M^2 |\mathbf{u}|_{W^{1,\infty}(M)}^2\} + \frac{C}{\varepsilon} \max_{M \in \mathcal{M}_h} \left\{ \frac{h_M^2}{\gamma_M} |\mathbf{u}|_{W^{1,\infty}(M)}^2 \right\} \right. \\
& \left. + \frac{C}{\varepsilon} \max_{M \in \mathcal{M}_h} \{\gamma_M^{-1} \|\mathbf{u}\|_{\infty, M}^2\} + C\varepsilon \max_{M \in \mathcal{M}_h} \{\tau_M^u |\mathbf{u}_h|_{W^{1,\infty}(M)}^2\} \right] \|\mathbf{e}_{u,h}\|_0^2.
\end{aligned}$$

Combining these estimates with the upper bounds for the remaining terms from the proof of Theorem 3.2.12 yields

$$\begin{aligned}
& \frac{1}{2} \partial_t \|\mathbf{e}_{u,h}\|_0^2 + (1 - 6\varepsilon) \|(\mathbf{e}_{u,h}, e_{p,h})\|_{LPS}^2 \leq \frac{1}{4} \|\partial_t \boldsymbol{\eta}_{u,h}\|_0^2 \\
& + \sum_{M \in \mathcal{M}_h} \left[\frac{C}{\varepsilon} \left(\frac{1}{h_M^2} + \frac{2}{\tau_M^u} \right) \|\boldsymbol{\eta}_{u,h}\|_{0,M}^2 + \frac{C}{\varepsilon} (\nu + \tau_M^u |\mathbf{u}_M|^2 + \gamma_M d) \|\nabla \boldsymbol{\eta}_{u,h}\|_{0,M}^2 \right. \\
& \left. + \frac{C}{\varepsilon} \min \left(\frac{d}{\nu}, \frac{1}{\gamma_M} \right) \|\eta_{p,h}\|_{0,M}^2 + \frac{C}{\varepsilon} \tau_M^u |\mathbf{u}_M|^2 \|\kappa_M^u(\nabla \mathbf{u})\|_{0,M}^2 \right] \\
& + \left[1 + \beta \|\mathbf{g}\|_\infty + |\mathbf{u}|_{W^{1,\infty}(\Omega)} + \varepsilon \max_{M \in \mathcal{M}_h} \{h_M^2 |\mathbf{u}|_{W^{1,\infty}(M)}^2\} + \frac{C}{\varepsilon} \max_{M \in \mathcal{M}_h} \left\{ \frac{h_M^2}{\gamma_M} |\mathbf{u}|_{W^{1,\infty}(M)}^2 \right\} \right. \\
& \left. + \frac{C}{\varepsilon} \max_{M \in \mathcal{M}_h} \{\gamma_M^{-1} \|\mathbf{u}\|_{\infty, M}^2\} + C\varepsilon \max_{M \in \mathcal{M}_h} \left(\tau_M^u |\mathbf{u}_h|_{W^{1,\infty}(M)}^2 \right) \right] \|\mathbf{e}_{u,h}\|_0^2 \\
& + \beta \|\mathbf{g}\|_\infty \|e_{\theta,h}\|_0^2 + C\beta \|\mathbf{g}\|_\infty \|\eta_{\theta,h}\|_0^2 \\
& + \frac{C}{\varepsilon} \sum_{E \in \mathcal{E}_h} \phi_E \|\eta_{p,h}\|_{0,E}^2 + \chi_{disc}(Q_h) \frac{C}{\varepsilon} \sum_{E \in \mathcal{E}_h} \frac{1}{\phi_E} \|\boldsymbol{\eta}_{u,h} \cdot \mathbf{n}_E\|_{0,E}^2. \tag{3.46}
\end{aligned}$$

For the Fourier equation, we proceed in a similar way as in the proof of Theorem 3.2.12: We subtract (3.2) from (2.10) with $\psi_h = e_{\theta,h} \in \Theta_h$ and reorder the terms as follows:

$$\begin{aligned}
& \frac{1}{2} \partial_t \|e_{\theta,h}\|_0^2 + \|[e_{\theta,h}]\|_{LPS}^2 = -(\partial_t \eta_{\theta,h}, e_{\theta,h}) - \alpha(\nabla \eta_{\theta,h}, \nabla e_{\theta,h}) \\
& + c_\theta(\mathbf{u}_h; \theta_h, e_{\theta,h}) - c_\theta(\mathbf{u}; \theta, e_{\theta,h}) - s_\theta(\mathbf{u}_h; \eta_{\theta,h}, e_{\theta,h}) + s_\theta(\mathbf{u}_h; \theta, e_{\theta,h}).
\end{aligned}$$

We include the estimate from Lemma 3.2.14 for the nonlinear terms

$$\begin{aligned}
& c_\theta(\mathbf{u}; \theta, e_{\theta,h}) - c_\theta(\mathbf{u}_h; \theta_h, e_{\theta,h}) \leq \frac{1}{4\varepsilon} \sum_{M \in \mathcal{M}_h} \frac{1}{h_M^2} \|\boldsymbol{\eta}_{u,h}\|_{0,M}^2 + \frac{C}{\varepsilon} \sum_{L \in \mathcal{L}_h} \frac{1}{\tau_L^\theta} \|\eta_{\theta,h}\|_{0,L}^2 \\
& + 3\varepsilon \|\boldsymbol{\eta}_{u,h}\|_{LPS}^2 + 3\varepsilon \|\mathbf{e}_{u,h}\|_{LPS}^2 + 7\varepsilon \|[e_{\theta,h}]\|_{LPS}^2 \\
& + \frac{1}{2} |\theta|_{W^{1,\infty}(\Omega)} \|\mathbf{e}_{u,h}\|_0^2 + \|e_{\theta,h}\|_0^2 \left(\frac{1}{2} |\theta|_{W^{1,\infty}(\Omega)} + C\varepsilon \max_{L \in \mathcal{L}_h} \{\tau_L^\theta |\mathbf{u}_h|_{W^{1,\infty}(L)}^2\} \right. \\
& \left. + \varepsilon \max_{M \in \mathcal{M}_h} \{h_M^2 |\theta|_{W^{1,\infty}(M)}^2\} + \frac{C}{\varepsilon} \max_{M \in \mathcal{M}_h} \left\{ \frac{h_M^2}{\gamma_M} |\theta|_{W^{1,\infty}(M)}^2 \right\} + \frac{C}{\varepsilon} \max_{M \in \mathcal{M}_h} \{\gamma_M^{-1} \|\theta\|_{\infty, M}^2\} \right)
\end{aligned}$$

and use $||| \mathbf{e}_{u,h} |||_{LPS}^2 = ||| (\mathbf{e}_{u,h}, 0) |||_{LPS}^2 \leq ||| (\mathbf{e}_{u,h}, e_{p,h}) |||_{LPS}^2$. This results in

$$\begin{aligned}
& \frac{1}{2} \partial_t \|e_{\theta,h}\|_0^2 + (1 - 9\varepsilon) \| [e_{\theta,h}] \|_{LPS}^2 \leq \frac{1}{4} \|\partial_t \eta_{\theta,h}\|_0^2 + \frac{C}{\varepsilon} \sum_{L \in \mathcal{L}_h} \frac{1}{\tau_L^\theta} \|\eta_{\theta,h}\|_{0,L}^2 \\
& + \frac{C}{\varepsilon} \sum_{M \in \mathcal{M}_h} \frac{1}{h_M^2} \|\boldsymbol{\eta}_{u,h}\|_{0,M}^2 + 3\varepsilon ||| \boldsymbol{\eta}_{u,h} |||_{LPS}^2 + 3\varepsilon ||| (\mathbf{e}_{u,h}, e_{p,h}) |||_{LPS}^2 + \frac{1}{2} \|\theta\|_{W^{1,\infty}(\Omega)} \|\mathbf{e}_{u,h}\|_0^2 \\
& + \left[1 + \frac{1}{2} \|\theta\|_{W^{1,\infty}(\Omega)} + \varepsilon \max_{M \in \mathcal{M}_h} \{h_M^2 |\theta|_{W^{1,\infty}(M)}^2\} + C\varepsilon \max_{L \in \mathcal{L}_h} (\tau_L^\theta |\mathbf{u}_h|_{W^{1,\infty}(L)}^2) \right] \\
& + \frac{C}{\varepsilon} \max_{M \in \mathcal{M}_h} \left\{ \frac{h_M^2}{\gamma_M} |\theta|_{W^{1,\infty}(M)}^2 \right\} + \frac{C}{\varepsilon} \max_{M \in \mathcal{M}_h} \left\{ \gamma_M^{-1} \|\theta\|_{\infty,M}^2 \right\} \|\mathbf{e}_{\theta,h}\|_0^2 \\
& + \frac{C}{\varepsilon} \sum_{L \in \mathcal{L}_h} \left[(\alpha + \tau_L^\theta |\mathbf{u}_L|^2) \|\nabla \eta_{\theta,h}\|_{0,L}^2 + \tau_L^\theta |\mathbf{u}_L|^2 \|\kappa_L^\theta(\nabla \theta)\|_{0,L}^2 \right]. \tag{3.47}
\end{aligned}$$

We utilize

$$||| \boldsymbol{\eta}_{u,h} |||_{LPS}^2 \leq \sum_{M \in \mathcal{M}_h} (\nu + \tau_M^u |\mathbf{u}_M|^2 + \gamma_M d) \|\nabla \boldsymbol{\eta}_{u,h}\|_{0,M}^2,$$

denote with $C > 0$ a constant independent of the problem parameters, h_M , h_L and the solutions and sum up the intermediate estimates for velocity (3.46) and temperature (3.47):

$$\begin{aligned}
& \frac{1}{2} \partial_t \|\mathbf{e}_{u,h}\|_0^2 + (1 - 9\varepsilon) ||| (\mathbf{e}_{u,h}, e_{p,h}) |||_{LPS}^2 + \frac{1}{2} \partial_t \|e_{\theta,h}\|_0^2 + (1 - 9\varepsilon) \| [e_{\theta,h}] \|_{LPS}^2 \\
& \leq \frac{1}{4} \|\partial_t \boldsymbol{\eta}_{u,h}\|_0^2 + \frac{1}{4} \|\partial_t \eta_{\theta,h}\|_0^2 + \frac{C}{\varepsilon} \sum_{M \in \mathcal{M}_h} \left(\frac{1}{h_M^2} + \frac{1}{\tau_M^u} \right) \|\boldsymbol{\eta}_{u,h}\|_{0,M}^2 \\
& + \left[1 + \beta \|\mathbf{g}\|_\infty + \|\mathbf{u}\|_{W^{1,\infty}(\Omega)} + \frac{1}{2} \|\theta\|_{W^{1,\infty}(\Omega)} + \varepsilon \max_{M \in \mathcal{M}_h} \{h_M^2 |\mathbf{u}|_{W^{1,\infty}(M)}^2\} \right] \\
& + \frac{C}{\varepsilon} \max_{M \in \mathcal{M}_h} \left\{ \frac{h_M^2}{\gamma_M} |\mathbf{u}|_{W^{1,\infty}(M)}^2 \right\} + \frac{C}{\varepsilon} \max_{M \in \mathcal{M}_h} \left\{ \gamma_M^{-1} \|\mathbf{u}\|_{\infty,M}^2 \right\} \\
& + C\varepsilon \max_{M \in \mathcal{M}_h} \left\{ \tau_M^u |\mathbf{u}_h|_{W^{1,\infty}(M)}^2 \right\} \|\mathbf{e}_{u,h}\|_0^2 \\
& + \sum_{M \in \mathcal{M}_h} \left(\frac{C}{\varepsilon} + C\varepsilon \right) (\nu + \tau_M^u |\mathbf{u}_M|^2 + \gamma_M d) \|\nabla \boldsymbol{\eta}_{u,h}\|_{0,M}^2 \\
& + \frac{C}{\varepsilon} \sum_{M \in \mathcal{M}_h} \left[\min \left(\frac{d}{\nu}, \frac{1}{\gamma_M} \right) \|\eta_{p,h}\|_{0,M}^2 + \tau_M^u |\mathbf{u}_M|^2 \|\kappa_M^u(\nabla \mathbf{u})\|_{0,M}^2 \right] \\
& + \frac{C}{\varepsilon} \sum_{E \in \mathcal{E}_h} \phi_E \| [\eta_{p,h}]_E \|_{0,E}^2 + \chi_{disc}(Q_h) \frac{C}{\varepsilon} \sum_{E \in \mathcal{E}_h} \frac{1}{\phi_E} \|\boldsymbol{\eta}_{u,h} \cdot \mathbf{n}_E\|_{0,E}^2 \\
& + \sum_{L \in \mathcal{L}_h} \left(\frac{C}{\varepsilon} \frac{1}{\tau_L^\theta} + C\beta \|\mathbf{g}\|_{\infty,L} \right) \|\eta_{\theta,h}\|_{0,L}^2 \\
& + \left[1 + \beta \|\mathbf{g}\|_\infty + \frac{1}{2} \|\theta\|_{W^{1,\infty}(\Omega)} + \varepsilon \max_{M \in \mathcal{M}_h} \{h_M^2 |\theta|_{W^{1,\infty}(M)}^2\} + C\varepsilon \max_{L \in \mathcal{L}_h} (\tau_L^\theta |\mathbf{u}_h|_{W^{1,\infty}(L)}^2) \right]
\end{aligned}$$

$$\begin{aligned}
& + \frac{C}{\varepsilon} \max_{M \in \mathcal{M}_h} \left\{ \frac{h_M^2}{\gamma_M} |\theta|_{W^{1,\infty}(M)}^2 \right\} + \frac{C}{\varepsilon} \max_{M \in \mathcal{M}_h} \left\{ \gamma_M^{-1} \|\theta\|_{\infty, M}^2 \right\} \Big] \|e_{\theta, h}\|_0^2 \\
& + \frac{C}{\varepsilon} \sum_{L \in \mathcal{L}_h} \left[(\alpha + \tau_L^\theta |\mathbf{u}_L|^2) \|\nabla \eta_{\theta, h}\|_{0, L}^2 + \tau_L^\theta |\mathbf{u}_L|^2 \|\kappa_L^\theta(\nabla \theta)\|_{0, L}^2 \right].
\end{aligned}$$

The choice $\varepsilon = \frac{1}{18}$ gives

$$\begin{aligned}
& \partial_t \|e_{u, h}\|_0^2 + \|(\mathbf{e}_{u, h}, e_{p, h})\|_{LPS}^2 + \partial_t \|e_{\theta, h}\|_0^2 + \|[e_{\theta, h}]\|_{LPS}^2 \\
& \lesssim \|\partial_t \boldsymbol{\eta}_{u, h}\|_0^2 + \|\partial_t \eta_{\theta, h}\|_0^2 + \sum_{M \in \mathcal{M}_h} \left(\frac{1}{h_M^2} + \frac{1}{\tau_M^u} \right) \|\boldsymbol{\eta}_{u, h}\|_{0, M}^2 \\
& + \left[1 + \beta \|\mathbf{g}\|_\infty + |\mathbf{u}|_{W^{1,\infty}(\Omega)} + |\theta|_{W^{1,\infty}(\Omega)} + \max_{M \in \mathcal{M}_h} \{h_M^2 |\mathbf{u}|_{W^{1,\infty}(M)}^2\} \right. \\
& + \max_{M \in \mathcal{M}_h} \left\{ \frac{h_M^2}{\gamma_M} |\mathbf{u}|_{W^{1,\infty}(M)}^2 \right\} + \max_{M \in \mathcal{M}_h} \left\{ \gamma_M^{-1} \|\mathbf{u}\|_{\infty, M}^2 \right\} + \max_{M \in \mathcal{M}_h} \left\{ \tau_M^u |\mathbf{u}_h|_{W^{1,\infty}(M)}^2 \right\} \Big] \|e_{u, h}\|_0^2 \\
& + \sum_{M \in \mathcal{M}_h} (\nu + \tau_M^u |\mathbf{u}_M|^2 + \gamma_M d) \|\nabla \boldsymbol{\eta}_{u, h}\|_{0, M}^2 \\
& + \sum_{M \in \mathcal{M}_h} \left[\min \left(\frac{d}{\nu}, \frac{1}{\gamma_M} \right) \|\eta_{p, h}\|_{0, M}^2 + \tau_M^u |\mathbf{u}_M|^2 \|\kappa_M^u(\nabla \mathbf{u})\|_{0, M}^2 \right] \\
& + \sum_{E \in \mathcal{E}_h} \phi_E \|\eta_{p, h}\|_{0, E}^2 + \chi_{disc}(Q_h) \sum_{E \in \mathcal{E}_h} \frac{1}{\phi_E} \|\boldsymbol{\eta}_{u, h} \cdot \mathbf{n}_E\|_{0, E}^2 \\
& + \sum_{L \in \mathcal{L}_h} \left[\left(\frac{1}{\tau_L^\theta} + \beta \|\mathbf{g}\|_{\infty, L} \right) \|\eta_{\theta, h}\|_{0, L}^2 + (\alpha + \tau_L^\theta |\mathbf{u}_L|^2) \|\nabla \eta_{\theta, h}\|_{0, L}^2 + \tau_L^\theta |\mathbf{u}_L|^2 \|\kappa_L^\theta(\nabla \theta)\|_{0, L}^2 \right] \\
& + \left[1 + \beta \|\mathbf{g}\|_\infty + |\theta|_{W^{1,\infty}(\Omega)} + \max_{M \in \mathcal{M}_h} \{h_M^2 |\theta|_{W^{1,\infty}(M)}^2\} + \max_{L \in \mathcal{L}_h} (\tau_L^\theta |\mathbf{u}_h|_{W^{1,\infty}(L)}^2) \right. \\
& \left. + \max_{M \in \mathcal{M}_h} \left\{ \frac{h_M^2}{\gamma_M} |\theta|_{W^{1,\infty}(M)}^2 \right\} + \max_{M \in \mathcal{M}_h} \left\{ \gamma_M^{-1} \|\theta\|_{\infty, M}^2 \right\} \right] \|e_{\theta, h}\|_0^2.
\end{aligned}$$

We can apply Gronwall's Lemma [A.3.5](#) for $\|(\mathbf{e}_{u, h}, e_{\theta, h})\|_0^2 := \|\mathbf{e}_{u, h}\|_0^2 + \|e_{\theta, h}\|_0^2$ since all terms on the right-hand side are integrable in time: This holds due to the regularity assumptions on \mathbf{u} , θ , Assumptions [3.2.3](#), [3.2.15](#) and $\mathbf{g} \in L^\infty(0, T; [L^\infty(\Omega)]^d)$. The Gronwall constant is

$$\begin{aligned}
C'_G(\mathbf{u}, \theta, \mathbf{u}_h) & = 1 + \beta \|\mathbf{g}\|_\infty + |\mathbf{u}|_{W^{1,\infty}(\Omega)} + |\theta|_{W^{1,\infty}(\Omega)} \\
& + \max_{M \in \mathcal{M}_h} \{h_M^2 |\mathbf{u}|_{W^{1,\infty}(M)}^2\} + \max_{M \in \mathcal{M}_h} \left\{ \frac{h_M^2}{\gamma_M} |\mathbf{u}|_{W^{1,\infty}(M)}^2 \right\} + \max_{M \in \mathcal{M}_h} \left\{ \gamma_M^{-1} \|\mathbf{u}\|_{\infty, M}^2 \right\} \\
& + \max_{M \in \mathcal{M}_h} \{h_M^2 |\theta|_{W^{1,\infty}(M)}^2\} + \max_{M \in \mathcal{M}_h} \left\{ \frac{h_M^2}{\gamma_M} |\theta|_{W^{1,\infty}(M)}^2 \right\} + \max_{M \in \mathcal{M}_h} \left\{ \gamma_M^{-1} \|\theta\|_{\infty, M}^2 \right\} \\
& + \max_{M \in \mathcal{M}_h} \left\{ \tau_M^u |\mathbf{u}_h|_{W^{1,\infty}(M)}^2 \right\} + \max_{L \in \mathcal{L}_h} \left\{ \tau_L^\theta |\mathbf{u}_h|_{W^{1,\infty}(L)}^2 \right\}
\end{aligned}$$

As the initial errors $\mathbf{e}_{u, h}(0)$, $e_{\theta, h}(0)$ vanish, we establish the desired result. \square

Corollary 3.2.17 (Method of quasi-optimal order with compatibility condition).

Let Assumptions 3.2.2, 3.2.3, 3.2.4, 3.2.5, 3.2.6 and 3.2.15 be valid. In addition, we require $\nabla Q_h|_M \subset \mathbf{D}_M^u$ for all $M \in \mathcal{M}_h$ and $\mathbf{u}_h(0) = j_u \mathbf{u}_0$, $\theta_h(0) = j_\theta \theta_0$. Let the solutions $(\mathbf{u}, p, \theta): [0, T] \rightarrow \mathbf{V}^{div} \times Q \times \Theta$, $(\mathbf{u}_h, p_h, \theta_h): [0, T] \rightarrow \mathbf{V}_h^{div} \times Q_h \times \Theta_h$ of (2.9)-(2.10) and (3.1)-(3.2) satisfy

$$\begin{aligned} \mathbf{u} &\in L^\infty(0, T; [W^{1,\infty}(\Omega)]^d) \cap L^2(0, T; [W^{k_u+1,2}(\Omega)]^d), \\ \partial_t \mathbf{u} &\in L^2(0, T; [W^{k_u,2}(\Omega)]^d), \quad p \in L^2(0, T; W^{k_p+1,2}(\Omega) \cap C(\Omega)), \\ \theta &\in L^\infty(0, T; W^{1,\infty}(\Omega)) \cap L^2(0, T; W^{k_\theta+1,2}(\Omega)), \\ \partial_t \theta &\in L^2(0, T; W^{k_\theta,2}(\Omega)), \\ \mathbf{u}_h(t) &\in [W^{1,\infty}(\Omega)]^d \quad \forall t \in [0, T]. \end{aligned}$$

Let $\chi_{disc}(Q_h) \in \{0, 1\}$ (vanishing if Q_h is continuous and $\chi_{disc}(Q_h) = 1$ if Q_h is discontinuous). The error can be bounded for $0 \leq t \leq T$ by

$$\begin{aligned} &\|\boldsymbol{\xi}_{u,h}\|_{L^\infty(0,t;L^2(\Omega))}^2 + \|\xi_{\theta,h}\|_{L^\infty(0,t;L^2(\Omega))}^2 + \int_0^t \left(\|(\boldsymbol{\xi}_{u,h}, \xi_{p,h})(\tau)\|_{LPS}^2 + \|[\xi_{\theta,h}(\tau)]_{LPS}^2 \right) d\tau \\ &\leq C \int_0^t e^{C'_{G,h}(\mathbf{u}, \theta, \mathbf{u}_h)(t-\tau)} \left\{ \sum_{M \in \mathcal{M}_h} h_M^{2k_u} \left[(\nu + \tau_M^u |\mathbf{u}_M|^2 + \gamma_M d + 1 + \frac{h_M^2}{\tau_M^u} \right. \right. \\ &\quad \left. \left. + \chi_{disc}(Q_h) \max_{T \subset M, E \in \partial T} \left\{ \frac{h_T}{\phi_E} \right\} \right] \|\mathbf{u}(\tau)\|_{W^{k_u+1,2}(\omega_M)}^2 \right. \\ &\quad \left. + \|\partial_t \mathbf{u}(\tau)\|_{W^{k_u,2}(\omega_M)}^2 + \tau_M^u |\mathbf{u}_M|^2 h_M^{2(s_u-k_u)} \|\mathbf{u}(\tau)\|_{W^{s_u+1,2}(\omega_M)}^2 \right] \\ &\quad + \sum_{M \in \mathcal{M}_h} h_M^{2(k_p+1)} \left[\min\left(\frac{d}{\nu}, \frac{1}{\gamma_M}\right) + \max_{T \subset M, E \in \partial T} \left\{ \frac{\phi_E}{h_T} \right\} \right] \|p(\tau)\|_{W^{k_p+1,2}(\omega_M)}^2 \\ &\quad + \sum_{L \in \mathcal{L}_h} h_L^{2k_\theta} \left[\left(\alpha + \tau_L^\theta |\mathbf{u}_L|^2 + \frac{h_L^2}{\tau_L^\theta} + h_L^2 \beta \|\mathbf{g}\|_{\infty,L} \right) \|\theta(\tau)\|_{W^{k_\theta+1,2}(\omega_L)}^2 \right. \\ &\quad \left. + \tau_L^\theta |\mathbf{u}_L|^2 h_L^{2(s_\theta-k_\theta)} \|\theta(\tau)\|_{W^{s_\theta+1,2}(\omega_L)}^2 + \|\partial_t \theta(\tau)\|_{W^{k_\theta,2}(\omega_L)}^2 \right] \Big\} d\tau \end{aligned} \quad (3.48)$$

with $s_u \in \{0, \dots, k_u\}$, $s_\theta \in \{0, \dots, k_\theta\}$ and the Gronwall constant

$$\begin{aligned} C'_G(\mathbf{u}, \theta, \mathbf{u}_h) &= 1 + \beta \|\mathbf{g}\|_\infty + |\mathbf{u}|_{W^{1,\infty}(\Omega)} + |\theta|_{W^{1,\infty}(\Omega)} \\ &\quad + \max_{M \in \mathcal{M}_h} \{h_M^2 |\mathbf{u}|_{W^{1,\infty}(M)}^2\} + \max_{M \in \mathcal{M}_h} \left\{ \frac{h_M^2}{\gamma_M} |\mathbf{u}|_{W^{1,\infty}(M)}^2 \right\} + \max_{M \in \mathcal{M}_h} \{\gamma_M^{-1} \|\mathbf{u}\|_{\infty,M}^2\} \\ &\quad + \max_{M \in \mathcal{M}_h} \{h_M^2 |\theta|_{W^{1,\infty}(M)}^2\} + \max_{M \in \mathcal{M}_h} \left\{ \frac{h_M^2}{\gamma_M} |\theta|_{W^{1,\infty}(M)}^2 \right\} + \max_{M \in \mathcal{M}_h} \{\gamma_M^{-1} \|\theta\|_{\infty,M}^2\} \\ &\quad + \max_{M \in \mathcal{M}_h} \left\{ \tau_M^u |\mathbf{u}_h|_{W^{1,\infty}(M)}^2 \right\} + \max_{L \in \mathcal{L}_h} \left\{ \tau_L^\theta |\mathbf{u}_h|_{W^{1,\infty}(L)}^2 \right\}. \end{aligned} \quad (3.49)$$

Proof. We split the semi-discrete errors according to

$$\xi_{u,h} = \boldsymbol{\eta}_{u,h} + \mathbf{e}_{u,h}, \quad \xi_{p,h} = \eta_{p,h} + e_{p,h}, \quad \xi_{\theta,h} = \eta_{\theta,h} + e_{\theta,h}$$

with the same interpolation operators as in Theorem 3.2.16 and use the triangle inequality. Most of the terms can be estimated as in Corollary 3.2.13. In addition, we take advantage of the trace inequality A.3.3:

$$\begin{aligned} \chi_{disc}(Q_h) \sum_{E \in \mathcal{E}_h} \frac{1}{\phi_E} \|\boldsymbol{\eta}_{u,h}(\tau) \cdot \mathbf{n}_E\|_{0,E}^2 \\ \leq \chi_{disc}(Q_h) C_{tr} \sum_{M \in \mathcal{M}_h} \sum_{T \subset M} \max_{E \in \partial T} \frac{1}{\phi_E} (h_T^{-1} \|\boldsymbol{\eta}_{u,h}(\tau)\|_{0,T}^2 + h_T \|\nabla \boldsymbol{\eta}_{u,h}(\tau)\|_{0,T}^2) \\ \leq \chi_{disc}(Q_h) C \sum_{M \in \mathcal{M}_h} \max_{T \subset M, E \in \partial T} \left\{ \frac{h_T}{\phi_E} \right\} h_M^{2k_u} \|\mathbf{u}(\tau)\|_{W^{k_u+1,2}(\omega_M)}^2 \end{aligned}$$

with $\chi_{disc}(Q_h) \in \{0, 1\}$. Here, we used $h_T \leq h_M \leq Ch_T$ and the approximation property of $j_u \mathbf{u}$ due to Assumption 3.2.6. This concludes the proof. \square

Indeed, we avoid the mesh restriction (3.43) in the above results. A drawback is that the Gronwall constant (3.49) now depends on $\tau_M^u |\mathbf{u}_h|_{W^{1,\infty}(M)}^2$ and $\tau_L^\theta |\mathbf{u}_h|_{W^{1,\infty}(L)}^2$ and thus on the discrete velocity. With a suitable choice of τ_M^u and τ_L^θ , we can relativize this disadvantage.

Compared to the previous Section 3.2.1, more premises are needed. In the following, we discuss possible settings where Theorem 3.2.16 and Corollary 3.2.17 are applicable. In order to establish Theorem 3.2.16, we require the additional Assumptions 3.2.6 and $\nabla Q_h|_M \subset \mathbf{D}_M^u$ for all $M \in \mathcal{M}_h$. The challenge is to guarantee Assumption 3.2.3 and 3.2.6 simultaneously: 3.2.3 requires a certain richness of the coarse space compared to the fine space so that the fluctuation operator has the desired approximation property, whereas the fine space has to be large enough, according to Lemma 3.2.7, such that Assumption 3.2.6 is satisfied.

In the argumentation below, we restrict ourselves to the fine and coarse velocity ansatz spaces; the temperature spaces can then be chosen in the same way. As shown in [MST07], the approximation property of κ_M^u (Assumption 3.2.3) is fulfilled, for example, if the polynomials of degree less or equal than $s_u - 1 \leq k_u - 1$ are in the coarse space: $[\mathbb{P}_{s_u-1}(M)]^d \subset \mathbf{D}_M^u$. Consider $s_u = k_u$. If we choose $Q_h = \mathbb{P}_{k_u-1}$ or $Q_h = \mathbb{P}_{-(k_u-1)}$ (in order to guarantee discrete inf-sup stability 2.2.1), the condition $\nabla Q_h|_M \subset \mathbf{D}_M^u$ holds.

From [MST07, MT14], we obtain the following variants for $(\mathbf{V}_h / \mathbf{D}_M^u) \wedge Q_h \wedge (\Theta_h / D_M^\theta)$:

- One-level methods:

$$\begin{aligned} (\mathbb{P}_{k_u}^+ / \mathbb{P}_{k_u-1}) \wedge \mathbb{P}_{k_u-1} \wedge (\mathbb{P}_{k_\theta}^+ / \mathbb{P}_{k_\theta-1}), & \quad (\mathbb{P}_{k_u}^+ / \mathbb{P}_{k_u-1}) \wedge \mathbb{P}_{-(k_u-1)} \wedge (\mathbb{P}_{k_\theta}^+ / \mathbb{P}_{k_\theta-1}), \\ (\mathbb{Q}_{k_u}^+ / \mathbb{P}_{k_u-1}) \wedge \mathbb{P}_{-(k_u-1)} \wedge (\mathbb{Q}_{k_\theta}^+ / \mathbb{P}_{k_\theta-1}), & \quad (\mathbb{Q}_{k_u} / \mathbb{P}_{k_u-1}) \wedge \mathbb{P}_{-(k_u-1)} \wedge (\mathbb{Q}_{k_\theta} / \mathbb{P}_{k_\theta-1}). \end{aligned}$$

- Two-level methods (for the construction of the coarse space, see [MST07, MT14]):
 $(\mathbb{P}_{k_u}/\mathbb{P}_{k_u-1}) \wedge \mathbb{P}_{-(k_u-1)} \wedge (\mathbb{P}_{k_\theta}/\mathbb{P}_{k_\theta-1}), \quad (\mathbb{Q}_{k_u}/\mathbb{Q}_{k_u-1}) \wedge \mathbb{Q}_{-(k_u-1)} \wedge (\mathbb{Q}_{k_\theta}/\mathbb{Q}_{k_\theta-1}),$
 $(\mathbb{Q}_{k_u}/\mathbb{P}_{k_u-1}) \wedge \mathbb{P}_{-(k_u-1)} \wedge (\mathbb{Q}_{k_\theta}/\mathbb{P}_{k_\theta-1}).$

For these choices of finite element spaces, the above analysis is valid. Note that we consider only $s_u = k_u$ and $s_\theta = k_\theta$. From (3.48) in Corollary 3.2.17, we obtain a method of quasi-optimal order k if $k := k_u = k_p + 1 = k_\theta$. Balancing the error bounds, we obtain a choice of the stabilization parameters as

$$\begin{aligned} \gamma_M &= \gamma_0, & \chi_{disc}(Q_h)\phi_0 h_T &\leq \phi_E \leq \bar{\phi}_0 h_T, \\ \underline{\tau}_0^u h_M^2 &\leq \tau_M^u(\mathbf{u}_M) \leq \bar{\tau}_0^u \|\mathbf{u}_h\|_{W^{1,\infty}(M)}^{-2}, & \underline{\tau}_0^\theta h_L^2 &\leq \tau_L^\theta(\mathbf{u}_L) \leq \bar{\tau}_0^\theta \|\mathbf{u}_h\|_{W^{1,\infty}(L)}^{-2} \end{aligned} \quad (3.50)$$

with tuning constants $\gamma_0, \phi_0, \bar{\phi}_0, \underline{\tau}_0^u, \bar{\tau}_0^u, \underline{\tau}_0^\theta, \bar{\tau}_0^\theta = \mathcal{O}(1)$. The reasons for the choice of γ_M are as in Section 3.2.1. For continuous pressure spaces Q_h , we may omit the pressure stabilization since in this case $\chi_{disc}(Q_h) = 0$. Note that the parameter bounds needed in Assumption 3.2.15 are met since we have for the streamline direction (due to Assumption 3.2.5)

$$\tau_M^u |\mathbf{u}_M|^2 \leq C \tau_M^u(\mathbf{u}_M) \|\mathbf{u}_h\|_{\infty, M}^2 \leq C \tau_M^u(\mathbf{u}_M) \|\mathbf{u}_h\|_{W^{1,\infty}(M)}^2$$

and analogously for $\tau_L^\theta |\mathbf{u}_L|^2$. Therefore, the Gronwall constant $C'_{G,h}(\mathbf{u}, \theta, \mathbf{u}_h)$ does not blow up.

3.3. Pressure Estimate

In order to derive an upper bound for the pressure error, we proceed in a similar manner as in Corollary 3.1.3 where stability of p_h is established.

Theorem 3.3.1 (Pressure estimate).

Let $(\mathbf{u}, p, \theta): [0, T] \rightarrow \mathbf{V}^{div} \times Q \times \Theta$, $(\mathbf{u}_h, p_h, \theta_h): [0, T] \rightarrow \mathbf{V}_h^{div} \times Q_h \times \Theta_h$ be solutions of (2.9)-(2.10) and (3.1)-(3.2) satisfying

$$\mathbf{u} \in L^\infty(0, T; [W^{1,\infty}(\Omega)]^d), \quad \mathbf{u}_h \in L^\infty(0, T; [L^\infty(\Omega)]^d).$$

Then we obtain the a priori estimate for the semi-discrete pressure error $\xi_{p,h} = p - p_h$ for $0 \leq t \leq T$

$$\begin{aligned} \|\xi_{p,h}\|_{L^2(0,t;L^2(\Omega))}^2 &\leq \frac{C}{\beta_h^2} \left\{ \|\partial_t \xi_{u,h}\|_{L^2(0,t;L^2(\Omega))}^2 + \beta^2 \|\mathbf{g}\|_{L^\infty(0,t;L^\infty(\Omega))}^2 \|\xi_{\theta,h}\|_{L^2(0,t;L^2(\Omega))}^2 \right. \\ &\quad \left. + (\|\mathbf{u}\|_{L^2(0,t;L^\infty(\Omega))}^2 + \|\mathbf{u}_h\|_{L^2(0,t;L^\infty(\Omega))}^2) \|\xi_{u,h}\|_{L^\infty(0,t;L^2(\Omega))}^2 \right\} \end{aligned}$$

$$\begin{aligned}
& + \int_0^t \left(\nu + C \max_{M \in \mathcal{M}_h} \{ \gamma_M^{-1} \|\mathbf{u}_h\|_{\infty, M}^2 \} + \max_{M \in \mathcal{M}_h} \{ \tau_M^u |\mathbf{u}_M|^2 \} + \max_{M \in \mathcal{M}_h} \{ \gamma_M d \} \right) \|\boldsymbol{\xi}_{u,h}\|_{LPS}^2 d\tau \\
& + \int_0^t \max_{M \in \mathcal{M}_h} \{ \tau_M^u |\mathbf{u}_M|^2 \} \sum_{M \in \mathcal{M}_h} \tau_M^u |\mathbf{u}_M|^2 \|\kappa_M^u(\nabla \mathbf{u})\|_{0,M}^2 d\tau \Big\}
\end{aligned}$$

with a constant $C > 0$ independent of the problem parameters, h_M , h_L and the solutions.

Proof. The discrete inf-sup condition from Assumption 2.2.1 gives that for $\xi_{p,h} \in Q_h$, there exists a unique $\mathbf{v}_h \in \mathbf{V}_h$ with

$$\nabla \cdot \mathbf{v}_h = \xi_{p,h}, \quad \|\nabla \mathbf{v}_h\|_0 \leq \frac{1}{\beta_h} \|\xi_{p,h}\|_0.$$

We subtract (3.1) from (2.9) and use $(\mathbf{v}_h, 0) \in \mathbf{V}_h \times Q_h$ as a test function. This leads to

$$\begin{aligned}
\beta_h \|\nabla \mathbf{v}_h\|_0 \|\xi_{p,h}\|_0 & \leq \|\xi_{p,h}\|_0^2 = (\xi_{p,h}, \nabla \cdot \mathbf{v}_h) = (\partial_t \boldsymbol{\xi}_{u,h}, \mathbf{v}_h) + (\nu \nabla \boldsymbol{\xi}_{u,h}, \nabla \mathbf{v}_h) \\
& + c_u(\mathbf{u}; \mathbf{u}, \mathbf{v}_h) - c_u(\mathbf{u}_h; \mathbf{u}_h, \mathbf{v}_h) + (\beta \mathbf{g} \boldsymbol{\xi}_{\theta,h}, \mathbf{v}_h) - s_u(\mathbf{u}_h; \mathbf{u}_h, \mathbf{v}_h) - t_h(\mathbf{u}_h; \mathbf{u}_h, \mathbf{v}_h) \\
& \leq \|\nabla \mathbf{v}_h\|_0 \left(\|\partial_t \boldsymbol{\xi}_{u,h}\|_{-1} + \nu \|\nabla \boldsymbol{\xi}_{u,h}\|_0 + \beta \|\mathbf{g}\|_{\infty} \|\boldsymbol{\xi}_{\theta,h}\|_{-1} \right) \\
& + c_u(\mathbf{u}; \mathbf{u}, \mathbf{v}_h) - c_u(\mathbf{u}_h; \mathbf{u}_h, \mathbf{v}_h) + s_u(\mathbf{u}_h; \boldsymbol{\xi}_{u,h}, \mathbf{v}_h) - s_u(\mathbf{u}_h; \mathbf{u}, \mathbf{v}_h) \\
& + t_h(\mathbf{u}_h; \boldsymbol{\xi}_{u,h}, \mathbf{v}_h),
\end{aligned}$$

where we used $(\nabla \cdot \mathbf{u}, q) = 0$ for all $q \in L^2(\Omega)$ in the last term. We further have

$$\begin{aligned}
s_u(\mathbf{u}_h; \boldsymbol{\xi}_{u,h}, \mathbf{v}_h) & \leq s_u(\mathbf{u}_h; \boldsymbol{\xi}_{u,h}, \boldsymbol{\xi}_{u,h})^{1/2} s_u(\mathbf{u}_h; \mathbf{v}_h, \mathbf{v}_h)^{1/2} \\
& \leq \|\boldsymbol{\xi}_{u,h}\|_{LPS} \max_{M \in \mathcal{M}_h} \{ \sqrt{\tau_M^u} |\mathbf{u}_M| \} \|\nabla \mathbf{v}_h\|_0, \\
-s_u(\mathbf{u}_h; \mathbf{u}, \mathbf{v}_h) & \leq \left(\sum_{M \in \mathcal{M}_h} \tau_M^u |\mathbf{u}_M|^2 \|\kappa_M^u(\nabla \mathbf{u})\|_{0,M}^2 \right)^{1/2} \max_{M \in \mathcal{M}_h} \{ \sqrt{\tau_M^u} |\mathbf{u}_M| \} \|\nabla \mathbf{v}_h\|_0, \\
t_h(\mathbf{u}_h; \boldsymbol{\xi}_{u,h}, \mathbf{v}_h) & \leq \|\boldsymbol{\xi}_{u,h}\|_{LPS} \max_{M \in \mathcal{M}_h} \{ \sqrt{\gamma_M d} \} \|\nabla \mathbf{v}_h\|_0.
\end{aligned}$$

Integration by parts of the convective terms, using $(\nabla \cdot \mathbf{u}, q) = 0$ for all $q \in L^2(\Omega)$ and applying the Poincaré inequality A.3.2 yield:

$$\begin{aligned}
& c_u(\mathbf{u}; \mathbf{u}, \mathbf{v}_h) - c_u(\mathbf{u}_h; \mathbf{u}_h, \mathbf{v}_h) \\
& = -(\mathbf{u} - \mathbf{u}_h, \mathbf{u} \cdot \nabla \mathbf{v}_h) - (\mathbf{u}_h, (\mathbf{u} - \mathbf{u}_h) \cdot \nabla \mathbf{v}_h) + \frac{1}{2} (\nabla \cdot (\mathbf{u} - \mathbf{u}_h), \mathbf{u}_h \cdot \mathbf{v}_h) \\
& \leq (\|\mathbf{u}\|_{\infty} + \|\mathbf{u}_h\|_{\infty}) \|\boldsymbol{\xi}_{u,h}\|_0 \|\nabla \mathbf{v}_h\|_0 + C \max_{M \in \mathcal{M}_h} \{ \gamma_M^{-1/2} \|\mathbf{u}_h\|_{\infty, M} \} \|\boldsymbol{\xi}_{u,h}\|_{LPS} \|\nabla \mathbf{v}_h\|_0.
\end{aligned}$$

We obtain

$$\begin{aligned} \beta_h \|\xi_{p,h}\|_0 &\leq \|\partial_t \xi_{u,h}\|_0 + \beta \|\mathbf{g}\|_\infty \|\xi_{\theta,h}\|_0 + (\|\mathbf{u}\|_\infty + \|\mathbf{u}_h\|_\infty) \|\xi_{u,h}\|_0 \\ &+ \left(\sqrt{\nu} + C \max_{M \in \mathcal{M}_h} \{ \gamma_M^{-1/2} \|\mathbf{u}_h\|_{\infty,M} \} + \max_{M \in \mathcal{M}_h} \{ \sqrt{\tau_M^u} |\mathbf{u}_M| \} + \max_{M \in \mathcal{M}_h} \{ \sqrt{\gamma_M d} \} \right) \|\xi_{u,h}\|_{LPS} \\ &+ \left(\sum_{M \in \mathcal{M}_h} \tau_M^u |\mathbf{u}_M|^2 \|\kappa_M^u (\nabla \mathbf{u})\|_{0,M}^2 \right)^{1/2} \max_{M \in \mathcal{M}_h} \{ \sqrt{\tau_M^u} |\mathbf{u}_M| \}. \end{aligned}$$

Squaring and integration in time result in the claim. \square

In the above estimate for the pressure error $\xi_{p,h}$, the results from Sections 3.2.1 or 3.2.2 can be inserted if the respective requirements are met.

Remark 3.3.2. If the convective terms are estimated in a standard way (using Lemma A.3.7), the dependence on $\|\mathbf{u}_h\|_\infty$ can be avoided, because we calculate

$$\begin{aligned} c_u(\mathbf{u}; \mathbf{u}, \mathbf{v}_h) - c_u(\mathbf{u}_h; \mathbf{u}_h, \mathbf{v}_h) &= c_u(\mathbf{u} - \mathbf{u}_h; \mathbf{u}, \mathbf{v}_h) - c_u(\mathbf{u} - \mathbf{u}_h; \mathbf{u} - \mathbf{u}_h, \mathbf{v}_h) + c_u(\mathbf{u}; \mathbf{u} - \mathbf{u}_h, \mathbf{v}_h) \\ &\leq C(\|\mathbf{u}\|_1 + \|\xi_{u,h}\|_1) \|\xi_{u,h}\|_1 \|\nabla \mathbf{v}_h\|_0 \\ &\leq C(\|\mathbf{u}\|_1 + \nu^{-1/2} \|\xi_{u,h}\|_{LPS}) \nu^{-1/2} \|\xi_{u,h}\|_{LPS} \|\nabla \mathbf{v}_h\|_0. \end{aligned}$$

However, the resulting error bound is not stable for vanishing ν .

Remark 3.3.3. The above a priori error estimate of the pressure suffers from the term $\|\partial_t \xi_{u,h}\|_{L^2(0,t;L^2(\Omega))}$. In [DAL15], we show for the Oseen problem that an error reduction occurs. A similar result was obtained in [BF07] for an edge stabilization method of the Navier-Stokes problem.

4. Fully Discrete Analysis

This chapter is dedicated to the behavior of the fully discrete algorithm in terms of convergence in time and space where grad-div and LPS-SU stabilizations are incorporated. We prove the stability of the fully discrete solution of the stabilized Oberbeck-Boussinesq model (3.1)-(3.2) and present a consistency analysis for the stabilized Navier-Stokes equations. In Section 2.3.1, we introduced the fully discrete scheme. For clarity, we repeat the important equations here and introduce some notations and simplifications we use in the following analysis.

Consider equidistant time steps of size Δt . Let $0 = t_0 < t_1 < \dots < t_N = T$. For $\mathbf{u}, \mathbf{v} \in \mathbf{V}$ and $\psi, \theta \in \Theta$, the LPS terms at time t_n are written as

$$\begin{aligned} s_u(\mathbf{w}, \mathbf{u}, \mathbf{y}, \mathbf{v}) &:= \sum_{M \in \mathcal{M}_h} \tau_M^n (\kappa_M^u((\mathbf{w}_M \cdot \nabla)\mathbf{u}), \kappa_M^u((\mathbf{y}_M \cdot \nabla)\mathbf{v}))_M, \\ s_\theta(\mathbf{w}, \psi, \mathbf{y}, \theta) &:= \sum_{L \in \mathcal{L}_h} \tau_L^n ((\kappa_L^\theta(\mathbf{w}_L \cdot \nabla)\psi), \kappa_L^\theta((\mathbf{y}_L \cdot \nabla)\theta))_L \end{aligned}$$

with element-wise constant $\mathbf{w}_M, \mathbf{w}_L, \mathbf{y}_M, \mathbf{y}_L \in \mathbb{R}^d$ as introduced in Section 2.2.3 and stabilization parameters that coincide with the semi-discrete, time-continuous ones at all t_n :

$$\tau_M^n = \tau_M^u(t_n), \quad \tau_L^n = \tau_L^\theta(t_n) \quad \text{for } M \in \mathcal{M}_h, L \in \mathcal{L}_h.$$

Note that this notation coincides with the definition from Section 2.2 if the first and third arguments are equal. For convenience, we assume a constant grad-div parameter $\gamma := \gamma_M$ for all $M \in \mathcal{M}_h$, i.e.,

$$t_h(\tilde{\mathbf{u}}_{ht}^n; \tilde{\mathbf{u}}_{ht}^n, \mathbf{v}_h) = \gamma(\nabla \cdot \tilde{\mathbf{u}}_{ht}^n, \nabla \cdot \mathbf{v}_h),$$

and the case $i_h \equiv 0$, since we use a continuous discrete pressure space for our simulations later. The extension to cell-wise linear and time dependent $\gamma_M^n = \gamma_M(t_n)$ can be proven easily.

Let $\theta_{ht}^{n*} := 2\theta_{ht}^{n-1} - \theta_{ht}^{n-2}$. For the analysis of the splitting algorithm, we consider the case of an incremental method, i.e., $\chi^{\text{rot}} = 0$. Then the fully discretized and stabilized scheme reads:

Find $\tilde{\mathbf{u}}_{ht}^n \in \mathbf{V}_h$ such that for all $\mathbf{v}_h \in \mathbf{V}_h$:

$$\begin{aligned} & \left(\frac{3\tilde{\mathbf{u}}_{ht}^n - 4\mathbf{u}_{ht}^{n-1} + \mathbf{u}_{ht}^{n-2}}{2\Delta t}, \mathbf{v}_h \right) + \nu(\nabla \tilde{\mathbf{u}}_{ht}^n, \nabla \mathbf{v}_h) + c_u(\tilde{\mathbf{u}}_{ht}^n; \tilde{\mathbf{u}}_{ht}^n, \mathbf{v}_h) + t_h(\tilde{\mathbf{u}}_{ht}^n; \tilde{\mathbf{u}}_{ht}^n, \mathbf{v}_h) \\ & + s_u(\tilde{\mathbf{u}}_{ht}^n, \tilde{\mathbf{u}}_{ht}^n, \tilde{\mathbf{u}}_{ht}^n, \mathbf{v}_h) - (p_{ht}^{n-1}, \nabla \cdot \mathbf{v}_h) + \beta(\mathbf{g}(t_n)\theta_{ht}^{n*}, \mathbf{v}_h) = (\mathbf{f}_u(t_n), \mathbf{v}_h), \\ & \tilde{\mathbf{u}}_{ht}^n|_{\partial\Omega} = 0. \end{aligned} \quad (4.1)$$

Find $\mathbf{u}_{ht}^n \in \mathbf{V}_h^{div}$ and $p_{ht}^n \in Q_h$ such that for all $\mathbf{y}_h \in \mathbf{Y}_h$ and $q_h \in Q_h$:

$$\begin{aligned} & \left(\frac{3\mathbf{u}_{ht}^n - 3\tilde{\mathbf{u}}_{ht}^n}{2\Delta t} + \nabla(p_{ht}^n - p_{ht}^{n-1}), \mathbf{y}_h \right) = 0, \\ & (\mathbf{u}_{ht}^n, \nabla q_h) = 0, \\ & \mathbf{u}_{ht}^n|_{\partial\Omega} = 0. \end{aligned} \quad (4.2)$$

Find $\theta_{ht}^n \in \Theta_h$ such that for all $\psi_h \in \Theta_h$:

$$\begin{aligned} & (D_t \theta_{ht}^n, \psi_h) + \alpha(\nabla \theta_{ht}^n, \nabla \psi_h) + c_\theta(\tilde{\mathbf{u}}_{ht}^n; \theta_{ht}^n, \psi_h) + s_\theta(\tilde{\mathbf{u}}_{ht}^n, \theta_{ht}^n, \tilde{\mathbf{u}}_{ht}^n, \psi_h) = (f_\theta(t_n), \psi_h), \\ & \theta_{ht}^n|_{\partial\Omega} = 0. \end{aligned} \quad (4.3)$$

The above scheme provides the existence of $\tilde{\mathbf{u}}_{ht}^n$, \mathbf{u}_{ht}^n , p_{ht}^n , θ_{ht}^n in every time step $1 \leq n \leq N$. This can be understood via induction. Given the solutions at time t_{n-1} and t_{n-2} , a solution $\tilde{\mathbf{u}}_{ht}^n$ of (4.1) exists by standard theory. The velocity \mathbf{u}_{ht}^n is given as the L^2 -projection of $\tilde{\mathbf{u}}_{ht}^n$ onto $\mathbf{V}_h^{div} \neq \{\mathbf{0}\}$. All $\mathbf{y}_h \in \mathbf{Y}_h$ can be written as $\mathbf{y}_h = \mathbf{w}_h + \nabla q_h \in \mathbf{Y}_h = \mathbf{V}_h^{div} \oplus \nabla Q_h$. If we insert $\mathbf{u}_{ht}^n := P_{div} \tilde{\mathbf{u}}_{ht}^n$ into the projection equation (4.2), we have:

$$\begin{aligned} & \left(\frac{3\mathbf{u}_{ht}^n - 3\tilde{\mathbf{u}}_{ht}^n}{2\Delta t} + \nabla(p_{ht}^n - p_{ht}^{n-1}), \mathbf{y}_h \right) = \frac{3}{2\Delta t} (P_{div} \tilde{\mathbf{u}}_{ht}^n - \tilde{\mathbf{u}}_{ht}^n, \mathbf{w}_h) + (\nabla(p_{ht}^n - p_{ht}^{n-1}), \mathbf{w}_h) \\ & + \frac{3}{2\Delta t} (\mathbf{u}_{ht}^n - \tilde{\mathbf{u}}_{ht}^n, \nabla q_h) + (\nabla(p_{ht}^n - p_{ht}^{n-1}), \nabla q_h) \\ & = \frac{3}{2\Delta t} (\mathbf{u}_{ht}^n - \tilde{\mathbf{u}}_{ht}^n, \nabla q_h) + (\nabla(p_{ht}^n - p_{ht}^{n-1}), \nabla q_h). \end{aligned}$$

Thus, the projection equation becomes a Poisson problem for the pressure p_{ht}^n . Therefore, its existence is guaranteed and (4.2) is satisfied. Obviously, θ_{ht}^n exists as well.

4.1. Stability of the Fully Discretized Quantities

In order to obtain stability for the fully discretized quantities, we are interested in suitable norms in which we want to control the solution and errors.

Definition 4.1.1 (Time-discrete norm).

Let $\mathbf{v}^n \in \mathbf{A}$ be vector-valued and $\psi^n \in B$ be scalar-valued quantities, where \mathbf{A} and B are normed spaces, $1 \leq n \leq N$. Let $\mathbf{v} = (\mathbf{v}^1, \dots, \mathbf{v}^N) \in \mathbf{A}^N$ and $\psi = (\psi^1, \dots, \psi^N) \in B^N$. The norms we want to control are defined by

$$\begin{aligned} \|\mathbf{v}\|_{l^2(0,T;\mathbf{A})}^2 &:= \Delta t \sum_{n=1}^N \|\mathbf{v}^n\|_{\mathbf{A}}^2, & \|\psi\|_{l^2(0,T;B)}^2 &:= \Delta t \sum_{n=1}^N \|\psi^n\|_B^2, \\ \|\mathbf{v}\|_{l^\infty(0,T;\mathbf{A})} &:= \max_{1 \leq n \leq N} \|\mathbf{v}^n\|_{\mathbf{A}}, & \|\psi\|_{l^\infty(0,T;B)} &:= \max_{1 \leq n \leq N} \|\psi^n\|_B. \end{aligned}$$

We denote analogously

$$\begin{aligned} \|\mathbf{v}\|_{l^2(0,T;LPS)}^2 &:= \Delta t \sum_{n=1}^N \|\|\mathbf{v}^n\|\|_{LPS}^2 \\ &= \Delta t \sum_{n=1}^N \left(\nu \|\nabla \mathbf{v}^n\|_0^2 + \gamma \|\nabla \cdot \mathbf{v}^n\|_0^2 + s_u(\tilde{\mathbf{u}}_{ht}^n, \mathbf{v}^n, \tilde{\mathbf{u}}_{ht}^n, \mathbf{v}^n) \right), \\ \|\psi\|_{l^2(0,T;LPS)}^2 &:= \Delta t \sum_{n=1}^N \|\|\psi^n\|\|_{LPS}^2 = \Delta t \sum_{n=1}^N \left(\alpha \|\nabla \psi^n\|_0^2 + s_\theta(\tilde{\mathbf{u}}_{ht}^n, \psi^n, \tilde{\mathbf{u}}_{ht}^n, \psi^n) \right). \end{aligned}$$

For quantities r that are continuous in time, we identify r with $(r(t_1), \dots, r(t_N))^T$, where $t_n := n\Delta t$.

Theorem 4.1.2 (Stability of the stabilized Oberbeck-Boussinesq model).

Let $\mathbf{f}_u \in l^2(0, T; [L^2(\Omega)]^d)$, $f_\theta \in l^2(0, T; L^2(\Omega))$ and $\mathbf{g} \in l^\infty(0, T; [L^\infty(\Omega)]^d)$. With $C > 0$, we have the following stability result for solutions $(\tilde{\mathbf{u}}_{ht}, \mathbf{u}_{ht}, p_{ht}, \theta_{ht}) \in (\mathbf{V}_h)^N \times (\mathbf{V}_h^{div})^N \times (Q_h)^N \times (\Theta_h)^N$ of (4.1)-(4.3):

$$\begin{aligned} &\|\tilde{\mathbf{u}}_{ht}\|_{l^\infty(0,T;L^2(\Omega))}^2 + \|\tilde{\mathbf{u}}_{ht}\|_{l^2(0,T;LPS)}^2 + (\Delta t)^2 \|\nabla p_{ht}\|_{l^\infty(0,T;L^2(\Omega))}^2 \\ &+ \|\theta_{ht}\|_{l^\infty(0,T;L^2(\Omega))}^2 + \|\theta_{ht}\|_{l^2(0,T;LPS)}^2 \\ &\leq C e^{C_{G,OB}} \left[\|\tilde{\mathbf{u}}_{ht}^0\|_0^2 + \|\tilde{\mathbf{u}}_{ht}^1\|_0^2 + \|2\mathbf{u}_{ht}^1 - \mathbf{u}_{ht}^0\|_0^2 + \|\|\tilde{\mathbf{u}}_{ht}^0\|\|_{LPS}^2 + \|\|\tilde{\mathbf{u}}_{ht}^1\|\|_{LPS}^2 \right. \\ &+ (\Delta t)^2 \|\nabla p_{ht}^0\|_0^2 + (\Delta t)^2 \|\nabla p_{ht}^1\|_0^2 + \|\theta_{ht}^1\|_0^2 + \|\theta_{ht}^0\|_0^2 + \|2\theta_{ht}^1 - \theta_{ht}^0\|_0^2 \\ &\left. + \|\|\theta_{ht}^0\|\|_{LPS}^2 + \|\|\theta_{ht}^1\|\|_{LPS}^2 + \left(\beta \|\mathbf{g}\|_{l^\infty(0,T;L^\infty(\Omega))} \right)^{-1} \left(\|\mathbf{f}_u\|_{l^2(0,T;L^2(\Omega))}^2 + \|f_\theta\|_{l^2(0,T;L^2(\Omega))}^2 \right) \right], \end{aligned}$$

provided $3\Delta t\beta\|\mathbf{g}\|_{l^\infty(0,T;L^\infty(\Omega))} < 1$ and with a Gronwall constant $C_{G,OB}$ behaving like

$$C_{G,OB} \sim T \left(1 - 3\Delta t\beta\|\mathbf{g}\|_{l^\infty(0,T;L^\infty(\Omega))}\right)^{-1}. \quad (4.4)$$

Proof. Due to the projection step (4.2) tested with $\mathbf{y}_h = \frac{8}{3}(\Delta t)^2 \nabla p_{ht}^{n-1}$ and the fact that $\mathbf{u}_{ht}^n \in \mathbf{V}_h^{div}$, we have

$$-4\Delta t(\tilde{\mathbf{u}}_{ht}^n, \nabla p_{ht}^{n-1}) + \frac{8(\Delta t)^2}{3}(\nabla(p_{ht}^n - p_{ht}^{n-1}), \nabla p_{ht}^{n-1}) = 0.$$

Testing with $\mathbf{v}_h = 4\Delta t\tilde{\mathbf{u}}_{ht}^n$ in (4.1) yields due to skew-symmetry of c_u

$$\begin{aligned} & 2\left(3\tilde{\mathbf{u}}_{ht}^n - 4\mathbf{u}_{ht}^{n-1} + \mathbf{u}_{ht}^{n-2}, \tilde{\mathbf{u}}_{ht}^n\right) + 4\Delta t\nu(\nabla\tilde{\mathbf{u}}_{ht}^n, \nabla\tilde{\mathbf{u}}_{ht}^n) + 4\Delta t\gamma(\nabla \cdot \tilde{\mathbf{u}}_{ht}^n, \nabla \cdot \tilde{\mathbf{u}}_{ht}^n) \\ & + 4\Delta ts_u(\tilde{\mathbf{u}}_{ht}^n, \tilde{\mathbf{u}}_{ht}^n, \tilde{\mathbf{u}}_{ht}^n, \tilde{\mathbf{u}}_{ht}^n) \\ & = -4\Delta tc_u(\tilde{\mathbf{u}}_{ht}^n; \tilde{\mathbf{u}}_{ht}^n, \tilde{\mathbf{u}}_{ht}^n) + 4\Delta t(\mathbf{f}_u(t_n), \tilde{\mathbf{u}}_{ht}^n) - 4\Delta t(\nabla p_{ht}^{n-1}, \tilde{\mathbf{u}}_{ht}^n) - 4\Delta t\beta(\mathbf{g}(t_n)\theta_{ht}^{n*}, \tilde{\mathbf{u}}_{ht}^n) \\ & = 4\Delta t(\mathbf{f}_u(t_n), \tilde{\mathbf{u}}_{ht}^n) - 4\Delta t(\nabla p_{ht}^{n-1}, \tilde{\mathbf{u}}_{ht}^n) - 4\Delta t\beta(\mathbf{g}(t_n)(2\theta_{ht}^{n-1} - \theta_{ht}^{n-2}), \tilde{\mathbf{u}}_{ht}^n). \end{aligned}$$

We add these two equations together and establish using Young's inequality

$$\begin{aligned} & 2\left(3\tilde{\mathbf{u}}_{ht}^n - 4\mathbf{u}_{ht}^{n-1} + \mathbf{u}_{ht}^{n-2}, \tilde{\mathbf{u}}_{ht}^n\right) + 4\Delta t\nu\|\nabla\tilde{\mathbf{u}}_{ht}^n\|_0^2 + 4\Delta t\gamma\|\nabla \cdot \tilde{\mathbf{u}}_{ht}^n\|_0^2 \\ & + 4\Delta ts_u(\tilde{\mathbf{u}}_{ht}^n, \tilde{\mathbf{u}}_{ht}^n, \tilde{\mathbf{u}}_{ht}^n, \tilde{\mathbf{u}}_{ht}^n) + \frac{8}{3}(\Delta t)^2(\nabla(p_{ht}^n - p_{ht}^{n-1}), \nabla p_{ht}^{n-1}) \\ & = 4\Delta t(\mathbf{f}_u(t_n), \tilde{\mathbf{u}}_{ht}^n) - 4\Delta t\beta(\mathbf{g}(t_n)(2\theta_{ht}^{n-1} - \theta_{ht}^{n-2}), \tilde{\mathbf{u}}_{ht}^n) \\ & \leq \frac{5\Delta t\beta\|\mathbf{g}(t_n)\|_\infty}{3}\|\tilde{\mathbf{u}}_{ht}^n\|_0^2 + \frac{12\Delta t}{5\beta\|\mathbf{g}(t_n)\|_\infty}\|\mathbf{f}_u(t_n)\|_0^2 + \frac{4\Delta t\beta\|\mathbf{g}(t_n)\|_\infty}{3}\|\tilde{\mathbf{u}}_{ht}^n\|_0^2 \\ & + 3\Delta t\beta\|\mathbf{g}(t_n)\|_\infty\|2\theta_{ht}^{n-1} - \theta_{ht}^{n-2}\|_0^2 \\ & \leq 3\Delta t\beta\|\mathbf{g}(t_n)\|_\infty\|\tilde{\mathbf{u}}_{ht}^n\|_0^2 + \frac{12\Delta t}{5\beta\|\mathbf{g}(t_n)\|_\infty}\|\mathbf{f}_u(t_n)\|_0^2 + 3\Delta t\beta\|\mathbf{g}(t_n)\|_\infty\|2\theta_{ht}^{n-1} - \theta_{ht}^{n-2}\|_0^2. \end{aligned} \quad (4.5)$$

Denote $\delta_t a^n := a^n - a^{n-1}$ and $\delta_{tt} a^n := \delta_t(\delta_t a^n)$. The first term on the left-hand side is splitted according to

$$\begin{aligned} & 2(3\tilde{\mathbf{u}}_{ht}^n - 4\mathbf{u}_{ht}^{n-1} + \mathbf{u}_{ht}^{n-2}, \tilde{\mathbf{u}}_{ht}^n) = 6(\tilde{\mathbf{u}}_{ht}^n, \tilde{\mathbf{u}}_{ht}^n - \mathbf{u}_{ht}^n) \\ & + 2(\tilde{\mathbf{u}}_{ht}^n - \mathbf{u}_{ht}^n, 3\mathbf{u}_{ht}^n - 4\mathbf{u}_{ht}^{n-1} + \mathbf{u}_{ht}^{n-2}) + 2(\mathbf{u}_{ht}^n, 3\mathbf{u}_{ht}^n - 4\mathbf{u}_{ht}^{n-1} + \mathbf{u}_{ht}^{n-2}) \\ & = I_1 + I_2 + I_3 \end{aligned}$$

$$\begin{aligned} \text{with } I_1 & := 3\|\tilde{\mathbf{u}}_{ht}^n\|_0^2 + 3\|\mathbf{u}_{ht}^n - \tilde{\mathbf{u}}_{ht}^n\|_0^2 - 3\|\mathbf{u}_{ht}^n\|_0^2, \\ I_2 & := 2(\tilde{\mathbf{u}}_{ht}^n - \mathbf{u}_{ht}^n, 3\mathbf{u}_{ht}^n - 4\mathbf{u}_{ht}^{n-1} + \mathbf{u}_{ht}^{n-2}), \\ I_3 & := \|\mathbf{u}_{ht}^n\|_0^2 + \|2\mathbf{u}_{ht}^n - \mathbf{u}_{ht}^{n-1}\|_0^2 + \|\delta_{tt}\mathbf{u}_{ht}^n\|_0^2 - \|\mathbf{u}_{ht}^{n-1}\|_0^2 - \|2\mathbf{u}_{ht}^{n-1} - \mathbf{u}_{ht}^{n-2}\|_0^2, \end{aligned}$$

where the following identities were taken advantage of:

$$2(a, a - b) = \|a\|_0^2 + \|a - b\|_0^2 - \|b\|_0^2, \quad (4.6)$$

$$2(a, 3a - 4b + c) = \|a\|_0^2 + \|2a - b\|_0^2 + \|a - 2b + c\|_0^2 - \|b\|_0^2 - \|2b - c\|_0^2. \quad (4.7)$$

The second term I_2 vanishes using (4.2) and due to $\mathbf{u}_{ht}^n \in \mathbf{V}_h^{div}$:

$$\begin{aligned} \frac{3}{4\Delta t} I_2 &= (\nabla(p_{ht}^n - p_{ht}^{n-1}), 3\mathbf{u}_{ht}^n - 4\mathbf{u}_{ht}^{n-1} + \mathbf{u}_{ht}^{n-2}) \\ &= -(p_{ht}^n - p_{ht}^{n-1}, \nabla \cdot (3\mathbf{u}_{ht}^n - 4\mathbf{u}_{ht}^{n-1} + \mathbf{u}_{ht}^{n-2})) = 0. \end{aligned}$$

We deploy this splitting and apply identity (4.6) to $\frac{8}{3}(\Delta t)^2(\nabla(p_{ht}^n - p_{ht}^{n-1}), \nabla p_{ht}^{n-1})$ in (4.5):

$$\begin{aligned} &3\|\tilde{\mathbf{u}}_{ht}^n\|_0^2 + 3\|\mathbf{u}_{ht}^n - \tilde{\mathbf{u}}_{ht}^n\|_0^2 - 2\|\mathbf{u}_{ht}^n\|_0^2 + \|2\mathbf{u}_{ht}^n - \mathbf{u}_{ht}^{n-1}\|_0^2 + \frac{4}{3}(\Delta t)^2\|\nabla p_{ht}^n\|_0^2 \\ &+ 4\Delta t\nu\|\nabla\tilde{\mathbf{u}}_{ht}^n\|_0^2 + 4\Delta t\gamma\|\nabla \cdot \tilde{\mathbf{u}}_{ht}^n\|_0^2 + \|\delta_{tt}\mathbf{u}_{ht}^n\|_0^2 + 4\Delta ts_u(\tilde{\mathbf{u}}_{ht}^n, \tilde{\mathbf{u}}_{ht}^n, \tilde{\mathbf{u}}_{ht}^n, \tilde{\mathbf{u}}_{ht}^n) \\ &\leq \|\tilde{\mathbf{u}}_{ht}^{n-1}\|_0^2 + \|2\mathbf{u}_{ht}^{n-1} - \mathbf{u}_{ht}^{n-2}\|_0^2 + \frac{4}{3}(\Delta t)^2\|\nabla p_{ht}^{n-1}\|_0^2 + \frac{4}{3}(\Delta t)^2\|\nabla(p_{ht}^n - p_{ht}^{n-1})\|_0^2 \\ &+ 3\Delta t\beta\|\mathbf{g}(t_n)\|_\infty\|\tilde{\mathbf{u}}_{ht}^n\|_0^2 + \frac{12\Delta t}{5\beta\|\mathbf{g}(t_n)\|_\infty}\|\mathbf{f}_u(t_n)\|_0^2 + 3\Delta t\beta\|\mathbf{g}(t_n)\|_\infty\|2\theta_{ht}^{n-1} - \theta_{ht}^{n-2}\|_0^2. \end{aligned}$$

Then we use that $\|\mathbf{u}_{ht}^n\|_0 \leq \|\tilde{\mathbf{u}}_{ht}^n\|_0$ because $\mathbf{u}_{ht}^n = P_{div}\tilde{\mathbf{u}}_{ht}^n$ is an orthogonal L^2 -projection:

$$\begin{aligned} &\|\tilde{\mathbf{u}}_{ht}^n\|_0^2 + 3\|\mathbf{u}_{ht}^n - \tilde{\mathbf{u}}_{ht}^n\|_0^2 + \|2\mathbf{u}_{ht}^n - \mathbf{u}_{ht}^{n-1}\|_0^2 + \frac{4}{3}(\Delta t)^2\|\nabla p_{ht}^n\|_0^2 \\ &+ 4\Delta t\nu\|\nabla\tilde{\mathbf{u}}_{ht}^n\|_0^2 + 4\Delta t\gamma\|\nabla \cdot \tilde{\mathbf{u}}_{ht}^n\|_0^2 + \|\delta_{tt}\mathbf{u}_{ht}^n\|_0^2 + 4\Delta ts_u(\tilde{\mathbf{u}}_{ht}^n, \tilde{\mathbf{u}}_{ht}^n, \tilde{\mathbf{u}}_{ht}^n, \tilde{\mathbf{u}}_{ht}^n) \\ &\leq \|\tilde{\mathbf{u}}_{ht}^{n-1}\|_0^2 + \|2\mathbf{u}_{ht}^{n-1} - \mathbf{u}_{ht}^{n-2}\|_0^2 + \frac{4}{3}(\Delta t)^2\|\nabla p_{ht}^{n-1}\|_0^2 + \frac{4}{3}(\Delta t)^2\|\nabla(p_{ht}^n - p_{ht}^{n-1})\|_0^2 \\ &+ 3\Delta t\beta\|\mathbf{g}(t_n)\|_\infty\|\tilde{\mathbf{u}}_{ht}^n\|_0^2 + \frac{12\Delta t}{5\beta\|\mathbf{g}(t_n)\|_\infty}\|\mathbf{f}_u(t_n)\|_0^2 + 3\Delta t\beta\|\mathbf{g}(t_n)\|_\infty\|2\theta_{ht}^{n-1} - \theta_{ht}^{n-2}\|_0^2. \end{aligned}$$

The projection equation (4.2) tested with $\mathbf{y}_h = \nabla(p_{ht}^n - p_{ht}^{n-1})$ yields

$$\begin{aligned} \frac{2\Delta t}{3}\|\nabla(p_{ht}^n - p_{ht}^{n-1})\|_0^2 &= -(\mathbf{u}_{ht}^n - \tilde{\mathbf{u}}_{ht}^n, \nabla(p_{ht}^n - p_{ht}^{n-1})) \\ &\leq \|\mathbf{u}_{ht}^n - \tilde{\mathbf{u}}_{ht}^n\|_0\|\nabla(p_{ht}^n - p_{ht}^{n-1})\|_0 \\ \Rightarrow \frac{4}{3}(\Delta t)^2\|\nabla(p_{ht}^n - p_{ht}^{n-1})\|_0^2 &\leq 3\|\mathbf{u}_{ht}^n - \tilde{\mathbf{u}}_{ht}^n\|_0^2. \end{aligned}$$

We insert this in the previous estimate and obtain

$$\begin{aligned} &\|\tilde{\mathbf{u}}_{ht}^n\|_0^2 + \|2\mathbf{u}_{ht}^n - \mathbf{u}_{ht}^{n-1}\|_0^2 + \frac{4}{3}(\Delta t)^2\|\nabla p_{ht}^n\|_0^2 + 4\Delta t\nu\|\nabla\tilde{\mathbf{u}}_{ht}^n\|_0^2 \\ &+ 4\Delta t\gamma\|\nabla \cdot \tilde{\mathbf{u}}_{ht}^n\|_0^2 + \|\delta_{tt}\mathbf{u}_{ht}^n\|_0^2 + 4\Delta ts_u(\tilde{\mathbf{u}}_{ht}^n, \tilde{\mathbf{u}}_{ht}^n, \tilde{\mathbf{u}}_{ht}^n, \tilde{\mathbf{u}}_{ht}^n) \end{aligned}$$

$$\begin{aligned}
&\leq \|\tilde{\mathbf{u}}_{ht}^{n-1}\|_0^2 + \|2\mathbf{u}_{ht}^{n-1} - \mathbf{u}_{ht}^{n-2}\|_0^2 + \frac{4}{3}(\Delta t)^2 \|\nabla p_{ht}^{n-1}\|_0^2 + 3\Delta t\beta \|\mathbf{g}(t_n)\|_\infty \|\tilde{\mathbf{u}}_{ht}^n\|_0^2 \\
&+ \frac{12\Delta t}{5\beta \|\mathbf{g}(t_n)\|_\infty} \|\mathbf{f}_u(t_n)\|_0^2 + 3\Delta t\beta \|\mathbf{g}(t_n)\|_\infty \|2\theta_{ht}^{n-1} - \theta_{ht}^{n-2}\|_0^2. \tag{4.8}
\end{aligned}$$

For the temperature, we test (4.3) with $\psi_h = 4\Delta t\theta_{ht}^n$ and take advantage of the skew-symmetry of c_θ :

$$\begin{aligned}
&2\left(3\theta_{ht}^n - 4\theta_{ht}^{n-1} + \theta_{ht}^{n-2}, \theta_{ht}^n\right) + 4\Delta t\alpha(\nabla\theta_{ht}^n, \nabla\theta_{ht}^n) + 4\Delta ts_\theta(\tilde{\mathbf{u}}_{ht}^n, \theta_{ht}^n, \tilde{\mathbf{u}}_{ht}^n, \theta_{ht}^n) \\
&= -4\Delta tc_\theta(\tilde{\mathbf{u}}_{ht}^n; \theta_{ht}^n, \theta_{ht}^n) + 4\Delta t(f_\theta(t_n), \theta_{ht}^n) \\
&= 4\Delta t(f_\theta(t_n), \theta_{ht}^n) \leq 3\Delta t\beta \|\mathbf{g}(t_n)\|_\infty \|\theta_{ht}^n\|_0^2 + \frac{4\Delta t}{3\beta \|\mathbf{g}(t_n)\|_\infty} \|f_\theta(t_n)\|_0^2.
\end{aligned}$$

For the first term on the left-hand side, it holds due to identity (4.7):

$$\begin{aligned}
2(3\theta_{ht}^n - 4\theta_{ht}^{n-1} + \theta_{ht}^{n-2}, \theta_{ht}^n) &= \|\theta_{ht}^n\|_0^2 + \|2\theta_{ht}^n - \theta_{ht}^{n-1}\|_0^2 + \|\delta_{tt}\theta_{ht}^n\|_0^2 \\
&\quad - \|\theta_{ht}^{n-1}\|_0^2 - \|2\theta_{ht}^{n-1} - \theta_{ht}^{n-2}\|_0^2.
\end{aligned}$$

We obtain

$$\begin{aligned}
&\|\theta_{ht}^n\|_0^2 + \|2\theta_{ht}^n - \theta_{ht}^{n-1}\|_0^2 + \|\delta_{tt}\theta_{ht}^n\|_0^2 + 4\Delta t\alpha \|\nabla\theta_{ht}^n\|_0^2 + 4\Delta ts_\theta(\tilde{\mathbf{u}}_{ht}^n, \theta_{ht}^n, \tilde{\mathbf{u}}_{ht}^n, \theta_{ht}^n) \\
&\leq \|\theta_{ht}^{n-1}\|_0^2 + \|2\theta_{ht}^{n-1} - \theta_{ht}^{n-2}\|_0^2 + 3\Delta t\beta \|\mathbf{g}(t_n)\|_\infty \|\theta_{ht}^n\|_0^2 + \frac{4\Delta t}{3\beta \|\mathbf{g}(t_n)\|_\infty} \|f_\theta(t_n)\|_0^2. \tag{4.9}
\end{aligned}$$

Adding (4.8) and (4.9) and summing up from $n = 2$ to $m \leq N$ give

$$\begin{aligned}
&\|\tilde{\mathbf{u}}_{ht}^m\|_0^2 + \|2\mathbf{u}_{ht}^m - \mathbf{u}_{ht}^{m-1}\|_0^2 + \frac{4}{3}(\Delta t)^2 \|\nabla p_{ht}^m\|_0^2 + \|\theta_{ht}^m\|_0^2 + \|2\theta_{ht}^m - \theta_{ht}^{m-1}\|_0^2 \\
&+ \sum_{n=2}^m \left[4\Delta t\nu \|\nabla \tilde{\mathbf{u}}_{ht}^n\|_0^2 + 4\Delta t\gamma \|\nabla \cdot \tilde{\mathbf{u}}_{ht}^n\|_0^2 + \|\delta_{tt}\mathbf{u}_{ht}^n\|_0^2 + \|\delta_{tt}\theta_{ht}^n\|_0^2 \right. \\
&+ 4\Delta t\alpha \|\nabla\theta_{ht}^n\|_0^2 + 4\Delta ts_u(\tilde{\mathbf{u}}_{ht}^n, \tilde{\mathbf{u}}_{ht}^n, \tilde{\mathbf{u}}_{ht}^n, \tilde{\mathbf{u}}_{ht}^n) + 4\Delta ts_\theta(\tilde{\mathbf{u}}_{ht}^n, \theta_{ht}^n, \tilde{\mathbf{u}}_{ht}^n, \theta_{ht}^n) \left. \right] \\
&\leq \|\tilde{\mathbf{u}}_{ht}^1\|_0^2 + \|2\mathbf{u}_{ht}^1 - \mathbf{u}_{ht}^0\|_0^2 + \frac{4}{3}(\Delta t)^2 \|\nabla p_{ht}^1\|_0^2 \\
&+ \|\theta_{ht}^1\|_0^2 + \|2\theta_{ht}^1 - \theta_{ht}^0\|_0^2 + \Delta t \sum_{n=2}^m 3\beta \|\mathbf{g}(t_n)\|_\infty \|2\theta_{ht}^{n-1} - \theta_{ht}^{n-2}\|_0^2 \\
&+ \Delta t \sum_{n=2}^m 3\beta \|\mathbf{g}(t_n)\|_\infty \left(\|\tilde{\mathbf{u}}_{ht}^n\|_0^2 + \|\theta_{ht}^n\|_0^2 \right) + \sum_{n=2}^m \frac{\Delta t}{\beta \|\mathbf{g}(t_n)\|_\infty} \left(\frac{12}{5} \|\mathbf{f}_u(t_n)\|_0^2 + \frac{4}{3} \|f_\theta(t_n)\|_0^2 \right) \\
&\leq \|\tilde{\mathbf{u}}_{ht}^1\|_0^2 + \|2\mathbf{u}_{ht}^1 - \mathbf{u}_{ht}^0\|_0^2 + \frac{4}{3}(\Delta t)^2 \|\nabla p_{ht}^1\|_0^2 + \|\theta_{ht}^1\|_0^2 + \|2\theta_{ht}^1 - \theta_{ht}^0\|_0^2 \\
&+ \Delta t \sum_{n=1}^m 3\beta \|\mathbf{g}(t_n)\|_\infty \left(\|\tilde{\mathbf{u}}_{ht}^n\|_0^2 + \|\theta_{ht}^n\|_0^2 + \|2\theta_{ht}^n - \theta_{ht}^{n-1}\|_0^2 \right)
\end{aligned}$$

$$+ \frac{\Delta t}{\beta \|\mathbf{g}\|_{l^\infty(0,T;L^\infty(\Omega))}} \sum_{n=2}^m \left(\frac{12}{5} \|\mathbf{f}_u(t_n)\|_0^2 + \frac{4}{3} \|f_\theta(t_n)\|_0^2 \right).$$

Provided $3\Delta t\beta\|\mathbf{g}\|_{l^\infty(0,T;L^\infty(\Omega))} < 1$, the discrete Gronwall Lemma [A.3.6](#) can be applied for $\|\tilde{\mathbf{u}}_{ht}^m\|_0^2 + \|\theta_{ht}^m\|_0^2 + \|2\theta_{ht}^m - \theta_{ht}^{m-1}\|_0^2$. Hence, for $2 \leq m \leq N$:

$$\begin{aligned} & \|\tilde{\mathbf{u}}_{ht}^m\|_0^2 + (\Delta t)^2 \|\nabla p_{ht}^m\|_0^2 + \|\theta_{ht}^m\|_0^2 + \|2\theta_{ht}^m - \theta_{ht}^{m-1}\|_0^2 \\ & + \Delta t \sum_{n=2}^m \left[\nu \|\nabla \tilde{\mathbf{u}}_{ht}^n\|_0^2 + \gamma \|\nabla \cdot \tilde{\mathbf{u}}_{ht}^n\|_0^2 + \alpha \|\nabla \theta_{ht}^n\|_0^2 \right. \\ & \left. + s_u(\tilde{\mathbf{u}}_{ht}^n, \tilde{\mathbf{u}}_{ht}^n, \tilde{\mathbf{u}}_{ht}^n, \tilde{\mathbf{u}}_{ht}^n) + s_\theta(\tilde{\mathbf{u}}_{ht}^n, \theta_{ht}^n, \tilde{\mathbf{u}}_{ht}^n, \theta_{ht}^n) \right] \\ & \leq e^{C_{G,OB}} \left[\|\tilde{\mathbf{u}}_{ht}^1\|_0^2 + \|2\mathbf{u}_{ht}^1 - \mathbf{u}_{ht}^0\|_0^2 + (\Delta t)^2 \|\nabla p_{ht}^1\|_0^2 + \|\theta_{ht}^1\|_0^2 + \|2\theta_{ht}^1 - \theta_{ht}^0\|_0^2 \right. \\ & \left. + \frac{C\Delta t}{\beta \|\mathbf{g}\|_{l^\infty(0,T;L^\infty(\Omega))}} \sum_{n=2}^m \left(\|\mathbf{f}_u(t_n)\|_0^2 + \|f_\theta(t_n)\|_0^2 \right) \right] \end{aligned}$$

with a Gronwall constant $C_{G,OB} \sim T \left(1 - 3\Delta t\beta\|\mathbf{g}\|_{l^\infty(0,T;L^\infty(\Omega))} \right)^{-1}$. \square

Thus, the fully discrete velocity and temperature are stable with respect to the fully discrete norms as introduced in [Definition 4.1.1](#). We can prove stability of the pressure by taking advantage of the discrete inf-sup condition. Note that one immediately obtains a certain stability of the pressure as $(\Delta t)^2 \|\nabla p_{ht}\|_{l^\infty(0,T;L^2(\Omega))}^2 \leq C$.

4.2. Fully Discrete Convergence Results

A proof of convergence for the fully discretized model is not trivial. Even for the Navier-Stokes equations, we run into technical difficulties we want to discuss in this section. The main challenge here is to handle both the pressure term and the convective term in the advection-diffusion equation [\(4.1\)](#).

The rotational correction scheme is analyzed in [\[GS04\]](#) for the linear Stokes problem. L^2 -convergence of the time-discretized velocity as $(\Delta t)^2$ is shown as expected. For the $W^{1,2}$ -velocity and the L^2 -pressure errors, improved convergence results of order $(\Delta t)^{3/2}$ can be obtained. It is argued there that the nonlinear terms do not corrupt the order of convergence and can therefore be omitted.

In our considerations [\[AD15\]](#), we observe that indeed, the order of convergence stems from the linear problem, but nonlinear terms add technical problems for the rotational correction scheme that cannot be handled easily. In order to extend the analysis of [\[GS04\]](#) to the nonlinear case - or worse the stabilized case -, one would need stability results and prior auxiliary estimates for the error that are not available for the rotational scheme, since one would need to control a term of the form $(\nabla \nabla \cdot \tilde{\mathbf{u}}_{ht}^n, \nabla p_{ht}^n)$.

Therefore, we pursue a different ansatz for the nonlinear case considering the incremental method. Our analysis is inspired by techniques from several authors who worked on the fully discretized Navier-Stokes equations: In [BC07], convergence results for a first order projection method for the fully discrete Navier–Stokes equations are given. The fractional step incremental projection method for the unstabilized Navier-Stokes equations with BDF2 time-discretization is analyzed in [Gue99]. Shen considers a different second order time-discretization scheme in [She96]. Neither author regards the dependence on constant problem parameters, in particular on ν . It is a stated aim of this thesis to point out the arising restrictions of our error estimates. Besides that, we take LPS SU and grad-div stabilization into account.

We desire to separately consider the errors produced by discretization in time and space. So we bound the total error via the triangle inequality according to:

$$\begin{aligned}\|\mathbf{u} - \tilde{\mathbf{u}}_{ht}\|_{l^\infty(0,T;L^2(\Omega))} &\leq \|\mathbf{u} - \mathbf{u}_h\|_{l^\infty(0,T;L^2(\Omega))} + \|\mathbf{u}_h - \tilde{\mathbf{u}}_{ht}\|_{l^\infty(0,T;L^2(\Omega))}, \\ \|\mathbf{u} - \tilde{\mathbf{u}}_{ht}\|_{l^2(0,T;LPS)} &\leq \|\mathbf{u} - \mathbf{u}_h\|_{l^2(0,T;LPS)} + \|\mathbf{u}_h - \tilde{\mathbf{u}}_{ht}\|_{l^2(0,T;LPS)}.\end{aligned}$$

The errors resulting from $\mathbf{u} - \mathbf{u}_h$ can be bounded by a semi-discrete analysis, e.g., similar to Chapter 3, which provides a bound for the time-continuous norm as

$$\|\mathbf{u} - \mathbf{u}_h\|_{L^\infty(0,T;L^2(\Omega))} + \|\mathbf{u} - \mathbf{u}_h\|_{L^2(0,T;LPS)} \lesssim h^{k_u}.$$

We use the fact that these norms provide an upper bound for the respective discrete norms; see Section 4.2.1. The estimates for $\mathbf{u}_h - \tilde{\mathbf{u}}_{ht}$ are presented in Section 4.2.2. In Section 4.2.3, we combine the results and derive an error bound on $\|p - p_{ht}\|_{l^2(0,T;L^2(\Omega))}$ via the inf-sup stability of the ansatz spaces.

Assumption 4.2.1 (For error due to spatial discretization).

We require for some $l \in \{1, 2\}$ (to be fixed later)

$$\mathbf{u} \in W^{l,2}(0, T; LPS), \quad \mathbf{u}_h \in W^{l,2}(0, T; LPS), \quad (4.10)$$

where $W^{l,2}(0, T; LPS)$ consists of functions $\mathbf{v} \in W^{l,2}(0, T; [W^{1,2}(\Omega)]^d)$ such that all time derivatives $\mathbf{v}^{(n)}$ ($n = 0, \dots, l$) are bounded with respect to $\|\cdot\|_{0,T;LPS}$. Moreover, assume that the conditions for Corollary 3.2.13 hold for the velocity. This includes in particular

$$\begin{aligned}\mathbf{u} &\in L^\infty(0, T; [W^{1,\infty}(\Omega)]^d) \cap L^2(0, T; [W^{k_u+1,2}(\Omega)]^d), \\ \partial_t \mathbf{u} &\in L^2(0, T; [W^{k_u,2}(\Omega)]^d), \quad p \in L^2(0, T; W^{k_p+1,2}(\Omega) \cap C(\Omega)).\end{aligned}$$

The latter conditions can be replaced by the premises of any other suitable semi-discrete a priori error estimate for the time dependent Navier-Stokes equations.

Assumption 4.2.2 (For linear error due to temporal discretization).

We require for the linear error due to time-discretization that there is a constant $C > 0$ (independent of n) such that for all $1 \leq n \leq N$:

$$\|R^n - R^{n-1}\|_0^2 + \|\nabla(p_h(t_n) - 2p_h(t_{n-1}) + p_h(t_{n-2}))\|_0^2 \leq C(\Delta t)^4, \quad (4.11)$$

$$\|\nabla(p_h(t_n) - p_h(t_{n-1}))\|_0 \leq C\Delta t, \quad (4.12)$$

$$\Delta t \sum_{n=1}^N \|R^n\|_{-1}^2 \leq C(\Delta t)^4, \quad (4.13)$$

where $R^n := D_t \mathbf{u}_h(t_n) - \partial_t \mathbf{u}_h(t_n)$ denotes the difference between of the time derivative and its BDF2-type discretization.

We remark that if $\mathbf{u}_h \in W^{3,\infty}(0, T; [L^2(\Omega)]^d)$ and $p_h \in W^{2,\infty}(0, T; H^1(\Omega))$, conditions (4.11) and (4.12) can be shown via (generalized) Taylor expansion. (4.13) can be derived from

$$\int_0^T \|\partial_{ttt} \mathbf{u}_h(\tau)\|_{-1}^2 + \|\partial_{tt} \mathbf{u}_h(\tau)\|_1^2 + \|\partial_{tt} p_h(\tau)\|_0^2 d\tau \leq C$$

using Taylor expansion. We refer to [She92] and [She96], where similar proofs are presented.

Assumption 4.2.3 (For nonlinear error due to temporal discretization).

For the nonlinear error due to temporal discretization, we require all conditions from Assumptions 4.2.1 and 4.2.2 as well as in addition

$$\mathbf{u} \in L^\infty(0, T; [W^{2,2}(\Omega)]^d); \quad (4.14)$$

in particular, we assume $\|\mathbf{u}\|_{L^\infty(0, T; W^{2,2}(\Omega))} \leq C$ with C independent of ν .

For the stabilization terms, we require the following properties. Let the cell-wise constant streamline direction be defined as

$$\mathbf{w}_M = \frac{1}{|M|} \int_M \mathbf{w}(\mathbf{x}) d\mathbf{x}$$

for all $M \in \mathcal{M}_h$. Furthermore, we require that s_u is linear in each argument; in particular, τ_M^n must not depend nonlinearly on the arguments of s_u . Let $i_h \equiv 0$ and assume $\gamma := \gamma_M$ for all $M \in \mathcal{M}_h$, i.e.,

$$t_h(\tilde{\mathbf{u}}_{ht}^n; \tilde{\mathbf{u}}_{ht}^n, \mathbf{v}_h) = \gamma(\nabla \cdot \tilde{\mathbf{u}}_{ht}^n, \nabla \cdot \mathbf{v}_h).$$

Note that the above setting of \mathbf{w}_M is in agreement with Assumption 3.2.5 that is needed for the semi-discrete analysis in Section 2.2.3. According to the grad-div parameter choice we discussed in the semi-discrete analysis, the assumption on t_h is reasonable.

Assumption 4.2.4 (For fully discrete error).

In addition to Assumption 4.2.3, let the following conditions be true for some $p \in \{1, 2\}$:

$$\mathbf{u} \in L^\infty(0, T; [W^{k_u+1, 2}(\Omega)]^d), \quad p \in W^{1, 2}(0, T; L^2(\Omega)), \quad \mathbf{u}_h \in W^{p, 2}(0, T; [L^2(\Omega)]^d).$$

4.2.1. Spatial Discretization of the Continuous Quantities

In order to make use of semi-discrete error estimates for $\mathbf{u} - \mathbf{u}_h$, we have to show equivalence of the time-discrete l^2 -norm and the time-continuous L^2 -norm. For this, we need some preparatory results. We do not show the proofs here; instead, we refer the reader to [AD15]. First, we state an interpolation result which is an extension of the Bramble-Hilbert Theorem.

Theorem 4.2.5 (Generalized Bramble-Hilbert Theorem).

Let X be a real, separable Hilbert space and $m \geq 1$ an integer. Denote by $\mathbb{P}^{m-1}(a, b; X)$ the space of polynomials $p: (a, b) \subset \mathbb{R} \rightarrow X$ of maximal order $m - 1$ (with respect to time) and with values in X . Then there exists $C > 0$ such that for any bounded intervals $(a, b) \subset (0, T)$ and any $f \in H^m(a, b; X)$, there exists a polynomial $q \in \mathbb{P}^{m-1}(a, b; X)$ satisfying $q(a) = f(a)$ and $q(b) = f(b)$ and

$$\|f - q\|_{H^k(a, b; X)} \leq C(b - a)^{m-k} \|f\|_{H^m(a, b; X)} \quad \forall k \in \mathbb{N}, k \leq m. \quad (4.15)$$

Lemma 4.2.6 (Equivalence of discrete and continuous norms).

Consider the set of points in time $\mathcal{N}_T = \{0 = t_0, \dots, t_N = T\}$, where we assume a constant time step size $\Delta t = T/N$ and $t_n = n\Delta t$, $n = 0, \dots, N$. Let X be a Banach space. Then there exist constants $c, C > 0$ such that the estimate

$$c\Delta t \sum_{i=0}^N \|f(t_i)\|_X^2 \leq \|f\|_{L^2(0, T; X)}^2 \leq C\Delta t \sum_{i=0}^N \|f(t_i)\|_X^2 \quad (4.16)$$

holds true for all functions $f: [0, T] \rightarrow X$ that are piecewise linear with respect to \mathcal{N}_T .

We can use the semi-discrete errors as an upper bound of the errors with respect to the time-discrete norms according to the result below. For the proof, we refer to [AD15].

Theorem 4.2.7 (Time-continuous quantities in time-discrete norms).

Let $\boldsymbol{\xi}_{u,h} = \mathbf{u} - \mathbf{u}_h$. Then it holds

$$\|\boldsymbol{\xi}_{u,h}\|_{l^\infty(0,T;L^2(\Omega))}^2 \leq \|\boldsymbol{\xi}_{u,h}\|_{L^\infty(0,T;L^2(\Omega))}^2$$

and if we additionally assume $\boldsymbol{\xi}_{u,h} \in H^l(0,T;LPS)$ for some $l \in \{1, 2\}$,

$$\begin{aligned} \|\boldsymbol{\xi}_{u,h}\|_{l^2(0,T;W^{1,2}(\Omega))}^2 &\leq C\|\boldsymbol{\xi}_{u,h}\|_{L^2(0,T;W^{1,2}(\Omega))}^2 + C(\Delta t)^{2l}, \\ \|\boldsymbol{\xi}_{u,h}\|_{l^2(0,T;LPS)}^2 &\leq C\|\boldsymbol{\xi}_{u,h}\|_{L^2(0,T;LPS)}^2 + C(\Delta t)^{2l}, \end{aligned}$$

provided that the right-hand sides exist.

Under the conditions of Corollary 3.2.13, for example, we can derive an a priori estimate of the semi-discrete error $\boldsymbol{\xi}_{u,h}$ in the fully discrete norms. Here, all terms resulting from the non-isothermal coupling are omitted.

Corollary 4.2.8 (Spatial convergence in discrete norms).

If Assumption 4.2.1 holds, the semi-discrete error can be bounded by

$$\begin{aligned} \|\boldsymbol{\xi}_{u,h}\|_{l^\infty(0,T;L^2(\Omega))}^2 &\leq \|\boldsymbol{\xi}_{u,h}\|_{L^\infty(0,T;L^2(\Omega))}^2 \\ &\leq C e^{C_{G,h}(\mathbf{u})} \int_0^T \left\{ \sum_{M \in \mathcal{M}_h} h_M^{2k_u} \left[(1 + \nu R e_M^2 + \tau_M^u |\mathbf{u}_M|^2 + d\gamma_M) \|\mathbf{u}(\tau)\|_{W^{k_u+1,2}(\omega_M)}^2 \right. \right. \\ &\quad \left. \left. + \tau_M^u |\mathbf{u}_M|^2 h_M^{2(s_u-k_u)} \|\mathbf{u}(\tau)\|_{W^{s_u+1,2}(\omega_M)}^2 + \|\partial_t \mathbf{u}(\tau)\|_{W^{k_u,2}(\omega_M)}^2 \right] \right. \\ &\quad \left. + \sum_{M \in \mathcal{M}_h} h_M^{2(k_p+1)} \min\left(\frac{d}{\nu}, \frac{1}{\gamma_M}\right) \|p(\tau)\|_{W^{k_p+1,2}(\omega_M)}^2 \right\} d\tau =: C \Xi_{\xi,u,h}, \\ \|\boldsymbol{\xi}_{u,h}\|_{l^2(0,T;LPS)}^2 &\leq C\|\boldsymbol{\xi}_{u,h}\|_{L^2(0,T;LPS)}^2 + C(\Delta t)^{2l} \leq C \Xi_{\xi,u,h} + C(\Delta t)^{2l} \end{aligned}$$

with $C_{G,h}(\mathbf{u}) \lesssim 1 + C|\mathbf{u}|_{L^\infty(0,T;W^{1,\infty}(\Omega))} + Ch^2|\mathbf{u}|_{L^\infty(0,T;W^{1,\infty}(\Omega))}^2 + C\|\mathbf{u}\|_{L^\infty(0,T;L^\infty(\Omega))}^2$.

Proof. The right-hand sides in Theorem 4.2.7 can be bounded by Corollary 3.2.13:

$$\begin{aligned} &\|\boldsymbol{\xi}_{u,h}\|_{L^\infty(0,T;[L^2(\Omega)]^d)}^2 + \|\boldsymbol{\xi}_{u,h}\|_{L^2(0,T;LPS)}^2 \\ &\leq C \int_0^T e^{C_{G,h}(\mathbf{u})(t-\tau)} \left\{ \sum_{M \in \mathcal{M}_h} h_M^{2k_u} \left[(1 + \nu R e_M^2 + \tau_M^u |\mathbf{u}_M|^2 + d\gamma_M) \|\mathbf{u}(\tau)\|_{W^{k_u+1,2}(\omega_M)}^2 \right. \right. \\ &\quad \left. \left. + \tau_M^u |\mathbf{u}_M|^2 h_M^{2(s_u-k_u)} \|\mathbf{u}(\tau)\|_{W^{s_u+1,2}(\omega_M)}^2 + \|\partial_t \mathbf{u}(\tau)\|_{W^{k_u,2}(\omega_M)}^2 \right] \right. \\ &\quad \left. + \sum_{M \in \mathcal{M}_h} h_M^{2(k_p+1)} \min\left(\frac{d}{\nu}, \frac{1}{\gamma_M}\right) \|p(\tau)\|_{W^{k_p+1,2}(\omega_M)}^2 \right\} d\tau \leq C e^{C_{G,h}(\mathbf{u})} \Xi_{\xi,u,h} \end{aligned}$$

with $C_{G,h}(\mathbf{u}) \lesssim 1 + C\|\mathbf{u}\|_{L^\infty(0,T;W^{1,\infty}(\Omega))} + Ch^2\|\mathbf{u}\|_{L^\infty(0,T;W^{1,\infty}(\Omega))}^2 + C\|\mathbf{u}\|_{L^\infty(0,T;L^\infty(\Omega))}^2$. \square

4.2.2. Temporal Discretization of the Space-Discrete Quantities

The time-discrete error $\mathbf{u}_h - \tilde{\mathbf{u}}_{ht}$ is handled by introducing a solution $\tilde{\mathbf{w}}_{ht}$ of an auxiliary linear problem as

$$\|\mathbf{u}_h - \tilde{\mathbf{u}}_{ht}\| \leq \|\mathbf{u}_h - \tilde{\mathbf{w}}_{ht}\| + \|\tilde{\mathbf{w}}_{ht} - \tilde{\mathbf{u}}_{ht}\| \quad (4.17)$$

with a suitable norm, where $(\tilde{\mathbf{w}}_{ht}, \mathbf{w}_{ht}, r_{ht}) \in (\mathbf{V}_h)^N \times (\mathbf{V}_h^{div})^N \times (Q_h)^N$ solves the problem:

Find $\tilde{\mathbf{w}}_{ht}^n \in \mathbf{V}_h$, $\mathbf{w}_{ht}^n \in \mathbf{V}_h^{div}$, $r_{ht}^n \in Q_h$ such that for all $\mathbf{v}_h \in \mathbf{V}_h$, $\mathbf{y}_h \in \mathbf{Y}_h$, $q_h \in Q_h$

$$\begin{aligned} & \left(\frac{3\tilde{\mathbf{w}}_{ht}^n - 4\mathbf{w}_{ht}^{n-1} + \mathbf{w}_{ht}^{n-2}}{2\Delta t}, \mathbf{v}_h \right) + \nu(\nabla \tilde{\mathbf{w}}_{ht}^n, \nabla \mathbf{v}_h) + \gamma(\nabla \cdot \tilde{\mathbf{w}}_{ht}^n, \nabla \cdot \mathbf{v}_h) \\ & = (\mathbf{f}_u(t_n), \mathbf{v}_h) - (\nabla r_{ht}^{n-1}, \mathbf{v}_h) - c_u(\mathbf{u}_h(t_n); \mathbf{u}_h(t_n), \mathbf{v}_h) - s_u(\mathbf{u}_h(t_n), \mathbf{u}_h(t_n), \mathbf{v}_h), \\ & \tilde{\mathbf{w}}_{ht}^n|_{\partial\Omega} = 0, \end{aligned} \quad (4.18)$$

$$\begin{aligned} & \left(\frac{3\mathbf{w}_{ht}^n - 3\tilde{\mathbf{w}}_{ht}^n}{2\Delta t} + \nabla(r_{ht}^n - r_{ht}^{n-1}), \mathbf{y}_h \right) = 0, \\ & (\nabla \cdot \mathbf{w}_{ht}^n, q_h) = 0, \\ & \mathbf{w}_{ht}^n|_{\partial\Omega} = 0. \end{aligned} \quad (4.19)$$

$\mathbf{u}_h - \tilde{\mathbf{w}}_{ht}$ is called linear error and is estimated in Lemma 4.2.14, $\tilde{\mathbf{w}}_{ht} - \tilde{\mathbf{u}}_{ht}$ denotes the so-called nonlinear error, see Lemma 4.2.16. Consistency estimates in time are obtained by combining the results of both auxiliary problems.

Definition 4.2.9 (Error splitting).

We denote the errors due to temporal discretization

$$\boldsymbol{\xi}_u^n := \mathbf{u}_h(t_n) - \mathbf{u}_{ht}^n, \quad \tilde{\boldsymbol{\xi}}_u^n := \mathbf{u}_h(t_n) - \tilde{\mathbf{u}}_{ht}^n, \quad \xi_p^n := p_h(t_n) - p_{ht}^n.$$

For the linear problem, we define the propagation operator $\delta_t a^n := a^n - a^{n-1}$ and the errors

$$\boldsymbol{\eta}_u^n := \mathbf{u}_h(t_n) - \mathbf{w}_{ht}^n, \quad \tilde{\boldsymbol{\eta}}_u^n := \mathbf{u}_h(t_n) - \tilde{\mathbf{w}}_{ht}^n, \quad \eta_p^n := p_h(t_n) - r_{ht}^n.$$

We introduce the nonlinear errors

$$\mathbf{e}_u^n := \mathbf{w}_{ht}^n - \mathbf{u}_{ht}^n, \quad \tilde{\mathbf{e}}_u^n := \tilde{\mathbf{w}}_{ht}^n - \tilde{\mathbf{u}}_{ht}^n, \quad \mathbf{e}_p^n := r_{ht}^n - p_{ht}^n.$$

Note that it holds $\tilde{\xi}_u^n = \tilde{\eta}_u^n + \tilde{e}_u^n$, $\xi_u^n = \eta_u^n + e_u^n$ and $\xi_p^n = \eta_p^n + e_p^n$.

For convergence rates of the desired order, estimates of the initial errors are needed. For this, we cite [AD15].

Lemma 4.2.10 (Initialization).

The initial errors due to temporal discretization can be bounded by

$$\|\tilde{\xi}_u^m\|_0^2 + \nu(\Delta t)^2 \|\tilde{\xi}_u^m\|_1^2 + (\Delta t)^2 \|\nabla \xi_p^m\|_0^2 \leq C(\Delta t)^4 \quad \forall m \in \{1, 2\},$$

provided the time step size satisfies

$$C \frac{\Delta t}{\nu^3} + C \frac{\Delta t}{\nu} \max_{M \in \mathcal{M}_h} \left\{ \frac{\tau_M^m}{h_M^d} \right\} + C \frac{\Delta t}{\nu} \max_{M \in \mathcal{M}_h} \left\{ \frac{\tau_M^m}{h_M^d} \right\}^2 \leq 1 \quad \forall m \in \{1, 2\}.$$

The initial linear errors can be bounded by

$$\|\tilde{\eta}_u^m\|_0^2 + \nu(\Delta t)^2 \|\tilde{\eta}_u^m\|_1^2 + (\Delta t)^2 \|\nabla \eta_p^m\|_0 \leq C(\Delta t)^4 \quad \forall m \in \{1, 2\}.$$

Proof. For the first time step, one takes advantage of the fact that the error at $t_0 = 0$ vanishes. For the next time steps, one uses the same techniques as for estimating the linear and nonlinear errors. See [AD15] for details. \square

The proofs for the linear error are a modification of the work in [GS04], where we work on the space-discrete level, add grad-div stabilization, handle the pressure term in a different way and do not consider the rotational correction.

Lemma 4.2.11 (Intermediate linear velocity error).

Let $\Delta t < \frac{1}{2}$ and Assumption 4.2.2 be valid. For all $1 \leq m \leq N$, it holds

$$\|\eta_u^m - \tilde{\eta}_u^m\|_0^2 \leq e^{C_{G,\text{lin}}(\Delta t)^4} \quad (4.20)$$

with $C_{G,\text{lin}} \sim T(1 - 2\Delta t)^{-1}$.

Proof. The error equation due to the difference between the Navier-Stokes momentum equation and the advection-diffusion step (4.18) reads

$$\begin{aligned} & \left(\frac{3\tilde{\eta}_u^n - 4\eta_u^{n-1} + \eta_u^{n-2}}{2\Delta t}, \mathbf{v}_h \right) + \nu(\nabla \tilde{\eta}_u^n, \nabla \mathbf{v}_h) + \gamma(\nabla \cdot \tilde{\eta}^n, \nabla \cdot \mathbf{v}_h) \\ & = (R^n, \mathbf{v}_h) - (\nabla(p_h(t_n) - r_{ht}^{n-1}), \mathbf{v}_h) \quad \forall \mathbf{v}_h \in \mathbf{V}_h \end{aligned} \quad (4.21)$$

with $R^n := D_t \mathbf{u}_h(t_n) - \partial_t \mathbf{u}_h(t_n)$ and due to the projection step (4.19), we have the error equation

$$\left(\frac{3\boldsymbol{\eta}_u^n - 3\tilde{\boldsymbol{\eta}}_u^n}{2\Delta t} + \nabla(r_{ht}^n - r_{ht}^{n-1}), \mathbf{y}_h \right) = 0 \quad \forall \mathbf{y}_h \in \mathbf{Y}_h. \quad (4.22)$$

We consider the difference between two consecutive time steps of the advection-diffusion error equation (4.21) and call this the propagation error equation for the advection-diffusion step. Since the propagation operator δ_t is linear, we establish:

$$\begin{aligned} & \left(\frac{3\delta_t \tilde{\boldsymbol{\eta}}_u^n - 4\delta_t \boldsymbol{\eta}_u^{n-1} + \delta_t \boldsymbol{\eta}_u^{n-2}}{2\Delta t}, \mathbf{v}_h \right) + \nu(\nabla \delta_t \tilde{\boldsymbol{\eta}}_u^n, \nabla \mathbf{v}_h) + \gamma(\nabla \cdot \delta_t \tilde{\boldsymbol{\eta}}_u^n, \nabla \cdot \mathbf{v}_h) \\ & = (\delta_t R^n, \mathbf{v}_h) - (\nabla \delta_t(p_h(t_n) - r_t^{n-1}), \mathbf{v}_h) \quad \forall \mathbf{v}_h \in \mathbf{V}_h. \end{aligned} \quad (4.23)$$

The propagation error for the projection error equation (4.22) is similarly defined by

$$\begin{aligned} 0 & = \left(\frac{3\delta_t \boldsymbol{\eta}_u^n - 3\delta_t \tilde{\boldsymbol{\eta}}_u^n}{2\Delta t}, \mathbf{y}_h \right) - (\nabla \delta_t(r_{ht}^n - r_{ht}^{n-1}), \mathbf{y}_h) \\ & = \left(\frac{3\delta_t \boldsymbol{\eta}_u^n - 3\delta_t \tilde{\boldsymbol{\eta}}_u^n}{2\Delta t}, \mathbf{y}_h \right) + (\nabla \delta_t(\eta_p^n - \eta_p^{n-1}), \mathbf{y}_h) \\ & \quad - (\nabla \delta_t(p_h(t_n) - p_h(t_{n-1})), \mathbf{y}_h) \quad \forall \mathbf{y}_h \in \mathbf{Y}_h. \end{aligned} \quad (4.24)$$

Testing (4.23) with $\mathbf{v}_h = 4\Delta t \delta_t \tilde{\boldsymbol{\eta}}_u^n$ gives

$$\begin{aligned} & 2 \left(3\delta_t \tilde{\boldsymbol{\eta}}_u^n - 4\delta_t \boldsymbol{\eta}_u^{n-1} + \delta_t \boldsymbol{\eta}_u^{n-2}, \delta_t \tilde{\boldsymbol{\eta}}_u^n \right) + 4\Delta t \nu (\nabla \delta_t \tilde{\boldsymbol{\eta}}_u^n, \nabla \delta_t \tilde{\boldsymbol{\eta}}_u^n) + 4\Delta t \gamma (\nabla \cdot \delta_t \tilde{\boldsymbol{\eta}}_u^n, \nabla \cdot \delta_t \tilde{\boldsymbol{\eta}}_u^n) \\ & = 4\Delta t (\delta_t R^n, \delta_t \tilde{\boldsymbol{\eta}}_u^n) \\ & \quad - 4\Delta t (\nabla \delta_t(p_h(t_{n-1}) - r_{ht}^{n-1}), \delta_t \tilde{\boldsymbol{\eta}}_u^n) - 4\Delta t (\nabla \delta_t(p_h(t_{n-1}) - p_h(t_n)), \delta_t \tilde{\boldsymbol{\eta}}_u^n). \end{aligned}$$

Now, we test the propagation error in the projection step (4.24) with $\mathbf{y}_h = \nabla \delta_t \eta_p^{n-1} = \nabla \delta_t(p_h(t_{n-1}) - r_{ht}^{n-1})$ and get after integration by parts for the first term

$$\begin{aligned} - \left(\frac{3}{2\Delta t} \delta_t \tilde{\boldsymbol{\eta}}_u^n, \nabla \delta_t(p_h(t_{n-1}) - r_{ht}^{n-1}) \right) & = -(\nabla \delta_t(\eta_p^n - \eta_p^{n-1}), \nabla \delta_t \eta_p^{n-1}) \\ & \quad + (\nabla \delta_t(p_h(t_n) - p_h(t_{n-1})), \nabla \delta_t \eta_p^{n-1}). \end{aligned}$$

Combining these and using that $\delta_t \boldsymbol{\eta}_u^n = P_H \delta_t \tilde{\boldsymbol{\eta}}_u^n$, therefore $\|\delta_t \boldsymbol{\eta}_u^n\| \leq \|\delta_t \tilde{\boldsymbol{\eta}}_u^n\|$, yield (in a similar way as in the proof of Theorem 4.1.2)

$$\begin{aligned} & \|\delta_t \tilde{\boldsymbol{\eta}}_u^n\|_0^2 + 3\|\delta_t \boldsymbol{\eta}_u^n - \delta_t \tilde{\boldsymbol{\eta}}_u^n\|_0^2 + \|2\delta_t \boldsymbol{\eta}_u^n - \delta_t \boldsymbol{\eta}_u^{n-1}\|_0^2 \\ & + \|\delta_{ttt} \boldsymbol{\eta}_u^n\|_0^2 - \|\delta_t \tilde{\boldsymbol{\eta}}_u^{n-1}\|_0^2 - \|2\delta_t \boldsymbol{\eta}_u^{n-1} - \delta_t \boldsymbol{\eta}_u^{n-2}\|_0^2 \\ & + 4\Delta t \nu \|\nabla \delta_t \tilde{\boldsymbol{\eta}}_u^n\|_0^2 + 4\Delta t \gamma \|\nabla \cdot \delta_t \tilde{\boldsymbol{\eta}}_u^n\|_0^2 + \frac{4}{3}(\Delta t)^2 \|\nabla \delta_t \eta_p^n\|_0^2 \end{aligned}$$

$$\begin{aligned}
&\leq \frac{4}{3}(\Delta t)^2 \|\nabla \delta_t \eta_p^n - \nabla \delta_t \eta_p^{n-1}\|_0^2 + \frac{4}{3}(\Delta t)^2 \|\nabla \delta_t \eta_p^{n-1}\|_0^2 \\
&\quad + 4\Delta t (\delta_t R^n, \delta_t \tilde{\boldsymbol{\eta}}_u^n) - 4\Delta t (\nabla \delta_t (p_h(t_{n-1}) - p_h(t_n)), \delta_t \tilde{\boldsymbol{\eta}}_u^n) \\
&\quad + \frac{8}{3}(\Delta t)^2 (\nabla \delta_t (p_h(t_n) - p_h(t_{n-1})), \nabla \delta_t \eta_p^{n-1}). \tag{4.25}
\end{aligned}$$

In order to handle the first term on the right-hand side, the projection propagation error equation (4.24) is tested with $\mathbf{y}_h = \nabla \delta_t (\eta_p^n - \eta_p^{n-1})$:

$$\begin{aligned}
\frac{2\Delta t}{3} \|\nabla \delta_t (\eta_p^n - \eta_p^{n-1})\|_0^2 &\leq \|\delta_t \boldsymbol{\eta}_u^n - \delta_t \tilde{\boldsymbol{\eta}}_u^n\|_0 \|\nabla \delta_t (\eta_p^n - \eta_p^{n-1})\|_0 \\
&\quad + \frac{2\Delta t}{3} (\nabla \delta_t (p_h(t_n) - p_h(t_{n-1})), \nabla \delta_t (\eta_p^n - \eta_p^{n-1})) \\
&\leq \frac{3}{4\Delta t} \|\delta_t \boldsymbol{\eta}_u^n - \delta_t \tilde{\boldsymbol{\eta}}_u^n\|_0^2 + \frac{\Delta t}{3} \|\nabla \delta_t (\eta_p^n - \eta_p^{n-1})\|_0^2 \\
&\quad + \frac{2\Delta t}{3} (\nabla \delta_{tt} p_h(t_n), \nabla \delta_t (\eta_p^n - \eta_p^{n-1}))
\end{aligned}$$

due to Young's inequality. Therefore, after multiplication with $4\Delta t$,

$$\frac{4}{3}(\Delta t)^2 \|\nabla \delta_t (\eta_p^n - \eta_p^{n-1})\|_0^2 \leq 3 \|\delta_t \boldsymbol{\eta}_u^n - \delta_t \tilde{\boldsymbol{\eta}}_u^n\|_0^2 + \frac{8}{3}(\Delta t)^2 (\nabla \delta_{tt} p_h(t_n), \nabla \delta_t (\eta_p^n - \eta_p^{n-1})).$$

We insert this into (4.25) and use Young's inequality:

$$\begin{aligned}
&\|\delta_t \tilde{\boldsymbol{\eta}}_u^n\|_0^2 + \|2\delta_t \boldsymbol{\eta}_u^n - \delta_t \boldsymbol{\eta}_u^{n-1}\|_0^2 \\
&\quad + \|\delta_{ttt} \boldsymbol{\eta}_u^n\|_0^2 - \|\delta_t \tilde{\boldsymbol{\eta}}_u^{n-1}\|_0^2 - \|2\delta_t \boldsymbol{\eta}_u^{n-1} - \delta_t \boldsymbol{\eta}_u^{n-2}\|_0^2 \\
&\quad + 4\Delta t \nu \|\nabla \delta_t \tilde{\boldsymbol{\eta}}_u^n\|_0^2 + 4\Delta t \gamma \|\nabla \cdot \delta_t \tilde{\boldsymbol{\eta}}^n\|_0^2 + \frac{4}{3}(\Delta t)^2 \|\nabla \delta_t \eta_p^n\|_0^2 \\
&\leq \frac{4}{3}(\Delta t)^2 \|\nabla \delta_t \eta_p^{n-1}\|_0^2 + 4\Delta t (\delta_t R^n, \delta_t \tilde{\boldsymbol{\eta}}_u^n) + 4\Delta t (\nabla \delta_{tt} p_h(t_n), \delta_t \tilde{\boldsymbol{\eta}}_u^n) \\
&\quad + \frac{8}{3}(\Delta t)^2 (\nabla \delta_{tt} p_h(t_n), \nabla \delta_t \eta_p^n) \\
&\leq \frac{4}{3}(\Delta t)^2 \|\nabla \delta_t \eta_p^{n-1}\|_0^2 + 4\Delta t \|\delta_t R^n\|_0^2 + \Delta t \|\delta_t \tilde{\boldsymbol{\eta}}_u^n\|_0^2 \\
&\quad + 4\Delta t \|\nabla \delta_{tt} p_h(t_n)\|_0^2 + \Delta t \|\delta_t \tilde{\boldsymbol{\eta}}_u^n\|_0^2 + \frac{8}{3} \Delta t \|\nabla \delta_{tt} p_h(t_n)\|_0^2 + \frac{2}{3}(\Delta t)^3 \|\nabla \delta_t \eta_p^n\|_0^2.
\end{aligned}$$

Summing up from $n = 3$ to $m \leq N$ gives

$$\begin{aligned}
&\|\delta_t \tilde{\boldsymbol{\eta}}_u^m\|_0^2 + \|2\delta_t \boldsymbol{\eta}_u^m - \delta_t \boldsymbol{\eta}_u^{m-1}\|_0^2 + \frac{4}{3}(\Delta t)^2 \|\nabla \delta_t \eta_p^m\|_0^2 \\
&\quad + \sum_{n=3}^m \left(\|\delta_{ttt} \boldsymbol{\eta}_u^n\|_0^2 + 4\Delta t \nu \|\nabla \delta_t \tilde{\boldsymbol{\eta}}_u^n\|_0^2 + 4\Delta t \gamma \|\nabla \cdot \delta_t \tilde{\boldsymbol{\eta}}^n\|_0^2 \right) \\
&\leq \|\delta_t \tilde{\boldsymbol{\eta}}_u^2\|_0^2 + \|2\delta_t \boldsymbol{\eta}_u^2 - \delta_t \boldsymbol{\eta}_u^1\|_0^2 + \frac{4}{3}(\Delta t)^2 \|\nabla \delta_t \eta_p^2\|_0^2
\end{aligned}$$

$$+ \Delta t \sum_{n=3}^m \left(2\|\delta_t \tilde{\boldsymbol{\eta}}_u^n\|_0^2 + \frac{2}{3}(\Delta t)^2 \|\nabla \delta_t \boldsymbol{\eta}_p^n\|_0^2 \right) + \Delta t \sum_{n=3}^m \left(4\|\delta_t R^n\|_0^2 + 7\|\nabla \delta_{tt} p_h(t_n)\|_0^2 \right).$$

Provided that $2\Delta t < 1$, the discrete Gronwall Lemma applied to the term $\|\delta_t \tilde{\boldsymbol{\eta}}_u^m\|_0^2 + \frac{4}{3}(\Delta t)^2 \|\nabla \delta_t \boldsymbol{\eta}_p^m\|_0^2$ yields

$$\begin{aligned} & \|\delta_t \tilde{\boldsymbol{\eta}}_u^m\|_0^2 + \|2\delta_t \boldsymbol{\eta}_u^m - \delta_t \boldsymbol{\eta}_u^{m-1}\|_0^2 + \frac{4}{3}(\Delta t)^2 \|\nabla \delta_t \boldsymbol{\eta}_p^m\|_0^2 \\ & + \sum_{n=3}^m \left(\|\delta_{ttt} \boldsymbol{\eta}_u^n\|_0^2 + 4\Delta t \nu \|\nabla \delta_t \tilde{\boldsymbol{\eta}}_u^n\|_0^2 + 4\Delta t \gamma \|\nabla \cdot \delta_t \tilde{\boldsymbol{\eta}}^n\|_0^2 \right) \\ & \leq e^{C_{G,\text{lin}}} \left[\|\delta_t \tilde{\boldsymbol{\eta}}_u^2\|_0^2 + \|2\delta_t \boldsymbol{\eta}_u^2 - \delta_t \boldsymbol{\eta}_u^1\|_0^2 + \frac{4}{3}(\Delta t)^2 \|\nabla \delta_t \boldsymbol{\eta}_p^2\|_0^2 \right. \\ & \left. + C\Delta t \sum_{n=3}^m \left(\|\delta_t R^n\|_0^2 + \|\nabla \delta_{tt} p_h(t_n)\|_0^2 \right) \right] \leq e^{C_{G,\text{lin}}} (\Delta t)^4. \end{aligned} \quad (4.26)$$

This holds since the first three terms on the right-hand side denote initial errors (that can be bounded by Lemma 4.2.10). Moreover, Assumption 4.2.2 ensures the estimate

$$\|\delta_t R^n\|_0^2 + \|\nabla \delta_{tt} p_h(t_n)\|_0^2 \leq C(\Delta t)^4$$

with C independent of n . $C_{G,\text{lin}} \sim T(1 - 2\Delta t)^{-1}$ denotes a Gronwall constant.

The intermediate result follows from the use of the projection error equation (4.22), from (4.26) and Assumption 4.2.2:

$$\begin{aligned} \|\boldsymbol{\eta}_u^n - \tilde{\boldsymbol{\eta}}_u^n\|_0 &= \frac{2\Delta t}{3} \|\nabla \delta_t r_{ht}^n\|_0 = \frac{2\Delta t}{3} \|\nabla (\delta_t \boldsymbol{\eta}_p^n - \delta_t p_h(t_n))\|_0 \\ &\leq \frac{2\Delta t}{3} \|\nabla \delta_t \boldsymbol{\eta}_p^n\|_0 + \frac{2\Delta t}{3} \|\delta_t \nabla p_h(t_n)\|_0 \leq C_{G,\text{lin}} (\Delta t)^2. \end{aligned}$$

□

To bound $\|\tilde{\boldsymbol{\eta}}_u^n\|_0$, we need the following operator.

Definition 4.2.12 (Grad-div stabilized inverse Stokes operator).

We define the grad-div stabilized space-discrete inverse Stokes operator $S: \mathbf{V}_h \rightarrow \mathbf{V}_h$ as the solution $(S\mathbf{v}_h, r_h) \in \mathbf{V}_h \times Q_h$ of the problem

$$\begin{aligned} \nu(\nabla S\mathbf{v}_h, \nabla \mathbf{w}_h) - (r_h, \nabla \cdot \mathbf{w}_h) + \gamma(\nabla \cdot S\mathbf{v}_h, \nabla \cdot \mathbf{w}_h) &= (\mathbf{v}_h, \mathbf{w}_h) & \forall \mathbf{w}_h \in \mathbf{V}_h, \\ (\nabla \cdot S\mathbf{v}_h, q_h) &= 0 & \forall q_h \in Q_h, \\ S\mathbf{v}_h|_{\partial\Omega} &= 0. & \end{aligned} \quad (4.27)$$

Further, let $|\mathbf{v}_h|_*^2 := (\mathbf{v}_h, S\mathbf{v}_h)$ for any $\mathbf{v}_h \in \mathbf{V}_h$.

Lemma 4.2.13 (Properties of the inverse Stokes operator).

Let $\varepsilon > 0$ be arbitrary. S has the following properties:

$$\begin{aligned}
\|\nabla S\mathbf{v}_h\|_0 &\leq \frac{1}{\nu}\|\mathbf{v}_h\|_0, \\
|\mathbf{v}_h|_*^2 &= (\mathbf{v}_h, S\mathbf{v}_h) = \nu(\nabla S\mathbf{v}_h, \nabla \mathbf{v}_h) + \gamma(\nabla \cdot S\mathbf{v}_h, \nabla \cdot \mathbf{v}_h) \\
&\geq \left(1 - \left(\frac{2\nu + \gamma}{\nu}\right)^2 \frac{\varepsilon}{4}\right) \|\mathbf{v}_h\|_0^2 - \frac{1}{\varepsilon} \|\mathbf{v}_h - \mathbf{v}_h^*\|_0^2 \quad \forall \mathbf{v}_h^* \in \mathbf{V}_h^{div}, \\
|\mathbf{v}_h|_*^2 &\leq \frac{1}{\nu} \|\mathbf{v}_h\|_0^2.
\end{aligned} \tag{4.28}$$

Proof. By testing (4.27) symmetrically with $\mathbf{w}_h = \mathbf{v}_h$, we derive an estimate for the solution in the $W^{1,2}$ -semi-norm

$$\begin{aligned}
\nu\|\nabla S\mathbf{v}_h\|_0^2 + \gamma\|\nabla \cdot S\mathbf{v}_h\|_0^2 &= (\mathbf{v}_h, S\mathbf{v}_h) - (r_h, \nabla \cdot S\mathbf{v}_h) = (\mathbf{v}_h, S\mathbf{v}_h) \leq \|\mathbf{v}_h\|_{-1} \|\nabla S\mathbf{v}_h\|_0 \\
\Rightarrow \|\nabla S\mathbf{v}_h\|_0 &\leq \frac{1}{\nu} \|\mathbf{v}_h\|_{-1} \leq \frac{1}{\nu} \|\mathbf{v}_h\|_0
\end{aligned}$$

due to the fact that $\|\mathbf{v}_h\|_{-1} \leq \|\mathbf{v}_h\|_0$. Thus, the upper bound for the semi-norm induced by the inverse Stokes operator can be derived as

$$|\mathbf{v}_h|_*^2 = (\mathbf{v}_h, S\mathbf{v}_h) \leq \|\mathbf{v}_h\|_{-1} \|\nabla S\mathbf{v}_h\|_0 \leq \frac{1}{\nu} \|\mathbf{v}_h\|_{-1}^2 \leq \frac{1}{\nu} \|\mathbf{v}_h\|_0^2.$$

Next, we are interested in a lower bound. If we add grad-div stabilization in [Gue99] (as in [AD15]), we can get $\|\nabla r_h\|_0 \leq C(2 + \frac{2}{\nu})\|\mathbf{v}_h\|_0$ and calculate with this

$$\begin{aligned}
|\mathbf{v}_h|_*^2 &= \nu(\nabla S\mathbf{v}_h, \nabla \mathbf{v}_h) + \gamma(\nabla \cdot S\mathbf{v}_h, \nabla \cdot \mathbf{v}_h) = \|\mathbf{v}_h\|_0^2 + (r_h, \nabla \cdot \mathbf{v}_h) \\
&= \|\mathbf{v}_h\|_0^2 - (\nabla r_h, \mathbf{v}_h - \mathbf{v}_h^*) \geq \|\mathbf{v}_h\|_0^2 - \|\nabla r_h\|_0 \|\mathbf{v}_h - \mathbf{v}_h^*\|_0 \\
&\geq \left(1 - \left(\frac{2\nu + \gamma}{\nu}\right)^2 \frac{\varepsilon}{4}\right) \|\mathbf{v}_h\|_0^2 - \frac{1}{\varepsilon} \|\mathbf{v}_h - \mathbf{v}_h^*\|_0^2
\end{aligned}$$

for all $\varepsilon > 0$ and arbitrary $\mathbf{v}_h^* \in \mathbf{V}_h^{div}$. □

Lemma 4.2.14 (Time convergence of the linear error).

If $\Delta t < \frac{1}{2}$ and Assumption 4.2.2 are valid, it holds for all $1 \leq m \leq N$

$$\begin{aligned}
\|\tilde{\boldsymbol{\eta}}_u^m\|_0^2 &\leq \frac{C}{\nu^2} e^{C_{G,\text{lin}}(\Delta t)^4}, \\
\nu\|\nabla \tilde{\boldsymbol{\eta}}_u^m\|_0^2 + \gamma\|\nabla \cdot \tilde{\boldsymbol{\eta}}_u^m\|_0^2 &\leq e^{C_{G,\text{lin}}(\Delta t)^2}
\end{aligned}$$

with $C_{G,\text{lin}} \sim T(1 - 2\Delta t)^{-1}$.

Proof. We test the advection-diffusion error equation (4.21) with the inverse Stokes operator applied to $4\Delta t \tilde{\boldsymbol{\eta}}_u^n$ and eliminate the terms containing $\boldsymbol{\eta}_u^{n-1}$, $\boldsymbol{\eta}_u^{n-2}$ via the projection error equation (4.22) tested with $S\tilde{\boldsymbol{\eta}}_u^n$. Using $S\tilde{\boldsymbol{\eta}}_u^n \in \mathbf{V}_h^{div}$ gives:

$$\begin{aligned} & 2(3\tilde{\boldsymbol{\eta}}_u^n - 4\tilde{\boldsymbol{\eta}}_u^{n-1} + \tilde{\boldsymbol{\eta}}_u^{n-2}, S\tilde{\boldsymbol{\eta}}_u^n) + 4\Delta t \nu (\nabla \tilde{\boldsymbol{\eta}}_u^n, \nabla S\tilde{\boldsymbol{\eta}}_u^n) + 4\Delta t \gamma (\nabla \cdot \tilde{\boldsymbol{\eta}}_u^n, \nabla \cdot S\tilde{\boldsymbol{\eta}}_u^n) \\ &= 4\Delta t (R^n, S\tilde{\boldsymbol{\eta}}_u^n) + 4\Delta t (\nabla \left(-p_h(t_n) + \frac{7}{3}r^{n-1} - \frac{5}{3}r^{n-2} + \frac{1}{3}r^{n-3} \right), S\tilde{\boldsymbol{\eta}}_u^n) = 4\Delta t (R^n, S\tilde{\boldsymbol{\eta}}_u^n). \end{aligned}$$

For the first term, we use the identity

$$\begin{aligned} 2(3\tilde{\boldsymbol{\eta}}_u^n - 4\tilde{\boldsymbol{\eta}}_u^{n-1} + \tilde{\boldsymbol{\eta}}_u^{n-2}, S\tilde{\boldsymbol{\eta}}_u^n) &= |\tilde{\boldsymbol{\eta}}_u^n|_*^2 + |2\tilde{\boldsymbol{\eta}}_u^n - \tilde{\boldsymbol{\eta}}_u^{n-1}|_*^2 + |\delta_{tt}\tilde{\boldsymbol{\eta}}_u^n|_*^2 \\ &\quad - |\tilde{\boldsymbol{\eta}}_u^{n-1}|_*^2 - |2\tilde{\boldsymbol{\eta}}_u^{n-1} - \tilde{\boldsymbol{\eta}}_u^{n-2}|_*^2. \end{aligned}$$

This can be understood via Definition 4.2.12 of S : For $\mathbf{v}_h, \mathbf{w}_h \in \mathbf{V}_h$, it holds

$$(\mathbf{v}_h, S\mathbf{w}_h) = \nu (\nabla S\mathbf{v}_h, \nabla S\mathbf{w}_h) + \gamma (\nabla \cdot S\mathbf{v}_h, \nabla \cdot S\mathbf{w}_h) = (\mathbf{w}_h, S\mathbf{v}_h)$$

and thus with the definition $|\mathbf{v}_h|_* = (\mathbf{v}_h, S\mathbf{v}_h)$ from Lemma 4.2.13

$$\begin{aligned} & 2(3\tilde{\boldsymbol{\eta}}_u^n - 4\tilde{\boldsymbol{\eta}}_u^{n-1} + \tilde{\boldsymbol{\eta}}_u^{n-2}, S\tilde{\boldsymbol{\eta}}_u^n) \\ &= (6\tilde{\boldsymbol{\eta}}_u^n - 4\tilde{\boldsymbol{\eta}}_u^{n-1} + \tilde{\boldsymbol{\eta}}_u^{n-2}, S\tilde{\boldsymbol{\eta}}_u^n) - 4(\tilde{\boldsymbol{\eta}}_u^n, S\tilde{\boldsymbol{\eta}}_u^{n-1}) + (\tilde{\boldsymbol{\eta}}_u^n, S\tilde{\boldsymbol{\eta}}_u^{n-2}) \\ &= (\tilde{\boldsymbol{\eta}}_u^n, S\tilde{\boldsymbol{\eta}}_u^n) + (2\tilde{\boldsymbol{\eta}}_u^n - \tilde{\boldsymbol{\eta}}_u^{n-1}, 2S\tilde{\boldsymbol{\eta}}_u^n - S\tilde{\boldsymbol{\eta}}_u^{n-1}) \\ &\quad + (\tilde{\boldsymbol{\eta}}_u^n - 2\tilde{\boldsymbol{\eta}}_u^{n-1} + \tilde{\boldsymbol{\eta}}_u^{n-2}, S\tilde{\boldsymbol{\eta}}_u^n - 2S\tilde{\boldsymbol{\eta}}_u^{n-1} + S\tilde{\boldsymbol{\eta}}_u^{n-2}) \\ &\quad - (\tilde{\boldsymbol{\eta}}_u^{n-1}, S\tilde{\boldsymbol{\eta}}_u^{n-1}) - (2\tilde{\boldsymbol{\eta}}_u^{n-1} - \tilde{\boldsymbol{\eta}}_u^{n-2}, 2S\tilde{\boldsymbol{\eta}}_u^{n-1} - S\tilde{\boldsymbol{\eta}}_u^{n-2}) \\ &= |\tilde{\boldsymbol{\eta}}_u^n|_*^2 + |2\tilde{\boldsymbol{\eta}}_u^n - \tilde{\boldsymbol{\eta}}_u^{n-1}|_*^2 + |\delta_{tt}\tilde{\boldsymbol{\eta}}_u^n|_*^2 - |\tilde{\boldsymbol{\eta}}_u^{n-1}|_*^2 - |2\tilde{\boldsymbol{\eta}}_u^{n-1} - \tilde{\boldsymbol{\eta}}_u^{n-2}|_*^2. \end{aligned}$$

With this, we get the following equation

$$\begin{aligned} & |\tilde{\boldsymbol{\eta}}_u^n|_*^2 + |2\tilde{\boldsymbol{\eta}}_u^n - \tilde{\boldsymbol{\eta}}_u^{n-1}|_*^2 + |\delta_{tt}\tilde{\boldsymbol{\eta}}_u^n|_*^2 + 4\Delta t \nu (\nabla \tilde{\boldsymbol{\eta}}_u^n, \nabla S\tilde{\boldsymbol{\eta}}_u^n) + 4\Delta t \gamma (\nabla \cdot \tilde{\boldsymbol{\eta}}_u^n, \nabla \cdot S\tilde{\boldsymbol{\eta}}_u^n) \\ &= 4\Delta t (R^n, S\tilde{\boldsymbol{\eta}}_u^n) + |\tilde{\boldsymbol{\eta}}_u^{n-1}|_*^2 + |2\tilde{\boldsymbol{\eta}}_u^{n-1} - \tilde{\boldsymbol{\eta}}_u^{n-2}|_*^2. \end{aligned}$$

Due to Lemma 4.2.13, the consistency error can be bounded as

$$4\Delta t (R^n, S\tilde{\boldsymbol{\eta}}_u^n) \leq \frac{4\Delta t}{\nu} \|R^n\|_{-1}^2 + \Delta t \nu \|S\tilde{\boldsymbol{\eta}}_u^n\|_1^2 \leq \frac{4\Delta t}{\nu} \|R^n\|_{-1}^2 + \Delta t \|\tilde{\boldsymbol{\eta}}_u^n\|_0^2.$$

Using (4.28) with $\varepsilon = 2 \left(\frac{\nu}{2\nu + \gamma} \right)^2$, the diffusive term and the grad-div stabilization can be estimated by

$$4\Delta t \nu (\nabla \tilde{\boldsymbol{\eta}}_u^n, \nabla S\tilde{\boldsymbol{\eta}}_u^n) + 4\Delta t \gamma (\nabla \cdot \tilde{\boldsymbol{\eta}}_u^n, \nabla \cdot S\tilde{\boldsymbol{\eta}}_u^n) \geq 2\Delta t \|\tilde{\boldsymbol{\eta}}_u^n\|_0^2 - c\Delta t \|\tilde{\boldsymbol{\eta}}_u^n - \boldsymbol{\eta}_u^n\|_0^2,$$

where $c = 2 \left(\frac{2\nu+\gamma}{\nu} \right)^2 \leq C(1 + \frac{\nu}{\gamma})^2$. Combining these estimates and summing up from $n = 3$ to $m \leq N$ yield

$$\begin{aligned} & |\tilde{\boldsymbol{\eta}}_u^m|_*^2 + |2\tilde{\boldsymbol{\eta}}_u^m - \tilde{\boldsymbol{\eta}}_u^{m-1}|_*^2 + \sum_{n=3}^m (|\delta_{tt}\tilde{\boldsymbol{\eta}}_u^n|_*^2 + \Delta t \|\tilde{\boldsymbol{\eta}}_u^n\|_0^2) \\ & \leq |\tilde{\boldsymbol{\eta}}_u^2|_*^2 + |2\tilde{\boldsymbol{\eta}}_u^2 - \tilde{\boldsymbol{\eta}}_u^1|_*^2 + \sum_{n=3}^m \left(\frac{4\Delta t}{\nu} \|R^n\|_{-1}^2 + c\Delta t \|\tilde{\boldsymbol{\eta}}_u^n - \boldsymbol{\eta}_u^n\|_0^2 \right) \leq \left(\frac{C}{\nu} + ce^{C_{G,\text{lin}}} \right) (\Delta t)^4 \end{aligned} \quad (4.29)$$

because of Lemma 4.2.11, Assumption 4.2.2 and initial error estimates: Lemma 4.2.13 implies that $|\cdot|_*$ can be bounded from above by $\|\cdot\|_0$; the combination with Lemma 4.2.10 gives the desired initial error bounds. In particular, we derive

$$\begin{aligned} \|\tilde{\boldsymbol{\eta}}_u\|_{l^2(0,T;L^2(\Omega))}^2 &= \Delta t \sum_{n=0}^N \|\tilde{\boldsymbol{\eta}}_u^n\|_0^2 \leq \left(\frac{C}{\nu} + \left(1 + \frac{\gamma}{\nu}\right)^2 e^{C_{G,\text{lin}}} \right) (\Delta t)^4 \\ &\leq \frac{C}{\nu^2} e^{C_{G,\text{lin}}} (\Delta t)^4. \end{aligned}$$

To get an l^∞ -estimate, we use (4.28) again with $\varepsilon = 2 \left(\frac{\nu}{2\nu+\gamma} \right)^2$ and obtain from (4.29) together with Lemma 4.2.11

$$\begin{aligned} \|\tilde{\boldsymbol{\eta}}_u\|_{l^\infty(0,T;L^2(\Omega))}^2 &\leq C \max_{1 \leq n \leq N} |\tilde{\boldsymbol{\eta}}_u^n|_*^2 + C \left(1 + \frac{\gamma}{\nu}\right)^2 \max_{1 \leq n \leq N} \|\tilde{\boldsymbol{\eta}}_u^n - \boldsymbol{\eta}_u^n\|_0^2 \\ &\leq \frac{C}{\nu^2} e^{C_{G,\text{lin}}} (\Delta t)^4. \end{aligned}$$

For the estimates for the $W^{1,2}$ -semi-norm, we again use calculations from Lemma 4.2.11. Due to (4.26), we have

$$\sum_{n=3}^m (\nu \|\nabla \delta_t \tilde{\boldsymbol{\eta}}_u^n\|_0^2 + \gamma \|\nabla \cdot \delta_t \tilde{\boldsymbol{\eta}}_u^n\|_0^2) \leq e^{C_{G,\text{lin}}} (\Delta t)^3$$

and therefore via triangle inequality and because of $N = T/\Delta t$:

$$\begin{aligned} \sqrt{\nu} \|\nabla \tilde{\boldsymbol{\eta}}_u^m\|_0 + \sqrt{\gamma} \|\nabla \cdot \tilde{\boldsymbol{\eta}}_u^m\|_0 &\leq \sum_{n=1}^m (\sqrt{\nu} \|\nabla \delta_t \tilde{\boldsymbol{\eta}}_u^n\|_0 + \sqrt{\gamma} \|\nabla \cdot \delta_t \tilde{\boldsymbol{\eta}}_u^n\|_0) \\ &\leq C \left(N \sum_{n=1}^m (\nu \|\nabla \delta_t \tilde{\boldsymbol{\eta}}_u^n\|_0^2 + \gamma \|\nabla \cdot \delta_t \tilde{\boldsymbol{\eta}}_u^n\|_0^2) \right)^{1/2} \leq e^{C_{G,\text{lin}}} \Delta t. \end{aligned}$$

□

Lemma 4.2.15 (Stability of $\nabla \mathbf{u}_h$).

Set $h := \max_{M \in \mathcal{M}_h} h_M$. Let Assumption 4.2.3 be valid and $\Delta t < 1$. Then we have

$$\|\mathbf{u}_h\|_{l^\infty(0,T;W^{1,2}(\Omega))}^2 \leq C + Ce^{C_{G,h}(\mathbf{u})} \frac{h^{2k_u} + h^{2k_p+2}}{\nu \Delta t}. \quad (4.30)$$

If we additionally assume $(h^{2k_u} + h^{2k_p+2}) \lesssim e^{-C_{G,h}(\mathbf{u})} \nu \Delta t$, it holds

$$\|\mathbf{u}_h\|_{l^\infty(0,T;W^{1,2}(\Omega))}^2 \leq C.$$

Proof. Thanks to Assumption 4.2.3, we can apply Corollary 4.2.8 and establish

$$\begin{aligned} \|\mathbf{u} - \mathbf{u}_h\|_{l^2(0,T;W^{1,2}(\Omega))}^2 &\leq C \left(\|\mathbf{u} - \mathbf{u}_h\|_{L^2(0,T;W^{1,2}(\Omega))}^2 + (\Delta t)^{2l} \right) \\ &\leq \frac{Ce^{C_{G,h}(\mathbf{u})}}{\nu} (h^{2k_u} + h^{2k_p+2}) + C(\Delta t)^{2l}, \\ \|\mathbf{u} - \mathbf{u}_h\|_{l^\infty(0,T;W^{1,2}(\Omega))}^2 &\leq \frac{C}{\Delta t} \|\mathbf{u} - \mathbf{u}_h\|_{l^2(0,T;W^{1,2}(\Omega))}^2 \\ &\leq Ce^{C_{G,h}(\mathbf{u})} \frac{h^{2k_u} + h^{2k_p+2}}{\nu \Delta t} + C(\Delta t)^{2l-1}. \end{aligned}$$

With this and $\mathbf{u} \in L^\infty(0, T; [W^{2,2}(\Omega)]^d)$ due to Assumption 4.2.3, we derive

$$\begin{aligned} \|\mathbf{u}_h\|_{l^\infty(0,T;W^{1,2}(\Omega))}^2 &\leq C \|\mathbf{u}\|_{l^\infty(0,T;W^{1,2}(\Omega))}^2 + C \|\mathbf{u} - \mathbf{u}_h\|_{l^\infty(0,T;W^{1,2}(\Omega))}^2 \\ &\leq C + Ce^{C_{G,h}(\mathbf{u})} \frac{h^{2k_u} + h^{2k_p+2}}{\nu \Delta t} + C(\Delta t)^{2l-1} \leq C \end{aligned}$$

because $(h^{2k_u} + h^{2k_p+2}) \lesssim e^{-C_{G,h}(\mathbf{u})} \nu \Delta t$ and $2l \geq 1$. \square

Now, let us turn our attention to the nonlinear error. The proof combines estimation strategies from [She96] with the handling of the discrete BDF2-type time derivative by [GS04] as well as adds grad-div and LPS stabilization and the thorough consideration of ν dependencies. Extra technical challenges matter since we do not require $\mathbf{u}_h \in L^\infty(0, T; [W^{2,2}(\Omega)]^d)$. In addition to the previous lemma, we make use of the insights from the linear error estimate (Lemma 4.2.14).

Lemma 4.2.16 (Time convergence of the nonlinear error).

Denote

$$\begin{aligned} K_{t,\text{nl}} := C\Delta t \|\mathbf{u}_h\|_{l^\infty(0,T;W^{1,2}(\Omega))}^2 &\left(\frac{\|\mathbf{u}_h\|_{l^\infty(0,T;W^{1,2}(\Omega))}^2}{\nu^3} + \max_{1 \leq n \leq N} \max_{M \in \mathcal{M}_h} \left\{ \frac{\tau_M^n}{h_M^d} \right\} \right) \\ &+ \frac{\|\mathbf{u}_h\|_{l^\infty(0,T;L^2(\Omega))}^2}{\nu} \max_{1 \leq n \leq N} \max_{M \in \mathcal{M}_h} \left\{ \frac{\tau_M^n}{h_M^d} \right\}^2. \end{aligned}$$

Under the conditions of Assumption 4.2.3, it holds with $C_{G,t} \sim T(1 - K_{t,\text{nl}})^{-1}$, for all $1 \leq m \leq N$:

$$\begin{aligned}
& \|\tilde{\mathbf{e}}_u^m\|_0^2 + (\Delta t)^2 \|\nabla e_p^m\|_0^2 + \sum_{n=1}^m \left[\Delta t \nu \|\nabla \tilde{\mathbf{e}}_u^n\|_0^2 + \Delta t \gamma \|\nabla \cdot \tilde{\mathbf{e}}_u^n\|_0^2 \right. \\
& \left. + \Delta t \sum_{M \in \mathcal{M}_h} \tau_M^n \|\kappa_M^u ((\tilde{\mathbf{u}}_M^n \cdot \nabla) \tilde{\mathbf{e}}_u^n)\|_{0,M}^2 \right] \\
& \leq e^{C_{G,t}} \left\{ \left(\frac{C}{\nu^3} + \frac{C}{\nu^2} \max_{1 \leq n \leq N} \max_{M \in \mathcal{M}_h} \{\tau_M^n / h_M^d\} + \frac{C}{\nu^3} \max_{1 \leq n \leq N} \max_{M \in \mathcal{M}_h} \{\tau_M^n / h_M^d\}^2 \right) (\Delta t)^4 \right. \\
& \left. + \frac{C}{\nu} \max_{1 \leq n \leq N} \max_{M \in \mathcal{M}_h} \{\tau_M^n |\tilde{\mathbf{u}}_M^n|^2\} (\Delta t)^2 + \frac{C}{\nu^3} e^{C_{G,h}(u)} (h^{2k_u} + h^{2k_p+2}) (\Delta t)^2 + \frac{C}{\nu^2} (\Delta t)^{2l+2} \right\},
\end{aligned}$$

provided that $(h^{2k_u} + h^{2k_p+2}) \lesssim e^{-C_{G,h}(u)} \nu \Delta t$ and $K_{t,\text{nl}} < 1$.

Proof. Subtracting the advection-diffusion equations for $\tilde{\mathbf{w}}_{ht}^n$ and $\tilde{\mathbf{u}}_{ht}^n$ from each other gives

$$\begin{aligned}
& \left(\frac{3\tilde{\mathbf{e}}_u^n - 4\mathbf{e}_u^{n-1} + \mathbf{e}_u^{n-2}}{2\Delta t}, \mathbf{v}_h \right) + \nu (\nabla \tilde{\mathbf{e}}_u^n, \nabla \mathbf{v}_h) + \gamma (\nabla \cdot \tilde{\mathbf{e}}_u^n, \nabla \cdot \mathbf{v}_h) \\
& + (\nabla e_p^{n-1}, \mathbf{v}_h) + c_u(\mathbf{u}_h(t_n); \mathbf{u}_h(t_n), \mathbf{v}_h) - c_u(\tilde{\mathbf{u}}_{ht}^n; \tilde{\mathbf{u}}_{ht}^n, \mathbf{v}_h) \\
& + s_u(\mathbf{u}_h(t_n), \mathbf{u}_h(t_n), \mathbf{u}_h(t_n), \mathbf{v}_h) - s_u(\tilde{\mathbf{u}}_{ht}^n, \tilde{\mathbf{u}}_{ht}^n, \tilde{\mathbf{u}}_{ht}^n, \mathbf{v}_h) = 0 \quad \forall \mathbf{v}_h \in \mathbf{V}_h
\end{aligned} \tag{4.31}$$

and for the projection equations for $\tilde{\mathbf{w}}_{ht}^n$ and $\tilde{\mathbf{u}}_{ht}^n$:

$$\left(\frac{3\mathbf{e}_u^n - 3\tilde{\mathbf{e}}_u^n}{2\Delta t} + \nabla(e_p^n - e_p^{n-1}), \mathbf{y}_h \right) = 0 \quad \forall \mathbf{y}_h \in \mathbf{Y}_h. \tag{4.32}$$

The advection-diffusion error equation (4.31) is tested symmetrically with $4\Delta t \tilde{\mathbf{e}}_u^n$ and the resulting pressure term $4\Delta t (\nabla e_p^{n-1}, \tilde{\mathbf{e}}_u^n)$ is handled via (4.32) tested with $\frac{8}{3}(\Delta t)^2 \nabla e_p^{n-1}$. As before, this yields

$$\begin{aligned}
& \|\tilde{\mathbf{e}}_u^n\|_0^2 + 3\|\mathbf{e}_u^n - \tilde{\mathbf{e}}_u^n\|_0^2 + \|2\mathbf{e}_u^n - \mathbf{e}_u^{n-1}\|_0^2 + \frac{4}{3}(\Delta t)^2 \|\nabla e_p^n\|_0^2 \\
& + 4\Delta t \nu \|\nabla \tilde{\mathbf{e}}_u^n\|_0^2 + 4\Delta t \gamma \|\nabla \cdot \tilde{\mathbf{e}}_u^n\|_0^2 + \|\delta_{tt} \mathbf{e}_u^n\|_0^2 + 4\Delta t (S_n, \tilde{\mathbf{e}}_u^n) \\
& \leq \|\tilde{\mathbf{e}}_u^{n-1}\|_0^2 + \|2\mathbf{e}_u^{n-1} - \mathbf{e}_u^{n-2}\|_0^2 + \frac{4}{3}(\Delta t)^2 \|\nabla e_p^{n-1}\|_0^2 \\
& + \frac{4}{3}(\Delta t)^2 \|\nabla(e_p^n - e_p^{n-1})\|_0^2 - 4\Delta t (Q_n, \tilde{\mathbf{e}}_u^n),
\end{aligned} \tag{4.33}$$

where

$$\begin{aligned}
(Q_n, \tilde{\mathbf{e}}_u^n) & := c_u(\mathbf{u}_h(t_n); \mathbf{u}_h(t_n), \tilde{\mathbf{e}}_u^n) - c_u(\tilde{\mathbf{u}}_{ht}^n; \tilde{\mathbf{u}}_{ht}^n, \tilde{\mathbf{e}}_u^n) \\
(S_n, \tilde{\mathbf{e}}_u^n) & := s_u(\mathbf{u}_h(t_n), \mathbf{u}_h(t_n), \mathbf{u}_h(t_n), \tilde{\mathbf{e}}_u^n) - s_u(\tilde{\mathbf{u}}_{ht}^n, \tilde{\mathbf{u}}_{ht}^n, \tilde{\mathbf{u}}_{ht}^n, \tilde{\mathbf{e}}_u^n).
\end{aligned}$$

Equation (4.32) tested with $\nabla(e_p^n - e_p^{n-1})$ gives

$$\frac{4}{3}(\Delta t)^2 \|\nabla(e_p^n - e_p^{n-1})\|_0^2 \leq 3\|e_u^n - \tilde{e}_u^n\|_0^2.$$

Due to $\tilde{e}_u^n + \tilde{\eta}_u^n = \mathbf{u}_h(t_n) - \tilde{\mathbf{u}}_{ht}^n$, we calculate for the convective term using skew-symmetry

$$\begin{aligned} (Q_n, \tilde{e}_u^n) &= c_u(\tilde{\eta}_u^n + \tilde{e}_u^n; \mathbf{u}_h(t_n), \tilde{e}_u^n) + c_u(\tilde{\mathbf{u}}_{ht}^n; \tilde{\eta}_u^n + \tilde{e}_u^n, \tilde{e}_u^n) \\ &= c_u(\tilde{\eta}_u^n + \tilde{e}_u^n; \mathbf{u}_h(t_n), \tilde{e}_u^n) + c_u(\mathbf{u}_h(t_n); \tilde{\eta}_u^n, \tilde{e}_u^n) \\ &\quad - c_u(\tilde{\eta}_u^n; \tilde{\eta}_u^n, \tilde{e}_u^n) - c_u(\tilde{e}_u^n; \tilde{\eta}_u^n, \tilde{e}_u^n) \end{aligned}$$

and make use of Lemma A.3.7 as well as the convergence results for the linear problem:

$$\begin{aligned} c_u(\tilde{e}_u^n; \mathbf{u}_h(t_n), \tilde{e}_u^n) &\leq C\|\tilde{e}_u^n\|_0^{1/2}\|\mathbf{u}_h(t_n)\|_1\|\tilde{e}_u^n\|_1^{3/2} \\ &\leq \frac{\nu}{32}\|\nabla\tilde{e}_u^n\|_0^2 + \frac{C}{\nu^3}\|\mathbf{u}_h(t_n)\|_1^4\|\tilde{e}_u^n\|_0^2, \\ c_u(\mathbf{u}_h(t_n); \tilde{\eta}_u^n, \tilde{e}_u^n) + c_u(\tilde{\eta}_u^n; \mathbf{u}_h(t_n), \tilde{e}_u^n) \\ &= c_u(\mathbf{u}(t_n); \tilde{\eta}_u^n, \tilde{e}_u^n) - c_u(\mathbf{u}(t_n) - \mathbf{u}_h(t_n); \tilde{\eta}_u^n, \tilde{e}_u^n) \\ &\quad + c_u(\tilde{\eta}_u^n; \mathbf{u}(t_n), \tilde{e}_u^n) - c_u(\tilde{\eta}_u^n; \mathbf{u}(t_n) - \mathbf{u}_h(t_n), \tilde{e}_u^n) \\ &\leq C\|\mathbf{u}(t_n)\|_2\|\tilde{\eta}_u^n\|_0\|\tilde{e}_u^n\|_1 + C\|\mathbf{u}(t_n) - \mathbf{u}_h(t_n)\|_1\|\tilde{\eta}_u^n\|_1\|\tilde{e}_u^n\|_1 \\ &\leq \frac{\nu}{32}\|\nabla\tilde{e}_u^n\|_0^2 + \frac{C\|\mathbf{u}(t_n)\|_2^2}{\nu}\|\tilde{\eta}_u^n\|_0^2 + \frac{C}{\nu}\|\tilde{\eta}_u^n\|_1^2\|\mathbf{u}(t_n) - \mathbf{u}_h(t_n)\|_1^2, \\ c_u(\tilde{\eta}_u^n; \tilde{\eta}_u^n, \tilde{e}_u^n) &\leq C\|\tilde{\eta}_u^n\|_1^2\|\tilde{e}_u^n\|_1 \leq \frac{\nu}{32}\|\nabla\tilde{e}_u^n\|_0^2 + \frac{C}{\nu}\|\tilde{\eta}_u^n\|_1^4, \\ c_u(\tilde{e}_u^n; \tilde{\eta}_u^n, \tilde{e}_u^n) &\leq C\|\tilde{\eta}_u^n\|_1\|\tilde{e}_u^n\|_1^2. \end{aligned}$$

From Lemma 4.2.14, we have that $\sqrt{\nu}\|\tilde{\eta}_u^n\|_{l^\infty(0,T;W^{1,2}(\Omega))} \leq \exp(C_{G,\text{lin}})\Delta t$. Provided that $C\Delta t \leq \nu^{3/2}/8$, we can estimate the last term

$$c_u(\tilde{e}_u^n; \tilde{\eta}_u^n, \tilde{e}_u^n) \leq C\|\tilde{\eta}_u^n\|_1\|\tilde{e}_u^n\|_1^2 \leq \frac{\nu}{32}\|\nabla\tilde{e}_u^n\|_0^2.$$

Taking $\|\tilde{\eta}_u\|_{l^\infty(0,T;L^2(\Omega))} \leq \frac{\exp(C_{G,\text{lin}})}{\nu}(\Delta t)^2$ and $\sqrt{\nu}\|\tilde{\eta}_u^n\|_{l^\infty(0,T;W^{1,2}(\Omega))} \leq \exp(C_{G,\text{lin}})\Delta t$ from Lemma 4.2.14 into account, we obtain in combination (with $\exp(C_{G,\text{lin}})$ hidden in C)

$$\begin{aligned} (Q^n, \tilde{e}_u^n) &\leq \frac{\nu}{8}\|\nabla\tilde{e}_u^n\|_0^2 + \frac{C\|\mathbf{u}_h(t_n)\|_1^4}{\nu^3}\|\tilde{e}_u^n\|_0^2 \\ &\quad + \frac{C\|\mathbf{u}(t_n)\|_2^2}{\nu^3}(\Delta t)^4 + \frac{C}{\nu^2}\|\mathbf{u}(t_n) - \mathbf{u}_h(t_n)\|_1^2(\Delta t)^2. \end{aligned} \quad (4.34)$$

Recall that s_u is supposed to be linear in each argument due to Assumption 4.2.3. For the stabilization terms, we have

$$\begin{aligned}
(S^n, \tilde{\mathbf{e}}_u^n) &= s_u(\mathbf{u}_h(t_n), \mathbf{u}_h(t_n), \mathbf{u}_h(t_n), \tilde{\mathbf{e}}_u^n) - s_u(\tilde{\mathbf{u}}_{ht}^n, \tilde{\mathbf{u}}_{ht}^n, \tilde{\mathbf{u}}_{ht}^n, \tilde{\mathbf{e}}_u^n) \\
&= s_u(\tilde{\mathbf{u}}_{ht}^n, \tilde{\boldsymbol{\eta}}_u^n + \tilde{\mathbf{e}}_u^n, \tilde{\mathbf{u}}_{ht}^n, \tilde{\mathbf{e}}_u^n) + s_u(\tilde{\boldsymbol{\eta}}_u^n + \tilde{\mathbf{e}}_u^n, \mathbf{u}_h(t_n), \tilde{\mathbf{u}}_{ht}^n, \tilde{\mathbf{e}}_u^n) \\
&\quad + s_u(\mathbf{u}_h(t_n), \mathbf{u}_h(t_n), \tilde{\boldsymbol{\eta}}_u^n + \tilde{\mathbf{e}}_u^n, \tilde{\mathbf{e}}_u^n) \\
&= s_u(\tilde{\mathbf{u}}_{ht}^n, \tilde{\boldsymbol{\eta}}_u^n, \tilde{\mathbf{u}}_{ht}^n, \tilde{\mathbf{e}}_u^n) + s_u(\tilde{\boldsymbol{\eta}}_u^n, \mathbf{u}_h(t_n), \tilde{\mathbf{u}}_{ht}^n, \tilde{\mathbf{e}}_u^n) + s_u(\mathbf{u}_h(t_n), \mathbf{u}_h(t_n), \tilde{\boldsymbol{\eta}}_u^n, \tilde{\mathbf{e}}_u^n) \\
&\quad + s_u(\tilde{\mathbf{u}}_{ht}^n, \tilde{\mathbf{e}}_u^n, \tilde{\mathbf{u}}_{ht}^n, \tilde{\mathbf{e}}_u^n) + s_u(\tilde{\mathbf{e}}_u^n, \mathbf{u}_h(t_n), \tilde{\mathbf{u}}_{ht}^n, \tilde{\mathbf{e}}_u^n) + s_u(\mathbf{u}_h(t_n), \mathbf{u}_h(t_n), \tilde{\mathbf{e}}_u^n, \tilde{\mathbf{e}}_u^n) \\
&=: I_1 + I_2 + I_3 + I_4 + I_5 + I_6.
\end{aligned}$$

According to Lemma A.3.8, Cauchy-Schwarz and Young's inequality, the terms $I_5 + I_6$ can be handled as

$$\begin{aligned}
|I_5 + I_6| &\leq C \|\mathbf{u}_h(t_n)\|_1^2 \max_{M \in \mathcal{M}_h} \{\tau_M^n / h_M^d\} \|\tilde{\mathbf{e}}_u^n\|_0^2 + \frac{1}{4} \sum_{M \in \mathcal{M}_h} \tau_M^n \|\kappa_M^u((\tilde{\mathbf{u}}_M^n \cdot \nabla) \tilde{\mathbf{e}}_u^n)\|_{0,M}^2 \\
&\quad + \frac{\nu}{8} \|\tilde{\mathbf{e}}_u^n\|_1^2 + \frac{C \|\mathbf{u}_h(t_n)\|_0^2 \|\mathbf{u}_h(t_n)\|_1^2}{\nu} \max_{M \in \mathcal{M}_h} \{\tau_M^n / h_M^d\}^2 \|\tilde{\mathbf{e}}_u^n\|_0^2.
\end{aligned}$$

For the remaining terms, we make use of Lemma 4.2.14, namely $\|\tilde{\boldsymbol{\eta}}_u\|_{l^\infty(0,T;L^2(\Omega))} \leq \frac{\exp(C_{G,\text{lin}})}{\nu} (\Delta t)^2$ and $\sqrt{\nu} \|\tilde{\boldsymbol{\eta}}_u^n\|_{l^\infty(0,T;W^{1,2}(\Omega))} \leq \exp(C_{G,\text{lin}}) \Delta t$:

$$\begin{aligned}
I_1 &= s_u(\tilde{\mathbf{u}}_{ht}^n, \tilde{\boldsymbol{\eta}}_u^n, \tilde{\mathbf{u}}_{ht}^n, \tilde{\mathbf{e}}_u^n) \\
&\leq C \sqrt{\max_{M \in \mathcal{M}_h} \{\tau_M^n |\tilde{\mathbf{u}}_M^n|^2\}} \|\tilde{\boldsymbol{\eta}}_u^n\|_1 \left(\sum_{M \in \mathcal{M}_h} \tau_M^n \|\kappa_M^u((\tilde{\mathbf{u}}_M^n \cdot \nabla) \tilde{\mathbf{e}}_u^n)\|_{0,M}^2 \right)^{1/2} \\
&\leq C \max_{M \in \mathcal{M}_h} \{\tau_M^n |\tilde{\mathbf{u}}_M^n|^2\} \|\tilde{\boldsymbol{\eta}}_u^n\|_1^2 + \frac{1}{4} \sum_{M \in \mathcal{M}_h} \tau_M^n \|\kappa_M^u((\tilde{\mathbf{u}}_M^n \cdot \nabla) \tilde{\mathbf{e}}_u^n)\|_{0,M}^2 \\
&\leq \frac{C}{\nu} \max_{M \in \mathcal{M}_h} \{\tau_M^n |\tilde{\mathbf{u}}_M^n|^2\} (\Delta t)^2 + \frac{1}{4} \sum_{M \in \mathcal{M}_h} \tau_M^n \|\kappa_M^u((\tilde{\mathbf{u}}_M^n \cdot \nabla) \tilde{\mathbf{e}}_u^n)\|_{0,M}^2, \\
I_2 &= s_u(\tilde{\boldsymbol{\eta}}_u^n, \mathbf{u}_h(t_n), \tilde{\mathbf{u}}_{ht}^n, \tilde{\mathbf{e}}_u^n) \\
&\leq C \max_{M \in \mathcal{M}_h} \{\tau_M^n / h_M^d\} \|\tilde{\boldsymbol{\eta}}_u^n\|_0^2 \|\mathbf{u}_h(t_n)\|_1^2 + \frac{1}{4} \sum_{M \in \mathcal{M}_h} \tau_M^n \|\kappa_M^u((\tilde{\mathbf{u}}_M^n \cdot \nabla) \tilde{\mathbf{e}}_u^n)\|_{0,M}^2 \\
&\leq \frac{C}{\nu^2} \max_{M \in \mathcal{M}_h} \{\tau_M^n / h_M^d\} (\Delta t)^4 + \frac{1}{4} \sum_{M \in \mathcal{M}_h} \tau_M^n \|\kappa_M^u((\tilde{\mathbf{u}}_M^n \cdot \nabla) \tilde{\mathbf{e}}_u^n)\|_{0,M}^2, \\
I_3 &= s_u(\mathbf{u}_h(t_n), \mathbf{u}_h(t_n), \tilde{\boldsymbol{\eta}}_u^n, \tilde{\mathbf{e}}_u^n) \leq C \max_{M \in \mathcal{M}_h} \{\tau_M^n / h_M^d\} \|\mathbf{u}_h(t_n)\|_0 \|\mathbf{u}_h(t_n)\|_1 \|\tilde{\boldsymbol{\eta}}_u^n\|_0 \|\tilde{\mathbf{e}}_u^n\|_1 \\
&\leq \frac{C}{\nu} \max_{M \in \mathcal{M}_h} \{\tau_M^n / h_M^d\}^2 \|\mathbf{u}_h(t_n)\|_0^2 \|\mathbf{u}_h(t_n)\|_1^2 \|\tilde{\boldsymbol{\eta}}_u^n\|_0^2 + \frac{\nu}{4} \|\tilde{\mathbf{e}}_u^n\|_1^2 \\
&\leq \frac{C}{\nu^3} \max_{M \in \mathcal{M}_h} \{\tau_M^n / h_M^d\}^2 \|\mathbf{u}_h(t_n)\|_0^2 \|\mathbf{u}_h(t_n)\|_1^2 (\Delta t)^4 + \frac{\nu}{4} \|\tilde{\mathbf{e}}_u^n\|_1^2.
\end{aligned}$$

Summarizing these terms yields

$$\begin{aligned}
-(S^n, \tilde{e}_u^n) + I_4 &\leq \frac{3}{4} \sum_{M \in \mathcal{M}_h} \tau_M^n \|\kappa_M^u ((\tilde{\mathbf{u}}_M^n \cdot \nabla) \tilde{e}_u^n)\|_{0,M}^2 + \frac{3\nu}{8} \|\tilde{e}_u^n\|_1^2 \\
&+ \left(C \|\mathbf{u}_h(t_n)\|_1^2 \max_{M \in \mathcal{M}_h} \{\tau_M^n / h_M^d\} + \frac{C \|\mathbf{u}_h(t_n)\|_0^2 \|\mathbf{u}_h(t_n)\|_1^2}{\nu} \max_{M \in \mathcal{M}_h} \{\tau_M^n / h_M^d\}^2 \right) \|\tilde{e}_u^n\|_0^2 \\
&+ \left(\frac{C}{\nu^2} \max_{M \in \mathcal{M}_h} \{\tau_M^n / h_M^d\} + \frac{C}{\nu^3} \max_{M \in \mathcal{M}_h} \{\tau_M^n / h_M^d\}^2 \|\mathbf{u}_h(t_n)\|_0^2 \|\mathbf{u}_h(t_n)\|_1^2 \right) (\Delta t)^4 \\
&+ \frac{C}{\nu} \max_{M \in \mathcal{M}_h} \{\tau_M^n |\tilde{\mathbf{u}}_M^n|^2\} (\Delta t)^2.
\end{aligned}$$

We insert the above estimates into (4.33), sum up from $n = 2$ to $m \leq N$ and obtain

$$\begin{aligned}
&\|\tilde{e}_u^m\|_0^2 + \|2e_u^m - e_u^{m-1}\|_0^2 + \frac{4}{3}(\Delta t)^2 \|\nabla e_p^m\|_0^2 \\
&+ \sum_{n=2}^m \left[2\Delta t \nu \|\nabla \tilde{e}_u^n\|_0^2 + 4\Delta t \gamma \|\nabla \cdot \tilde{e}_u^n\|_0^2 + \|\delta_{tt} e_u^n\|_0^2 + \Delta t \sum_{M \in \mathcal{M}_h} \tau_M^n \|\kappa_M^u ((\tilde{\mathbf{u}}_M^n \cdot \nabla) \tilde{e}_u^n)\|_{0,M}^2 \right] \\
&\leq \|\tilde{e}_u^1\|_0^2 + \|2e_u^1 - e_u^0\|_0^2 + \frac{4}{3}(\Delta t)^2 \|\nabla e_p^1\|_0^2 + 4\Delta t \sum_{n=2}^m \left\{ \left(\frac{C \|\mathbf{u}_h(t_n)\|_1^4}{\nu^3} \right. \right. \\
&+ C \|\mathbf{u}_h(t_n)\|_1^2 \max_{M \in \mathcal{M}_h} \{\tau_M^n / h_M^d\} + \frac{C \|\mathbf{u}_h(t_n)\|_0^2 \|\mathbf{u}_h(t_n)\|_1^2}{\nu} \max_{M \in \mathcal{M}_h} \{\tau_M^n / h_M^d\}^2 \left. \right\} \|\tilde{e}_u^n\|_0^2 \\
&+ \left(\frac{C \|\mathbf{u}(t_n)\|_2^2 + C}{\nu^3} + \frac{C}{\nu^2} \max_{M \in \mathcal{M}_h} \left(\frac{\tau_M^n}{h_M^d} \right) + \frac{C}{\nu^3} \max_{M \in \mathcal{M}_h} \left(\frac{\tau_M^n}{h_M^d} \right)^2 \|\mathbf{u}_h(t_n)\|_0^2 \|\mathbf{u}_h(t_n)\|_1^2 \right) (\Delta t)^4 \\
&+ \left. \frac{C}{\nu} \max_{M \in \mathcal{M}_h} \{\tau_M^n |\tilde{\mathbf{u}}_M^n|^2\} (\Delta t)^2 + \frac{C}{\nu^2} \|\mathbf{u}(t_n) - \mathbf{u}_h(t_n)\|_1^2 (\Delta t)^2 \right\}. \tag{4.35}
\end{aligned}$$

Due to the estimates for the initial errors of the time-discretized problem and the linear auxiliary problem (see Lemma 4.2.10), the initial errors of the nonlinear problem also converge suitably

$$\|\tilde{e}_u^1\|_0^2 + \|2e_u^1 - e_u^0\|_0^2 + \frac{4}{3}(\Delta t)^2 \|\nabla e_p^1\|_0^2 \leq C(\Delta t)^4.$$

In addition, we consult Theorem 4.2.7 and Corollary 4.2.8 in order to establish

$$\begin{aligned}
\|\mathbf{u} - \mathbf{u}_h\|_{l^2(0,T;W^{1,2}(\Omega))}^2 &\leq C \|\mathbf{u}(t_n) - \mathbf{u}_h(t_n)\|_{L^2(0,T;W^{1,2}(\Omega))}^2 + C(\Delta t)^{2l} \\
&\leq \frac{1}{\nu} \|\mathbf{u}(t_n) - \mathbf{u}_h(t_n)\|_{L^2(0,T;LPS)}^2 + C(\Delta t)^{2l} \leq \frac{C}{\nu} e^{C_{G,h}(\mathbf{u})} (h^{2k_u} + h^{2k_p+2}) + C(\Delta t)^{2l}.
\end{aligned}$$

Provided that $(h^{2k_u} + h^{2k_p+2}) \lesssim e^{-C_{G,h}(u)} \nu \Delta t$ and

$$K_{t,\text{nl}} = C \Delta t \|\mathbf{u}_h\|_{l^\infty(0,T;W^{1,2}(\Omega))}^2 \left(\frac{\|\mathbf{u}_h\|_{l^\infty(0,T;W^{1,2}(\Omega))}^2}{\nu^3} + \max_{1 \leq n \leq N} \max_{M \in \mathcal{M}_h} \{\tau_M^n / h_M^d\} \right. \\ \left. + \frac{\|\mathbf{u}_h\|_{l^\infty(0,T;L^2(\Omega))}^2}{\nu} \max_{1 \leq n \leq N} \max_{M \in \mathcal{M}_h} \{\tau_M^n / h_M^d\}^2 \right) < 1,$$

application of the discrete Gronwall Lemma A.3.6 for $\|\tilde{\mathbf{e}}_u^m\|_0^2$ in (4.35) yields

$$\|\tilde{\mathbf{e}}_u^m\|_0^2 + (\Delta t)^2 \|\nabla e_p^m\|_0^2 + \sum_{n=1}^m \left[\Delta t \nu \|\nabla \tilde{\mathbf{e}}_u^n\|_0^2 + \Delta t \gamma \|\nabla \cdot \tilde{\mathbf{e}}_u^n\|_0^2 \right. \\ \left. + \Delta t \sum_{M \in \mathcal{M}_h} \tau_M^n \|\kappa_M^u((\tilde{\mathbf{u}}_M^n \cdot \nabla) \tilde{\mathbf{e}}_u^n)\|_{0,M}^2 \right] \\ \leq e^{C_{G,t}} \left\{ \left(\frac{C \|\mathbf{u}\|_{l^\infty(0,T;H^2(\Omega))}^2}{\nu^3} + \frac{C}{\nu^2} \max_{1 \leq n \leq N} \max_{M \in \mathcal{M}_h} \{\tau_M^n / h_M^d\} \right. \right. \\ \left. \left. + \frac{C}{\nu^3} \max_{1 \leq n \leq N} \max_{M \in \mathcal{M}_h} \{\tau_M^n / h_M^d\}^2 \|\mathbf{u}_h\|_{l^\infty(0,T;L^2(\Omega))}^2 \|\mathbf{u}_h\|_{l^\infty(0,T;W^{1,2}(\Omega))}^2 \right) (\Delta t)^4 \right. \\ \left. + \frac{C}{\nu} \max_{1 \leq n \leq N} \max_{M \in \mathcal{M}_h} \{\tau_M^n |\tilde{\mathbf{u}}_M^n|^2\} (\Delta t)^2 + \frac{C}{\nu^3} e^{C_{G,h}(u)} (h^{2k_u} + h^{2k_p+2}) (\Delta t)^2 + \frac{C}{\nu^2} (\Delta t)^{2l+2} \right\} \\ \leq e^{C_{G,t}} \left\{ \left(\frac{C}{\nu^3} + \frac{C}{\nu^2} \max_{1 \leq n \leq N} \max_{M \in \mathcal{M}_h} \{\tau_M^n / h_M^d\} + \frac{C}{\nu^3} \max_{1 \leq n \leq N} \max_{M \in \mathcal{M}_h} \{\tau_M^n / h_M^d\}^2 \right) (\Delta t)^4 \right. \\ \left. + \frac{C}{\nu} \max_{1 \leq n \leq N} \max_{M \in \mathcal{M}_h} \{\tau_M^n |\tilde{\mathbf{u}}_M^n|^2\} (\Delta t)^2 + \frac{C}{\nu^3} e^{C_{G,h}(u)} (h^{2k_u} + h^{2k_p+2}) (\Delta t)^2 + \frac{C}{\nu^2} (\Delta t)^{2l+2} \right\},$$

where Lemma 4.2.15 for $\|\mathbf{u}_h\|_{l^\infty(0,T;W^{1,2}(\Omega))}$ is taken into account and $C_{G,t} \sim T(1 - K_{t,\text{nl}})^{-1}$ denotes the Gronwall constant. \square

Now, we are prepared to state an estimate for the total error due to temporal discretization. For this purpose, we combine Lemmas 4.2.14 and 4.2.16.

Theorem 4.2.17 (Time convergence of the semi-discrete quantities).

Under the assumptions of Lemmas 4.2.14 and 4.2.16, it holds

$$\|\tilde{\boldsymbol{\xi}}_u\|_{l^\infty(0,T;L^2(\Omega))}^2 \leq \frac{C}{\nu^2} e^{C_{G,\text{lin}}} (\Delta t)^4 + \Xi_{e,u,t}, \\ \|\tilde{\boldsymbol{\xi}}_u\|_{l^2(0,T;LPS)}^2 = \nu \|\nabla \tilde{\boldsymbol{\xi}}_u\|_{l^2(0,T;L^2(\Omega))}^2 + \gamma \|\nabla \cdot \tilde{\boldsymbol{\xi}}_u\|_{l^2(0,T;L^2(\Omega))}^2 \\ + \Delta t \sum_{n=1}^N \sum_{M \in \mathcal{M}_h} \tau_M^n \|\kappa_M^u((\tilde{\mathbf{u}}_M^n \cdot \nabla) \tilde{\boldsymbol{\xi}}_u^n)\|_0^2 \leq e^{C_{G,\text{lin}}} (\Delta t)^2 + \Xi_{e,u,t}$$

with the abbreviation

$$\begin{aligned} \Xi_{e,u,t} := & e^{C_{G,t}} \left\{ \left(\frac{C}{\nu^3} + \frac{C}{\nu^2} \max_{1 \leq n \leq N} \max_{M \in \mathcal{M}_h} \{ \tau_M^n / h_M^d \} + \frac{C}{\nu^3} \max_{1 \leq n \leq N} \max_{M \in \mathcal{M}_h} \{ \tau_M^n / h_M^d \}^2 \right) (\Delta t)^4 \right. \\ & \left. + \frac{C}{\nu} \max_{1 \leq n \leq N} \max_{M \in \mathcal{M}_h} \{ \tau_M^n |\tilde{\mathbf{u}}_M^n|^2 \} (\Delta t)^2 + \frac{C}{\nu^3} e^{C_{G,h}(u)} (h^{2k_u} + h^{2k_p+2}) (\Delta t)^2 + \frac{C}{\nu^2} (\Delta t)^{2l+2} \right\}. \end{aligned}$$

Proof. For the linear error, Lemma 4.2.14 yields if $\Delta t < \frac{1}{2}$

$$\|\tilde{\boldsymbol{\eta}}_u^m\|_0^2 \leq \frac{C}{\nu^2} e^{C_{G,\text{lin}}} (\Delta t)^4, \quad \nu \|\nabla \tilde{\boldsymbol{\eta}}_u^m\|_0^2 + \gamma \|\nabla \cdot \tilde{\boldsymbol{\eta}}_u^m\|_0^2 \leq e^{C_{G,\text{lin}}} (\Delta t)^2$$

with $C_{G,\text{lin}} \sim T(1 - 2\Delta t)^{-1}$. The nonlinear error is bounded by Lemma 4.2.16 as

$$\begin{aligned} & \|\tilde{\mathbf{e}}_u^m\|_0^2 + (\Delta t)^2 \|\nabla e_p^m\|_0^2 + \sum_{n=1}^m \left[\Delta t \nu \|\nabla \tilde{\mathbf{e}}_u^n\|_0^2 + \Delta t \gamma \|\nabla \cdot \tilde{\mathbf{e}}_u^n\|_0^2 \right. \\ & \left. + \Delta t \sum_{M \in \mathcal{M}_h} \tau_M^n \|\kappa_M^u((\tilde{\mathbf{u}}_M^n \cdot \nabla) \tilde{\mathbf{e}}_u^n)\|_{0,M}^2 \right] \\ & \leq e^{C_{G,t}} \left\{ \left(\frac{C}{\nu^3} + \frac{C}{h^d \nu^2} \max_{1 \leq n \leq N} \max_{M \in \mathcal{M}_h} \{ \tau_M^n \} + \frac{C}{\nu^3 h^{2d}} \max_{1 \leq n \leq N} \max_{M \in \mathcal{M}_h} \{ \tau_M^n \}^2 \right) (\Delta t)^4 \right. \\ & \left. + \frac{C}{\nu} \max_{1 \leq n \leq N} \max_{M \in \mathcal{M}_h} \{ \tau_M^n |\tilde{\mathbf{u}}_M^n|^2 \} (\Delta t)^2 + \frac{C}{\nu^3} e^{C_{G,h}(u)} (h^{2k_u} + h^{2k_p+2}) (\Delta t)^2 + \frac{C}{\nu^2} (\Delta t)^{2l+2} \right\}, \end{aligned}$$

provided that $(h^{2k_u} + h^{2k_p+2}) \lesssim e^{-C_{G,h}(u)} \nu \Delta t$ and

$$\begin{aligned} K_{t,\text{nl}} = C \Delta t \|\mathbf{u}_h\|_{l^\infty(0,T;W^{1,2}(\Omega))}^2 & \left(\frac{\|\mathbf{u}_h\|_{l^\infty(0,T;W^{1,2}(\Omega))}^2}{\nu^3} + \max_{1 \leq n \leq N} \max_{M \in \mathcal{M}_h} \{ \tau_M^n / h_M^d \} \right. \\ & \left. + \frac{\|\mathbf{u}_h\|_{l^\infty(0,T;L^2(\Omega))}^2}{\nu} \max_{1 \leq n \leq N} \max_{M \in \mathcal{M}_h} \{ \tau_M^n / h_M^d \}^2 \right) < 1. \end{aligned}$$

We further notice for any $M \in \mathcal{M}_h$ and $1 \leq n \leq N$

$$\begin{aligned} \tau_M^n \|\kappa_M^u((\tilde{\mathbf{u}}_M^n \cdot \nabla) \tilde{\boldsymbol{\xi}}_u^n)\|_{0,M}^2 & \leq 2\tau_M^n \|\kappa_M^u((\tilde{\mathbf{u}}_M^n \cdot \nabla) \tilde{\boldsymbol{\eta}}_u^n)\|_{0,M}^2 + 2\tau_M^n \|\kappa_M^u((\tilde{\mathbf{u}}_M^n \cdot \nabla) \tilde{\mathbf{e}}_u^n)\|_{0,M}^2 \\ & \leq C \tau_M^n |\tilde{\mathbf{u}}_M^n|^2 \|\tilde{\boldsymbol{\eta}}_u^n\|_{1,M}^2 + C \tau_M^n \|\kappa_M^u((\tilde{\mathbf{u}}_M^n \cdot \nabla) \tilde{\mathbf{e}}_u^n)\|_{0,M}^2 \\ & \leq \frac{C}{\nu} \tau_M^n |\tilde{\mathbf{u}}_M^n|^2 (\Delta t)^2 + C \tau_M^n \|\kappa_M^u((\tilde{\mathbf{u}}_M^n \cdot \nabla) \tilde{\mathbf{e}}_u^n)\|_{0,M}^2. \end{aligned}$$

In combination, we establish the claim. \square

4.2.3. Errors of the Fully Discretized Scheme

For convenience, we define the total error by

$$\tilde{\zeta}_u^n := \mathbf{u}(t_n) - \tilde{\mathbf{u}}_{ht}^n, \quad \zeta_u^n := \mathbf{u}(t_n) - \mathbf{u}_{ht}^n, \quad \zeta_p^n := p(t_n) - p_{ht}^n.$$

We combine the estimates for the discretizations in time and space into the theorem below.

Theorem 4.2.18 (Fully discrete error).

Let Assumption 4.2.4 be valid. Besides, let $(h^{2k_u} + h^{2k_p+2}) \lesssim e^{-C_{G,h}(\mathbf{u})\nu\Delta t}$ and

$$\begin{aligned} K_{t,nl} = C\Delta t \|\mathbf{u}_h\|_{l^\infty(0,T;W^{1,2}(\Omega))}^2 & \left(\frac{\|\mathbf{u}_h\|_{l^\infty(0,T;W^{1,2}(\Omega))}^2}{\nu^3} + \max_{1 \leq n \leq N} \max_{M \in \mathcal{M}_h} \{\tau_M^n / h_M^d\} \right. \\ & \left. + \frac{\|\mathbf{u}_h\|_{l^\infty(0,T;L^2(\Omega))}^2}{\nu} \max_{1 \leq n \leq N} \max_{M \in \mathcal{M}_h} \{\tau_M^n / h_M^d\}^2 \right) < 1. \end{aligned}$$

With $h = \max_{M \in \mathcal{M}_h}$ and the notation from the previous results

$$\begin{aligned} \Xi_{e,u,t} & := e^{C_{G,t}} \left\{ \left(\frac{C}{\nu^3} + \frac{C}{\nu^2} \max_{1 \leq n \leq N} \max_{M \in \mathcal{M}_h} \{\tau_M^n / h_M^d\} + \frac{C}{\nu^3} \max_{1 \leq n \leq N} \max_{M \in \mathcal{M}_h} \{\tau_M^n / h_M^d\}^2 \right) (\Delta t)^4 \right. \\ & \left. + \frac{C}{\nu} \max_{1 \leq n \leq N} \max_{M \in \mathcal{M}_h} \{\tau_M^n |\tilde{\mathbf{u}}_M^n|^2\} (\Delta t)^2 + \frac{C}{\nu^3} e^{C_{G,h}(\mathbf{u})} (h^{2k_u} + h^{2k_p+2}) (\Delta t)^2 + \frac{C}{\nu^2} (\Delta t)^{2l+2} \right\}, \\ \Xi_{\xi,u,h} & := e^{C_{G,h}(\mathbf{u})} \int_0^T \left\{ \sum_{M \in \mathcal{M}_h} h_M^{2k_u} \left[(1 + \nu R e_M^2 + \tau_M^u |\mathbf{u}_M|^2 + d\gamma_M) \|\mathbf{u}(\tau)\|_{W^{k_u+1,2}(\omega_M)}^2 \right. \right. \\ & \left. \left. + \tau_M^u |\mathbf{u}_M|^2 h_M^{2(s_u-k_u)} \|\mathbf{u}(\tau)\|_{W^{s_u+1,2}(\omega_M)}^2 + \|\partial_t \mathbf{u}(\tau)\|_{W^{k_u,2}(\omega_M)}^2 \right] \right. \\ & \left. + \sum_{M \in \mathcal{M}_h} h_M^{2(k_p+1)} \min\left(\frac{d}{\nu}, \frac{1}{\gamma_M}\right) \|p(\tau)\|_{W^{k_p+1,2}(\omega_M)}^2 \right\} d\tau \end{aligned}$$

and $C_{G,h}(\mathbf{u}) \lesssim 1 + C\|\mathbf{u}\|_{L^\infty(0,T;W^{1,\infty}(\Omega))} + Ch^2\|\mathbf{u}\|_{L^\infty(0,T;W^{1,\infty}(\Omega))}^2 + C\|\mathbf{u}\|_{L^\infty(0,T;L^\infty(\Omega))}^2$, the fully discrete errors can be bounded as

$$\|\tilde{\zeta}_u\|_{l^\infty(0,T;L^2(\Omega))}^2 \leq \frac{C}{\nu^2} e^{C_{G,\text{lin}}} (\Delta t)^4 + C \Xi_{e,u,t} + C \Xi_{\xi,u,h} =: \Xi_{\zeta,u,L^2},$$

$$\begin{aligned} \|\tilde{\zeta}_u\|_{l^2(0,T;LPS)}^2 & \leq e^{C_{G,\text{lin}}} (\Delta t)^2 + C \Xi_{e,u,t} \\ & + C \left(1 + \frac{1}{\nu} \max_{1 \leq n \leq N} \max_{M \in \mathcal{M}_h} \{\tau_M^n |\tilde{\mathbf{u}}_M^n|^2\} \right) ((\Delta t)^{2l} + \Xi_{\xi,u,h}) =: \Xi_{\zeta,u,LPS}, \end{aligned}$$

$$\begin{aligned} \|\zeta_p\|_{l^2(0,T;L^2(\Omega))}^2 & \leq \left(\frac{C}{(\Delta t)^2} + C \right) \Xi_{\zeta,u,L^2} \\ & + C \left(\nu + \gamma + \max_{1 \leq n \leq N} \max_{M \in \mathcal{M}_h} \{\tau_M^n |\tilde{\mathbf{u}}_M^n|^2\} \right) \Xi_{\zeta,u,LPS} \end{aligned}$$

$$+ C \frac{\Xi_{\zeta_u, LPS}^2}{\Delta t \nu^2} + C \max_{1 \leq n \leq N} \max_{M \in \mathcal{M}_h} \{\tau_M^n |\tilde{\mathbf{u}}_M^n|^2 h_M^{2s_u}\}^2 \|\mathbf{u}\|_{l^\infty(0, T; W^{s_u+1, 2}(\Omega))}^2 + C(\Delta t)^2.$$

Proof. We meld Corollary 4.2.8 (for the spatial results) and Theorem 4.2.17 (for the temporal results). Further, we use that

$$s_u(\tilde{\mathbf{u}}_{ht}^n, \tilde{\zeta}_u^n, \tilde{\mathbf{u}}_{ht}^n, \tilde{\zeta}_u^n) \leq 2s_u(\tilde{\mathbf{u}}_{ht}^n, \tilde{\xi}_u^n, \tilde{\mathbf{u}}_{ht}^n, \tilde{\xi}_u^n) + 2s_u(\tilde{\mathbf{u}}_{ht}^n, \xi_{u,h}^n, \tilde{\mathbf{u}}_{ht}^n, \xi_{u,h}^n),$$

where we already have a bound for the first term and estimate the second one as

$$s_u(\tilde{\mathbf{u}}_{ht}^n, \xi_{u,h}^n, \tilde{\mathbf{u}}_{ht}^n, \xi_{u,h}^n) \leq \max_{M \in \mathcal{M}_h} \{\tau_M^n |\tilde{\mathbf{u}}_M^n|^2\} \|\xi_{u,h}^n\|_1^2 \leq \frac{\max_{M \in \mathcal{M}_h} \{\tau_M^n |\tilde{\mathbf{u}}_M^n|^2\}}{\nu} \|\xi_{u,h}^n\|_{LPS}^2.$$

In combination, we obtain the estimates for

$$\begin{aligned} \|\tilde{\zeta}_u\|_{l^\infty(0, T; L^2(\Omega))}^2 &\leq C \|\tilde{\xi}_u\|_{l^\infty(0, T; L^2(\Omega))}^2 + C \|\xi_{u,h}\|_{l^\infty(0, T; L^2(\Omega))}^2, \\ \|\tilde{\zeta}_u\|_{l^2(0, T; LPS)}^2 &\leq C \|\tilde{\xi}_u\|_{l^2(0, T; LPS)}^2 \\ &\quad + C \left(1 + \frac{1}{\nu} \max_{1 \leq n \leq N} \max_{M \in \mathcal{M}_h} \{\tau_M^n |\tilde{\mathbf{u}}_M^n|^2\}\right) \|\xi_{u,h}\|_{l^2(0, T; LPS)}^2. \end{aligned}$$

In order to derive an estimate for the pressure error in the $L^2(\Omega)$ -norm, we utilize the discrete inf-sup stability of the ansatz spaces, i.e.,

$$\exists \mathbf{w}_h \in \mathbf{V}_h: \|\nabla \mathbf{w}_h\|_0 \leq \|\zeta_p^n\|_0 / \beta_h, \quad (\nabla \cdot \mathbf{w}_h, \zeta_p^n) = \|\zeta_p^n\|_0^2. \quad (4.36)$$

Tested with \mathbf{w}_h , the advection-diffusion error equation for the fully discrete error reads:

$$\begin{aligned} &\left(\frac{3\tilde{\zeta}_u^n - 4\zeta_u^{n-1} + \zeta_u^{n-2}}{2\Delta t}, \mathbf{w}_h \right) + \nu (\nabla \tilde{\zeta}_u^n, \nabla \mathbf{w}_h) + \gamma (\nabla \cdot \tilde{\zeta}_u^n, \nabla \cdot \mathbf{w}_h) \\ &= -c_u(\mathbf{u}(t_n); \mathbf{u}(t_n), \mathbf{w}_h) + c_u(\tilde{\mathbf{u}}_{ht}^n; \tilde{\mathbf{u}}_{ht}^n, \mathbf{w}_h) + s_u(\tilde{\mathbf{u}}_{ht}^n, \tilde{\mathbf{u}}_{ht}^n, \tilde{\mathbf{u}}_{ht}^n, \mathbf{w}_h) \\ &\quad + (D_t \mathbf{u}(t_n) - \partial_t \mathbf{u}(t_n), \mathbf{w}_h) - (\nabla(p(t_n) - p_{ht}^{n-1}), \mathbf{w}_h), \end{aligned}$$

where $D_t \mathbf{u}(t_n) = (3\mathbf{u}(t_n) - 4\mathbf{u}(t_{n-1}) + \mathbf{u}(t_{n-2})) / (2\Delta t)$ and $\partial_t \mathbf{u}$ is the time derivative of \mathbf{u} . With $\tilde{\zeta}_u^n = \tilde{\xi}_u^n + \xi_{u,h}^n$, we obtain

$$\begin{aligned} \|\nabla \mathbf{w}_h\|_0 \|\zeta_p^{n-1}\|_0 &\leq \frac{1}{\beta_h} \|\zeta_p^{n-1}\|_0^2 = -(\nabla \zeta_p^{n-1}, \mathbf{w}_h) \\ &\leq \left\| \frac{3\tilde{\zeta}_u^n - 4\zeta_u^{n-1} + \zeta_u^{n-2}}{2\Delta t} \right\|_{-1} \|\nabla \mathbf{w}_h\|_0 + \nu \|\nabla \tilde{\zeta}_u^n\|_0 \|\nabla \mathbf{w}_h\|_0 + \gamma \|\nabla \cdot \tilde{\zeta}_u^n\|_0 \|\nabla \cdot \mathbf{w}_h\|_0 \\ &\quad + c_u(\mathbf{u}(t_n); \mathbf{u}(t_n), \mathbf{w}_h) - c_u(\tilde{\mathbf{u}}_{ht}^n; \tilde{\mathbf{u}}_{ht}^n, \mathbf{w}_h) + s_u(\tilde{\mathbf{u}}_{ht}^n, \tilde{\mathbf{u}}_{ht}^n, \tilde{\mathbf{u}}_{ht}^n, \mathbf{w}_h) \\ &\quad + \|D_t \mathbf{u}(t_n) - \partial_t \mathbf{u}(t_n)\|_{-1} \|\nabla \mathbf{w}_h\|_0 + \|p(t_n) - p(t_{n-1})\|_0 \|\nabla \cdot \mathbf{w}_h\|_0. \end{aligned}$$

The convective terms can be estimated according to Lemma A.3.7:

$$\begin{aligned}
c_u(\mathbf{u}(t_n); \mathbf{u}(t_n), \mathbf{w}_h) - c_u(\tilde{\mathbf{u}}_{ht}^n; \tilde{\mathbf{u}}_{ht}^n, \mathbf{w}_h) &= c_u(\tilde{\boldsymbol{\zeta}}_u^n; \mathbf{u}(t_n), \mathbf{w}_h) - c_u(\tilde{\mathbf{u}}_{ht}^n; \tilde{\boldsymbol{\zeta}}_u^n, \mathbf{w}_h) \\
&= c_u(\tilde{\boldsymbol{\zeta}}_u^n; \mathbf{u}(t_n), \mathbf{w}_h) - c_u(\mathbf{u}(t_n); \tilde{\boldsymbol{\zeta}}_u^n, \mathbf{w}_h) - c_u(\tilde{\boldsymbol{\zeta}}_u^n; \tilde{\boldsymbol{\zeta}}_u^n, \mathbf{w}_h) \\
&\leq C \|\tilde{\boldsymbol{\zeta}}_u^n\|_0 \|\mathbf{u}(t_n)\|_2 \|\mathbf{w}_h\|_1 + C \|\tilde{\boldsymbol{\zeta}}_u^n\|_1^2 \|\mathbf{w}_h\|_1.
\end{aligned}$$

For the LPS SU stabilization, we calculate

$$\begin{aligned}
s_u(\tilde{\mathbf{u}}_{ht}^n, \tilde{\mathbf{u}}_{ht}^n, \tilde{\mathbf{u}}_{ht}^n, \mathbf{w}_h) &= s_u(\tilde{\mathbf{u}}_{ht}^n, \mathbf{u}(t_n) - \tilde{\boldsymbol{\zeta}}_u^n, \tilde{\mathbf{u}}_{ht}^n, \mathbf{w}_h) \\
&\leq C \sum_{M \in \mathcal{M}_h} \tau_M^n |\tilde{\mathbf{u}}_M^n|^2 \|\kappa_M^u(\mathbf{u}(t_n))\|_{0,M} \|\mathbf{w}_h\|_{1,M} \\
&\quad + C \sum_{M \in \mathcal{M}_h} \tau_M^n \|\kappa_M^u((\tilde{\mathbf{u}}_M^n \cdot \nabla) \tilde{\boldsymbol{\zeta}}_u^n)\|_{0,M} |\tilde{\mathbf{u}}_M^n| \|\mathbf{w}_h\|_{1,M} \\
&\leq C \left(\max_{M \in \mathcal{M}_h} \{ \tau_M^n |\tilde{\mathbf{u}}_M^n|^2 \|\kappa_M^u(\mathbf{u}(t_n))\|_{0,M} \} \right. \\
&\quad \left. + \sum_{M \in \mathcal{M}_h} \tau_M^n |\tilde{\mathbf{u}}_M^n| \|\kappa_M^u((\tilde{\mathbf{u}}_M^n \cdot \nabla) \tilde{\boldsymbol{\zeta}}_u^n)\|_{0,M} \right) \|\nabla \mathbf{w}_h\|_0 \\
&\leq C \left(\max_{M \in \mathcal{M}_h} \{ \tau_M^n |\tilde{\mathbf{u}}_M^n|^2 h_M^{s_u} \|\mathbf{u}(t_n)\|_{W^{s_u+1,2}(\omega_M)} \} \right. \\
&\quad \left. + \sum_{M \in \mathcal{M}_h} \tau_M^n |\tilde{\mathbf{u}}_M^n| \|\kappa_M^u((\tilde{\mathbf{u}}_M^n \cdot \nabla) \tilde{\boldsymbol{\zeta}}_u^n)\|_{0,M} \right) \|\nabla \mathbf{w}_h\|_0
\end{aligned}$$

with $s_u \in \{0, \dots, k_u\}$ due to the approximation property of κ_M^u . Now, we take the estimates for $\|\tilde{\boldsymbol{\zeta}}_u\|_{l^\infty(0,T;L^2(\Omega))}$ and $\|\tilde{\boldsymbol{\zeta}}_u\|_{l^2(0,T;LPS)}$ as well as $\Delta t \sum_{n=1}^N \|p(t_n) - p(t_{n-1})\|_0^2 \leq C(\Delta t)^2$ into account. The latter holds because of $p \in W^{1,2}(0,T;L^2(\Omega))$ due to Assumption 4.2.4, Lemma 4.2.6 and Taylor expansion. It follows that:

$$\begin{aligned}
\Delta t \sum_{n=1}^N \|\zeta_p^{n-1}\|_0^2 &\leq C \left\{ \frac{1}{(\Delta t)^2} \|\tilde{\boldsymbol{\zeta}}_u\|_{l^\infty(0,T;L^2(\Omega))}^2 + \nu^2 \|\nabla \tilde{\boldsymbol{\zeta}}_u\|_{l^2(0,T;L^2(\Omega))}^2 \right. \\
&\quad + \gamma^2 \|\nabla \cdot \tilde{\boldsymbol{\zeta}}_u\|_{l^2(0,T;L^2(\Omega))}^2 + \|\tilde{\boldsymbol{\zeta}}_u\|_{l^\infty(0,T;L^2(\Omega))}^2 \|\mathbf{u}\|_{l^2(0,T;H^2(\Omega))}^2 \\
&\quad + \|\tilde{\boldsymbol{\zeta}}_u\|_{l^\infty(0,T;W^{1,2}(\Omega))}^2 \|\tilde{\boldsymbol{\zeta}}_u\|_{l^2(0,T;W^{1,2}(\Omega))}^2 \\
&\quad + \max_{1 \leq n \leq N} \max_{M \in \mathcal{M}_h} \{ \tau_M^n |\tilde{\mathbf{u}}_M^n|^2 h_M^{s_u} \}^2 \|\mathbf{u}\|_{l^\infty(0,T;W^{s_u+1,2}(\Omega))}^2 \\
&\quad \left. + \max_{1 \leq n \leq N} \max_{M \in \mathcal{M}_h} \{ \tau_M^n |\tilde{\mathbf{u}}_M^n|^2 \} \Delta t \sum_{n=1}^N \sum_{M \in \mathcal{M}_h} \tau_M^n \|\kappa_M^u((\tilde{\mathbf{u}}_M^n \cdot \nabla) \tilde{\boldsymbol{\zeta}}_u^n)\|_{0,M}^2 + (\Delta t)^2 \right\} \\
&\leq C \left(\frac{1}{(\Delta t)^2} + \|\mathbf{u}\|_{l^2(0,T;H^2(\Omega))}^2 \right) \Xi_{\zeta,u,L2} \\
&\quad + C \left(\nu + \gamma + \max_{1 \leq n \leq N} \max_{M \in \mathcal{M}_h} \{ \tau_M^n |\tilde{\mathbf{u}}_M^n|^2 \} \right) \Xi_{\zeta,u,LPS} + C \frac{\Xi_{\zeta,u,LPS}^2}{\Delta t \nu^2} \\
&\quad + C \max_{1 \leq n \leq N} \max_{M \in \mathcal{M}_h} \{ \tau_M^n |\tilde{\mathbf{u}}_M^n|^2 h_M^{s_u} \}^2 \|\mathbf{u}\|_{l^\infty(0,T;W^{s_u+1,2}(\Omega))}^2 + C(\Delta t)^2,
\end{aligned}$$

where we utilized

$$\begin{aligned} \|\tilde{\zeta}_u\|_{l^\infty(0,T;W^{1,2}(\Omega))}^2 \|\tilde{\zeta}_u\|_{l^2(0,T;W^{1,2}(\Omega))}^2 &\leq \frac{1}{\Delta t} \|\tilde{\zeta}_u\|_{l^2(0,T;W^{1,2}(\Omega))}^4 \\ &\leq \frac{\exp(C_{G,\text{lin}})}{\Delta t \nu^2} \|\tilde{\zeta}_u\|_{l^2(0,T;LPS)}^4 \leq \frac{C}{\Delta t \nu^2} \Xi_{\zeta,u,LPS}^2. \end{aligned}$$

With $\|\mathbf{u}\|_{l^\infty(0,T;H^2(\Omega))}^2 \leq \|\mathbf{u}\|_{L^\infty(0,T;H^2(\Omega))}^2 \leq C$ because of Assumption 4.2.4, the claim is established. \square

We derive a method of quasi-optimal order by bounding the right-hand side in Theorem 4.2.18 in terms of the fully discretized parameters.

Corollary 4.2.19 (Method of quasi-optimal order).

Let the conditions of Theorem 4.2.18 with $l = 1$ hold true. If the problem parameters satisfy

$$\begin{aligned} \gamma = \gamma_0, \quad \nu Re_M^2 \lesssim 1, \quad \tau_M^n \lesssim \min \left\{ \frac{(\Delta t)^2}{\nu^2 |\tilde{\mathbf{u}}_M^n|^2}, \frac{1}{|\tilde{\mathbf{u}}_M^n|^2 h_M^{2(s_u - k_u)}}, h_M^{d-2(s_u - k_u)} \right\}, \\ \Delta t \lesssim \min \{ h_M^{d/(2p)-2(s_u - k_u)}, \nu^3 \}, \quad h^{2k_u} + h^{2k_p+2} \lesssim e^{-C_{G,h}(\mathbf{u})} \nu \Delta t, \end{aligned}$$

the error due to spatial and temporal discretizations can be bounded by

$$\begin{aligned} \|\tilde{\zeta}_u\|_{l^\infty(0,T;L^2(\Omega))}^2 &\lesssim \frac{e^{C_{G,t}}}{\nu^3} (\Delta t)^4 + e^{C_{G,h}(\mathbf{u})} (h^{2k_u} + h^{2(k_p+1)}), \\ \|\tilde{\zeta}_u\|_{l^2(0,T;LPS)}^2 &\lesssim e^{C_{G,\text{lin}}} (\Delta t)^2 + e^{C_{G,h}(\mathbf{u})} (h^{2k_u} + h^{2(k_p+1)}), \\ \|\zeta_p\|_{l^2(0,T;L^2(\Omega))}^2 &\lesssim \frac{e^{C_{G,t}}}{\nu^3} (\Delta t)^2 + e^{C_{G,h}(\mathbf{u})} \frac{h^{2k_u} + h^{2(k_p+1)}}{(\Delta t)^2}. \end{aligned}$$

Proof. For $l = 1$ and the parameter choice stated in the corollary, we balance the following terms in Theorem 4.2.18

$$\begin{aligned} &\left(\frac{1}{\nu^3} + \frac{C}{h^d \nu^2} \max_{1 \leq n \leq N} \max_{M \in \mathcal{M}_h} \{\tau_M^n\} + \frac{C}{\nu^3 h^{2d}} \max_{1 \leq n \leq N} \max_{M \in \mathcal{M}_h} \{\tau_M^n\}^2 \right) (\Delta t)^4 \\ &+ \frac{C}{\nu} \max_{1 \leq n \leq N} \max_{M \in \mathcal{M}_h} \{\tau_M^n |\tilde{\mathbf{u}}_M^n|^2\} (\Delta t)^2 + \frac{C}{\nu^2} (\Delta t)^{2l+2} \lesssim \frac{1}{\nu^3} (\Delta t)^4. \end{aligned} \quad (4.37)$$

Theorem 4.2.18 provides an upper bound of the fully discrete error that still depends both on semi-discrete and on fully discrete stabilization parameters. In order to be able to compare and balance them, we bound the semi-discrete streamline velocity by the following argument. Choose the partitioning $\mathcal{N}_t := \{[(n-1)\Delta t, n\Delta t]\}_{n=1}^{N=T/\Delta t}$ and a piecewise linear

nodal basis ϕ_n . Define $\hat{\mathbf{u}}_{ht}(t)$ by the finite element approximation of $\tilde{\mathbf{u}}_{ht}$ and choose τ_M^u as the finite element approximation of τ_M^n :

$$\hat{\mathbf{u}}_{ht} := \sum_{n=1}^N \tilde{\mathbf{u}}_{ht}^n \phi_n, \quad \tau_M^u := \sum_{n=1}^N \tau_M^n \phi_n.$$

In particular, according to this construction, we can achieve $\hat{\mathbf{u}}_{ht} \in W^{2,2}(0, T; [L^2(\Omega)]^d)$, $\tau_M^u \in W^{2,2}(0, T; L^2(\Omega))$ and $\tau_M^u(t_n) = \tau_M^n$ for all $1 \leq n \leq N$. With the abbreviation $K_u := \|\mathbf{u}\|_{L^\infty(0, T; W^{k_u+1, 2}(\omega_M))}^2$ and $\hat{\mathbf{u}}_M(t) := \frac{1}{|M|} \int_M \hat{\mathbf{u}}_{ht}(\mathbf{x}) d\mathbf{x}$, it holds due to Lemma A.3.8 and Lemma 4.2.6 for all $M \in \mathcal{M}_h$

$$\begin{aligned} & \int_0^T \tau_M^u(t) |\mathbf{u}_M(t)|^2 \|\mathbf{u}(t)\|_{W^{k_u+1, 2}(\omega_M)}^2 dt \\ & \leq CK_u \int_0^T \tau_M^u(t) |\hat{\mathbf{u}}_M(t)|^2 dt + CK_u \int_0^T \tau_M^u(t) |\mathbf{u}_M(t) - \hat{\mathbf{u}}_M(t)|^2 dt \\ & \leq CK_u \|\sqrt{\tau_M^u} \hat{\mathbf{u}}_M\|_{L^2(0, T)}^2 + Ch_M^{-d} K_u \|\sqrt{\tau_M^u} (\mathbf{u}_h - \hat{\mathbf{u}}_{ht})\|_{L^2(0, T; L^2(M))}^2 \\ & \leq CK_u \|\sqrt{\tau_M^n} \hat{\mathbf{u}}_M\|_{l^2(0, T)}^2 + Ch_M^{-d} K_u \left(\|\sqrt{\tau_M^n} (\mathbf{u}_h - \tilde{\mathbf{u}}_{ht})\|_{l^2(0, T; L^2(M))}^2 + C(\Delta t)^{2p} \right) \\ & \leq CK_u \left(\max_{1 \leq n \leq N} \{\tau_M^n |\tilde{\mathbf{u}}_M^n|^2\} + \frac{\max_{1 \leq n \leq N} \{\tau_M^n\}}{h_M^d} \|\tilde{\boldsymbol{\xi}}_u\|_{l^2(0, T; L^2(M))}^2 + C \frac{(\Delta t)^{2p}}{h_M^d} \right). \end{aligned}$$

Now, we use the estimate due to Theorem 4.2.17 as

$$\|\tilde{\boldsymbol{\xi}}_u\|_{l^2(0, T; L^2(M))}^2 \leq \|\tilde{\boldsymbol{\xi}}_u\|_{l^\infty(0, T; L^2(\Omega))}^2 \leq \frac{C}{\nu^2} e^{C_{G, \text{lin}}(\Delta t)^4} + \Xi_{e, u, t},$$

together with the balance from (4.37). Hence, the theorem yields for the error in $L^2(\Omega)$:

$$\begin{aligned} & \|\tilde{\boldsymbol{\xi}}_u\|_{l^\infty(0, T; L^2(\Omega))}^2 \leq \frac{C}{\nu^2} e^{C_{G, \text{lin}}(\Delta t)^4} \\ & + e^{C_{G, t}} \left\{ \left(\frac{C}{\nu^3} + \frac{C}{\nu^2} \max_{1 \leq n \leq N} \max_{M \in \mathcal{M}_h} \{\tau_M^n / h_M^d\} + \frac{C}{\nu^3} \max_{1 \leq n \leq N} \max_{M \in \mathcal{M}_h} \{\tau_M^n / h_M^d\}^2 \right) (\Delta t)^4 \right. \\ & + \frac{C}{\nu} \max_{1 \leq n \leq N} \max_{M \in \mathcal{M}_h} \{\tau_M^n |\tilde{\mathbf{u}}_M^n|^2\} (\Delta t)^2 + \frac{C e^{C_{G, h}(\mathbf{u})}}{\nu^3} (h^{2k_u} + h^{2k_p+2}) (\Delta t)^2 + \frac{C}{\nu^2} (\Delta t)^{2l+2} \left. \right\} \\ & + C \int_0^T e^{C_{G, h}(\mathbf{u})(t-\tau)} \left\{ \sum_{M \in \mathcal{M}_h} h_M^{2k_u} \left[(1 + \nu R e_M^2 + \tau_M^u |\mathbf{u}_M|^2 + d\gamma_M) \|\mathbf{u}(\tau)\|_{W^{k_u+1, 2}(\omega_M)}^2 \right. \right. \\ & + \tau_M^u |\mathbf{u}_M|^2 h_M^{2(s_u - k_u)} \|\mathbf{u}(\tau)\|_{W^{s_u+1, 2}(\omega_M)}^2 + \|\partial_t \mathbf{u}(\tau)\|_{W^{k_u, 2}(\omega_M)}^2 \left. \right] \\ & + \sum_{M \in \mathcal{M}_h} h_M^{2(k_p+1)} \min\left(\frac{d}{\nu}, \frac{1}{\gamma_M}\right) \|p(\tau)\|_{W^{k_p+1, 2}(\omega_M)}^2 \left. \right\} d\tau \\ & \lesssim \left(1 + \max_{1 \leq n \leq N} \max_{M \in \mathcal{M}_h} \{\tau_M^n / h_M^d\} (1 + h_M^{2(s_u - k_u)}) \right) \left[\frac{e^{C_{G, t}}}{\nu^3} (\Delta t)^4 \right. \end{aligned}$$

$$\begin{aligned}
& + e^{C_{G,h}(\mathbf{u})} \frac{(\Delta t)^2}{\nu^3} (h^{2k_u} + h^{2k_p+2}) \Big] + h^{2k_p+2} e^{C_{G,h}(\mathbf{u})} \min\left(\frac{d}{\nu}, \frac{1}{\gamma}\right) \\
& + h^{2k_u} e^{C_{G,h}(\mathbf{u})} \left[1 + \nu R e_M^2 + d\gamma + (1 + h^{2(s_u-k_u)}) \max_{1 \leq n \leq N} \max_{M \in \mathcal{M}_h} \left\{ \tau_M^n |\tilde{\mathbf{u}}_M|^2 + C \frac{(\Delta t)^{2p}}{h_M^d} \right\} \right] \\
& \leq \frac{e^{C_{G,t}}}{\nu^3} (\Delta t)^4 + (h^{2k_u} + h^{2k_p+2}) e^{C_{G,h}(\mathbf{u})},
\end{aligned}$$

where $\Delta t \lesssim \min\{h_M^{d/(2p)-2(s_u-k_u)}, \nu^3\}$ and the parameter choices

$$\gamma = \gamma_0, \quad \nu R e_M^2 \lesssim 1, \quad \tau_M^n \lesssim \min \left\{ \frac{(\Delta t)^2}{\nu^2 |\tilde{\mathbf{u}}_M^n|^2}, \frac{1}{|\tilde{\mathbf{u}}_M^n|^2 h_M^{2(s_u-k_u)}}, h_M^{d-2(s_u-k_u)} \right\}$$

were utilized. The suggested parameter design arises because Theorem 4.2.18 is only applicable if $(h^{2k_u} + h^{2k_p+2}) \lesssim e^{-C_{G,h}(\mathbf{u})} \nu \Delta t$ and $\Delta t \lesssim \nu^3$. The estimates for $\|\tilde{\zeta}_u\|_{l^2(0,T;LPS)}^2$ and $\|\zeta_p\|_{l^2(0,T;L^2(\Omega))}^2$ are shown similarly. \square

Remark 4.2.20. The error estimates in Theorem 4.2.18 suggest a parameter choice as

$$\begin{aligned}
\gamma = \gamma_0, \quad \nu R e_M^2 \lesssim 1, \quad \tau_M^n \lesssim \min \left\{ \frac{(\Delta t)^2}{\nu^2 |\tilde{\mathbf{u}}_M^n|^2}, \frac{1}{|\tilde{\mathbf{u}}_M^n|^2 h_M^{2(s_u-k_u)}}, h_M^{d-2(s_u-k_u)} \right\}, \\
\Delta t \lesssim \min\{h^{d/(2p)-2(s_u-k_u)}, \nu^3\}, \quad h^{2k_u} + h^{2k_p+2} \lesssim e^{-C_{G,h}(\mathbf{u})} \nu \Delta t,
\end{aligned}$$

see Corollary 4.2.19. For the above analysis, discrete inf-sup stability of the ansatz spaces is required. We assume Taylor-Hood elements satisfying $k_u = k_p + 1$ and a coarse space with $s_u = k_u$.

Now, let us discuss a feasible choice of $p \in \{1, 2\}$. Consider $p = 1$ first. For $d \in \{2, 3\}$, the condition $\Delta t \lesssim h^{d/(2p)}$ is fulfilled if we choose $\Delta t \sim h^{3/2}$ (for $h < 1$). Note that the requirement $h^{2k_u} \lesssim e^{-C_{G,h}(\mathbf{u})} \nu \Delta t$ has to be fulfilled simultaneously by a small enough grid size (or sufficiently high polynomial order k_u). This leads to the requirement

$$h^{2k_u-3/2} \lesssim e^{-C_{G,h}(\mathbf{u})} \nu;$$

in particular, higher order velocity spaces $k_u > 1$ would be required. In case of $p = 2$, the choice $\Delta t \sim h^{3/4}$ (for $h < 1$) would be sufficient. This would relax the condition on the mesh size considerably in the sense that first order ansatz spaces are not excluded:

$$h^{2k_u-3/4} \lesssim e^{-C_{G,h}(\mathbf{u})} \nu.$$

We point out that this challenge arises since it is desired to express the right-hand side in Theorem 4.2.18 in terms of fully discretized stabilization parameters (which are the ones that are actually implemented in our algorithm).

With the mentioned choices and $p = 2$, we obtain a quasi-optimal estimate for Taylor-Hood elements as

$$\begin{aligned}\|\tilde{\zeta}_u\|_{l^\infty(0,T;L^2(\Omega))}^2 &\lesssim \frac{e^{C_{G,t}}}{\nu^3}(\Delta t)^4 + e^{C_{G,h}(\mathbf{u})}h^{2k_u}, \\ \|\tilde{\zeta}_u\|_{l^2(0,T;LPS)}^2 &\lesssim e^{C_{G,\text{lin}}}(\Delta t)^2 + e^{C_{G,h}(\mathbf{u})}h^{2k_u}, \\ \|\zeta_p\|_{l^2(0,T;L^2(\Omega))}^2 &\lesssim \frac{e^{C_{G,t}}}{\nu^3}(\Delta t)^2 + e^{C_{G,h}(\mathbf{u})}h^{2k_u-3/2}.\end{aligned}$$

Let us remark that the suboptimal spatial error in the L^2 -norm leads to a suboptimal pressure estimate as well. One has to put more effort into this (e.g. with the Aubin-Nitsche Lemma considering the dual problem or using weaker norms) to obtain the desired order.

Remark 4.2.21. A similar convergence analysis can be performed for the coupled Oberbeck-Boussinesq model. The first step is to add the error equation for the temperature step and the error advection-diffusion equation where the reaction term $\beta\mathbf{g}\theta$ is included. The reaction term can be handled as in Theorem 4.1.2. The remaining Navier-Stokes terms stemming from the advection-diffusion step are treated as in the above estimates. The terms from the temperature step can be dealt with in a similar way; the analysis is even easier because the Fourier equation does not incorporate a pressure term or different time-discrete temperature approximations. Note that α plays a similar role as ν for the temperature.

4.3. Critical Examination of the Required Assumptions

One objective of convergence analysis is to have as few restrictions and assumptions as possible. If we recall Assumptions 4.2.1, 4.2.2, 4.2.3 and 4.2.4 or the bounds on the time step size as ν^3 , this desire is not supplied. In this section, we have a closer look at the requirements of our analysis and demonstrate where they are originated.

For the semi-discrete error $\mathbf{u} - \mathbf{u}_h$, we need a continuous solution satisfying

$$\begin{aligned}\mathbf{u} &\in L^\infty(0, T; [W^{1,\infty}(\Omega)]^d) \cap L^2(0, T; [W^{k_u+1,2}(\Omega)]^d), \\ \partial_t \mathbf{u} &\in L^2(0, T; [W^{k_u,2}(\Omega)]^d), \quad p \in L^2(0, T; W^{k_p+1,2}(\Omega) \cap C(\Omega))\end{aligned}$$

according to Assumption 4.2.1. This is not too restrictive, it is comparable with the requirements in [BF07], for instance. In order to utilize the time-continuous $L^2(0, T; LPS)$ -norm as an upper bound of the discrete one, we need to assume for some $l \in \{1, 2\}$

$$\mathbf{u} \in W^{l,2}(0, T; LPS), \quad \mathbf{u}_h \in W^{l,2}(0, T; LPS).$$

As our analysis suggests, $l = 1$ suffices (this can be understood by looking at the nonlinear temporal error).

The auxiliary semi-discrete velocity \mathbf{u}_h and pressure p_h play the role of (time-)continuous quantities in the estimates for the temporal discretization (Section 4.2.2). Hence, Assumption 4.2.2 demands

$$\begin{aligned} \|R^n - R^{n-1}\|_0^2 + \|\nabla(p_h(t_n) - 2p_h(t_{n-1}) + p_h(t_{n-2}))\|_0^2 &\leq C(\Delta t)^4, \\ \Delta t \sum_{n=1}^N \|R^n\|_{-1}^2 &\leq C(\Delta t)^4, \\ \|\nabla(p_h(t_n) - p_h(t_{n-1}))\|_0 &\leq C\Delta t \end{aligned}$$

with $R^n = D_t \mathbf{u}_h(t_n) - \partial_t \mathbf{u}_h(t_n)$. This is needed for the proof of the linear part of the error introduced by temporal discretizations. As argued in [She96] (see also [She92]), these conditions can be derived from certain regularity assumptions on \mathbf{u}_h and p_h that can be shown to hold for the continuous solutions \mathbf{u} , p of the Navier-Stokes equations if the data are smooth enough (cf. [HR82]). Unfortunately, Assumption 4.2.2 is not reducible to the continuous quantities because the semi-discrete analysis does not yield estimates for $\nabla p - \nabla p_h$ or $\partial_t \mathbf{u} - \partial_t \mathbf{u}_h$.

For the nonlinear (temporal) error, we combine all these conditions in Assumption 4.2.3 and additionally that $\|\mathbf{u}\|_{L^\infty(0,T;W^{2,2}(\Omega))} \leq C$ with C independent of ν . The striking condition we have for Lemma 4.2.16 reads

$$\begin{aligned} K_{t,\text{nl}} = C\Delta t \|\mathbf{u}_h\|_{l^\infty(0,T;W^{1,2}(\Omega))}^2 &\left(\frac{\|\mathbf{u}_h\|_{l^\infty(0,T;W^{1,2}(\Omega))}^2}{\nu^3} + \max_{1 \leq n \leq N} \max_{M \in \mathcal{M}_h} \{\tau_M^n / h_M^d\} \right. \\ &\left. + \frac{\|\mathbf{u}_h\|_{l^\infty(0,T;L^2(\Omega))}^2}{\nu} \max_{1 \leq n \leq N} \max_{M \in \mathcal{M}_h} \{\tau_M^n / h_M^d\}^2 \right) < 1 \end{aligned}$$

and is due to the estimates for the convective and stabilization terms. The most restrictive term $\Delta t < C\nu^3$ gives rise to an upper bound for the error growing as

$$\exp\left(\frac{T}{1 - \Delta t / \nu^3}\right).$$

Even if the LPS SU stabilization was omitted, the requirement

$$C\Delta t \frac{\|\mathbf{u}_h\|_{l^\infty(0,T;W^{1,2}(\Omega))}^4}{\nu^3} < 1$$

arises due to the convective term. This bound is crucial for the application of the discrete Gronwall Lemma A.3.6. The critical step is to bound

$$\begin{aligned} c_u(\tilde{\mathbf{e}}_u^n; \mathbf{u}_h(t_n), \tilde{\mathbf{e}}_u^n) &\leq C \|\tilde{\mathbf{e}}_u^n\|_0^{1/2} \|\mathbf{u}_h(t_n)\|_1 \|\tilde{\mathbf{e}}_u^n\|_1^{3/2} \\ &\leq \frac{\nu}{32} \|\nabla \tilde{\mathbf{e}}_u^n\|_0^2 + \frac{C}{\nu^3} \|\mathbf{u}_h(t_n)\|_1^4 \|\tilde{\mathbf{e}}_u^n\|_0^2 \end{aligned} \quad (4.38)$$

in (4.34) in the proof of the nonlinear error $\tilde{\mathbf{e}}_u^n$. Here, the problem is that we do not assume $\mathbf{u}_h \in L^\infty(0, T; [W^{2,2}(\Omega)]^d)$ a priori. We put effort already in Lemma 4.2.15 to prove that $\mathbf{u}_h \in L^\infty(0, T; [W^{1,2}(\Omega)]^d)$. However, we emphasize that this critical estimate containing ν^3 could be avoided if we assumed $\mathbf{u}_h \in L^\infty(0, T; [W^{2,2}(\Omega)]^d)$.

A related problem arises for the term

$$\begin{aligned} &c_u(\mathbf{u}_h(t_n); \tilde{\boldsymbol{\eta}}_u^n, \tilde{\mathbf{e}}_u^n) + c_u(\tilde{\boldsymbol{\eta}}_u^n; \mathbf{u}_h(t_n), \tilde{\mathbf{e}}_u^n) \\ &= c_u(\mathbf{u}(t_n); \tilde{\boldsymbol{\eta}}_u^n, \tilde{\mathbf{e}}_u^n) - c_u(\mathbf{u}(t_n) - \mathbf{u}_h(t_n); \tilde{\boldsymbol{\eta}}_u^n, \tilde{\mathbf{e}}_u^n) \\ &\quad + c_u(\tilde{\boldsymbol{\eta}}_u^n; \mathbf{u}(t_n), \tilde{\mathbf{e}}_u^n) - c_u(\tilde{\boldsymbol{\eta}}_u^n; \mathbf{u}(t_n) - \mathbf{u}_h(t_n), \tilde{\mathbf{e}}_u^n) \\ &\leq C \|\mathbf{u}(t_n)\|_2 \|\tilde{\boldsymbol{\eta}}_u^n\|_0 \|\tilde{\mathbf{e}}_u^n\|_1 + C \|\mathbf{u}(t_n) - \mathbf{u}_h(t_n)\|_1 \|\tilde{\boldsymbol{\eta}}_u^n\|_1 \|\tilde{\mathbf{e}}_u^n\|_1 \\ &\leq \frac{\nu}{32} \|\nabla \tilde{\mathbf{e}}_u^n\|_0^2 + \frac{C \|\mathbf{u}(t_n)\|_2^2}{\nu} \|\tilde{\boldsymbol{\eta}}_u^n\|_0^2 + \frac{C}{\nu} \|\tilde{\boldsymbol{\eta}}_u^n\|_1^2 \|\mathbf{u}(t_n) - \mathbf{u}_h(t_n)\|_1^2. \end{aligned}$$

Although we do not have $\mathbf{u}_h \in L^\infty(0, T; [W^{2,2}(\Omega)]^d)$, we need to estimate the linear error $\tilde{\boldsymbol{\eta}}_u^n$ in the L^2 -norm in order to reach the full order of temporal convergence as $(\Delta t)^2$. So we need to go back to the continuous solution \mathbf{u} that is assumed to be in $L^\infty(0, T; [W^{2,2}(\Omega)]^d)$ (Assumption 4.2.3). This is still quite restrictive. Note that the term $\|\mathbf{u}(t_n) - \mathbf{u}_h(t_n)\|_1^2$ is handled via the semi-discrete results, see Corollary 4.2.8: Provided $\mathbf{u}_h \in W^{l,2}(0, T; LPS)$, it holds

$$\begin{aligned} \|\mathbf{u} - \mathbf{u}_h\|_{l^2(0, T; W^{1,2}(\Omega))}^2 &\leq C \|\mathbf{u}(t_n) - \mathbf{u}_h(t_n)\|_{L^2(0, T; W^{1,2}(\Omega))}^2 + C(\Delta t)^{2l} \\ &\leq \frac{1}{\nu} \|\mathbf{u}(t_n) - \mathbf{u}_h(t_n)\|_{L^2(0, T; LPS)}^2 + C(\Delta t)^{2l} \leq \frac{C}{\nu} e^{C_{G,h}(\mathbf{u})} (h^{2k_u} + h^{2k_p+2}) + C(\Delta t)^{2l}. \end{aligned}$$

The assumption with $l = 1$ is sufficient to obtain convergence of the fully discrete L^2 -error as $(\Delta t)^2$. We remark that this technique - introduction of $\mathbf{u}(t_n)$ - does not help for the critical term (4.38):

$$\begin{aligned} c_u(\tilde{\mathbf{e}}_u^n; \mathbf{u}_h(t_n), \tilde{\mathbf{e}}_u^n) &= c_u(\tilde{\mathbf{e}}_u^n; \mathbf{u}(t_n), \tilde{\mathbf{e}}_u^n) + c_u(\tilde{\mathbf{e}}_u^n; \mathbf{u}_h(t_n) - \mathbf{u}(t_n), \tilde{\mathbf{e}}_u^n) \\ &\leq \|\tilde{\mathbf{e}}_u^n\|_0 \|\mathbf{u}(t_n)\|_2 \|\tilde{\mathbf{e}}_u^n\|_1 + C \|\tilde{\mathbf{e}}_u^n\|_0^{1/2} \|\mathbf{u}_h(t_n) - \mathbf{u}(t_n)\|_1 \|\tilde{\mathbf{e}}_u^n\|_1^{3/2} \\ &\leq \frac{\nu}{32} \|\nabla \tilde{\mathbf{e}}_u^n\|_0^2 + C \frac{\|\mathbf{u}(t_n)\|_2^2}{\nu} \|\tilde{\mathbf{e}}_u^n\|_0^2 + \frac{C}{\nu^3} \|\mathbf{u}_h(t_n) - \mathbf{u}(t_n)\|_1^4 \|\tilde{\mathbf{e}}_u^n\|_0^2 \end{aligned}$$

$$\leq \frac{\nu}{32} \|\nabla \tilde{\mathbf{e}}_u^n\|_0^2 + C \left(\frac{\|\mathbf{u}(t_n)\|_2^2}{\nu} + e^{2C_{G,h}(\mathbf{u})} \frac{h^{4k_u} + h^{4k_p+4}}{\nu^5(\Delta t)^2} + C(\Delta t)^{4l-2} \right) \|\tilde{\mathbf{e}}_u^n\|_0^2, \quad (4.39)$$

where we inserted the estimate

$$\begin{aligned} \|\mathbf{u} - \mathbf{u}_h\|_{l^\infty(0,T;W^{1,2}(\Omega))}^2 &\leq \frac{C}{\Delta t} \|\mathbf{u} - \mathbf{u}_h\|_{l^2(0,T;W^{1,2}(\Omega))}^2 \\ &\leq \frac{C}{\Delta t} \left(\|\mathbf{u} - \mathbf{u}_h\|_{L^2(0,T;W^{1,2}(\Omega))}^2 + (\Delta t)^{2l} \right) \leq C e^{C_{G,h}(\mathbf{u})} \frac{h^{2k_u} + h^{2k_p+2}}{\nu \Delta t} + C(\Delta t)^{2l-1}. \end{aligned}$$

With the requirement $h^{2k_u} + h^{2k_p+2} \lesssim e^{-C_{G,h}(\mathbf{u})} \nu \Delta t$ and (4.39), we obtain a comparable condition $\Delta t \lesssim \nu^3$.

For the nonlinear estimate in Lemma 4.2.16, we suppose that the LPS SU parameter τ_M^n must not depend nonlinearly on the arguments of s_u . This contradicts the findings from Chapter 3, where we suggest a choice as $h_M/|\tilde{\mathbf{u}}_M|$. The linearity of s_u in each argument is important to combine the terms

$$s_u(\mathbf{u}_h(t_n), \mathbf{u}_h(t_n), \mathbf{u}_h(t_n), \tilde{\mathbf{e}}_u^n) - s_u(\tilde{\mathbf{u}}_{ht}^n, \tilde{\mathbf{u}}_{ht}^n, \tilde{\mathbf{u}}_{ht}^n, \tilde{\mathbf{e}}_u^n).$$

The critical point is that the respective first arguments in these two terms differ. Again, we observe that this is a problem due to the (auxiliary) introduction of \mathbf{u}_h .

In addition, we need

$$\mathbf{u} \in L^\infty(0, T; [W^{k_u+1,2}(\Omega)]^d), \quad p \in W^{1,2}(0, T; L^2(\Omega)),$$

see Assumption 4.2.4, to establish Theorem 4.2.18. Compared with the previously discussed conditions, this one is not critical.

Another challenge arises if we want to balance the error bounds in Theorem 4.2.18 in order to obtain a method of desired order; see Corollary 4.2.19. Theorem 4.2.18 provides an upper bound that still depends both on semi-discrete (i.e., time-continuous) and on fully discrete stabilization parameters. We desire to express the right-hand side only by fully discretized parameters as these are the quantities used in a numerical procedure. In order to bound the semi-discrete streamline velocity by the fully discrete one, we need the additional condition:

$$\mathbf{u}_h \in W^{p,2}(0, T; [L^2(\Omega)]^d), \quad p \in \{1, 2\}.$$

Moreover, the restriction

$$\Delta t \lesssim h^{d/(2p)-2(s_u-k_u)}$$

arises from this. The parameter choice according to Corollary 4.2.19 reads

$$\gamma = \gamma_0, \quad \nu Re_M^2 \lesssim 1, \quad \tau_M^n \lesssim \min \left\{ \frac{(\Delta t)^2}{\nu^2 |\tilde{\mathbf{u}}_M^n|^2}, \frac{1}{|\tilde{\mathbf{u}}_M^n|^2 h^{2(s_u - k_u)}}, h^d \right\},$$

$$\Delta t \lesssim \min \{ h^{d/(2p) - 2(s_u - k_u)}, \nu^3 \}, \quad h^{2k_u} + h^{2k_p + 2} \lesssim e^{-C_{G,h}(\mathbf{u})} \nu \Delta t.$$

If $p = 1$ holds, this leads to a high polynomial order $k_u > 1$ and small grid size; for $p = 2$ the restriction on the polynomial order can be diminished (see Remark 4.2.20). This issue could be avoided by omitting the LPS SU stabilization or by leaving out the introduction of the semi-discrete solution.

Note that in [AD15], we additionally pursue a second ansatz to discretize in time first and afterwards in space. We point out that this leads to less restrictive parameter bounds as $\Delta t \lesssim \nu^{3/2}$ and $\tau_M^n \lesssim |\mathbf{u}_M|^{-2}$ (if $s_u = k_u$). This strategy also suffers from the introduction of a semi-discrete velocity (discrete in time, continuous in space): One cannot show the desired order of convergence with respect to spatial discretization, unless certain regularity properties for the semi-discrete quantity are assumed. Anyway, we infer that the parameter choice from Corollary 4.2.19 might be too restrictive. So we do not focus on this during our numerical simulations.

In conclusion, it seems favorable for a fully discrete analysis, to omit the intermediate step via $\mathbf{u} - \tilde{\mathbf{u}}_{ht} = (\mathbf{u} - \mathbf{u}_h) + (\mathbf{u}_h - \tilde{\mathbf{u}}_{ht})$ and estimate the complete difference immediately. Then, regularity assumptions for \mathbf{u}_h are no longer necessary. Moreover, we conjecture that the challenges due to the LPS SU stabilization can be reduced significantly. Regularity of \mathbf{u} alone would lead to a diminished constraint on Δt . One would desire to estimate the convective terms more carefully. Note that an additional difficulty arises compared with usual procedures: $\tilde{\mathbf{u}}_{ht}^n$ is not weakly solenoidal in this segregation algorithm.

5. Numerical Examples

Stabilization techniques are designed to improve the accuracy of a numerical method. We discuss if grad-div and local projection stabilization in streamline direction serve this purpose in the sense that they damp unphysical oscillations and act as a turbulence model. Because we restrict ourselves to the consideration of inf-sup stable elements and continuous discrete pressure spaces in this chapter, no pressure stabilization is needed. We address the question of a suitable parameter design. It is desired to find a parameter choice that performs well for a large class of numerical test cases. Therefore, we consider a variety of different isothermal and temperature driven flow examples in the following.

First, we validate the theoretical convergence results with respect to the mesh width h and the time step size Δt obtained from the previous chapters.

In Sections 5.1 and 5.2, we consider isothermal flow. The influence of grad-div stabilization on the spatial errors for different Reynolds numbers is studied in both sections. The additional effect of LPS SU stabilization is examined in Section 5.2. Enriched elements are used as well. Section 5.3 is dedicated to spatial and temporal convergence for a non-isothermal example in dependence on α and β . The errors for various stabilization parameters in combination with different choices of finite elements for the temperature are presented.

The remaining examples are dedicated to more realistic flow. In Sections 5.4 and 5.5, the performance of grad-div and LPS SU stabilization is considered for laminar isothermal and non-isothermal flow. Different stabilization parameters (in combination with different coarse spaces) are compared.

Transient flow examples are regarded in Sections 5.6 and 5.7. Section 5.6 contains a turbulent isothermal test case. The energy spectrum of this isotropic flow gives insight whether grad-div stabilization alone is sufficient as an implicit turbulence model or whether additional LPS SU stabilization is needed in order to prevent an unphysical energy increase. It is studied theoretically and numerically how the LPS SU parameter locally depends on \mathbf{u}_h and the mesh width h . These findings are tested in Section 5.7 for non-isothermal flow with Rayleigh numbers $10^5 \leq Ra \leq 10^9$. For high Rayleigh numbers, where the flow becomes transient, grad-div and LPS SU are considered as well as different finite elements and grids. Based on the Nusselt number, we discuss how these aspects affect the quality of the numerical solution.

For the isothermal examples, we seek for solutions of the Navier-Stokes equations

$$\begin{aligned} \partial_t \mathbf{u} - \nu \Delta \mathbf{u} + (\mathbf{u} \cdot \nabla) \mathbf{u} + \nabla p &= \mathbf{f}_u \quad \text{in } (0, T) \times \Omega, \\ \nabla \cdot \mathbf{u} &= 0 \quad \text{in } (0, T) \times \Omega, \end{aligned} \tag{5.1}$$

whereas for the non-isothermal ones, we consider the Oberbeck-Boussinesq model (2.7). The discrete solutions are calculated using stabilized finite element methods with inf-sup stable velocity and pressure spaces. For our numerical simulations, we take advantage of the C++-FEM package `deal.II`, see [BHK07, BHH⁺15], which provides important tools for solving differential equations using finite elements: These include tools for defining domains and grid generation, matrix assembling and handling of degrees of freedom. The time-discretization used is the rotational pressure-correction projection method introduced in Section 2.3.

For the convergence studies, we denote the velocity error $\|\mathbf{u}(T) - \tilde{\mathbf{u}}_{ht}^N\|_0$ in the L^2 -norm at the end of the considered time interval $T = N\Delta t$ with $L^2(u)$. $H^1(u)$ describes the error in the semi-norm $\|\nabla(\mathbf{u}(T) - \tilde{\mathbf{u}}_{ht}^N)\|_0$ and $L^2(\operatorname{div} u)$ stands for $\|\nabla \cdot \tilde{\mathbf{u}}_{ht}^N\|_0$. The notation for pressure and temperature is analogous.

Throughout the numerical experiments, the one-level approach as described in Section 2.2.3 is used when LPS SU stabilization applied, i.e., $\mathcal{M}_h = \mathcal{T}_h$ and $\mathcal{L}_h = \mathcal{T}_h$. Furthermore, a continuous pressure ansatz space is used; therefore, we set $i_h \equiv 0$. For convenience, we write $\mathbf{u}_h, p_h, \theta_h$ in this chapter instead of the fully discrete $\tilde{\mathbf{u}}_{ht}, p_{ht}, \theta_{ht}$.

5.1. Isothermal Convergence Results: 3D No-Flow Problem

This example serves to examine the effect of grad-div stabilization in case of different viscosities ν . We published the results of this section in [ADL15].

5.1.1. Features of the Test Case

We consider the No-Flow test problem in three dimensions with exact stationary solution

$$\mathbf{u}(\mathbf{x}) \equiv \mathbf{0}, \quad p(\mathbf{x}) = x^3 + y^2 + z^2 + x - 1 \quad \text{in } \Omega = (0, 1)^3$$

for $\mathbf{x} = (x, y, z)^T$ and forcing term $\mathbf{f}_u(\mathbf{x}) = (3x^2 + 1, 3y^2, 3z^2)^T$. Note that \mathbf{f}_u is a gradient field. The used grids are randomly distorted by 1% as shown in Figure B.1 in the appendix. The grid size h is determined as an average cell diameter.

As discussed in [Lin14], this test is relevant for the numerical simulation of coupled flow problems, where forcing terms with large gradient parts can cause poor mass conservation for vanishing ν .

5.1.2. Numerical Experiments

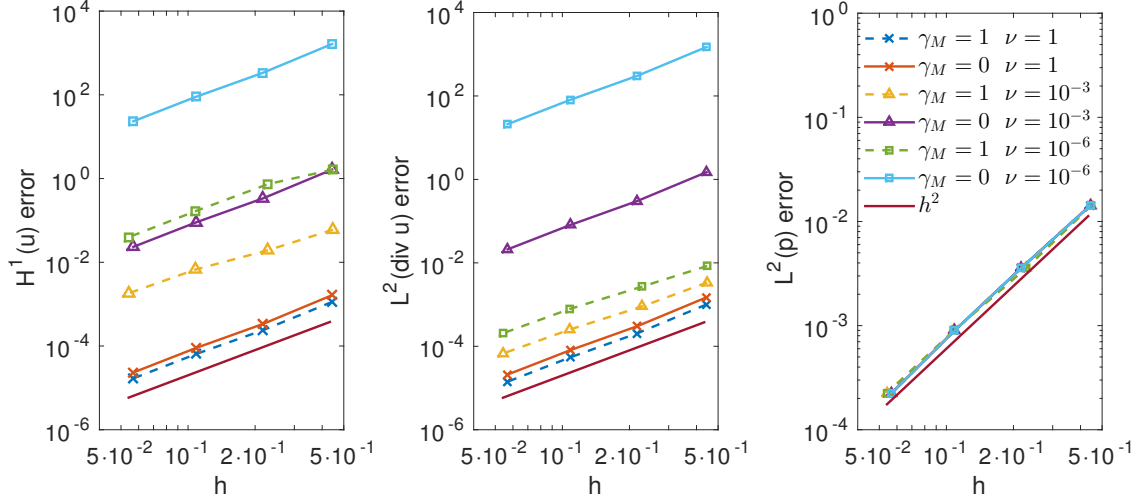


Figure 5.1.: No-Flow test for $\mathbb{Q}_2 \wedge \mathbb{Q}_1$ elements for \mathbf{u} and p and $\nu \in \{1, 10^{-3}, 10^{-6}\}$ with and without grad-div stabilization: H^1 -velocity error (left), L^2 -divergence error (middle), L^2 -pressure error (right).

In Figure 5.1, we study spatial convergence of different errors in order to validate the findings of Chapter 3. The errors for all $\nu \in \{1, 10^{-3}, 10^{-6}\}$ show the expected rates, even in the unstabilized case: The H^1 -velocity, L^2 -pressure and L^2 -divergence errors behave like

$$\|\nabla(\mathbf{u} - \mathbf{u}_h)\|_0 \sim h^2, \quad \|p - p_h\|_0 \sim h^2, \quad \|\nabla \cdot \mathbf{u}_h\|_0 \sim h^2.$$

For different ν , the velocity errors differ by orders of magnitude. Without grad-div stabilization the error in the H^1 -semi-norm is proportional to ν^{-1} . By using $\gamma_M = 1$, this behavior can be improved such that the error scales like $\nu^{-1/2}$, see Figure 5.1. This result is conforming with the analytical result as the squared H^1 -semi-norm is multiplied by ν in the definition of $\|\cdot\|_{LPS}$. The pressure errors neither depend on ν nor on the use of stabilization.

5.2. Isothermal Convergence Results: 2D Couzy Problem

The Couzy problem was proposed by Couzy [Cou95] and involves an analytical solution of the Navier-Stokes equations. Hence, it is suited to study convergence of the numerical (stabilized) approximations to this solution. We are interested in finding the optimal grad-div parameter for different Reynolds numbers Re and in the influence of LPS SU stabilization. Some of the following results were presented in our paper [DAL15].

5.2.1. Features of the Test Case

Consider a test problem in $\Omega = (0, 1)^2$. It is constructed such that

$$\begin{aligned} \mathbf{u}(\mathbf{x}) &= \sin(\pi t) \left(-\cos\left(\frac{\pi}{2}x\right) \sin\left(\frac{\pi}{2}y\right), \sin\left(\frac{\pi}{2}x\right) \cos\left(\frac{\pi}{2}y\right) \right)^T, \\ p(\mathbf{x}) &= -\pi \sin\left(\frac{\pi}{2}x\right) \sin\left(\frac{\pi}{2}y\right) \sin(\pi t) \end{aligned}$$

is a solution of the Navier-Stokes problem (5.1). The forcing term \mathbf{f}_u , the initial condition and the Dirichlet boundary data are deduced from the exact solution.

We consider different Reynolds numbers $Re \in \{1, 10^3, 10^6, 10^9\}$. $(\mathbb{Q}_2/\mathbb{Q}_1) \wedge \mathbb{Q}_1$ or enriched $(\mathbb{Q}_2^+/\mathbb{Q}_1) \wedge \mathbb{Q}_1$ elements for the velocity fine and coarse space and the pressure are used. Isotropic grids with mesh size h are applied. Since we are interested in the spatial approximation properties of the proposed methods here, we evaluate the error after 1000 time steps of size $\Delta t = 10^{-5}$.

5.2.2. Numerical Experiments

In Figure 5.2, we show the dependence on a constant grad-div parameter γ_M for $Re = 10^3$ and $\mathbb{Q}_2 \wedge \mathbb{Q}_1$ elements for velocity and pressure. The convergence diagrams for the velocity and divergence errors show a significant influence of γ_M , whereas the pressure error is not affected (see appendix, Figure B.2). A deviation from the optimal convergence rates of the velocity or divergence errors is observed if γ_M is too large or too small (or zero).

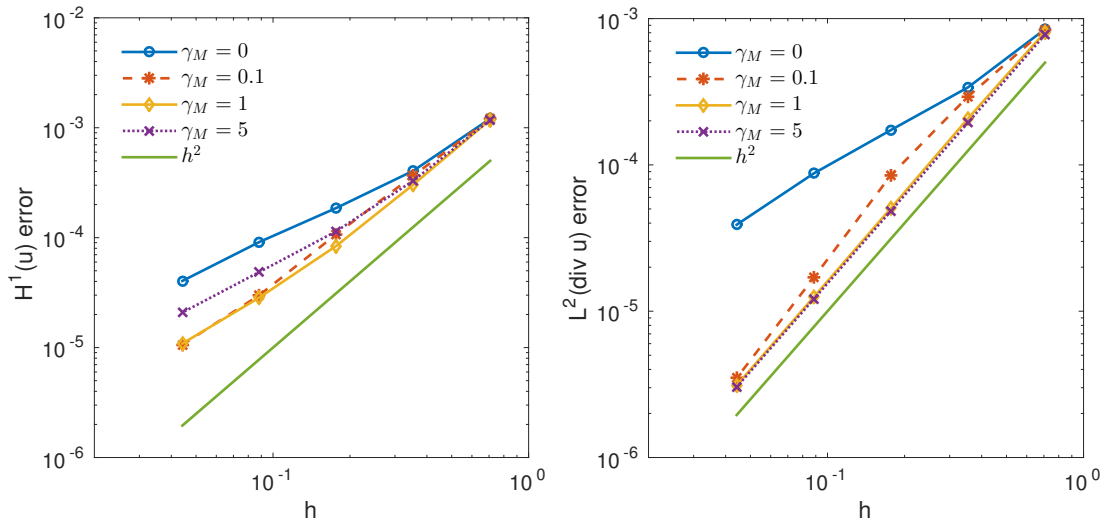


Figure 5.2.: Two-dimensional Couzy test with $Re = 10^3$: Dependence of the H^1 -velocity error (left) and the L^2 -divergence error (right) on the grad-div parameter γ_M for $\mathbb{Q}_2 \wedge \mathbb{Q}_1$ elements.

The dependence of the errors on Re for optimized grad-div parameter γ_M is considered in Figure 5.3 for $\mathbb{Q}_2 \wedge \mathbb{Q}_1$ elements. The L^2 -velocity and L^2 -pressure errors are shown in the appendix, Figure B.3. We observe that a grad-div parameter of magnitude $\mathcal{O}(1)$ is adequate for all Reynolds numbers. A deviation from the optimal convergence rates of the H^1 - and L^2 -velocity errors occurs for higher Reynolds numbers on fine meshes. This can be explained by a too large time step size. On the other hand, optimal rates are found for $L^2(\operatorname{div} u)$ and $L^2(p)$.

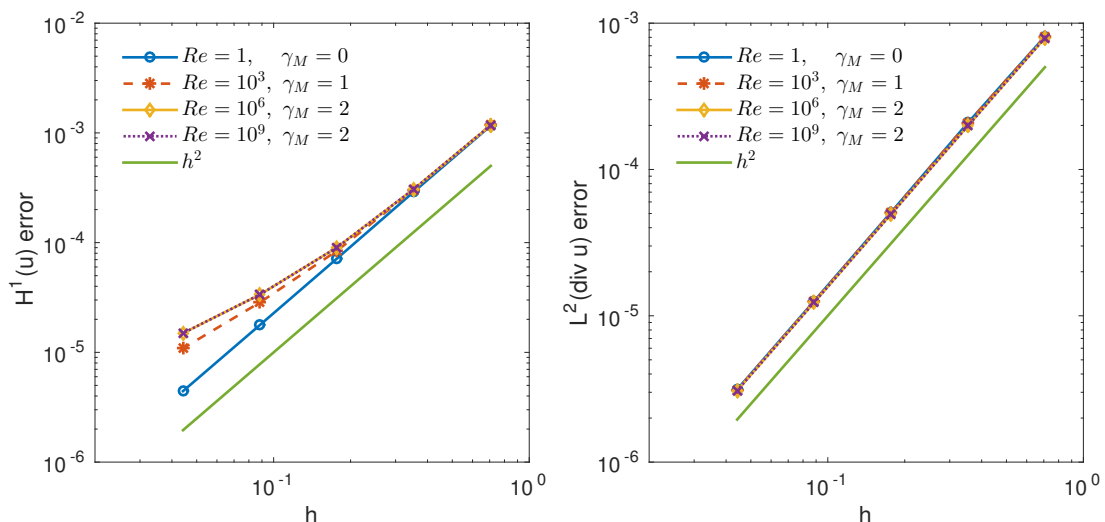


Figure 5.3.: Two-dimensional Couzy test with optimized grad-div parameter γ_M : Dependence of the H^1 -velocity error (left) and the L^2 -divergence error (right) on Re for $\mathbb{Q}_2/\mathbb{Q}_1$.

In Figure 5.4, we compare the effect of LPS SU stabilization and enrichment for $Re = 10^3$. $(\mathbb{Q}_2/\mathbb{Q}_1) \wedge \mathbb{Q}_1$ and $(\mathbb{Q}_2^+/\mathbb{Q}_1) \wedge \mathbb{Q}_1$ elements are combined with grad-div stabilization only and with additional LPS SU stabilization, i.e. $\tau_M^u \in \{0, \frac{1}{2}h/\|\mathbf{u}_h\|_{\infty, M}, \|\mathbf{u}_h\|_{\infty, M}^{-2}\}$. L^2 -velocity and L^2 -divergence errors can be found in the appendix, Figure B.4.

For Taylor-Hood elements, LPS SU stabilization does not influence the errors notably; the convergence rate in the velocity errors in H^1 and L^2 is reduced for fine grids. Enriched elements can improve this situation. In the grad-div stabilized cases with $\tau_M^u \in \{0, \frac{1}{2}h/\|\mathbf{u}_h\|_{\infty, M}\}$, the expected rates are obtained. In contrast, using an enriched velocity space in conjunction with $\tau_M^u = \|\mathbf{u}_h\|_{\infty, M}^{-2} \leq |\mathbf{u}_M|^{-2}$, the order of convergence drops by up to a half for the finest grids. This leads to the conclusion that the upper bound obtained from the semi-discrete analysis in Chapter 3 might be too large. The pressure error is unaffected by different LPS SU parameters. Enriched elements deteriorate the divergence error slightly but convergence rates as h^2 are observed in all cases.

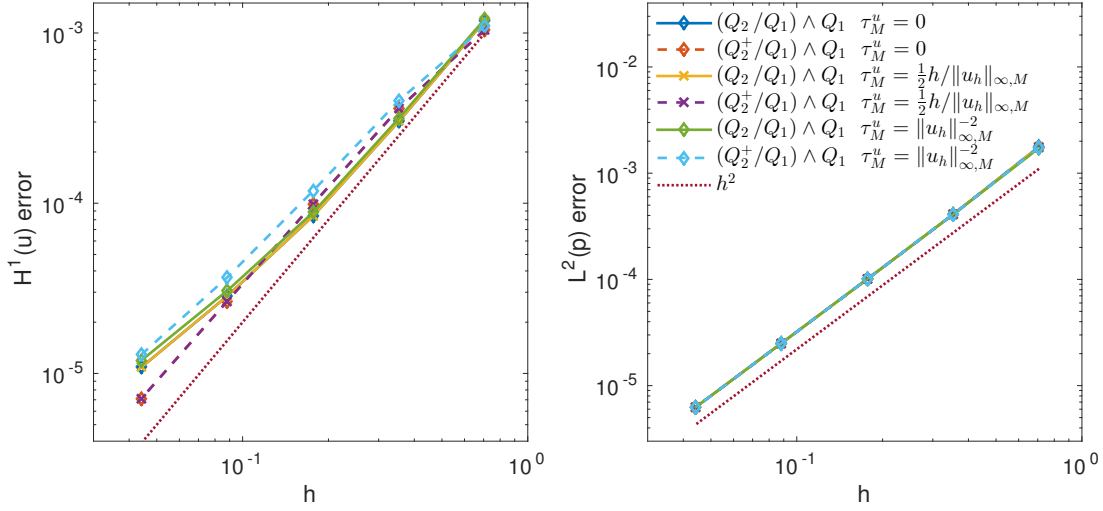


Figure 5.4.: Two-dimensional Couzy test for $Re = 10^3$ with $\gamma_M = 1$: H^1 -velocity error (left) and L^2 -pressure error (right) for different LPS SU parameters τ_M^u for $(Q_2/Q_1) \wedge Q_1$ and $(Q_2^+/Q_1) \wedge Q_1$ elements.

5.3. Non-Isothermal Convergence Results: 2D Traveling Wave

The test case consists of a convection driven temperature peak moving through a domain. After the peak hits a boundary, it is transported out of the domain. This example is constructed such that an analytical solution is known. It captures the nature of convection-diffusion equations but is coupled with a momentum equation according to the Oberbeck-Boussinesq model.

In this section, we verify the theoretical convergence results in space and time numerically. The influence of LPS stabilization is discussed.

5.3.1. Features of the Test Case

We consider a time dependent, two-dimensional solution of the Oberbeck-Boussinesq equations (2.7) for different parameters $\nu, \alpha, \beta > 0$ in a box $\Omega = (0, 1)^2$ with $t \in [0, 6 \cdot 10^{-3}]$:

$$\begin{aligned} \mathbf{u}(x, y, t) &= (100, 0)^T, \quad p(x, y, t) = 0, \\ \theta(x, y, t) &= (1 + 3200\alpha t)^{-1/2} \exp\left(-\left(\frac{1}{2} + 100tx\right)^2 \left(\frac{1}{800} + 4\alpha t\right)^{-1}\right), \\ \mathbf{f}_u(x, y, t) &= \left(0, -\beta(1 + 3200\alpha t)^{-1/2} \exp\left(-200(1 + 3200\alpha t)^{-1}(1 + 200t - 2x)^2\right)\right)^T, \\ f_\theta(x, y, t) &= 0 \end{aligned}$$

with $\mathbf{g} \equiv (0, -1)^T$ and (time dependent) Dirichlet boundary conditions for \mathbf{u} and θ , where the right-hand sides \mathbf{f}_u, f_θ are calculated such that (\mathbf{u}, p, θ) solves the equations. Initially, the temperature peak is located at $x = \frac{1}{2}$ and moves in x -direction until it finally hits the wall at $x = 1, t = 0.005$ and is transported out of the domain. Note that the movement of the peak is one-dimensional.

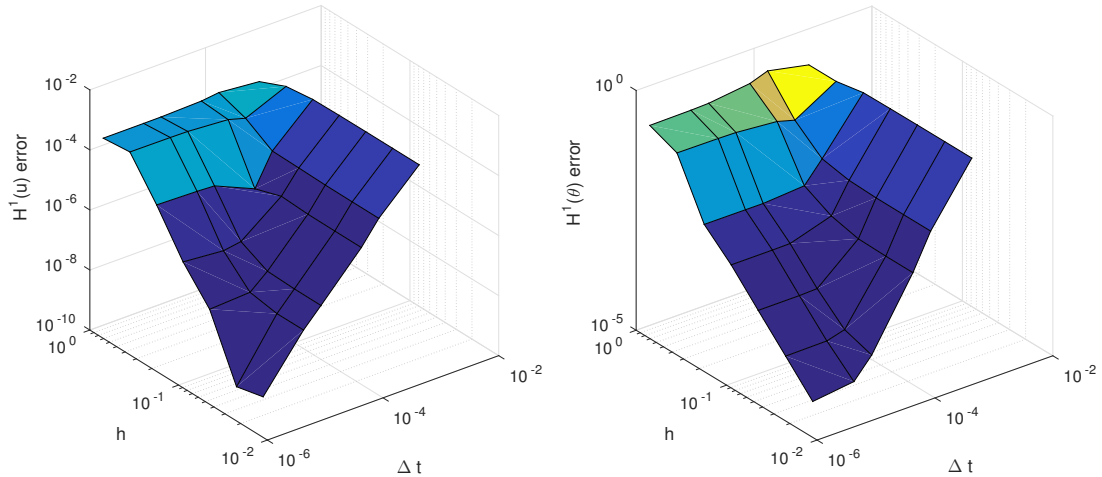


Figure 5.5.: Velocity (left) and temperature (right) H^1 -errors in dependence of Δt and h , $(\nu, \alpha, \beta) = (1, 1, 1)$.

The mesh is randomly distorted by 1%; h denotes an average cell diameter. The fully discrete error depends both on the time step size Δt and the mesh size h . We want to study the induced errors separately. So we have to choose the other parameter small enough such that the error of interest dominates. Otherwise, its order of convergence would be corrupted by the error introduced by the other quantity (see Figure 5.5).

We use $\mathbb{Q}_2 \wedge \mathbb{Q}_1 \wedge (\mathbb{Q}_2/\mathbb{Q}_1)$ or $\mathbb{Q}_2 \wedge \mathbb{Q}_1 \wedge (\mathbb{Q}_2^+/\mathbb{Q}_1)$ elements for velocity, pressure and fine and coarse temperature. Since only the temperature ansatz spaces are varied here, we write $\mathbb{Q}_2^{(+)}/\mathbb{Q}_1$ for convenience.

5.3.2. Numerical Experiments: Spatial Convergence

Different parameter settings for (ν, α, β) are considered and the errors in temperature, velocity and pressure are examined. Note that the continuous solutions \mathbf{u} and p are part of the semi-discrete ansatz spaces \mathbf{V}_h and Q_h . Furthermore, the influence of small viscosity ν is discussed in Sections 5.1, 5.2. Therefore, we focus on the case of moderate ν , where no stabilization for the momentum equation is needed ($\gamma_M = 0, \tau_M^u = 0$). The temperature errors are displayed here; spatial errors for velocity and pressure can be found in the appendix, Section B.3.

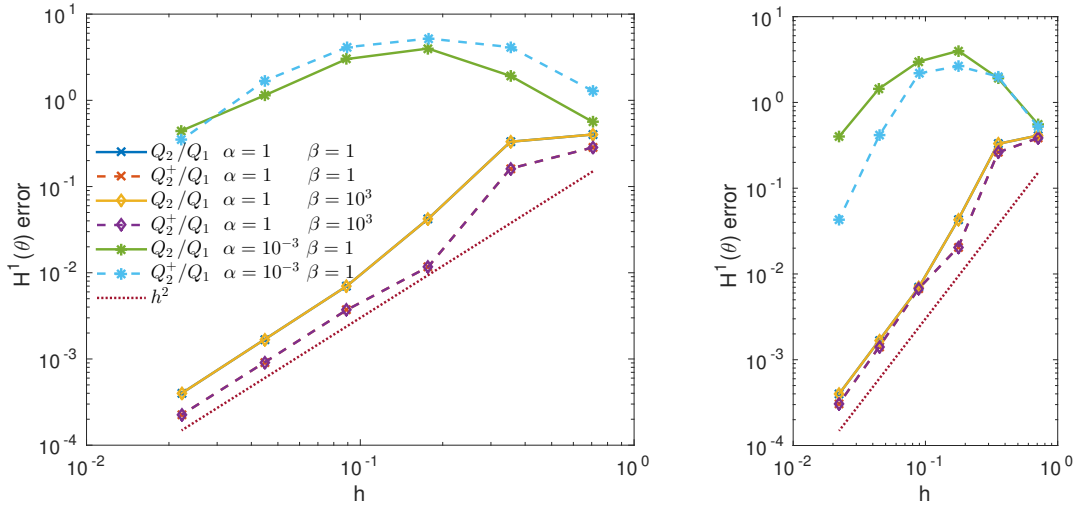


Figure 5.6.: Temperature H^1 -errors for different finite elements and choices of α and β with $\tau_L^\theta = 0$ (left) and $\tau_L^\theta = h/\|\mathbf{u}_h\|_{\infty,L}$ (right), $\nu = 1$.

As presented in Figure 5.6, the cases with $\alpha = 1$ show the expected order of convergence $\|\theta - \theta_h\|_{H^1(\Omega)} \sim h^2$ even without stabilization. Adding LPS stabilization for θ does not corrupt this result. Note that even a high parameter β does not require any stabilization: Neither the discrete temperature nor velocity or pressure fail to converge properly (see Figure 5.6 and appendix, Figures B.5 and B.6). In the interesting case $\alpha = 10^{-3}$, the temperature H^1 -errors become very large in the unstabilized case. LPS stabilization, especially in combination with Q_2^+/Q_1 elements for θ_h , cures this situation (Figure 5.6 right). We point out that if the mesh width restriction

$$Re_M = \frac{h_M \|\mathbf{u}_h\|_{\infty,M}}{\nu} \leq \frac{1}{\sqrt{\nu}}, \quad Pe_L = \frac{h_L \|\mathbf{u}_h\|_{\infty,L}}{\alpha} \leq \frac{1}{\sqrt{\alpha}},$$

that we obtained from the semi-discrete analysis in Section 3.2.1, is violated, no deterioration of the error is detected.

In the unstabilized case as well as in case of LPS SU with Q_2/Q_1 elements for the temperature, the spurious oscillations of the discrete temperature cannot be captured. These wiggles are directly visible in Figure 5.7, where $\theta_h(x, y = 0.5, t = 0.005)$ is plotted for $x \in [0, 0.95]$, and in Figure 5.8, that shows a temperature segment at time $t = 0.005$. The improvement becomes obvious in both illustrations if we use enriched elements Q_2^+/Q_1 .

In Figure 5.9, we study the influence of LPS stabilization for the temperature in case of small $\alpha = 10^{-3}$ in more detail. Different choices of the fine space are considered as well as stabilization parameters. Surprisingly, Q_2/Q_1 elements for the temperature do not

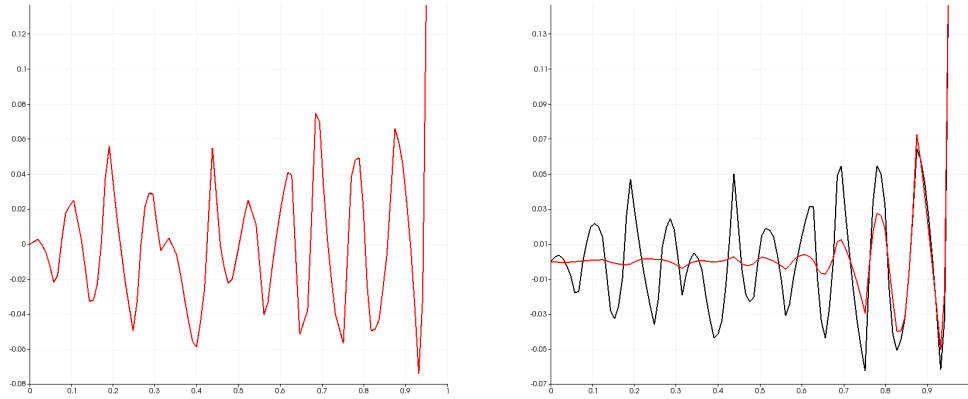


Figure 5.7.: Plot over temperature at $y = 0.5$ ($x \in [0, 0.95]$) at time $t = 0.005$ with $h = 1/16$ in case of $\mathbb{Q}_2/\mathbb{Q}_1$ elements (left) for $\tau_L^\theta = 0$ (black line) and for $\tau_L^\theta = \|\mathbf{u}_h\|_{\infty,L}^{-2}$ (red line), $\mathbb{Q}_2^+/\mathbb{Q}_1$ elements (right) for $\tau_L^\theta = 0$ (black line) and for $\tau_L^\theta = \|\mathbf{u}_h\|_{\infty,L}^{-2}$ (red line), $(\nu, \alpha, \beta) = (1, 10^{-3}, 1)$. The black line lies directly underneath the red one in the left picture.



Figure 5.8.: Temperature segment $x \in [0, 1]$, $y \in [0.35, 0.65]$ at $t = 0.005$ in case of $\mathbb{Q}_2/\mathbb{Q}_1$ elements (left) and $\mathbb{Q}_2^+/\mathbb{Q}_1$ elements (right) for $\tau_L^\theta = \|\mathbf{u}_h\|_{\infty,L}^{-2}$, $(\nu, \alpha, \beta) = (1, 10^{-3}, 1)$

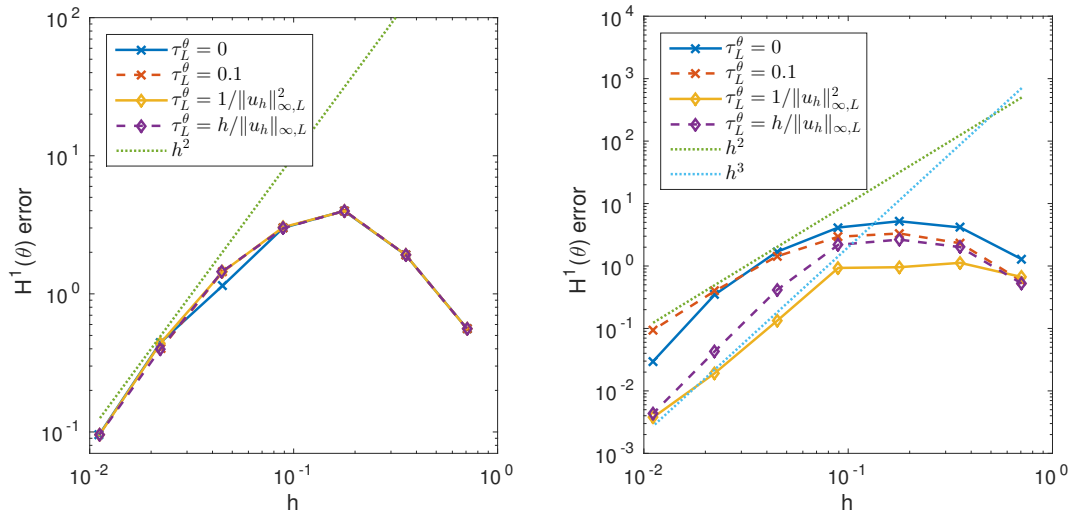


Figure 5.9.: Temperature H^1 -errors for different choices of τ_L^θ in case of $\mathbb{Q}_2/\mathbb{Q}_1$ elements (left) and $\mathbb{Q}_2^+/\mathbb{Q}_1$ elements (right), $(\nu, \alpha, \beta) = (1, 10^{-3}, 1)$.

improve the error considerably; only for one mesh size, we observe a slightly smaller H^1 -error, cf. Figure 5.9 (left). However, if $\mathbb{Q}_2^+/\mathbb{Q}_1$ elements are used for the temperature, LPS SU diminishes the error (Figure 5.9, right).

Figure 5.9 confirms the theoretical discussion that τ_L^θ has to be chosen to be at most $\tau_L^\theta = \|\mathbf{u}_h\|_{\infty,L}^{-2}$; a larger parameter is even worse than the unstabilized case. Our experiments suggest a choice of τ_L^θ as $\min\{h/\|\mathbf{u}_h\|_{\infty,L}, \|\mathbf{u}_h\|_{\infty,L}^{-2}\}$. The error decreases rapidly and is reduced by a factor of at least 10^1 compared to $\tau_L^\theta = 0$.

Figure B.7 in the appendix illustrates that the temperature error does not harm the other quantities considerably through the coupling.

5.3.3. Numerical Experiments: Convergence in Time

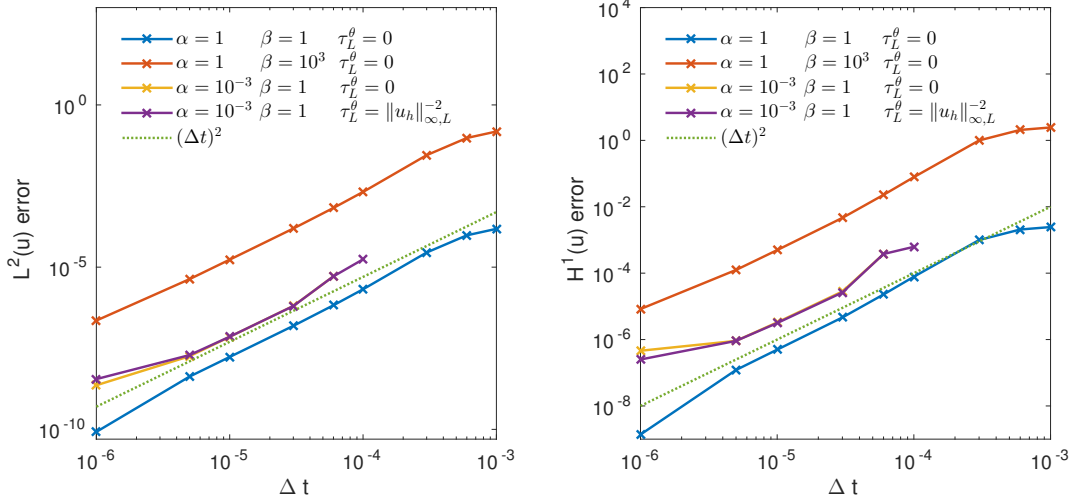


Figure 5.10.: Velocity L^2 - (left) and velocity H^1 -errors (right) for different choices of α and β with $\mathbb{Q}_2^+/\mathbb{Q}_1$ elements.

Figure 5.10 shows errors depending on the time step size Δt at fixed end time $T = 0.006$ and validates the theoretical convergence results of Chapter 4 in time: For the considered regimes of (ν, α, β) , the error $\|\mathbf{u}(T) - \tilde{\mathbf{u}}_{ht}^N\|_0$ is of order $\mathcal{O}((\Delta t)^2)$ as expected. Note that the error on the finest grid is corrupted by the error due to spatial discretization. The error $\|\theta(T) - \theta_{ht}^N\|_0$ shows a similar behavior, see Figure B.8 in the appendix. The errors $\|\nabla(\mathbf{u}(T) - \tilde{\mathbf{u}}_{ht}^N)\|_0$ and $\|p(T) - p_{ht}^N\|_0$ show an even better behavior than $\mathcal{O}(\Delta t)$. An improvement to $\mathcal{O}((\Delta t)^{3/2})$ is anticipated since we used the rotational correction scheme in our implementation (see [GS04] for the linear Stokes case).

5.4. Isothermal Laminar Flow: 2D Blasius Boundary Layers

Named after H. Blasius, a Blasius boundary layer is among the simplest applications of Prandtl's boundary layer theory. It describes the two-dimensional laminar boundary layer that develops if there is steady flow with free stream velocity u_∞ parallel to the x -axis across a flat plate. In [DAL15], some of the following numerical results are shown.

5.4.1. Features of the Test Case

The plate is parallel to the x -axis, starts at $(x = 0, y = 0)$ and is infinitely long downstream, see Figure 5.11. According to [SG00], the attached laminar boundary layer $u = u_\infty f'(\eta)$

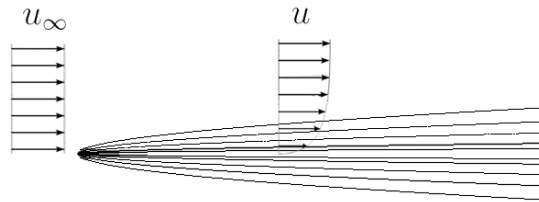


Figure 5.11.: Blasius flow.

developing along the plate can be quite well described by the Blasius profile. It is an exact solution of Prandtl's boundary layer equations, that are given by

$$\begin{aligned} 2f'''(\eta) + f(\eta)f''(\eta) &= 0, \\ f(0) = f'(0) &= 0, \quad \lim_{\eta \rightarrow \infty} f'(\eta) = 1, \end{aligned} \tag{5.2}$$

where $\eta = y\sqrt{u_\infty/(\nu x)}$ is a dimensionless variable.

Let us write $\mathbf{u} = (u, v)^T$ and $\mathbf{x} = (x, y)^T \in \Omega$. We start from the stationary Navier-Stokes equations, assume that viscous forces outside the boundary layer are negligible and the flow is tangential to the boundary layer. Then, the equations can be reduced to Prandtl's boundary layer equations

$$u \frac{\partial u}{\partial x} + v \frac{\partial u}{\partial y} = -\frac{\partial p}{\partial x} + \nu \frac{\partial^2 u}{\partial y^2}, \tag{5.3}$$

$$\frac{\partial p}{\partial y} = 0, \tag{5.4}$$

$$\frac{\partial u}{\partial x} + \frac{\partial v}{\partial y} = 0 \tag{5.5}$$

with boundary conditions $u(y = 0) = v(y = 0) = 0$, $\lim_{y \rightarrow \infty} u(y) = u_\infty$ and Bernoulli's equation for the outer flow

$$\frac{\partial p}{\partial x} = -u_\infty(x) \frac{du_\infty(x)}{dx}.$$

Since u_∞ is constant, we have that $dp/dx = 0$. In case of an infinitely thin plate, we introduce a dimensionless coordinate

$$\eta = y \sqrt{\frac{u_\infty}{\nu x}}$$

and use that the continuity equation (5.5) can be integrated by a streamfunction $\Psi(x, y)$. A dimensionless streamfunction $f(\eta)$ can be introduced by $\Psi = \sqrt{\nu u_\infty x} f(\eta)$. Therefore, it holds

$$u = \frac{\partial \Psi}{\partial y} = u_\infty f'(\eta), \quad v = -\frac{\partial \Psi}{\partial x} = \frac{1}{2} \sqrt{\frac{\nu u_\infty}{x}} (\eta f' - f).$$

Inserting this into (5.3) yields the universal ordinary differential equation, which describes the profile of the boundary layer (5.2).

Reference data are available in [How38]. For our numerical example, we consider a bounded domain $\Omega = (-0.5, 0.5)^2$, where an infinitely thin plate ranges from the middle of the domain $(0, 0)$ to the right wall $(0.5, 0)$. Homogeneous Dirichlet boundary conditions are used at the plate and Dirichlet data $(u_\infty = 1, 0)$ at the left, top and bottom walls are used. Neumann boundary conditions are posed on the right wall in order to disassemble an infinitely long plate. In the following, we consider Blasius flow at $\nu = 10^{-3}$. We evaluate the results once (after a fixed time T), when the numerical solution reached a stationary state.

5.4.2. Numerical Experiments

Using a discretization with Taylor-Hood elements $\mathbb{Q}_2 \wedge \mathbb{Q}_1$ for velocity and pressure in combination with grad-div stabilization $\gamma_M = 1$ on a structured rectangular mesh, we observe spurious wiggles of magnitude up to 10% of the velocity in front of the plate, see Figure 5.12. On the other hand, the boundary layer profile is in good agreement with the reference data from [How38].

In the following, the aim is to remove the unphysical oscillations while preserving or even improving the approximation of the boundary layer with as few mesh points as possible. We want to investigate if LPS SU stabilization has the desired effect and which parameter τ_M^u is suited. Figure 5.13 shows that in addition to grad-div, a LPS SU parameter $\tau_M^u = 1/\|\mathbf{u}_h\|_{\infty, M}^2$ can damp out the oscillations in front of the plate if $(\mathbb{Q}_2/\mathbb{Q}_1) \wedge \mathbb{Q}_1$ elements are used for velocity fine and coarse space and pressure. Smaller parameters τ_M^u of order

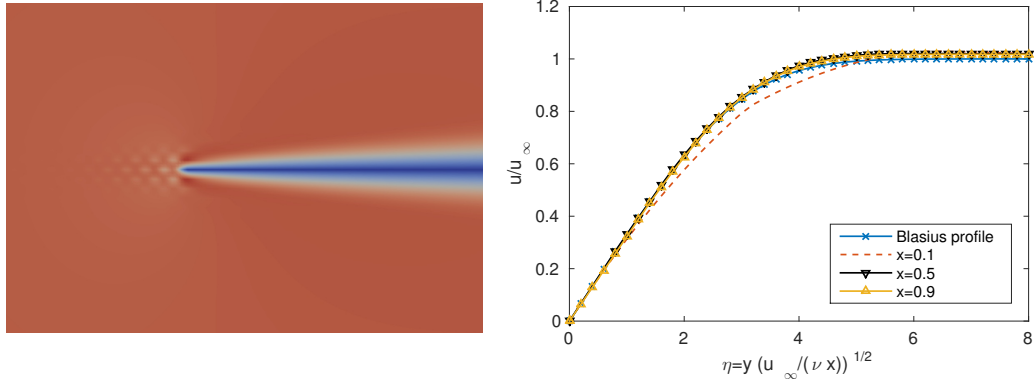


Figure 5.12.: Flow over a horizontal plate at $\nu = 10^{-3}$, $\gamma_M = 1$, $\tau_M^u = 0$, $h = 2^{-5}$: Velocity magnitude near the plate (left) and Blasius profiles at different x (right).

$\mathcal{O}(h^2)$ do not remove the wiggles. $\tau_M^u \sim \mathcal{O}(h)$ already yields an improvement but does not provide as much damping as the choice of order $\mathcal{O}(1)$. Enriched elements lead to similar results, see Figure B.9 in the appendix. We also refer the reader to the appendix, Figure B.10 in order to check that the choice $\tau_M^u = \frac{1}{2}h/\|\mathbf{u}_h\|_{\infty,M}$ in conjunction with $(\mathbb{Q}_2/\mathbb{Q}_1) \wedge \mathbb{Q}_1$ elements and with enriched $(\mathbb{Q}_2^+/\mathbb{Q}_1) \wedge \mathbb{Q}_1$ elements is comparable to $\tau_M^u = h/\|\mathbf{u}_h\|_{\infty,M}^2$. For the coarse space $\mathbf{D}_M^u = \mathbb{Q}_1$, we do not observe an influence of different stabilization parameters with respect to the Blasius profile. In this example, the flow away from the plate is given by $(1,0)$. In particular, this means that using parameters depending in any way on \mathbf{u}_h changes the behavior in the boundary layer only. There, the reference data is of the form

$$f'(\eta) = \eta f''(0) - \frac{(f'')^2 \eta^4}{2 \cdot 4!} + \mathcal{O}(\eta^5).$$

Hence, the streamline derivative is approximately linear away from the stagnation point. In particular, the velocity is well approximated in the coarse space $\mathbf{D}_M^u = \mathbb{Q}_1$. Therefore, the profile is almost unaffected by different choices of the LPS SU parameter. Using an empty coarse space or $\mathbf{D}_M^u = \mathbb{Q}_0$ in conjunction with a constant parameter $\tau_M^u = 1$ perturbs the approximation of the Blasius profile. In addition to the thickening of the boundary layer, the oscillations are rather smeared than damped out (cf. Figure 5.14). If the parameter is chosen in the magnitude $\mathcal{O}(h^2)$ for $\mathbf{D}_M^u = \emptyset$ or $\mathcal{O}(h)$ for $\mathbf{D}_M^u = \mathbb{Q}_0$ (as suggested by the semi-discrete analysis), the boundary profile is nearly unaffected.

We furthermore study refinement strategies near the plate in order to improve the numerical solution. In the appendix, Figures B.11 and B.12, meshes are tested that are refined near the boundary in different ways. The produced grids and the resulting velocity magnitude in case of grad-div stabilization $\gamma_M = 1$ are shown. The oscillations in front of the plate cannot be suppressed by a fine mesh only; a mesh is needed that damps out the

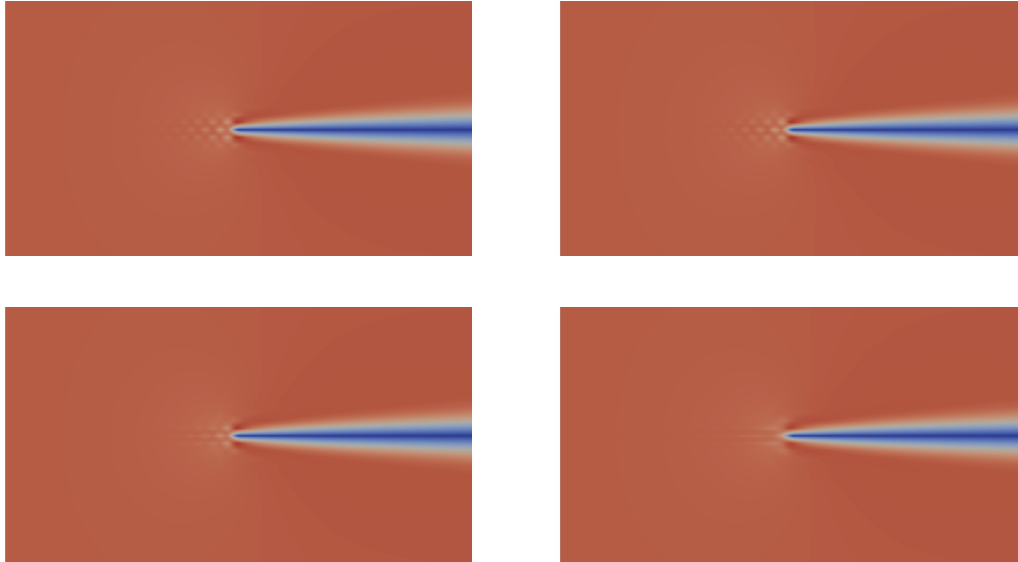


Figure 5.13.: Blasius flow with $\nu = 10^{-3}$ for $\gamma_M = 1$ and different choices of the stabilization parameter τ_M^u with $(\mathbb{Q}_2/\mathbb{Q}_1) \wedge \mathbb{Q}_1$ elements: $\tau_M^u = 0$ (top left), $\tau_M^u = h^2/\|\mathbf{u}_h\|_{\infty,M}^2$ (top right), $\tau_M^u = h/\|\mathbf{u}_h\|_{\infty,M}^2$ (bottom left), $\tau_M^u = 1/\|\mathbf{u}_h\|_{\infty,M}^2$ (bottom right).

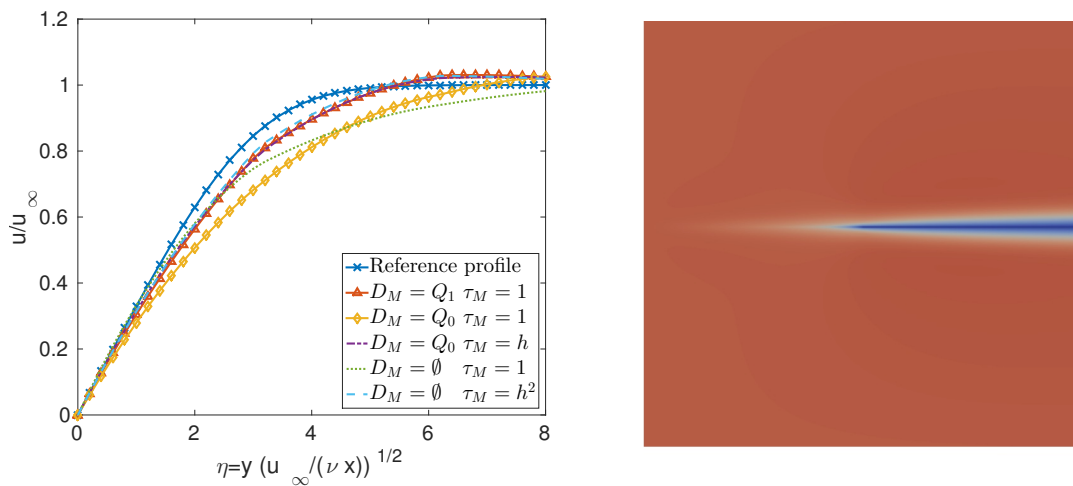


Figure 5.14.: Profiles for different coarse spaces D_M^u (denoted by D_M) and stabilization parameters τ_M^u with constant $\gamma_M = 1$ at $x = 0.1$ (left) and velocity magnitude for $D_M^u = \emptyset$, $\tau_M^u = 1$ (right).

wiggles by being rather coarse in front of the plate. Simultaneously, the domain near the plate has to be resolved in order to approximate the Blasius profile correctly. Therefore, we define a refinement criterion based on diminishing the total variation (TVD) in order to control the velocity difference within a cell

$$tol_T := \sum_{i=1}^d \left(\max_{\mathbf{x} \in T} |u_i(\mathbf{x})| - \min_{\mathbf{x} \in T} |u_i(\mathbf{x})| \right)$$

on each element $T \in \mathcal{T}_h$ for $\mathbf{u}_h = (u_1, \dots, u_d)^T$ in d dimensions. In this example, we want to ensure $tol_T \approx 0.1$ for all $T \in \mathcal{T}_h$. If this is not fulfilled, which is the case near the boundary layer, the cell is refined. Indeed, this results in a rather coarse mesh away from the plate that removes the spurious wiggles without any further stabilization than grad-div $\gamma_M = 1$; see Figure 5.15 (left) and Figure B.13 in the appendix. Figure 5.15 (right), where we increase the Reynolds number to 10^4 , 10^5 and 10^6 , shows that this criterion is stable with respect to Re . It leads to convincing approximations of the reference Blasius profile with errors less than 1%.

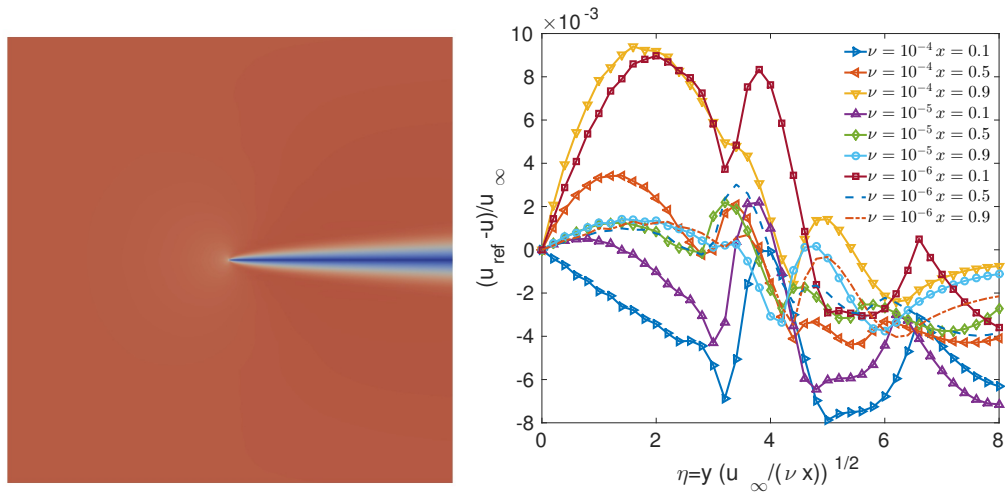


Figure 5.15.: TGV based refinement criterion with $\gamma_M = 1$: Velocity magnitude for $\nu = 10^{-3}$ (left), comparison of boundary layer profiles for different ν (right).

In conclusion, the desired effect can be achieved in the following ways, since the boundary layer has to be resolved sufficiently and the oscillations in front of the plate have to be removed: In case of isotropic meshes, LPS SU stabilization in addition to grad-div provides damping. Alternatively, the grid can be refined in a way that is adjusted to the test case, i.e., it adds grid diffusion in front of the plate.

5.5. Non-Isothermal Laminar Flow: 2D Heated Cavity

The heated cavity is an example for flow in a rectangular enclosure, that is relevant for many industrial applications like cooling of electronic devices or venting in buildings, see e.g. [MH96] for analysis of such a problem. The effects of convection resulting from a heated wall in presence of a gravitational force can be examined.

5.5.1. Features of the Test Case

We consider laminar, non-isothermal flow in a cavity. The left vertical wall of the two-dimensional domain $\Omega = (0, 1)^2$ is heated, the right one is cooled. The flow is then driven by this difference, no external forces occur. Due to the gravity $\mathbf{g} \equiv (0, -1)^T$, the fluid rises at the warm wall and sinks at the cold one.

Dirichlet boundary conditions for the temperature $\theta_{\text{left}} = 0.5$, $\theta_{\text{right}} = -0.5$ and homogeneous Dirichlet boundary conditions for the velocity are applied. We use the Prandtl number $Pr = 0.71$ of air at room temperature and vary the Rayleigh number Ra .

We solve the following dimensionless formulation of the Oberbeck-Boussinesq equations:

$$\begin{aligned} \partial_t \mathbf{u} - Pr \Delta \mathbf{u} + (\mathbf{u} \cdot \nabla) \mathbf{u} + \nabla p - Pr Ra \theta \mathbf{e}_y &= 0 && \text{in } (0, T) \times \Omega, \\ \nabla \cdot \mathbf{u} &= 0 && \text{in } (0, T) \times \Omega, \\ \partial_t \theta - \Delta \theta + (\mathbf{u} \cdot \nabla) \theta &= 0 && \text{in } (0, T) \times \Omega \end{aligned}$$

with Prandtl and Rayleigh numbers as introduced in Definition 2.1.1. The variables are of the order of the respective characteristic quantities.

The mesh is adapted to resolve the boundary layer and is randomly distorted by 1% (see appendix, Figure B.14). Here, the equidistant grid points are transformed by mappings $T_{ab}: [0, 1]^2 \rightarrow [0, 1]^2$ of the form

$$(x, y)^T \mapsto T_{ab}((x, y)^T) := \left(x - \frac{1}{2\pi}(1-a)\sin(2\pi x), y - \frac{1}{2\pi}(1-b)\sin(2\pi y) \right)^T$$

with parameters $0 < a, b < 1$ chosen as $a \approx Nu^{-1}$ and $b \approx Nu^{-1/3}$, as suggested in [Löw11]. The so-called Nusselt number Nu is introduced in the section below; for the grid generation, we use reference values from the literature. We point out that in case of $Ra = 10^4$, the maximal aspect ratio of the cells is approximately 1 : 2.8. For the highest Rayleigh number considered, the maximal aspect ratio is nearly 1 : 50.8. The aspect ratio of neighboring cells does not differ much. Note that the analytical results from Chapters 3 and 4 hold for isotropic meshes. This numerical test case goes beyond this. We refer the reader to [Ape99], where the approximation properties of finite element spaces on anisotropic meshes are

studied and local error estimates are derived.

Throughout this section, we use $(\mathbb{Q}_2/\mathbb{Q}_1) \wedge \mathbb{Q}_1 \wedge (\mathbb{Q}_2/\mathbb{Q}_1)$ elements.

5.5.2. Description of Benchmark Quantities

In order to validate the numerical results, we evaluate certain benchmarks and compare them with results from the literature.

The heat flux is defined as $\mathbf{q} := \mathbf{u}\theta - \alpha\nabla\theta$. In this example, we are interested in the heat transport from the warm left wall to the cold one, so we consider the horizontal heat flux $q_x(x, y, t) = u_x\theta - \alpha\frac{\partial\theta}{\partial x}$. From the total horizontal heat flux

$$\langle q_x \rangle_y(x, t) := \int_0^1 q_x(x, y, t) dy, \quad (5.6)$$

the dimensionless Nusselt number Nu is calculated as the ratio between the convective heat transport h and the diffusive heat transport for motionless fluid in an area A :

$$Nu(x, t) = \frac{h(x, t)L}{\alpha} \quad \text{with } h(x, t) = \frac{\langle q_x \rangle_y(x, t)}{A\Delta\theta}. \quad (5.7)$$

In the dimensionless context, this reduces to $Nu(x, t) = \langle q_x \rangle_y(x, t)$. It is an easy calculation that $Nu(x, t)$ is independent of x when a steady state is reached. Using the stationary equation for θ and the fact that \mathbf{u} is solenoidal gives

$$\begin{aligned} \frac{\partial \langle q_x \rangle_y(x)}{\partial x} &= \int_0^1 \left(\frac{\partial u_x}{\partial x} \theta + u_x \frac{\partial \theta}{\partial x} - \alpha \frac{\partial^2 \theta}{\partial x^2} \right) dy = \int_0^1 \left(-\frac{\partial u_y}{\partial y} \theta - u_y \frac{\partial \theta}{\partial y} + \alpha \frac{\partial^2 \theta}{\partial y^2} \right) dy \\ &= \int_0^1 \left(-\frac{\partial}{\partial y} (u_y \theta) + \alpha \frac{\partial^2 \theta}{\partial y^2} \right) dy \\ &= (u_y \theta)(x, 0) - (u_y \theta)(x, 1) + \alpha \frac{\partial \theta}{\partial y}(x, 1) - \alpha \frac{\partial \theta}{\partial y}(x, 0) = 0 \end{aligned}$$

due to the Dirichlet boundary conditions of \mathbf{u} and θ .

For two-dimensional flow, the streamfunction $\nabla\Phi := \mathbf{u}^\perp = (-u_y, u_x)^T$ can be defined. Local extrema indicate centers of a vortex and can be used as benchmarks. We solve for Φ numerically through the associated Poisson problem

$$\begin{aligned} \Delta\Phi &= \nabla \cdot (\nabla\Phi) = \nabla \cdot \mathbf{u}^\perp \quad \text{in } (0, T) \times \Omega, \\ \Phi &= 0 \quad \text{in } (0, T) \times \partial\Omega, \end{aligned}$$

as described in [L ow11]. We compare the absolute values of the global extrema, denoted by Φ_{\max} , with values from the literature.

5.5.3. Numerical Experiments

The velocity magnitude and temperature for different Rayleigh numbers $Ra \in \{10^4, 10^6, 10^7\}$ are presented in Figure 5.16; in the appendix, Figure B.15 all $Ra \in \{10^4, 10^5, 10^6, 10^7\}$ are depicted as an overview. No stabilization and $N = 64^2$ cells are used. In all of these cases, the flow is laminar and the solution reaches a stationary state that is shown in the pictures.

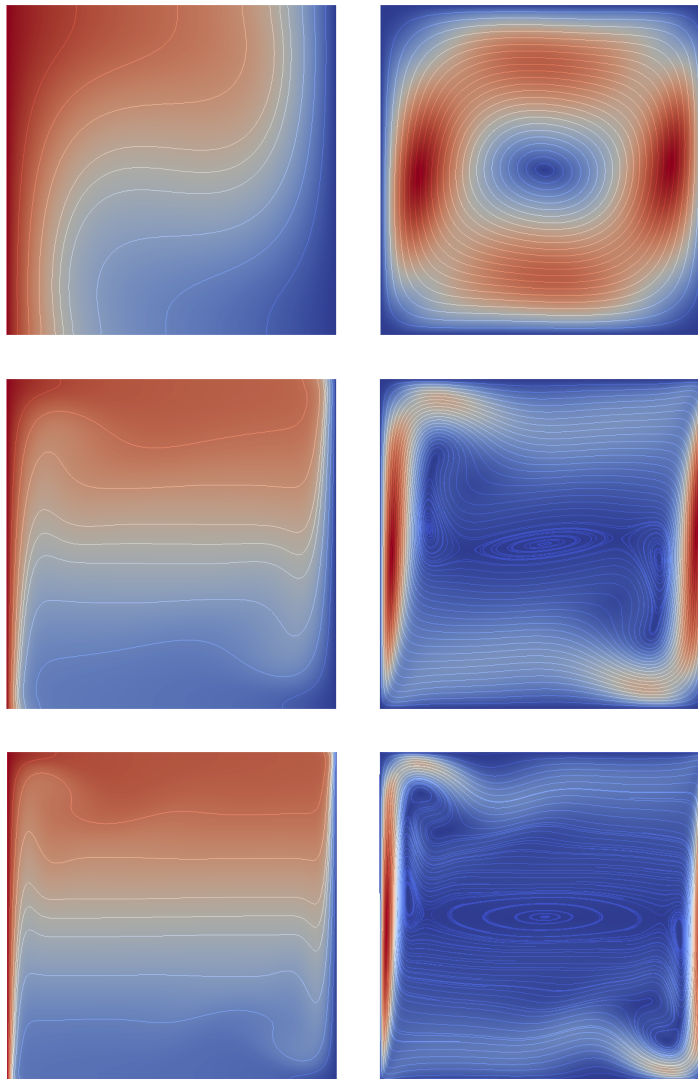


Figure 5.16.: Heated cavity, temperature (left) and velocity magnitude (right) with streamlines, without stabilization, $Pr = 0.71$, $Ra \in \{10^4, 10^6, 10^7\}$, $N = 64^2$.

For small Rayleigh numbers, a central main vortex of highest velocity occurs. For higher Ra , the boundary layer in the temperature near the heated and cooled walls becomes

thinner and the fluid in the middle of the cavity becomes almost motionless. Boundary layers within the velocity also emerge with growing Ra as the flow near the walls becomes faster.

Not only this behavior but also the benchmark quantities in Table 5.1 are in good agreement with the literature [Löw11, LQ91]. Even for $Ra = 10^7$, no stabilization for neither velocity nor temperature is needed. Note that for our simulations, we use a grid that is transformed in a way consistent with [Löw11] but distorted randomly. We observe grid convergence of the Nusselt number and of Φ_{\max} . Furthermore, Nu^{avg} is approximated better than $Nu(0.5)$, as expected, since $Nu(x)$ for some fixed $x \in [0, 1]$ depends on how well the temperature gradient near the walls is resolved. However, Nu^{avg} is averaged over $x \in [0, 1]$ and is subject to the temperature difference only:

$$\int_0^1 \frac{\partial \theta_h}{\partial x} dx = \theta_h(1, y) - \theta_h(0, y) = \theta_{\text{left}} - \theta_{\text{right}}.$$

Nonetheless, we observe that Nu^{avg} and $Nu(0.5)$ are very similar. In case of the exact solution, they would coincide as the solution reaches a steady state.

Ra	\sqrt{N}	$(Nu^{\text{avg}})^{\text{ref}}$	Nu^{avg}	$Nu(0.5)^{\text{ref}}$	$Nu(0.5)$	$(\sqrt{Ra}\Phi_{\max})^{\text{ref}}$	$\sqrt{Ra}\Phi_{\max}$
10^4	16	-	2.24478	-	2.23529	-	5.07359
	32	2.24481	2.24481	2.24195	2.24436	5.07367	5.07367
	64	2.24482	2.24482	2.24410	2.24656	5.07367	5.07367
	128	2.24482	2.24482	2.24464	2.24719	5.07367	5.07367
10^5	16	-	4.52124	-	4.52350	-	9.60613
	32	4.52162	4.52162	4.52283	4.52194	9.61490	9.6151
	64	4.52163	4.52163	4.52192	4.52095	9.61570	9.61572
	128	4.52164	4.52164	4.52170	4.52074	9.61637	9.61638
10^6	16	-	8.81573	-	8.85490	-	16.8347
	32	8.82502	8.82502	8.82484	8.82173	16.79189	16.7934
	64	8.82519	8.82519	8.82546	8.82189	16.81011	16.8103
	128	8.82520	8.82520	8.82530	8.82174	16.81013	16.8102
10^7	16	-	15.3718	-	16.0458	-	43.1554
	32	16.51578	16.5156	16.4921	16.4710	30.18100	30.1805
	64	16.52302	16.5230	16.5211	16.5017	30.16094	30.1612
	128	16.52309	16.5231	16.5228	16.5033	30.16377	30.1638

Table 5.1.: Nusselt numbers Nu and global extrema of the streamfunction Φ_{\max} for different Ra and different numbers of cells N (at stationary point), compared with simulations by [Löw11].

For our purpose to study stabilization, the case of even higher Rayleigh numbers is more interesting. [LQB98] investigates the transition point, when unsteady and even turbulent flow occurs inside a differentially heated cavity. The critical Rayleigh number is found to be $Ra_{crit} \in [1.81 \cdot 10^8, 1.83 \cdot 10^8]$, where the flow becomes unsteady.

We consider a flow with $Ra = 10^8$, which is slightly below this critical value. In Figure 5.17, temperature and velocity are displayed without and with grad-div stabilization. $N = 64^2$ cells are used within the cavity. Although a stationary solution is expected, the unstabilized results are unstable and show unphysical oscillations and vortices in both the velocity and the temperature; no steady state is reached. Grad-div stabilization with $\gamma_M = 1$ cures this situation.

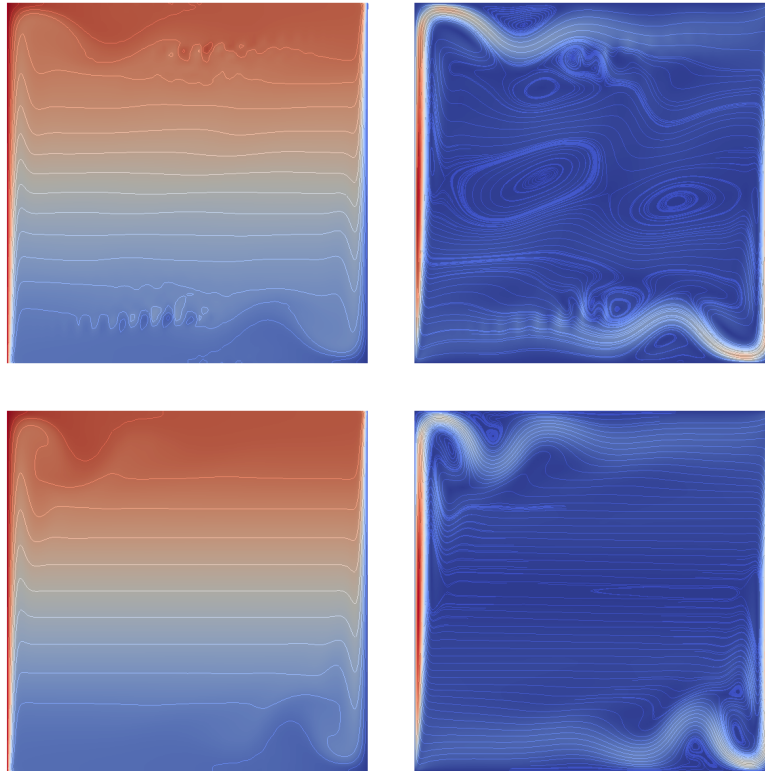


Figure 5.17.: Heated cavity with $Pr = 0.71$ and $Ra = 10^8$, temperature (left) and velocity (right) with streamlines without (top) and with grad-div stabilization (bottom), $N = 64^2$.

Table 5.2 compares the resulting benchmark values for different stabilization scenarios with [LQ91]. The presented values are obtained via averaging in time. Again, in all cases, we observe that refinement of the grid yields better agreement with the reference data. There is a considerable difference in the quality of the benchmarks if no stabilization is

\sqrt{N}	16	32	64	reference
Nu^{avg}	18.7694	27.3830	30.0965	30.225
Nu^{avg} GD	24.5473	27.9058	30.2237	
Nu^{avg} SUt	24.7862	27.9774	30.2238	
Nu^{avg} SUut	26.5130	28.2333	30.2239	
$Nu(0.5)$	23.4069	29.2566	29.5245	30.225
$Nu(0.5)$ GD	30.9351	27.1668	30.1839	
$Nu(0.5)$ SUt	29.5851	27.5024	30.1838	
$Nu(0.5)$ SUut	27.4597	28.7397	30.1825	
$\sqrt{Ra}\Phi_{\text{max}}$	113.7240	96.2385	55.3487	53.8475
$\sqrt{Ra}\Phi_{\text{max}}$ GD	108.2694	88.4510	53.8126	
$\sqrt{Ra}\Phi_{\text{max}}$ SUt	109.1343	88.3693	53.8135	
$\sqrt{Ra}\Phi_{\text{max}}$ SUut	104.7587	87.1177	53.8136	

Table 5.2.: Nusselt numbers Nu and extrema of the streamfunction Φ_{max} for $Ra = 10^8$ and different numbers of cells N (averaged over $t \in [0.07; 0.1]$) with different stabilizations, compared with benchmarks by [LQ91], that are obtained by using $N = 128^2$ cells. GD denotes $(\gamma_M, \tau_M^u, \tau_L^\theta) = (1, 0, 0)$, SUt $(\gamma_M, \tau_M^u, \tau_L^\theta) = (1, 0, \|\mathbf{u}_h\|_{\infty, M}^{-2})$, SUut $(\gamma_M, \tau_M^u, \tau_L^\theta) = (1, \frac{1}{2}h/\|\mathbf{u}_h\|_{\infty, M}, \|\mathbf{u}_h\|_{\infty, M}^{-2})$.

applied compared to the stabilized case. Adding LPS SU stabilization for temperature and velocity yields slightly better results than grad-div stabilization only. Note that anisotropic grids are used that are adapted to resolve the boundary layers.

5.6. Isothermal Turbulent Flow: 3D Taylor-Green Vortex

It is well known that dissipation occurs at the smallest scales in a flow, see the book of [Pop00]. In case of turbulent flow, these are, in general, not resolved by a numerical procedure unless through direct numerical simulation (DNS). Due to the development of smaller and smaller eddies in turbulent flow, this is not feasible in our situation. An alternative to solve the Navier-Stokes equations numerically is large eddy simulation (LES). The goal is to solve a given differential equation numerically on a grid that is too coarse to resolve all scales. So the influence of the small non-resolved scales has to be modeled. The most important issue in turbulence modeling is how to choose the model such that the dissipation of kinetic energy on the small scales is represented correctly. Otherwise, an unphysical energy increase occurs. The choice of a suitable turbulence model is a problem that has been looked at many times and is still not answered in a satisfactory way. There are many different ansatzes for this problem, see e.g. [BIL05, Joh12, Sag06] for introductions and mathematical considerations. More recent developments incorporate

characteristics and local behavior of the flow, as in [NTC⁺11], for instance, or make use of the idea of variational multiscale methods (cf. [RL10]).

In order to investigate the adequacy of grad-div and LPS SU stabilization as an implicit LES subgrid model, we consider the case of a three-dimensional Taylor-Green vortex (TGV). The Taylor-Green vortex is a commonly used and simple flow to study isotropic turbulence. The energy cascade produces smaller and smaller eddies and vortex stretching occurs.

5.6.1. Features of the Test Case

As in [CBCP15], we consider the flow in a periodic box $\Omega = (0, a)^3$ with some $a > 0$ that we vary as needed. With $b > 0$, the initial values are

$$\begin{aligned} \mathbf{u}_0 &= b \cdot \begin{pmatrix} \cos\left(\frac{2\pi}{a}x\right) \sin\left(\frac{2\pi}{a}y\right) \sin\left(\frac{2\pi}{a}z\right) \\ -\sin\left(\frac{2\pi}{a}x\right) \cos\left(\frac{2\pi}{a}y\right) \sin\left(\frac{2\pi}{a}z\right) \\ 0 \end{pmatrix}, \\ p_0 &= b \cdot \frac{1}{16} \left(\cos\left(\frac{4\pi}{a}x\right) + \cos\left(\frac{4\pi}{a}y\right) \right) \left(\cos\left(\frac{4\pi}{a}z\right) + 2 \right). \end{aligned}$$

The initial energy is concentrated on the wave numbers $\mathbf{k} = (\pm a, \pm a, \pm a)$. Note that $\|\mathbf{u}_0\|_\infty = b$. The parameters a, b will prove beneficial to study the proper choice of stabilization parameters in dependence on h and \mathbf{u}_h . Two settings are taken into consideration, namely $\{a = 2\pi, b = 1\}$ and $\{a = 8/\sqrt{3}, b = 1/10\}$. In order to examine the effects of stabilization on turbulent flow, we solve the problem for $\nu = 10^{-4}$ in case of $\{a = 2\pi, b = 1\}$ and $\nu = 10^{-5}$ if $\{a = 8/\sqrt{3}, b = 1/10\}$, whereas [CBCP15] uses $Re = 1,600$. [BMO⁺83] states that the flow is nearly isotropic for sufficiently high $Re \geq 1,000$.

We consider $t \in [0, 10/b]$ and $(\mathbb{Q}_2/\mathbb{Q}_1) \wedge \mathbb{Q}_1$ elements for fine and coarse velocity space and pressure. Isotropic grids are used, which means $h_M =: h$ for all $M \in \mathcal{M}_h$.

5.6.2. Description of Benchmark Quantities

In order to validate the numerical results, we compute the energy spectrum of the numerical solution at time t as

$$E(k, t) = \frac{1}{2} \sum_{k-\frac{1}{2} \leq |\mathbf{k}| \leq k+\frac{1}{2}} \hat{\mathbf{u}}(\mathbf{k}, t) \cdot \hat{\mathbf{u}}(\mathbf{k}, t)$$

with the Fourier transform $\hat{\mathbf{u}}(\mathbf{k}, t) = \int_\Omega \mathbf{u}(\mathbf{x}, t) \exp(-i\mathbf{k}\mathbf{x}) d\mathbf{x}$.

Denote by $K_0 > 0$ a dimensionless constant and by ε the turbulent dissipation rate. Kol-

Kolmogorov's second hypothesis states that in the inertial subrange, the energy is distributed like

$$E(k, t) = K_0 \varepsilon^{2/3} k^{-5/3},$$

assuming locally isotropic turbulence. We refer the reader to [Pop00] for details. This relation is also known as Kolmogorov's $-5/3$ -law.

5.6.3. Theoretical Justification for the Choice of the LPS SU Parameter

In this section, we discuss theoretical arguments that give insight into the proper choice of the LPS SU parameter τ_M^u , especially its dependence on the mean velocity on a cell \mathbf{u}_M and the globally used grid size h . Unfortunately, these considerations are not valid universally; they apply to isotropic homogeneous turbulence and give no answer to the case of wall bounded flow, for instance.

Parameters for the Smagorinsky model that are suited to represent the influence of small scales are derived in [Lil67]. We follow this argumentation and apply it to our situation: The LPS SU stabilization is interpreted as a turbulence model and is postulated to be of the form

$$\tau_M^u (\kappa_M^u (\mathbf{u}_M \cdot \nabla \mathbf{u}_h), \kappa_M^u (\mathbf{u}_M \cdot \nabla \mathbf{v}_h)) \quad \text{with} \quad \tau_M^u = \widetilde{\tau}_M \frac{h^\beta}{|\mathbf{u}_M|^\gamma}$$

and $\widetilde{\tau}_M > 0$ and some $\beta, \gamma \in \mathbb{R}$ to be determined by the following discussion. In case of isotropic turbulence, the energy spectrum is of the form

$$E(k, t) = K_0 \varepsilon^{2/3} k^{-5/3},$$

where ε represents the turbulent dissipation rate and simultaneously the energy transfer rate across a given wave number. Assume that the turbulent kinetic energy production and dissipation are in balance on a cell, i.e.,

$$\varepsilon = \tau_M^u \|\kappa_M^u (\mathbf{u}_M \cdot \nabla \mathbf{u}_h)\|_{0,M}^2. \quad (5.8)$$

In order to determine β and γ , we conduct dimensional analysis for (5.8). The notation $[\cdot]$ indicates the physical unit of a quantity.

$$\begin{aligned} \frac{m^2}{s^3} = [\varepsilon] &= \left[\tau_M^u \|\kappa_M^u (\mathbf{u}_M \cdot \nabla \mathbf{u}_h)\|_{0,M}^2 \right] = [\tau_M^u] \left(\frac{1}{m} \frac{m^2}{s^2} \right)^2 = [\tau_M^u] \frac{m^2}{s^4} \\ \Rightarrow [\tau_M^u] &= s = [h |\mathbf{u}_M|^{-1}] \end{aligned}$$

and thus, $\gamma = 1$ and $\beta = 1$.

Now, we desire to find a suitable constant $\widetilde{\tau}_M$. Denote by k_c the resolution limit wave number of the coarse space \mathbf{D}_M^u with respect to the velocity and by k_f the resolution limit wave number of \mathbf{V}_h . For the case of $(\mathbb{Q}_2/\mathbb{Q}_1) \wedge \mathbb{Q}_1$ elements and $a = 1$, it holds $k_f = \frac{3}{2}h^{-1}$ and $k_c/k_f = 1/2$. Due to Plancherel's theorem for the Fourier transform, we calculate from (5.8)

$$\begin{aligned} \|\kappa_M^u \nabla \mathbf{u}_h\|_{0,M}^2 &= \int_{k_c}^{k_f} k^2 E(k) dk = K_0 \int_{k_c}^{k_f} k^{1/3} \varepsilon^{2/3} dk \\ &= K_0 (\tau_M^u)^{2/3} \|\kappa_M^u (\mathbf{u}_M \cdot \nabla \mathbf{u}_h)\|_{0,M}^{4/3} \int_{k_c}^{k_f} k^{1/3} dk \\ &= K_0 (\tau_M^u)^{2/3} \|\kappa_M^u (\mathbf{u}_M \cdot \nabla \mathbf{u}_h)\|_{0,M}^{4/3} k_f^{4/3} \left(1 - \left(\frac{k_c}{k_f}\right)^{4/3}\right) \\ &= K_0 (\tau_M^u)^{2/3} \|\kappa_M^u (\mathbf{u}_M \cdot \nabla \mathbf{u}_h)\|_{0,M}^{4/3} k_f^{4/3} \left(1 - \left(\frac{1}{2}\right)^{4/3}\right) \left(\frac{3}{2}\right)^{4/3} h^{-4/3} \\ &= K_0 \frac{h^{2/3}}{\|\mathbf{u}_M\|_{0,M}^{2/3}} \widetilde{\tau}_M^{2/3} \|\kappa_M^u (\mathbf{u}_M \cdot \nabla \mathbf{u}_h)\|_{0,M}^{4/3} \left(1 - \left(\frac{1}{2}\right)^{4/3}\right) \left(\frac{3}{2}\right)^{8/3} h^{-8/3}. \end{aligned}$$

This yields a formula for $\widetilde{\tau}_M$. However, this would lead to a highly nonlinear stabilization term and is not feasible for our implementation. Therefore, we content ourselves with the insights from the dimensional analysis and choose $\widetilde{\tau}_M$ empirically. We point out that the finding $\tau_M^u \sim \frac{h}{|\mathbf{u}_M|}$ already reduces the range of possible parameters considerably.

5.6.4. Numerical Experiments

The initial condition of the TGV problem defines the large scale structures and vortices. For high Reynolds numbers, the kinetic energy is transported to the small scales due to vortex stretching.

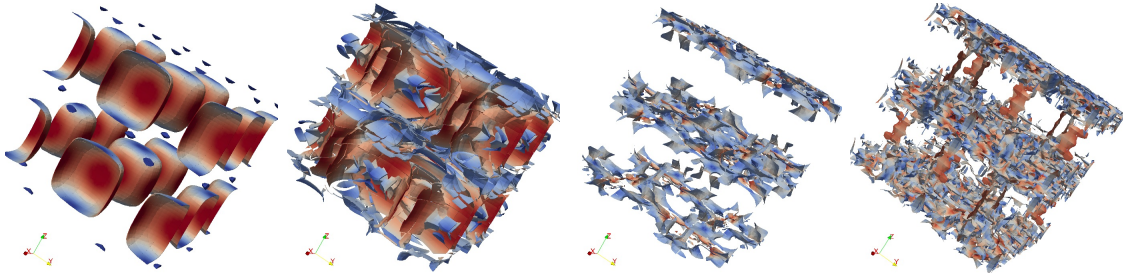


Figure 5.18.: Iso-surfaces for $|\boldsymbol{\omega}| = 1$ at $t = 0$ (left), $|\boldsymbol{\omega}| = 1$ at $t = 2$ (second from left), $|\boldsymbol{\omega}| = 2.5$ at $t = 4$ (second from right), $|\boldsymbol{\omega}| = 4$ at $t = 9$ (right) with $h = \pi/8$, $\{a = 2\pi, b = 1\}$ and grad-div stabilization $\gamma_M = 1$.

Figure 5.18 illustrates the mechanisms of the energy cascade in case of $\nu = 10^{-4}$ with the setup from [CBCP15] $\{a = 2\pi, b = 1\}$ ($h = \pi/8$). At the beginning, the flow is governed by large vortices, that decay into smaller eddies with high vorticity magnitude $|\omega|$. In order to validate the appropriate choice of stabilization parameters, we show energy spectra at time $t = 8/b$ for $\nu = 10^{-4}$. In this regime, the flow can be assumed to be nearly isotropic, so we compare the spectra with Kolmogorov's $-5/3$ law. Note that for a given mesh width h , the displayed spectrum cannot be resolved properly for larger frequencies than $k \sim h^{-1}$.

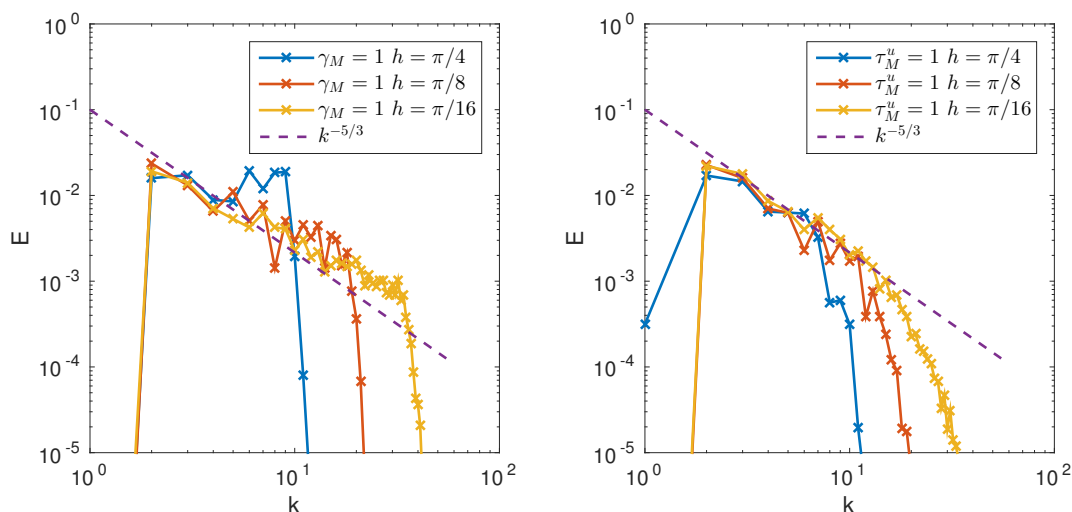


Figure 5.19.: Energy spectra at $t = 9$ for different mesh widths with $\gamma_M = 1$ (left) and with $\gamma_M = 1, \tau_M^u = 1$ (right), $\{a = 2\pi, b = 1\}$.

In Figure 5.19, the energy spectra with grad-div stabilization $\gamma_M = 1$ (left) and with grad-div combined with LPS SU $\gamma_M = 1, \tau_M^u = 1$ (right) are presented for mesh widths $h \in \{\pi/4, \pi/8, \pi/16\}$. Grad-div stabilization alone does not provide enough dissipation because on all grids, one observes that the smallest resolved scales carry too much energy. Additional LPS SU stabilization is more dissipative; the combination $\gamma_M = 1, \tau_M^u = 1$ is therefore more suited as a turbulence model than grad-div stabilization only. Indeed, the classical Smagorinsky model (with optimized stabilization parameter) shows a similar behavior; see Figure B.16 in the appendix.

Now, we are interested if there are choices for τ_M^u that are more suited as a turbulence model than $\tau_M^u = 1$. In order to be able to examine the influence of $|\mathbf{u}_M|$ and h , we scale the TGV problem such that $\Omega = (0, 8/\sqrt{3})^3$ and $\|\mathbf{u}_0\|_\infty = 1/10$; this means that we set $a = 8/\sqrt{3}$ and $b = 1/10$. The viscosity of the problem is $\nu = 10^{-5}$.

First, we consider how τ_M^u depends on $|\mathbf{u}_M|$. The semi-discrete analysis yields an upper bound of $\tau_M^u \leq |\mathbf{u}_M|^{-2}$; the dimensional analysis of Section 5.6.3 suggests a choice as

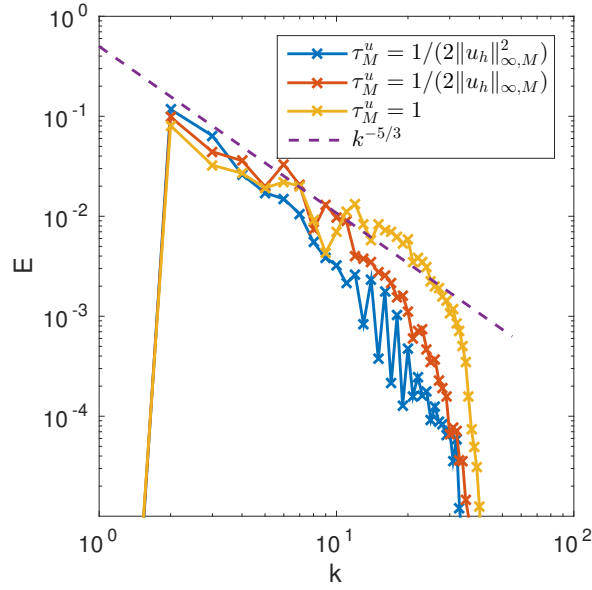


Figure 5.20.: Energy spectra at $t = 80$, $h = 1/(4\sqrt{3})$, $\|\mathbf{u}_0\|_\infty = 1/10$ for considering the dependence of the LPS SU parameter on $|\mathbf{u}_M|$.

$\tau_M^u \sim h|\mathbf{u}_M|^{-1}$. Figure 5.20 shows the combination of grad-div stabilization $\gamma_M = 1$ with different LPS SU choices $\|\mathbf{u}_h\|_{\infty, M}^{-\gamma} \leq |\mathbf{u}_M|^{-\gamma}$ with $\gamma \in \{0, 1, 2\}$. It illustrates that $\tau_M^u \sim \|\mathbf{u}_h\|_{\infty, M}^{-2} \leq |\mathbf{u}_M|^{-2}$ is indeed too dissipative and thus unfeasible. Note that the choice $\tau_M^u = 1$ is less dissipative on the small scales but shows more deviations from the $-5/3$ -law on the coarse scales than $\tau_M^u \sim \|\mathbf{u}_h\|_{\infty, M}^{-1}$.

Hence, we exclude $\tau_M^u \sim |\mathbf{u}_M|^{-2}$ from our further contemplations and look at the h -dependence more closely. In Figure 5.21, stabilization as $\gamma_M = 1$, $\tau_M^u \sim h^\beta/\|\mathbf{u}_h\|_{\infty, M}$ is shown for $\beta \in \{0, 1\}$ and for $h = 1/(4\sqrt{3})$ (left) and $h = 1/(8\sqrt{3})$ (right). The choice $\beta = 1$ yields much better results than $\beta = 0$ for both mesh sizes. So we can rule out that the improvement arises from a constant (i.e., h -independent) multiplicative factor in the LPS SU parameter. This is in good agreement with the knowledge from Section 5.6.3. On the grid $h = 1/(4\sqrt{3})$, we observe again that $\tau_M^u = 1$ is less dissipative on the small scales but deviates more from the $-5/3$ -law on the coarse scales than $\tau_M^u \sim h/\|\mathbf{u}_h\|_{\infty, M}$. Surprisingly, for $h = 1/(8\sqrt{3})$, these choices show very similar behavior, meaning that stabilization is needed most in cells where $(8\sqrt{3})\|\mathbf{u}_h\|_{\infty, M} \approx 1$. Since even for the initial condition, it holds $\|\mathbf{u}_0\|_{\infty, M} \leq 0.1$, this indicates cells of relatively large mean velocity within the domain. We remark that $\tau_M^u = 1$ is not suited as a universal choice: A LPS SU parameter as 0.1 corrupts the errors in Section 5.3, where a different flow example is considered. Therefore, a parameter is desired that incorporates properties of the flow.

In summary, the numerical tests as well as the theoretical arguments show that for isotropic

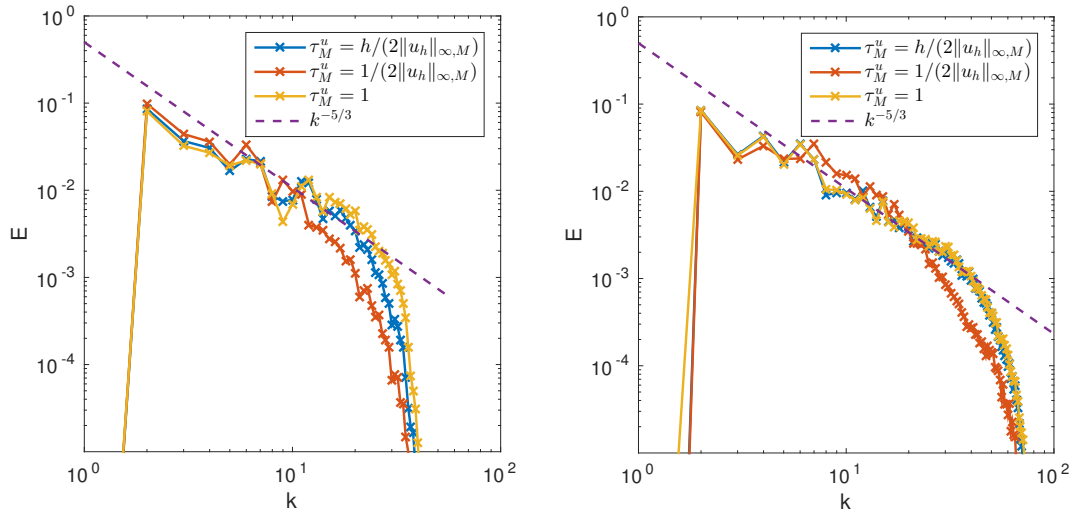


Figure 5.21.: Energy spectra at $t = 80$, $\|\mathbf{u}_0\|_\infty = 1/10$ for considering the dependence of the LPS SU parameter on h , $h = 1/(4\sqrt{3})$ (left), $h = 1/(8\sqrt{3})$ (right).

turbulence a choice of $\tau_M^u \sim h|\mathbf{u}_M|^{-1}$ is suited to act as an implicit turbulence model; grad-div stabilization alone is not dissipative enough.

5.7. Non-Isothermal Flow: 3D Rayleigh–Bénard Convection

The classical Rayleigh–Bénard test case describes flow driven by a temperature gradient between a heated bottom plate and a cooled top plate. This is an example of a natural convection phenomenon, that is widely studied experimentally and analytically, cf. [BPA00, AGL09, HSW11].

If the temperature difference is very small and the viscous damping is dominating, only heat conduction occurs without material transport. For small thermal diffusivity and/or larger temperature gradients, the heat is transported through convection. There is an upflow of warm fluid. However, gravity pulls the cooler liquid from the top to the bottom plate and acts against the viscous damping force in the fluid. The non-dimensional Rayleigh number Ra expresses the ratio between these forces; at high Rayleigh numbers, instabilities develop.

5.7.1. Features of the Test Case

We consider Rayleigh–Bénard convection in a three-dimensional cylindrical domain

$$\Omega := \left\{ (x, y, z) \in \left(-\frac{1}{2}, \frac{1}{2}\right)^3 \mid \sqrt{x^2 + y^2} \leq \frac{1}{2}, |z| \leq \frac{1}{2} \right\}$$

with aspect ratio $\Gamma = 1$ for Prandtl number $Pr = 0.786$ and different Rayleigh numbers $10^5 \leq Ra \leq 10^9$. The aspect ratio is determined as $\Gamma = D/H$, where $D = 1$ denotes the diameter and $H = 1$ the height of the cylinder. The Oberbeck-Boussinesq approximation with gravitational acceleration $\mathbf{g} \equiv (0, 0, -1)^T$ in z -direction is used. The temperature is fixed by Dirichlet boundary conditions at the bottom and top plates as $\theta_{bottom} = 0.5$, $\theta_{top} = -0.5$; the vertical wall is adiabatic with Neumann boundary conditions $\frac{\partial \theta}{\partial \mathbf{n}} = 0$. Homogeneous Dirichlet boundary data for the velocity are prescribed. Let $T = 1000$. As in [WSW12], the dimensionless equations read

$$\begin{aligned} \partial_t \mathbf{u} - Pr^{1/2} Ra^{-1/2} \Gamma^{-3/2} \Delta \mathbf{u} + (\mathbf{u} \cdot \nabla) \mathbf{u} + \nabla p - \theta \mathbf{e}_z &= 0 & \text{in } (0, T) \times \Omega, \\ \nabla \cdot \mathbf{u} &= 0 & \text{in } (0, T) \times \Omega, \\ \partial_t \theta - Pr^{-1/2} Ra^{-1/2} \Gamma^{-3/2} \Delta \theta + (\mathbf{u} \cdot \nabla) \theta &= 0 & \text{in } (0, T) \times \Omega. \end{aligned}$$

Simulations with different triangulations are run, see Figure 5.22. One grid is isotropic and globally refined. Furthermore, a mesh that is anisotropically refined near the walls is applied in order to resolve boundary layers. This is implemented using a transformation of the isotropic mesh; the mapping $T_{xyz}: \Omega \rightarrow \Omega$ is of the form

$$T_{xyz}: (x, y, z)^T \mapsto \left(\frac{x}{r} \cdot \frac{\tanh(4r)}{2 \tanh(2)}, \frac{y}{r} \cdot \frac{\tanh(4r)}{2 \tanh(2)}, \frac{\tanh(4z)}{2 \tanh(2)} \right)^T \quad (5.9)$$

with $r := \sqrt{x^2 + y^2}$. The identity mapping $T_{Id}: (x, y, z)^T \mapsto (x, y, z)^T$ indicates the isotropic grid.

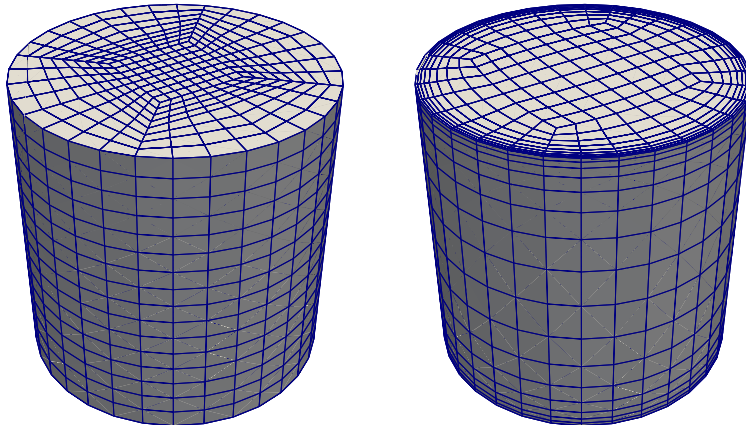


Figure 5.22.: Isotropic mesh (left) and anisotropic mesh that is transformed via T_{xyz} (right) with $N = 10 \cdot 8^3$ cells.

We use these triangulations with N cells, where $N \in \{10 \cdot 8^3, 10 \cdot 16^3\}$, as well as a time step size $\Delta t = 0.1$ for the coarser mesh and $\Delta t = 0.05$ for the finer mesh.

5.7.2. Description of Benchmark Quantities

As a benchmark quantity, the Nusselt number Nu is used. Recall that the vertical heat flux q_z from the warm wall to the cold one is defined by

$$q_z = u_z \theta - \alpha \frac{\partial \theta}{\partial z}.$$

With $B := \{(x, y) \in (-\frac{1}{2}, \frac{1}{2})^2 \mid \sqrt{x^2 + y^2} \leq \frac{1}{2}\}$, the total vertical heat flux at fixed z is calculated as

$$\langle q_z \rangle_{x,y}(z, t) = \int_B q_z(x, y, z, t) dx dy$$

and yields the dimensionless Nusselt number \bar{Nu} by averaging in time:

$$Nu(z) = \Gamma \left(\alpha |B| (T - t_0) |\theta_{bottom} - \theta_{top}| \right)^{-1} \int_{t_0}^T \langle q_z \rangle_{x,y}(z, t) dt \quad (5.10)$$

with a suitable interval $[t_0, T]$. It is well known that the time averaged Nusselt number does not depend on z . This can be understood via the maximum principle. In order to assess the quality of our simulations, we compute the Nusselt number for different $z \in \{-0.5, -0.25, 0, 0.25, 0.5\}$, where the heat transfer is integrated over a disk at fixed z . Then we compare these quantities with the Nusselt number Nu^{avg} calculated as the heat transfer averaged over the whole cylinder Ω :

$$Nu^{\text{avg}} := \Gamma \left(\alpha |\Omega| (T - t_0) |\theta_{bottom} - \theta_{top}| \right)^{-1} \int_{t_0}^T \int_{\Omega} q_z(x, y, z, t) dx dy dz dt. \quad (5.11)$$

The maximal deviation σ within the domain is evaluated according to

$$\sigma := \max\{|Nu^{\text{avg}} - Nu(z)|, z \in \{-0.5, -0.25, 0, 0.25, 0.5\}\}.$$

We compare the Nusselt numbers from our simulations with DNS results by [WSW12] and calculate σ , which is desired to be small. The reference Nusselt numbers are denoted Nu^{ref} .

5.7.3. Numerical Experiments

For high Rayleigh numbers, boundary layers occur in this test case. In order to resolve these layers in the numerical solution, the grid is transformed via T_{xyz} throughout this section unless it is stated otherwise.

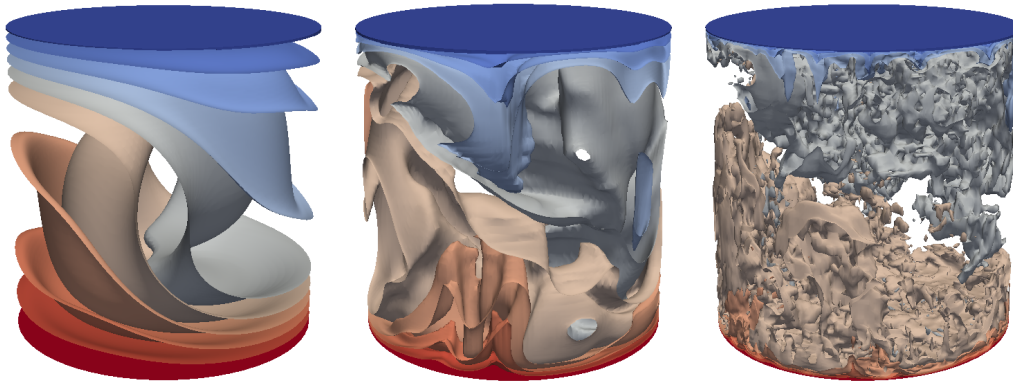


Figure 5.23.: Temperature iso-surfaces at $T = 1000$ for $Pr = 0.786$, $Ra = 10^5$ (left), $Ra = 10^7$ (middle), $Ra = 10^9$ (right), $N = 10 \cdot 16^3$, $\gamma_M = 0.1$.

A snapshot of temperature iso-surfaces for different Ra at $T = 1000$ is shown in Figure 5.23. $N = 10 \cdot 16^3$ cells, grad-div stabilization with $\gamma_M = 0.1$ and $\mathbb{Q}_2 \wedge \mathbb{Q}_1 \wedge \mathbb{Q}_2$ elements for velocity, pressure and temperature are used. In the appendix, Figure B.17, we also show streamlines of the associated velocity. Whereas the large scale behavior shows one large convection cell (upflow of warm fluid and descent of cold fluid) in all cases in a similar fashion, with larger Ra , smaller structures and thin boundary layers occur. For $Ra = 10^5$, the flow reaches a steady state, whereas $Ra \in \{10^7, 10^9\}$ results in transient flow. This is in good qualitative agreement with simulations run by [WSW12].

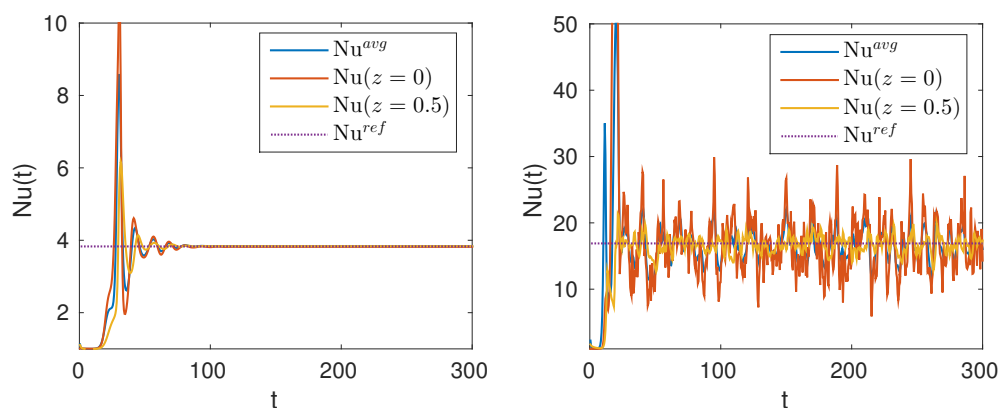


Figure 5.24.: Time development of the Nusselt number in case of grad-div stabilization $\gamma_M = 1$ for $t \in [0, 300]$, $Pr = 0.786$, $Ra = 10^5$ (left) and $Ra = 10^7$ (right), $N = 10 \cdot 8^3$.

For steady flow, the Nusselt number is constant in time and does not depend on z . In case of unsteady flow, we are interested in time averaged Nusselt numbers as suggested in [AGL09]. Indeed, Figure 5.24 illustrates that for steady flow at $Ra = 10^5$, the Nusselt number also reaches a steady state, while Nu fluctuates around a steady state for $Ra = 10^7$ and higher. We start the time averaging at $t_0 = 150$ after the peaks at the beginning vanished and the flow is built up.

First, we want to examine whether stabilization is needed in this example and determine the optimal grad-div parameter depending on Ra if necessary. We run simulations on the coarser mesh with $N = 10 \cdot 8^3$, $T = 1000$ and $\Delta t = 0.1$; different grad-div parameters γ_M in conjunction with $\mathbb{Q}_2 \wedge \mathbb{Q}_1 \wedge \mathbb{Q}_1$ elements are used. The resulting benchmark quantities are presented in Table 5.3 and compared with results from [WSW12], indicated by Nu^{ref} .

Ra	γ_M	Nu^{avg}	σ	Nu^{ref}
10^5	0	3.8396	0.0356	3.83
	1	3.8364	0.0307	
	0.1	3.8372	0.0303	
	0.01	3.8377	0.0319	
10^6	0	8.6457	0.3378	8.6
	1	8.5148	0.0542	
	0.1	8.6475	0.0190	
	0.01	8.6376	0.1122	
10^7	0	16.4143	1.8302	16.9
	1	16.7361	0.1569	
	0.1	16.8767	0.1068	
	0.01	16.9937	0.5567	
	0.001	16.9605	1.3452	
10^8	0	37.7301	29.4731	31.9
	1	30.7236	0.7044	
	0.1	31.2902	0.6957	
	0.01	32.6444	1.0782	
10^9	0	118.7932	137.5588	63.1
	1	48.1509	2.2666	
	0.1	48.7784	1.9513	
	0.01	55.5231	1.3464	
	0.001	82.1364	5.3807	

Table 5.3.: Averaged Nusselt numbers and maximal deviations σ for different Ra and different grad-div parameters γ_M , averaged over time $t \in [150, 1000]$, $N = 10 \cdot 8^3$.

Only for $Ra = 10^5$, the unstabilized case $\gamma_M = 0$ gives satisfactory values for Nu^{avg} and σ ; the discrepancy from Nu^{ref} is only 0.25%. Addition of grad-div stabilization does not corrupt this result. For higher Rayleigh numbers, $\gamma_M = 0$ leads to Nusselt numbers strongly depending on z and differing from the reference value by a large amount, for example by more than 88% of the absolute value Nu^{ref} in case of $Ra = 10^9$. Even negative Nusselt numbers occur for some z . Grad-div stabilization $\gamma_M = 0.01$ can reduce these differences to 12% for $Ra = 10^9$. Also, the deviation within the domain can be diminished considerably for all $Ra > 10^5$. The optimal grad-div parameter found by these experiments lies in the range $\gamma_M \in [0.01, 0.1]$ for all considered Rayleigh numbers. We infer that this parameter can be chosen independently from Ra .

Anyway, for all $Ra \in \{10^5, 10^6, 10^7, 10^8\}$, the reference values Nu^{ref} obtained by DNS can be approximated surprisingly well with the help of grad-div stabilization on a mesh with only $N = 10 \cdot 8^3$ cells. Also, the Nusselt number varies little with respect to different z .

Ra	γ_M	τ_M^u	τ_L^θ	Nu_{th}^{avg}	σ_{th}	Nu_{bb}^{avg}	σ_{bb}	Nu^{ref}
10^9	0.01	0	0	55.5231	1.3464	58.1419	1.4833	63.1
	0.01	1	0	52.7697	1.4125	53.4583	1.6291	
	0.01	hu1	0	53.8371	1.4130	58.2691	1.4702	
	0.01	0	1	51.3556	4.0768	55.4918	2.7713	
	0.01	0	hu1	52.4530	3.4847	56.5274	3.0578	
	0.01	1	1	50.0199	3.5080	52.0606	3.8839	
	0.01	hu1	hu1	51.8141	3.4344	54.0410	3.3333	

Table 5.4.: Averaged Nusselt numbers and maximal deviations σ for different choices of stabilization and finite element spaces, $Ra = 10^9$, averaged over time $t \in [150, 1000]$, $N = 10 \cdot 8^3$. The subscript th indicates that $(\mathbb{Q}_2/\mathbb{Q}_1) \wedge \mathbb{Q}_1 \wedge (\mathbb{Q}_2/\mathbb{Q}_1)$ elements are used and $(\mathbb{Q}_2^+/\mathbb{Q}_1) \wedge \mathbb{Q}_1 \wedge (\mathbb{Q}_2^+/\mathbb{Q}_1)$ are denoted by bb . The label $hu1$ indicates that $\tau_{M/L}^{u/\theta} = \frac{1}{2}h/\|\mathbf{u}_h\|_{\infty, M/L}$.

In order to examine the influence of additional LPS SU, we give an overview for different parameters with $(\mathbb{Q}_2/\mathbb{Q}_1) \wedge \mathbb{Q}_1 \wedge (\mathbb{Q}_2/\mathbb{Q}_1)$, indicated by th , and enriched $(\mathbb{Q}_2^+/\mathbb{Q}_1) \wedge \mathbb{Q}_1 \wedge (\mathbb{Q}_2^+/\mathbb{Q}_1)$ finite elements, denoted by bb , in Table 5.4; $Ra = 10^9$ and the optimal grad-div parameter $\gamma_M = 0.01$ are used. Note that the Nusselt numbers calculated with enriched elements are in better agreement with the reference value than using $(\mathbb{Q}_2/\mathbb{Q}_1) \wedge \mathbb{Q}_1 \wedge (\mathbb{Q}_2/\mathbb{Q}_1)$ elements. Our simulations support the conclusion that additional LPS SU stabilization is not needed in case of anisotropic grids that are adapted to the specific problem; grad-div suffices and is even more favorable. Stabilization of the velocity as $\tau_M^u \sim h/\|\mathbf{u}_h\|_{\infty, M}$ performs better than other LPS SU variants. In case of enriched elements, this choice gives slightly better results than grad-div stabilization only.

We present a larger variety of parameter choices for $Ra = 10^9$, $N = 10 \cdot 8^3$ and $(\mathbb{Q}_2/\mathbb{Q}_1) \wedge \mathbb{Q}_1 \wedge (\mathbb{Q}_2/\mathbb{Q}_1)$ elements in the appendix, Table B.1. The addition of LPS SU stabilization

with any tested parameter does not improve the benchmark quantities and yields even worse results. It is prominent that $\tau_M^u \sim \|\mathbf{u}_h\|_{\infty,M}^{-2}$, $\tau_L^\theta \sim \|\mathbf{u}_h\|_{\infty,L}^{-2}$ or a combination of both give rise to big deviations σ and poor Nusselt numbers. Therefore, we exclude this choice for the further studies presented in this section.

Ra	γ_M	τ_M^u	τ_L^θ	$Nu_{Id,th}^{\text{avg}}$	$\sigma_{Id,th}$	$Nu_{Id,bb}^{\text{avg}}$	$\sigma_{Id,bb}$	Nu^{ref}
10^9	0.01	0	0	41.4584	40.1989	47.5335	23.4029	63.1
	0.01	hu1	0	38.7093	43.0326	44.2998	24.7851	
	0.01	0	hu1	37.6081	10.8360	54.2603	16.5349	
	0.01	hu1	hu1	37.0516	10.3065	49.1255	12.9235	

Table 5.5.: Averaged Nusselt numbers and maximal deviations σ for $Ra = 10^9$ and different stabilization parameters, averaged over time $t \in [150, 1000]$, $N = 10 \cdot 8^3$. The subscript Id means that an isotropic grid is used. The additional th indicates that $(\mathbb{Q}_2/\mathbb{Q}_1) \wedge \mathbb{Q}_1 \wedge (\mathbb{Q}_2/\mathbb{Q}_1)$ elements are used and $(\mathbb{Q}_2^+/\mathbb{Q}_1) \wedge \mathbb{Q}_1 \wedge (\mathbb{Q}_2^+/\mathbb{Q}_1)$ are denoted by bb . The label $hu1$ indicates that $\tau_{M/L}^{u/\theta} = \frac{1}{2}h/\|\mathbf{u}_h\|_{\infty,M/L}$.

As mentioned before, we also test an isotropic grid, which is not particularly refined in boundary layer regions. In Table 5.5, we investigate the use of different stabilization variants in combination with $(\mathbb{Q}_2/\mathbb{Q}_1) \wedge \mathbb{Q}_1 \wedge (\mathbb{Q}_2/\mathbb{Q}_1)$, indicated by th , and enriched $(\mathbb{Q}_2^+/\mathbb{Q}_1) \wedge \mathbb{Q}_1 \wedge (\mathbb{Q}_2^+/\mathbb{Q}_1)$ elements, denoted by bb . The coarser mesh $N = 10 \cdot 8^3$ is applied. In general, the calculated benchmarks differ from the reference value Nu^{ref} by a larger amount than ones obtained on a grid that is refined within the boundary layer, even with the same number of cells, see also Table 5.4. However, in case of an isotropic grid, the deviation is very large if grad-div stabilization is used solely; LPS SU stabilization becomes relevant: Since small temperature structures in the boundary layer are not resolved, their influence has to be modeled. Additional stabilization for the temperature serves this purpose. For instance, in case of $(\mathbb{Q}_2/\mathbb{Q}_1) \wedge \mathbb{Q}_1 \wedge (\mathbb{Q}_2/\mathbb{Q}_1)$ elements, it reduces $\sigma_{Id,th}$ from nearly 97% of the absolute value of the calculated Nusselt number $Nu_{Id,th}^{\text{avg}}$ in case of $(\gamma_M, \tau_M^u, \tau_L^\theta) = (0.01, 0, 0)$ to less than 30% if $\tau_L^\theta = \frac{1}{2}h/\|\mathbf{u}_h\|_{\infty,L}$. The use of enriched elements improves the results; a Nusselt number $Nu_{Id,bb}^{\text{avg}} = 54.2603$ is reached for $(\gamma_M, \tau_M^u, \tau_L^\theta) = (0.01, 0, \frac{1}{2}h/\|\mathbf{u}_h\|_{\infty,L})$. LPS SU stabilization of the velocity is not sufficient, since it does not improve the situation for the temperature. In fact, whether LPS SU for the velocity is applied or omitted does not change the benchmark quantities considerably.

We verify the obtained insights for a finer mesh with $N = 10 \cdot 16^3$ cells that is anisotropically refined via T_{xyz} and $(\mathbb{Q}_2/\mathbb{Q}_1) \wedge \mathbb{Q}_1 \wedge (\mathbb{Q}_2/\mathbb{Q}_1)$ elements for different Rayleigh numbers. The resulting benchmark quantities are presented in Table 5.6. As expected, the averaged Nusselt numbers are in better agreement with the reference data than for the coarser grid ($N = 10 \cdot 8^3$, see Table 5.4). Nevertheless, regarding the question of a suitable parameter

Ra	γ_M	τ_M^u	τ_L^θ	Nu^{avg}	σ	Nu^{ref}
10^5	0.1	0	0	3.8402	0.0024	3.83
10^7	0.1	0	0	17.0254	0.0475	16.9
10^9	0.1	0	0	59.0524	1.0905	63.1
	0.1	hu1	0	57.9408	1.0853	
	0.1	0	hu1	58.7353	0.9786	
	0.1	hu1	hu1	57.6262	1.1909	
	0.01	0	0	60.4889	1.1574	
	0.01	hu1	0	59.1612	1.2727	
	0.01	0	hu1	59.6733	0.9801	
	0.01	hu1	hu1	58.7159	1.2264	
	0.001	0	0	64.1406	3.4328	

Table 5.6.: Averaged Nusselt numbers and maximal deviations σ for different Ra and different stabilization parameters, averaged over time $t \in [150, 1000]$, $N = 10 \cdot 16^3$. The label hu1 indicates that $\tau_{M/L}^{u/\theta} = \frac{1}{2}h/\|\mathbf{u}_h\|_{\infty, M/L}$.

design, the results are qualitatively comparable with the ones obtained with the coarser grid: The grad-div parameter plays the key role, LPS SU does not yield a considerable improvement.

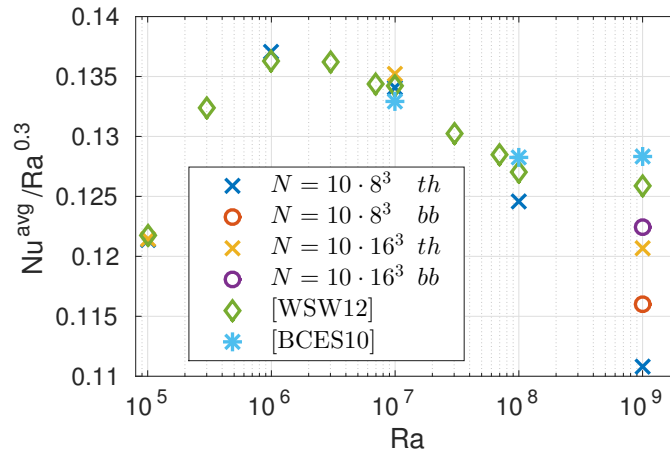


Figure 5.25.: $Nu/Ra^{0.3}$ ($\Gamma = 1$, $Pr = 0.786$) for an anisotropic grid with $N \in \{10 \cdot 8^3, 10 \cdot 16^3\}$ cells, compared with DNS data from [WSW12] ($\Gamma = 1$, $Pr = 0.786$) and [BCES10] ($\Gamma = 1$, $Pr = 0.7$). The label *th* indicates that $(Q_2/Q_1) \wedge Q_1 \wedge (Q_2/Q_1)$ elements are used and $(Q_2^+/Q_1) \wedge Q_1 \wedge (Q_2^+/Q_1)$ are denoted by *bb*. For $10^5 \leq Ra \leq 10^8$, $\gamma_M = 0.1$ is chosen; $\gamma_M = 0.01$ in case of $Ra = 10^9$.

Figure 5.25 provides an overview over the obtained results (using the respective optimal stabilization parameters and an anisotropic grid that is transformed via T_{xyz}). We compare the reduced Nusselt numbers $Nu/Ra^{0.3}$ for different finite element spaces, indicated by th and bb as above, with DNS data from the literature. The Grossmann-Lohse theory from [GL00] suggests that there is a scaling law of the Nusselt number depending on Ra (at fixed Pr) that holds over wide parameter ranges. The reduced Nusselt number calculated in our experiments is nearly constant. However, one does not observe a global behavior of the Nusselt number as $Nu \propto Ra^{0.3}$. But as in [WSW12], a smooth transition between different Ra -regimes $Ra \leq 10^6$, $10^6 \leq Ra \leq 10^8$ and $Ra \geq 10^8$ can be expected. The existence of different regimes is also mentioned in [AGL09].

	N	#DoF(u)	#DoF(p)	#DoF(θ)	$Nu_{\gamma_M=0.01}^{\text{avg}}$	$\sigma_{\gamma_M=0.01}$	Nu^{ref}
th	$10 \cdot 8^3$	129 987	5 729	43 329	55.5231	1.3464	63.1
bb	$10 \cdot 8^3$	176 067	5 729	58 689	58.1419	1.4833	
th	$10 \cdot 16^3$	1 011 075	43 329	337 025	60.4889	1.1574	
bb	$10 \cdot 16^3$	1 379 715	43 329	459 905	61.3628	0.4668	

Table 5.7.: Nusselt numbers $Nu_{\gamma_M=0.01}^{\text{avg}}$ and deviation $\sigma_{\gamma_M=0.01}$ for $Ra = 10^9$, $(\gamma_M, \tau_M^u, \tau_L^\theta) = (0.01, 0, 0)$ for different numbers of degrees of freedom for discrete velocity #DoF(u), pressure #DoF(p) and temperature #DoF(θ). th indicates that $(\mathbb{Q}_2/\mathbb{Q}_1) \wedge \mathbb{Q}_1 \wedge (\mathbb{Q}_2/\mathbb{Q}_1)$ elements are used and bb signifies $(\mathbb{Q}_2^+/\mathbb{Q}_1) \wedge \mathbb{Q}_1 \wedge (\mathbb{Q}_2^+/\mathbb{Q}_1)$ elements. The grids are transformed via T_{xyz} .

Let us take a step back and compare the accuracy of the benchmarks for different numbers of degrees of freedom (DoFs) of the discrete ansatz spaces: In Table 5.7, we list the results for the Nusselt numbers $Nu_{\gamma_M=0.01}^{\text{avg}}$ and deviation $\sigma_{\gamma_M=0.01}$ with grad-div stabilization $\gamma_M = 0.01$ only for different numbers of cells and varying ansatz spaces. This parameter choice provides the best results for $Ra = 10^9$ regarding the Nusselt number and shows small deviations within the domain. It is striking that the use of enrichment for fixed number of cells N leads to an improvement of the benchmarks that is high compared with the number of additional DoFs. Taking a larger N also gives a better approximation but introduces massively more DoFs. We point out that in the DNS in [WSW12], a fourth-order-accurate finite-volume code is used. For $Ra = 10^9$, a mesh with $384 \times 1024 \times 768$ is applied. Altogether, this results in more than $1.5 \cdot 10^9$ unknowns (1,509,949,440 degrees of freedom for velocity, pressure and temperature).

All in all, our simulations illustrate that we obtain surprisingly well approximated benchmark quantities even on relatively coarse meshes. The key ingredients are grad-div stabilization and a grid that resolves the boundary layer. In case of isotropic grids, that are not adapted to the problem, LPS SU stabilization for the temperature becomes necessary. Bubble enrichment enhances the accuracy on all grids.

6. Discussion and Conclusion

This thesis is devoted to the numerical solution of non-isothermal incompressible flow problems. A key objective is to obtain accurate approximate solutions, meaning that the model is theoretically and empirically founded. Hence, we introduce the Oberbeck-Boussinesq equations in Chapter 2, that are justified as a suitable mathematical model for incompressible non-isothermal flow with small temperature differences. We consider stabilized finite element methods in order to circumvent the need for direct numerical simulation and adapt the local projection stabilization method to the Oberbeck-Boussinesq model.

The discretization in time is described in Section 2.3. The so-called rotational pressure-correction projection method is used, which incorporates an approximation in time of second order. Projection methods go back to [Cho69, Tem69] and allow for a decoupling of pressure and velocity. To our best knowledge, we apply this method to the Oberbeck-Boussinesq model for the first time.

The analytical assessment of the stabilized method in Chapters 3 and 4 proves accuracy. We also desire to validate the theoretical results empirically and derive a parameter design that performs well. These issues are addressed below.

6.1. Discussion of the Analytical Results

A semi-discrete analysis for the Oberbeck-Boussinesq model is conducted in Chapter 3 for inf-sup stable elements. The techniques used here are based on the analysis from the publications [DAL15] and [ADL15], which are joint work with my supervisor Prof. Dr. Gert Lube and my colleague Daniel Arndt. The analysis is conducted for the Oseen and the Navier-Stokes problem. In this thesis, we prove stability of the semi-discrete velocity, temperature and pressure solutions of the stabilized Oberbeck-Boussinesq model, see Section 3.1. The key idea for proving a priori error estimates is to split the semi-discrete error into an interpolation error and a consistency error. The estimates require relatively mild regularity assumptions for the continuous solutions. The convective terms are treated carefully in order to circumvent an exponential deterioration of the error with vanishing diffusion. We make use of two special interpolation operators.

Section 3.2.1 is dedicated to the approach relying on the existence of a (quasi-)local interpolation operator $j_u: \mathbf{V}^{div} \rightarrow \mathbf{V}_h^{div}$ preserving the divergence (see [GS03]). This is based

on the inf-sup stability of the discrete velocity and pressure spaces.

We obtain a method of optimal order $k := \min\{k_u = k_p + 1, k_\theta\}$ provided that

$$Re_M = \frac{h_M \|\mathbf{u}_h\|_{\infty, M}}{\nu} \leq \frac{1}{\sqrt{\nu}} \quad \text{and} \quad Pe_L = \frac{h_L \|\mathbf{u}_h\|_{\infty, L}}{\alpha} \leq \frac{1}{\sqrt{\alpha}}$$

for all $M \in \mathcal{M}_h$ and $L \in \mathcal{L}_h$, which gives a restriction on the local mesh widths h_M and h_L . This condition is in agreement with our results from [DAL15] for the Oseen equation. In [MST07], the global condition

$$Re_\Omega := \frac{\|\mathbf{b}\|_\infty C_P}{\nu} \leq \frac{1}{\sqrt{\nu}}$$

is required, that cannot be ensured by grid refinement.

We argue that the method is applicable to almost all combinations of approximation and projection spaces $\mathbf{V}_h/\mathbf{D}_M^u$ and Θ_h/D_L^θ since the assumptions required for the proof are not very restrictive. Furthermore, we suggest a suitable parameter design depending on the coarse space \mathbf{D}_M^u . Note that a broad range of LPS SU parameters τ_M^u, τ_L^θ is possible. In particular, the errors do not deteriorate if τ_M^u, τ_L^θ are set to zero. The LPS SU as well as the pressure jump stabilization give additional control over the stabilized quantities. In contrast, in case of equal-order velocity and pressure ansatz spaces, a distinct choice for the LPS parameter can be suggested (cf. [LRL08]).

As [JLR13] illustrates for the Stokes problem, the design of the grad-div parameter γ_M is still an open question. An equilibration argument in our analysis only suggests a choice for γ_M that is not viable in practice. It is indicated by our analysis and numerical experiments that $\gamma_M = \mathcal{O}(1)$ is a feasible compromise. We point out that grad-div stabilization proves essential for the independence of the Gronwall constant $C_G(\mathbf{u})$ of ν .

In order to remove the restrictions $Re_M \leq \nu^{-1/2}$, $Pe_L \leq \alpha^{-1/2}$, we perform a more thorough estimation of the convective terms in Section 3.2.2. For this second approach, an interpolation operator with additional orthogonality properties is required. In [MST07], it is shown that this operator exists if a compatibility condition of inf-sup type between the approximation and projection velocity and temperature ansatz spaces holds. The compatibility condition restricts the range of possible ansatz spaces for fine and coarse velocity and temperature ansatz spaces. The constructed operator has the necessary approximation properties we need for our analysis. However, in case of the velocity, it does not map to \mathbf{V}_h^{div} in general. As a consequence, a mixed velocity-pressure term has to be handled in the analysis. This is handled by an additional requirement for the pressure ansatz space: $\nabla Q_h|_M \subset \mathbf{D}_M^u$ is assumed for all $M \in \mathcal{M}_h$. In case of discontinuous pressure spaces Q_h , the pressure jump stabilization term becomes important. We review combinations of finite element spaces where these assumptions hold true. The resulting Gronwall constant

occurring as an upper bound of the error depends on $\tau_M^u |\mathbf{u}_h|_{W^{1,\infty}(M)}^2$ and $\tau_L^\theta |\mathbf{u}_h|_{W^{1,\infty}(L)}^2$ and thus on the discrete velocity. A suitable choice of τ_M^u and τ_L^θ is needed to prevent a potential blow up of the Gronwall constant. Furthermore, balancing the error bounds yields a different parameter design with $\gamma_M = \mathcal{O}(1)$ and

$$h_M^2 \lesssim \tau_M^u(\mathbf{u}_M) \lesssim \|\mathbf{u}_h\|_{W^{1,\infty}(M)}^{-2}, \quad h_L^2 \lesssim \tau_L^\theta(\mathbf{u}_L) \lesssim \|\mathbf{u}_h\|_{W^{1,\infty}(L)}^{-2},$$

indicating that LPS SU cannot be omitted.

In Chapter 4, we perform a fully discrete analysis. Stability of the fully discrete solution of the stabilized Oberbeck-Boussinesq model is shown in Section 4.1. Spatial and temporal convergence is proved in Section 4.2 for the stabilized Navier-Stokes equations; the extension to the thermally coupled problem is omitted for convenience but can be performed in a similar fashion as the stability result.

In our technical report [AD15], where the results were published originally, we present two strategies to estimate the errors produced by discretization in time and space separately. In this thesis, we confine ourselves to the splitting

$$\mathbf{u} - \tilde{\mathbf{u}}_{ht} = (\mathbf{u} - \mathbf{u}_h) + (\mathbf{u}_h - \tilde{\mathbf{u}}_{ht})$$

for reasons of clarity and comprehensibility. This approach already reveals the used estimation techniques. Thus, we can take advantage of the semi-discrete a priori results. In Section 4.2.1, we transfer the semi-discrete error estimates in the time-continuous norms to estimates in the time-discrete norms. We put some considerations into this; for details, we refer to [AD15]. Note that in [AD15], the second ansatz is to discretize in time first and afterwards in space.

In Section 4.2.2, we estimate the error introduced by time-discretization of the space-discrete quantities $\mathbf{u}_h - \tilde{\mathbf{u}}_{ht}$. In order to do so, we split the error again into a linear and a nonlinear one. The linear error can be handled in a similar way as in [GS04] (for the space-continuous Stokes problem), whereas we consider the space-discrete grad-div stabilized problem. In [GS04], it is argued that the convective terms do not compromise the temporal errors and are therefore omitted. This is true in fact; the order of convergence in time is restricted by the linear part of the problem. Nonetheless, the nonlinear terms introduce notable technical difficulties and requirements. In particular, the convective terms lead to an unfeasible restriction of the time step size as $\Delta t \sim \nu^3$. This is required for the application of the discrete Gronwall Lemma. Otherwise, even higher regularity assumptions on \mathbf{u}_h would be needed. The convective terms are taken into account in the literature by [BC07] (for a first order projection method applied to Navier-Stokes), [Gue99] (for the unstabilized Navier-Stokes equations with BDF2 time-discretization), [She96] (for a differ-

ent second order time-discretization scheme of the unstabilized Navier-Stokes equations, acting in the space-continuous case), for instance. The dependence on critical problem parameters, in particular on ν , is not considered there. We consider the LPS SU and grad-div stabilized Navier-Stokes equations. In addition, it is a defined goal of this thesis to point out the restrictions for the time step size, mesh width and other parameters arising due to our error estimates.

We combine the temporal and spatial errors (from Sections 4.2.1 and 4.2.2) and derive a fully discrete error estimate in Section 4.2.3. The pressure error is bounded using the discrete inf-sup condition. This allows us to discuss a suitable design of the stabilization parameters and point out requirements, especially on the time step size:

$$\gamma = \gamma_0, \quad \nu Re_M^2 \lesssim 1, \quad \tau_M^n \lesssim \min \left\{ \frac{(\Delta t)^2}{\nu^2 |\tilde{\mathbf{u}}_M^n|^2}, \frac{1}{|\tilde{\mathbf{u}}_M^n|^2 h_M^{2(s_u - k_u)}}, h_M^{d-2(s_u - k_u)} \right\},$$

$$\Delta t \lesssim \min \{ h^{d/(2p)-2(s_u - k_u)}, \nu^3 \}, \quad h^{2k_u} + h^{2k_p+2} \lesssim e^{-C_{G,h}(u)} \nu \Delta t.$$

Note that this leads to the impression to omit the LPS SU stabilization completely. In contrast, the second strategy presented in [AD15] suggests a parameter choice for τ_M^n that is comparable with the one obtained from the usual semi-discrete analysis from Chapter 3. We infer that the above parameter design is too restrictive and can be circumvented.

The fully discrete analysis is furthermore afflicted with the auxiliary introduction of a semi-discrete, stabilized velocity \mathbf{u}_h ; in fact, both ansatzes from [AD15] face this challenge if the same quasi-optimal rates are desired. This leads to regularity assumptions for the semi-discrete velocity.

Hence, a promising alternative would be to omit a splitting of the error. This would lead to less requirements; mainly, assumptions on the continuous solution (\mathbf{u}, p) would suffice. More thorough estimates of the convective and stabilization terms would also lead to less restrictive conditions. However, the fact that $\tilde{\mathbf{u}}_{ht}^n$ is not weakly solenoidal in this segregation algorithm might lead to difficulties compared to usual techniques.

Note that the theoretical results from Chapters 3 and 4 assume homogeneous Dirichlet boundary conditions. Our numerical test cases often do not fit into this setting. Different boundary data often give rise to additional complications in the analysis. For example, the so-called “do-nothing“ condition of outflow character is built such that it does not affect the flow (in order to simulate significantly larger domains):

$$(\nu \nabla \mathbf{u} - p \mathbb{I}) \cdot \mathbf{n} = 0 \quad \text{on the outflow boundary.}$$

This is a very common condition and used in [Gre91], for instance. But as pointed out in [BMZ14], there are few analytical results. In particular, there are still stability issues

that are addressed by [BMZ14]. However, we do not observe numerical effects of these difficulties in our simulations.

6.2. Discussion of the Numerical Results

A highly parallel CFD solver based on the C++-FEM package `deal.II` for the time dependent Navier-Stokes problem was developed by D. Arndt from Göttingen. As part of this thesis, the implementation is extended to the non-isothermal case by myself, in particular, to include the coupling with the Fourier equation. Together with D. Arndt, we implemented the bubble enrichment of finite element spaces as introduced in Section 2.2.2. In Sections 5.1, 5.2 and 5.3, the proven convergence rates in h and Δt towards the respective analytical solution of the Navier-Stokes or Oberbeck-Boussinesq equations are validated numerically. Especially Sections 5.1 and 5.2 show that for small viscosities, grad-div stabilization guarantees the appropriate behavior of the errors; its use already diminishes the errors notably. A suitable parameter choice is $\gamma_M = \mathcal{O}(1)$ in all examples and for a broad range of ν . Adding LPS SU stabilization does not improve the results to a similar amount but does not harm neither. We point out that a choice as $\tau_{M/L}^{u/\theta} \sim h/\|\mathbf{u}_h\|_{\infty,M/L}$ seems favorable. Using enriched elements improves the errors in general. Note that more degrees of freedom are used here but the inf-sup stability of discrete velocity and pressure spaces is weaker in the sense that a larger velocity ansatz space is used.

The non-isothermal example of a temperature peak moving through a domain and hitting a Dirichlet wall with $\mathbf{u} \cdot \mathbf{n} > 0$ eventually is considered in Section 5.3. The case of large Rayleigh numbers and small α is the most interesting one since the calculated errors are large. When the peak hits the wall, in the unstabilized case, one observes spurious temperature oscillations in the solution spreading across the whole domain. One would expect a stabilizing effect of LPS SU because it affects the flow in streamline direction, where the wiggles occur. LPS SU combined with $\mathbb{Q}_2/\mathbb{Q}_1$ elements for the fine and coarse temperature spaces are not capable of reducing these oscillations. Only the use of LPS SU stabilization with $\mathbb{Q}_2^+/\mathbb{Q}_1$ for the fine and coarse spaces can damp the oscillations. The resulting errors decrease and the convergence rate in h is even improved. This example shows that the upper bound $\tau_L^\theta \lesssim \|\mathbf{u}_h\|_{\infty,L}^{-2}$, that is in agreement with the semi-discrete analysis, should not be exceeded since a larger stabilization parameter $\tau_L^\theta = 0.1$ deteriorates the results. The temporal accuracy, i.e., convergence rates with respect to the time step size, is as expected (or better) for all stabilization choices. The LPS SU parameter $\tau_L^\theta = \|\mathbf{u}_h\|_{\infty,L}^{-2}$ does not corrupt this though it is not of order $(\Delta t)^2$ as suggested by the fully discrete analysis from Chapter 4. As discussed before, we conclude that this requirement is not sharp due to the rather rough estimates of the convective and stabilization terms as well as the auxiliary introduction of a semi-discrete velocity.

From these insights, we infer that for the analytical solutions of Sections 5.1 and 5.2, grad-div stabilization $\gamma_M = \mathcal{O}(1)$ suffices to handle small ν . Section 5.3 suggests that if the main flow hits a Dirichlet wall in wall-normal direction, streamline upwinding LPS, especially in combination with enriched elements, damps occurring oscillations. The mesh width restriction found by the analysis in Section 3.2.1 cannot be observed empirically.

The other examples describe more realistic flow, where no analytical solution is known. In Section 5.4, laminar isothermal flow over a horizontal plate is considered. For a Reynolds number of 10^3 , spurious wiggles occur in front of the plate if an isotropic grid is used. This setting is comparable to the situation of a Dirichlet wall with $\mathbf{u} \cdot \mathbf{n} > 0$. These unphysical oscillations can be damped by using LPS SU stabilization; grad-div is not sufficient. For this laminar example, τ_M^u has to be chosen of order $\mathcal{O}(h^0)$ if fine and coarse space are $\mathbb{Q}_2/\mathbb{Q}_1$; a scaling as $\mathcal{O}(h^2)$ does not provide enough damping. The correct choice strongly depends on the used coarse space, as suggested by the theory in Chapter 3: If the coarse space is smaller than \mathbb{Q}_1 , the choice of $\mathcal{O}(h^0)$ damps too much. The best results are obtained if the grid is refined near the boundary layer, especially at the beginning of the plate, and coarse away from the plate where wiggles appear. In this case, LPS SU stabilization is not needed as mesh diffusivity serves the stabilization purpose. Therefore, it can be stated that LPS SU stabilization damps oscillations in the numerical solution that occur especially for globally refined isotropic grids.

The heated cavity in Section 5.5 allows us to assess the effect of grad-div and LPS SU stabilization in case of non-isothermal flow in a stationary regime $10^4 \leq Ra \leq 10^8$ near transition to the time dependent case. For a large range of $10^4 \leq Ra \leq 10^7$, no stabilization is needed in order to capture the expected flow characteristics. Near the transition point, grad-div stabilization is needed in order to overcome numerical instabilities. The positive effect is also reflected in the benchmark quantities. LPS SU for velocity or temperature provides only a slight improvement because the grid is resolved within the boundary layers.

For the case of isotropic turbulence (Taylor-Green vortex, Section 5.6), we investigate numerically whether grad-div and LPS SU serve as implicit turbulence models. A comparison with Kolmogorov's $-5/3$ -law for the energy cascade shows that grad-div stabilization alone does not provide enough dissipation in order to model the influence of the small non-resolved scales. Additional LPS SU stabilization acts in a similar way as the classical Smagorinsky model in the sense that it prevents that the energy for the smallest resolved scales increases. The theoretical reasoning due to dimensional analysis as well as the numerical tests suggest a parameter choice as $\tau_M^u \sim h/\|\mathbf{u}_h\|_{\infty, M}$. Note that $\tau_M^u = 1$ also seems appropriate but is not suited as a universal choice for different flow examples. So LPS SU is capable of adding dissipation to the fluid but - like the Smagorinsky model - is too dissipative. This is not very surprising as LPS SU is not adapted to the nature

of isotropic turbulence: It adds stabilization in the particular direction of the mean flow within a cell, whereas for the isotropic Taylor-Green vortex no direction is distinguished. Therefore, it would be interesting to test a turbulent example with clear main flow like the turbulent channel, for instance.

Rayleigh–Bénard convection in Section 5.7 is a transient non-isothermal example. In case of unsteady flow, grad-div stabilization and anisotropic grids are needed to compute benchmarks comparable to DNS results from the literature. The numerical tests show that a grad-div parameter $\gamma_M \in \{0.01, 0.1\}$ performs best for all $Ra \in \{10^5, 10^6, 10^7, 10^8, 10^9\}$. We point out that the use of grad-div proves crucial for the stability of the numerical solution for high Rayleigh numbers. LPS SU for the temperature becomes necessary if isotropic grids are used, where the boundary layers within the temperature are not resolved.

Summarizing, one can state that grad-div stabilization improves the numerical behavior in all considered examples. Not only the errors can be diminished but also benchmark quantities can be approximated better. A positive effect of LPS SU stabilization cannot be stated universally (at least, it does not harm in most cases). But for certain circumstances and settings, this technique is indeed favorable: Local projection stabilization is an adequate turbulence model and damps oscillations in case of transient flow for isotropic, globally refined grids. We point out that bubble enrichment of the fine (velocity and temperature) finite element spaces yields an improvement especially when used in the context of LPS SU stabilization.

6.3. Conclusion

In this thesis, we consider the Oberbeck-Boussinesq model that is suited to model non-isothermal incompressible flow if the flow is driven by small temperature differences. In order to diminish instabilities of the numerical solution, we apply LPS SU and grad-div stabilization in combination with inf-sup stable velocity-pressure elements. A pressure-correction projection method of second order is used for discretization in time. Our analytical and experimental results imply that the method has advantageous properties in the sense explained below.

The semi-discrete and fully discrete settings are analyzed; both the semi-discrete and the fully discrete solutions of the stabilized problem are stable. A priori error estimates of the expected order can be shown and lead to suggestions for a suitable parameter design, that is tested numerically afterwards. The analysis relies strongly on the discrete inf-sup stability of the finite element spaces: Estimates for velocity and pressure can be performed separately. A drawback of inf-sup stable elements (compared to equal-order) is that no precise parameter design is obtained by the analysis; instead, a range of possible choices

is suggested. This means that the choice of stabilization parameters is an important issue for the numerical tests. When the LPS SU stabilization is interpreted as an implicit turbulence model, we can make a clear assertion using dimensional analysis.

The empirical tests of a suitable parameter choice are in good agreement with the parameter design obtained by the semi-discrete analysis. However, a violation of the mesh width restriction as obtained in Section 3.2.1 does not lead to a deterioration of the errors in the numerical solutions. In addition, the parameter bound for the LPS SU parameter we found through the fully discrete analysis does not lead to a sufficient stabilization (in cases where LPS SU yields an improvement). This supports the wish for a more thorough consideration of the convective and stabilization terms in the fully discrete setting and a direct estimation of the fully discrete error without introduction of an auxiliary semi-discrete problem.

In order to perform sound empirical tests, we consider a variety of numerical examples. These sustain the conclusion that grad-div stabilization with $\gamma_M = \mathcal{O}(1)$ is important for robustness of the method. As it was pointed out by [Lin14], a proper choice of γ_M is important for improved mass conservation, in particular for volume forces of gradient type. The work of [dFGAJN15] for the time-dependent Oseen problem (with Taylor-Hood elements) confirms our observation that grad-div stabilization alone is often sufficient to obtain stable approximate solutions. In general, LPS SU does not deteriorate the results in any of the examined cases. LPS SU stabilization is recommendable if (isotropic) grids are used that are not well adapted to the specific example. In case of dominating convection, spurious oscillations can be suppressed by a large amount. Especially, enrichment of the discrete ansatz spaces for velocity and temperature by bubble functions leads to an improvement of the results.

A. Mathematical Tools and Notation

A.1. Notation

Let $\Omega \subset \mathbb{R}^d$, $d \in \{2, 3\}$, denote a bounded open domain with Lipschitz boundary. Vector-valued quantities are written in bold letters. We write for the Euclidean coordinates,

$$\mathbf{x} = (x, y)^T = (x_1, x_2)^T \in \mathbb{R}^2 \quad \text{or} \quad \mathbf{x} = (x, y, z)^T = (x_1, x_2, x_3)^T \in \mathbb{R}^3$$

and for the components of vectors, we use the notation

$$\begin{aligned} \mathbf{v} &= (v_1, \dots, v_d)^T \in \mathbb{R}^d, \\ \text{or: } \mathbf{v} &= (v_x, v_y)^T \in \mathbb{R}^2, \quad \mathbf{v} = (v_x, v_y, v_z)^T \in \mathbb{R}^3. \end{aligned}$$

For velocity components, we can also write $\mathbf{u} = (u, v, w)^T \in \mathbb{R}^3$. We denote the gradient with respect to the spatial variables of vector or scalar fields with $\nabla := \nabla_x$. Let $\nabla \cdot$ indicate the divergence of a vector field, \otimes the tensor product and \times the cross product.

A.2. Function Spaces

Let $K \subset \Omega$. We denote with $C(K)$ the space of continuous functions $v: K \rightarrow \mathbb{R}$. For $p \in [1, \infty]$, the Lebesgue space $L^p(K)$ is the function space containing all measurable functions $u: K \rightarrow \mathbb{R}$, such that

$$\begin{aligned} \|u\|_{L^p(K)} &:= \left(\int_K |u(\mathbf{x})|^p d\mathbf{x} \right)^{1/p} < \infty \quad \text{for } p \in [1, \infty), \\ \|u\|_{L^\infty(K)} &:= \text{ess sup}_{\mathbf{x} \in K} |u(\mathbf{x})| < \infty. \end{aligned}$$

$L^p(K)$ are Banach spaces. Additionally, $L^2(K)$ is a Hilbert space with respect to the inner product

$$(u, v)_{L^2(K)} := \int_K u(\mathbf{x})v(\mathbf{x})d\mathbf{x}.$$

The dual pairing of a Banach space X and its dual space X' is written as $\langle \cdot, \cdot \rangle_{X' \times X}$.

We fix some notation: Throughout this thesis, we use

$$\begin{aligned} \|u\|_0 &:= \|u\|_{L^2(\Omega)}, & \|u\|_{0,K} &:= \|u\|_{L^2(K)}, \\ \|u\|_\infty &:= \|u\|_{L^\infty(\Omega)}, & \|u\|_{\infty,K} &:= \|u\|_{L^\infty(K)}, \\ (u, v) &:= (u, v)_{L^2(\Omega)}, & (u, v)_K &:= (u, v)_{L^2(K)} \end{aligned}$$

if not stated otherwise. Moreover, let

$$L_*^2(\Omega) := \{q \in L^2(\Omega) : \int_\Omega q(\mathbf{x}) d\mathbf{x} = 0\}.$$

Let $m \in \mathbb{N}_0$ and $\alpha = (\alpha_1, \dots, \alpha_n)$ denote a multiindex of length $|\alpha| := \sum_{i=1}^n \alpha_i$. The Sobolev space $W^{m,p}(\Omega)$ consists of all m -times weakly differentiable functions $u: \Omega \rightarrow \mathbb{R}$ such that

$$\begin{aligned} \|u\|_{W^{m,p}(\Omega)} &:= \left(\sum_{0 \leq |\alpha| \leq m} \|D^\alpha u\|_{L^p(\Omega)}^p \right)^{1/p} < \infty \quad \text{for } p \in [1, \infty), \\ \|u\|_{W^{m,\infty}(\Omega)} &:= \max_{0 \leq |\alpha| \leq m} \|D^\alpha u\|_{L^\infty(\Omega)} < \infty, \end{aligned}$$

where $D^\alpha u$ denotes the α -th weak partial derivative. In particular, we have $L^p(\Omega) = W^{0,p}(\Omega)$. Note that $W^{m,p}(\Omega)$ are Banach spaces and

$$H^m(\Omega) := W^{m,2}(\Omega)$$

are Hilbert spaces. Further, $H_0^m(\Omega) = W_0^{m,2}(\Omega) := \{u \in H^m(\Omega) \mid u|_{\partial\Omega} = 0\}$. Note that on the space $W_0^{1,2}(\Omega)$, the norms $\|\cdot\|_{W^{1,2}(\Omega)}$ and $\|\nabla(\cdot)\|_0$ are equivalent (due to the Poincaré inequality [A.3.2](#)).

For the Hilbert spaces (with $p = 2$), we use the abbreviations in this thesis

$$\|u\|_m := \|u\|_{W^{m,2}(\Omega)}, \quad \|u\|_{m,K} := \|u\|_{W^{m,2}(K)}.$$

The Euclidean norm for vectors is denoted by $|\cdot|$. Besides, we write for products of two vectors $\mathbf{v}, \mathbf{w} \in \mathbb{R}^d$:

$$\mathbf{v}\mathbf{w} = \mathbf{v} \cdot \mathbf{w} = \sum_{i=1}^d v_i w_i.$$

Let $[L^p(\Omega)]^d$ be the space of all functions $\mathbf{u}: \Omega \rightarrow \mathbb{R}^d$ such that all components of \mathbf{u} are $L^p(\Omega)$ -functions. For convenience, we denote the respective norm with $\|\cdot\|_{L^p(\Omega)}$ as well; for example, in case of the L^2 -norm:

$$\|\mathbf{u}\|_0 := \left(\int_{\Omega} |\mathbf{u}(\mathbf{x})|^2 d\mathbf{x} \right)^{1/2}.$$

The spaces $[W^{m,p}(\Omega)]^d$ and the associated norms are defined analogously.

For evolution equations, we need the notion of functions depending on time with values in Banach or Hilbert spaces. We refer the reader to [Zei86] for details.

Definition A.2.1 (Bochner spaces).

Let $(Z, \|\cdot\|_Z)$ be a Banach space, $0 < T < \infty$. For $1 \leq p < \infty$ and vector-valued functions $u: (0, T) \rightarrow Z$ with values in Z , we define

$$L^p(0, T; Z) := \{u: (0, T) \rightarrow Z \text{ measurable} \mid \|u\|_{L^p(0, T; Z)} < \infty\},$$

where

$$\|u\|_{L^p(0, T; Z)} := \left(\int_0^T \|u(t)\|_Z^p dt \right)^{1/p},$$

and for $p = \infty$

$$L^\infty(0, T; Z) := \{u: (0, T) \rightarrow Z \text{ measurable} \mid \exists M \in (0, \infty): \|u(t)\|_Z < M \text{ in } (0, T) \text{ a. e.}\}.$$

If vector valued functions $\mathbf{u}: (0, T) \rightarrow [Z]^d$ are considered, the respective norms are also denoted as $\|\mathbf{u}\|_{L^p(0, T; Z)}$ for convenience. The notation

$$\|u\|_{L^\infty(0, T; W^{1,p}(\Omega))} := \text{ess sup}_{t \in (0, T)} \|\nabla u(t)\|_p$$

indicates the use of the semi-norm $\|\nabla(\cdot)\|_p$ instead of $\|\cdot\|_{W^{1,p}(\Omega)}$.

A function $u: [0, T] \rightarrow Z$ is called continuous in $t_0 \in [0, T]$ if

$$\lim_{\tau \rightarrow 0, t_0 + \tau \in [0, T]} \|u(t_0 + \tau) - u(t_0)\|_Z = 0.$$

We denote with $C(0, T; Z)$ the space of all functions $u: [0, T] \rightarrow Z$ that are continuous in all points $t_0 \in [0, T]$.

Generalized time derivatives can be defined as follows.

Definition A.2.2 (Generalized time derivatives).

Let $u \in L^1(0, T; Y)$ and $w \in L^1(0, T; Z)$ with Banach spaces Y, Z . Then w is called n -th generalized derivative of u on $(0, T)$ if it holds

$$\int_0^T \phi^{(n)}(t)u(t) dt = (-1)^n \int_0^T \phi(t)w(t) dt \quad \forall \phi \in C_0^\infty(0, T). \quad (\text{A.1})$$

We write $u^{(n)}(t) := w(t)$ or for $n = 1$, $\partial_t u(t) := w(t)$.

For real, separable Hilbert spaces X and $1 < p, q < \infty$ with $\frac{1}{p} + \frac{1}{q} = 1$, we can reformulate (A.1). Let $u \in L^p(0, T; X)$. If there exists $w \in L^q(0, T; X)$ with

$$\int_0^T (u(t), v)_X \phi^{(n)}(t) dt = (-1)^n \int_0^T (w(t), v)_X \phi(t) dt \quad \forall v \in X \quad \forall \phi \in C_0^\infty(0, T),$$

then the generalized derivative $u^{(n)}$ exists as $u^{(n)} = w$. It holds

$$\frac{d^n}{dt^n} (u(t), v)_X = (u^{(n)}(t), v)_X \quad \forall v \in X, t \in (0, T) \text{ a. e.} \quad (\text{A.2})$$

This gives rise to the following Sobolev spaces. Let X be a real, separable Hilbert space and $m \in \mathbb{N}$. For $1 < p, q < \infty$ with $\frac{1}{p} + \frac{1}{q} = 1$, we set

$$W^{m,p}(0, T; X) := \left\{ v \in L^p(0, T; X) \mid v^{(n)} \in L^q(0, T; X), n = 1, \dots, m \right\}. \quad (\text{A.3})$$

A.3. Inequalities and Auxiliary Calculations

A.3.1. Useful Inequalities

Lemma A.3.1 (Young's inequality).

Let $x, y \in \mathbb{R}$ and $\varepsilon > 0$ arbitrary. Then the following holds for $1 < p, q < \infty$ satisfying $\frac{1}{p} + \frac{1}{q} = 1$:

$$|xy| \leq \varepsilon |x|^p + \frac{(p\varepsilon)^{1-q}}{q} |y|^q. \quad (\text{A.4})$$

Proof. A proof is given in [Alt02]. □

Lemma A.3.2 (Poincaré's inequality).

Let $\Omega \subset \mathbb{R}^d$ be a bounded open domain. Then there is $C > 0$ depending only on the domain such that for all $u \in W_0^{1,2}(\Omega)$, it holds

$$\|u\|_0 \leq C \|\nabla u\|_0.$$

Proof. See [Dzi10]. □

Lemma A.3.3 (Trace inequality).

Let $\Omega \subset \mathbb{R}^d$, $d \in \{2, 3\}$, with Lipschitz boundary $\partial\Omega$. Let \mathcal{T}_h be a quasi-regular triangulation of Ω . Denote \mathcal{E}_h as the set of inner element faces $E \notin \partial\Omega$ of \mathcal{T}_h . Let h_T denote the outer radius of a cell $T \in \mathcal{T}_h$. Then there is $C_{tr} > 0$ such that for all $v \in W^{1,2}(\Omega)$

$$\|v\|_{0,E}^2 \leq C_{tr}(h_T^{-1}\|v\|_{0,T}^2 + h_T\|\nabla v\|_{0,T}^2).$$

Proof. We refer the reader to [HKW06]. □

A.3.2. Variants of Gronwall's Lemma

Lemma A.3.4 (Gronwall Lemma, integral version).

Let $T \in \mathbb{R}^+ \cup \{\infty\}$ and $\phi, g \in L^\infty(0, T)$. Moreover, let $\lambda \in L^1(0, T)$ denote a function which is non-negative almost everywhere in $[0, T]$. Assume g is monotonically increasing, positive and continuous in $[0, T]$. If the inequality

$$\phi(t) \leq g(t) + \int_0^t \lambda(s)\phi(s)ds$$

is fulfilled almost everywhere in $[0, T]$, then the following holds true almost everywhere in $0 \leq t \leq T$:

$$\phi(t) \leq g(t) \exp\left(\int_0^t \lambda(s)ds\right). \tag{A.5}$$

Proof. A proof can be found in [QV08]. □

Lemma A.3.5 (Gronwall Lemma, differential version).

Let $T \in \mathbb{R}^+ \cup \{\infty\}$, $t_0 \in [0, T)$ and let $\phi \in W^{1,1}(0, T)$ denote a function on $[0, T]$ that satisfies the inequality

$$\frac{d}{dt}\phi(t) \leq \lambda(t)\phi(t) + g(t)$$

almost everywhere in (t_0, T) with functions $\lambda, g \in L^1(t_0, T)$. Then the following holds true almost everywhere in $t_0 \leq t \leq T$:

$$\phi(t) \leq \phi(t_0)e^{\Lambda(t)} + \int_{t_0}^t e^{\Lambda(t)-\Lambda(s)}g(s)ds \tag{A.6}$$

with $\Lambda(t) := \int_{t_0}^t \lambda(s)ds$.

Proof. The proof is a corollary of the integral version (Lemma A.3.4). □

Lemma A.3.6 (Discrete Gronwall Lemma).

Consider $T > 0$ and $0 \leq k \leq T$. Let y^n, h^n, g^n, f^n be non-negative sequences satisfying for all $0 \leq m \leq [T/k]$

$$y^m + k \sum_{n=0}^m h^n \leq B + k \sum_{n=0}^m (g^n y^n + f^n) \quad \text{with } k \sum_{n=0}^{[T/k]} g^n \leq M$$

for some $M > 0$. Assume $kg^n < 1$ and let $\sigma = \max_{0 \leq n \leq [T/k]} (1 - kg^n)^{-1}$. Then for all $0 \leq m \leq [T/k]$, it holds

$$y^m + k \sum_{n=1}^m h^n \leq \exp(\sigma M) \left(B + k \sum_{n=0}^m f^n \right). \quad (\text{A.7})$$

Proof. A proof of this result can be found in [Tem95]. □

A.3.3. Estimates for the Convective Term**Lemma A.3.7.**

Let $\Omega \subset \mathbb{R}^d$, $d \leq 4$, $\mathbf{u}, \mathbf{v}, \mathbf{w} \in [W_0^{1,2}(\Omega)]^d$. The convective term

$$c(\mathbf{u}, \mathbf{v}, \mathbf{w}) = \frac{1}{2} ((\mathbf{u} \cdot \nabla \mathbf{v}, \mathbf{w}) - (\mathbf{u} \cdot \nabla \mathbf{w}, \mathbf{v}))$$

can be estimated in the following ways

$$c(\mathbf{u}, \mathbf{v}, \mathbf{w}) \leq \begin{cases} C \|\mathbf{u}\|_1 \|\mathbf{v}\|_1 \|\mathbf{w}\|_1, \\ C \|\mathbf{u}\|_2 \|\mathbf{v}\|_0 \|\mathbf{w}\|_1 & \forall \mathbf{u} \in [W^{2,2}(\Omega) \cap W_0^{1,2}(\Omega)]^d, \\ C \|\mathbf{u}\|_2 \|\mathbf{v}\|_1 \|\mathbf{w}\|_0 & \forall \mathbf{u} \in [W^{2,2}(\Omega) \cap W_0^{1,2}(\Omega)]^d, \\ C \|\mathbf{u}\|_1 \|\mathbf{v}\|_2 \|\mathbf{w}\|_0 & \forall \mathbf{v} \in [W^{2,2}(\Omega) \cap W_0^{1,2}(\Omega)]^d \end{cases}$$

with some $C > 0$. Furthermore, for $d \leq 3$, it holds

$$\begin{aligned} c(\mathbf{u}, \mathbf{v}, \mathbf{u}) &\leq C \|\mathbf{u}\|_0^{1/2} \|\mathbf{u}\|_1^{3/2} \|\mathbf{v}\|_1, \\ c(\mathbf{u}, \mathbf{v}, \mathbf{w}) &\leq C \|\mathbf{u}\|_1 \|\mathbf{v}\|_1^{1/2} \|\mathbf{v}\|_2^{1/2} \|\mathbf{w}\|_0 \quad \forall \mathbf{v} \in [W^{2,2}(\Omega) \cap W_0^{1,2}(\Omega)]^d. \end{aligned}$$

Proof. The proof utilizes Hölder's inequality and the Sobolev inequalities. We refer the reader to [Tem95]. □

Lemma A.3.8.

Let $\Omega \subset \mathbb{R}^d$, $\mathbf{u} \in [L^2(\Omega)]^d$ and $\mathbf{w} \in [W^{1,2}(\Omega)]^d$. Denote by \mathbf{u}_M the average over a cell $M \subset \Omega$, i.e.,

$$\mathbf{u}_M := \frac{1}{|M|} \int_M \mathbf{u}(\mathbf{x}) \, d\mathbf{x},$$

where $|M|$ denotes the measure of M in \mathbb{R}^d . Then it holds

$$\|(\mathbf{u}_M \cdot \nabla) \mathbf{w}\|_{0,M}^2 \leq \frac{1}{|M|} \|\mathbf{u}\|_{0,M}^2 \|\mathbf{w}\|_{1,M}^2.$$

Proof. Let $|\cdot|$ denote the vector norm in \mathbb{R}^d . Then we have via the Cauchy-Schwarz inequality:

$$|\mathbf{u}_M|^2 = \frac{1}{|M|^2} \left| \int_M \mathbf{u}(\mathbf{x}) \, d\mathbf{x} \right|^2 = \frac{1}{|M|^2} |(\mathbf{u}, \mathbf{1})_M|^2 \leq \frac{1}{|M|^2} \|\mathbf{u}\|_{0,M}^2 \|\mathbf{1}\|_{0,M}^2 = \frac{1}{|M|} \|\mathbf{u}\|_{0,M}^2.$$

Finally, for the streamline derivative:

$$\begin{aligned} \|(\mathbf{u}_M \cdot \nabla) \mathbf{w}\|_{0,M}^2 &= \sum_{i=1}^d \left\| \sum_{j=1}^d u_{M,j} \frac{\partial w_i}{\partial x_j} \right\|_{0,M}^2 \leq \sum_{i=1}^d \left(\sum_{j=1}^d \left\| u_{M,j} \frac{\partial w_j}{\partial x_i} \right\|_{0,M} \right)^2 \\ &= \sum_{i=1}^d \left(\sum_{j=1}^d |u_{M,j}| \left\| \frac{\partial w_j}{\partial x_i} \right\|_{0,M} \right)^2 \leq \sum_{i=1}^d \left(\sum_{j=1}^d |u_{M,j}|^2 \right) \left(\sum_{j=1}^d \left\| \frac{\partial w_j}{\partial x_i} \right\|_{0,M}^2 \right) \\ &= \left(\sum_{j=1}^d |u_{M,j}|^2 \right) \sum_{i,j} \left\| \frac{\partial w_j}{\partial x_i} \right\|_{0,M}^2 = |\mathbf{u}_M|^2 \|\mathbf{w}\|_1^2 \leq \frac{1}{|M|} \|\mathbf{u}\|_{0,M}^2 \|\mathbf{w}\|_{1,M}^2. \end{aligned}$$

□

A.4. Existence Results

Let X be a Hilbert space with scalar product $(\cdot, \cdot)_X$ and induced norm $\|\cdot\|_X$. Consider the variational problem:

Find $u \in X$ such that

$$a(u, v) = f(v) \quad \forall v \in X, \tag{A.8}$$

where $a: X \times X \rightarrow \mathbb{R}$ is a bilinear form and $f: X \rightarrow \mathbb{R}$ a linear functional. The Lax-Milgram Lemma states sufficient conditions for the existence and uniqueness of solutions of (A.8). A proof can be found in [Cia02].

Theorem A.4.1 (Lax-Milgram Lemma).

Assume that the bilinear form $a: X \times X \rightarrow \mathbb{R}$ is continuous, i.e.,

$$\exists \alpha_1 > 0: \quad |a(v, w)| \leq \alpha_1 \|v\|_X \|w\|_X \quad \forall v, w \in X,$$

and X -elliptic (or coercive), i.e.,

$$\exists \alpha_2 > 0: \quad a(v, v) \geq \alpha_2 \|v\|_X^2 \quad \forall v \in X.$$

Further, let the linear functional $f: X \rightarrow \mathbb{R}$ be continuous. Then problem (A.8) has a unique solution.

For evolution problems, we state a generalization of the Peano Theorem, which is an implication of the Fixed Point Theorem of Schauder (see [Zei86] for full proofs).

Let $(Y, \|\cdot\|_Y)$ be a Banach space, $f: D(f) \subset \mathbb{R} \times Y \rightarrow Y$ and $x_0 \in Y$. Consider an initial value problem of the form:

Find $x: [0, T] \rightarrow Y$ such that

$$\frac{d}{dt}x(t) = f(t, x(t)), \quad x(t_0) = x_0 \in Y. \quad (\text{A.9})$$

We assume that f is a compact operator, meaning that f is continuous and maps bounded sets $M \subset D(f)$ to relatively compact sets $f(M) \subset Y$. I.e., for all $\varepsilon > 0$, there are $y_1, \dots, y_{n(\varepsilon)} \in f(M)$ satisfying

$$\min_{1 \leq i \leq n(\varepsilon)} \|y_i - y\|_Y < \varepsilon \quad \forall y \in f(M).$$

Theorem A.4.2 (Generalized Peano Theorem).

For $t_0 \in \mathbb{R}$ and $x_0 \in Y$, define

$$Q_R := \{(t, y) \in \mathbb{R} \times Y: |t - t_0| \leq a, \quad |y - x_0| \leq R\}$$

with fixed numbers $a, R \in (0, \infty)$. Let $f|_{Q_R}: Q_R \rightarrow Y$ be compact and $\|f(t, y)\|_Y \leq K$ for all $(t, y) \in Q_R$ with fixed $K > 0$. Let $c := \min(a, R/K)$. Then the initial value problem (A.9) has at least one solution $x(\cdot) \in C^1(t_0 - c, t_0 + c; Y)$.

B. Appendix: Numerical Examples

In this chapter, we present some results that are mentioned in Chapter 5 but not shown there for reasons of space.

B.1. Isothermal Convergence Results: 3D No-Flow Problem

In order to investigate the influence of grad-div stabilization, we consider the No-Flow test problem in three dimensions with exact stationary solution

$$\mathbf{u}(\mathbf{x}) \equiv \mathbf{0}, \quad p(\mathbf{x}) = x^3 + y^2 + z^2 + x - 1 \quad \text{in } \Omega = (0, 1)^3$$

for $\mathbf{x} = (x, y, z)^T$ and forcing term $\mathbf{f}_u(\mathbf{x}) = (3x^2 + 1, 3y^2, 3z^2)^T$. The used grids are randomly distorted by 1% as shown below in Figure B.1.

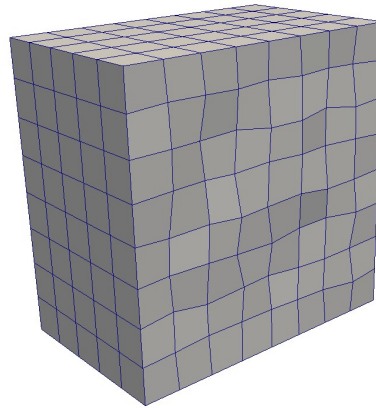


Figure B.1.: No-Flow test: Cut through mesh.

B.2. Isothermal Convergence Results: 2D Couzy Problem

The Couzy test problem in $\Omega = (0, 1)^2$ is constructed such that

$$\begin{aligned} \mathbf{u}(\mathbf{x}) &= \sin(\pi t) \left(-\cos\left(\frac{\pi}{2}x\right) \sin\left(\frac{\pi}{2}y\right), \sin\left(\frac{\pi}{2}x\right) \cos\left(\frac{\pi}{2}y\right) \right)^T, \\ p(\mathbf{x}) &= -\pi \sin\left(\frac{\pi}{2}x\right) \sin\left(\frac{\pi}{2}y\right) \sin(\pi t) \end{aligned}$$

is a solution of the Navier-Stokes problem. The dependence of the velocity and pressure L^2 -errors on a constant grad-div parameter $\gamma_M \in \{0, 0.1, 1, 5\}$ for $Re = 10^3$ and $\mathbb{Q}_2 \wedge \mathbb{Q}_1$ elements is shown in Figure B.2.

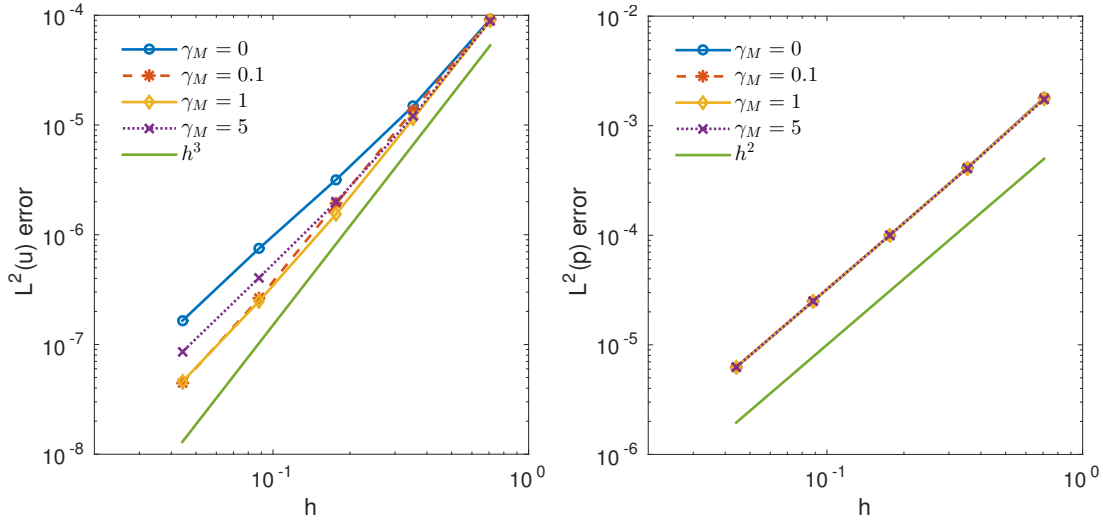


Figure B.2.: Two-dimensional Couzy test with $Re = 10^3$: Dependence of the L^2 -velocity error (left) and the L^2 -pressure error (right) on the grad-div parameter γ_M for $\mathbb{Q}_2 \wedge \mathbb{Q}_1$ elements.

The dependence of the L^2 -velocity and L^2 -pressure errors on Re for optimized grad-div parameters γ_M are considered in Figure B.3.

L^2 -velocity and L^2 -divergence errors for different LPS variants can be found in Figure B.4. We compare the effect of LPS SU stabilization and enrichment for $Re = 10^3$. $(\mathbb{Q}_2/\mathbb{Q}_1) \wedge \mathbb{Q}_1$ and $(\mathbb{Q}_2^+/\mathbb{Q}_1) \wedge \mathbb{Q}_1$ elements are combined with grad-div stabilization only and with additional LPS SU stabilization, i.e., $\tau_M^u \in \{0, \frac{1}{2}h/\|\mathbf{u}_h\|_{\infty, M}, \|\mathbf{u}_h\|_{\infty, M}^{-2}\}$.

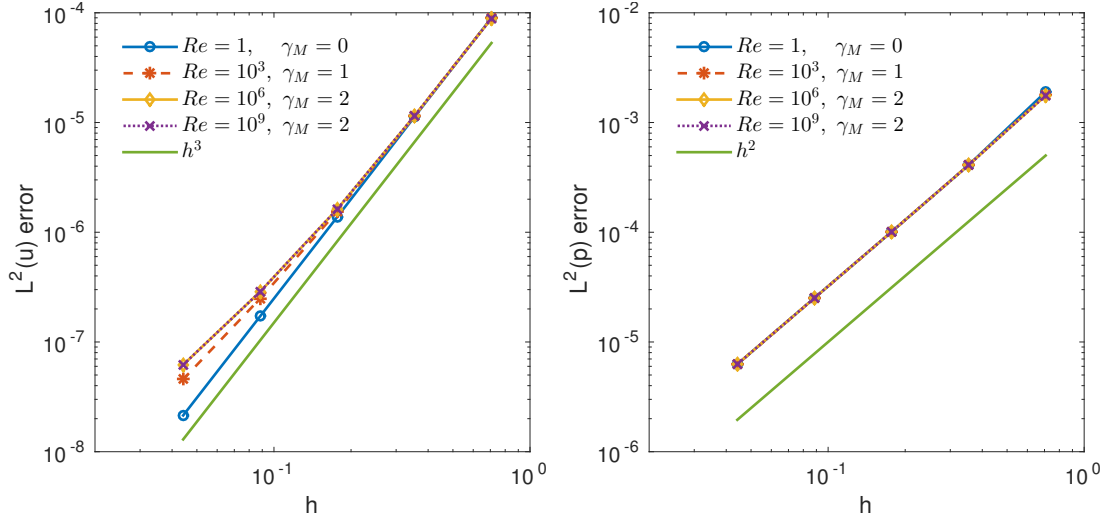


Figure B.3.: Two-dimensional Couzy test with optimized grad-div parameter γ_M : Dependence of the L^2 -velocity error (left) and the L^2 -pressure error (right) on Re for $\mathbb{Q}_2 \wedge \mathbb{Q}_1$.

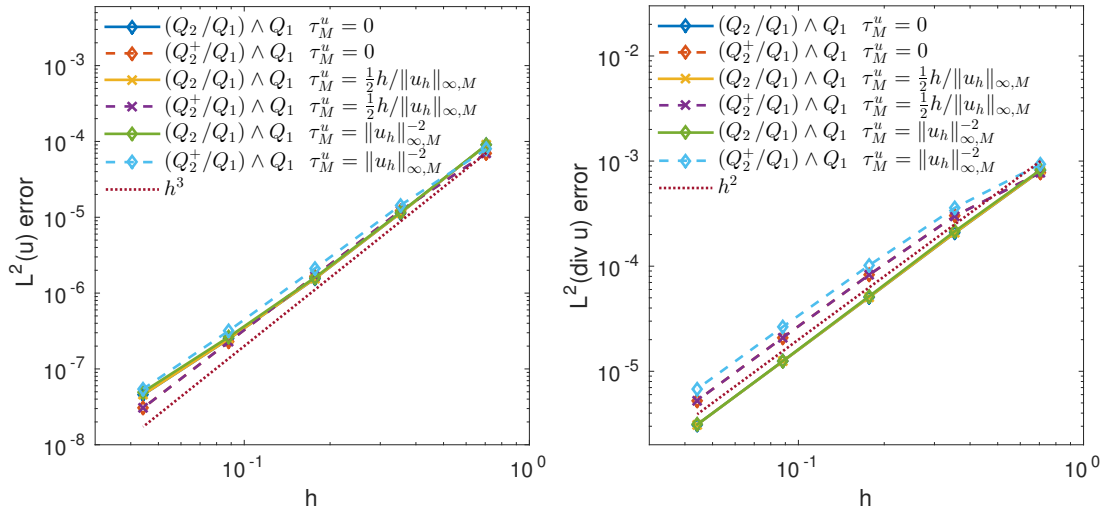


Figure B.4.: Two-dimensional Couzy test for $Re = 10^3$ with $\gamma_M = 1$: L^2 -velocity error (left) and L^2 -divergence error (right) for different LPS SU parameters τ_M^u for $(Q_2/Q_1) \wedge Q_1$ and $(Q_2^+/Q_1) \wedge Q_1$ elements.

B.3. Non-Isothermal Convergence Results: 2D Traveling Wave

We consider a time dependent, two-dimensional solution of the Oberbeck-Boussinesq equations for different parameters ν, α, β in a box $\Omega = (0, 1)^2$ with $t \in [0, 6 \cdot 10^{-3}]$:

$$\begin{aligned} \mathbf{u}(x, y, t) &= (100, 0)^T, \quad p(x, y, t) = 0, \\ \theta(x, y, t) &= (1 + 3200\alpha t)^{-1/2} \exp\left(-\left(\frac{1}{2} + 100tx\right)^2 \left(\frac{1}{800} + 4\alpha t\right)^{-1}\right), \\ \mathbf{f}_u(x, y, t) &= \left(0, -\beta(1 + 3200\alpha t)^{-1/2} \exp\left(-200(1 + 3200\alpha t)^{-1}(1 + 200t - 2x)^2\right)\right)^T, \\ f_\theta(x, y, t) &= 0 \end{aligned}$$

with $\mathbf{g} \equiv (0, -1)^T$ and (time dependent) Dirichlet boundary conditions for \mathbf{u} and θ .

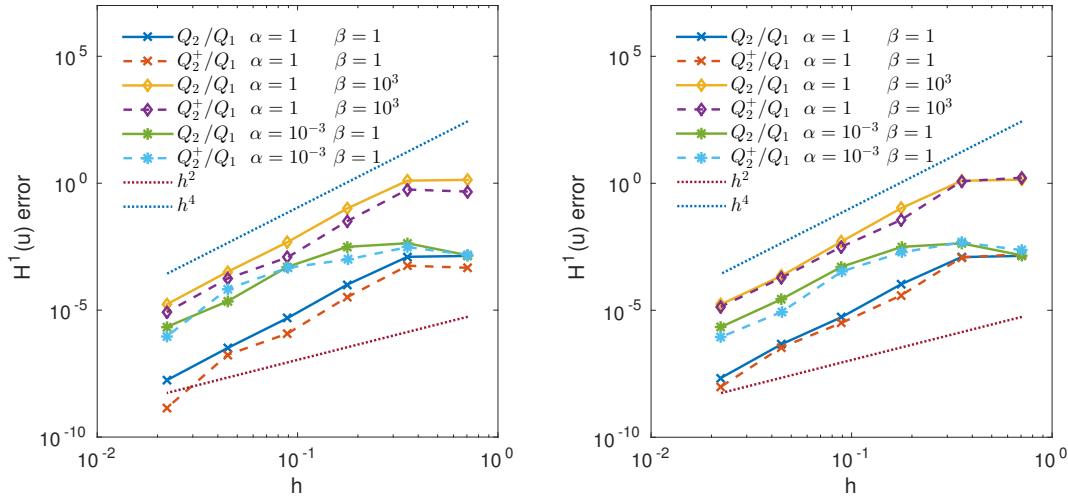


Figure B.5.: Velocity H^1 -errors for different finite elements and choices of α and β with $\tau_L^\theta = 0$ (left) and $\tau_L^\theta = h/\|\mathbf{u}_h\|_{\infty, L}$ (right).

Different stabilization parameter settings for (ν, α, β) and the resulting errors in velocity and pressure are considered in Figures B.5, B.6. With respect to desired convergence rates in velocity and pressure, even large β and small α do not require any stabilization. However, the errors are larger by orders of magnitude compared to the case $\alpha = 1, \beta = 1$. We point out that for small α , the temperature errors are improved by LPS SU stabilization (with $\tau_L^\theta > 0$). This does not affect the velocity and pressure errors considerably.

In Figure B.7, the influence of LPS stabilization for the temperature in case of small $\alpha = 10^{-3}$ is studied in more detail. Different choices of the fine space are considered as well as stabilization parameters. Whereas the temperature error is affected by these variations notably (see Figure 5.9), velocity and pressure errors are not in that amount.

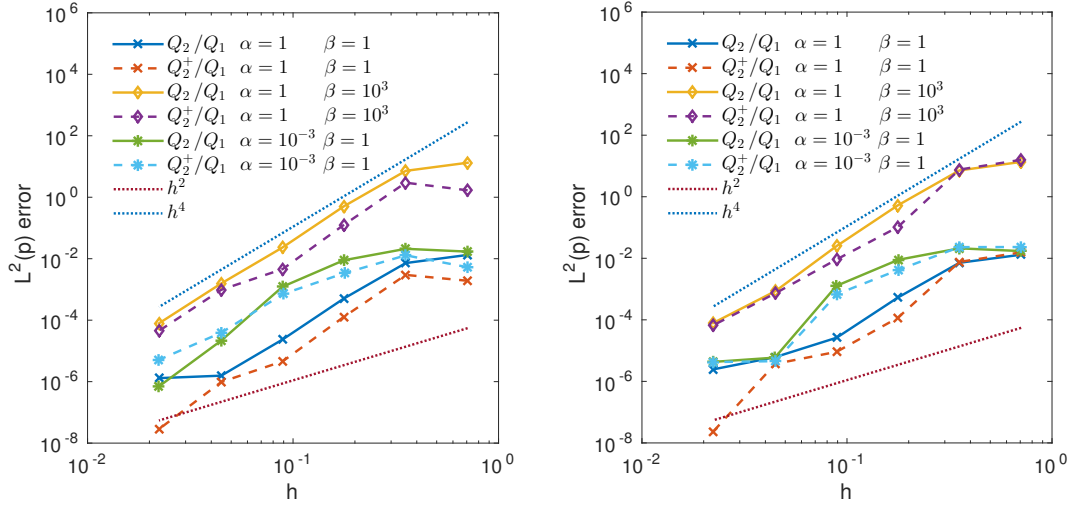


Figure B.6.: Pressure L^2 -errors for different finite elements and choices of α and β with $\tau_L^\theta = 0$ (left) and $\tau_L^\theta = h / \|u_h\|_{\infty, L}$ (right).

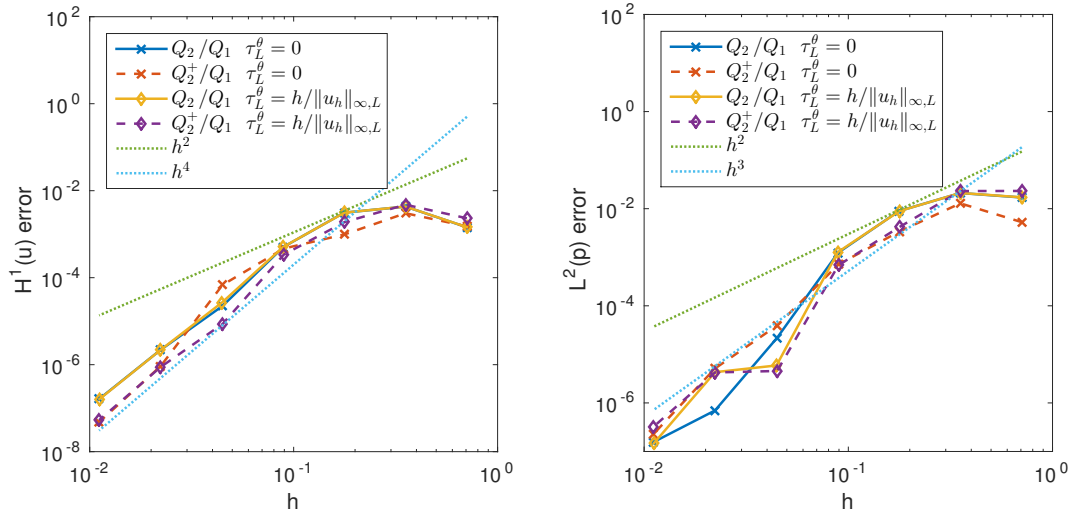


Figure B.7.: Velocity H^1 -errors (left) and pressure L^2 -errors (right) for different choices of τ_L^θ and finite elements, $(\nu, \alpha, \beta) = (1, 10^{-3}, 1)$.

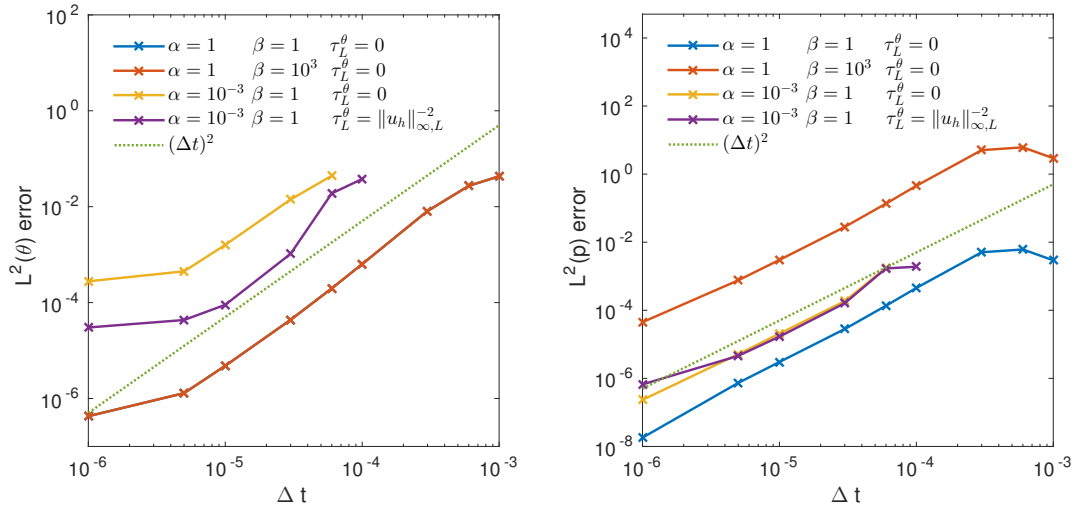


Figure B.8.: Temperature L^2 - (left) and pressure L^2 -errors (right) for different choices of α and β with $\mathbb{Q}_2^+/\mathbb{Q}_1$ elements.

Figure B.8 shows errors depending on the time step size Δt at fixed end time $T = 0.006$. The error $\|\theta(T) - \theta_{ht}^N\|_0$ is of order $\mathcal{O}((\Delta t)^2)$ as expected. Note that the error on the finest grid is corrupted by the error due to spatial discretization. The error $\|p(T) - p_{ht}^N\|_0$ shows an even better behavior than $\mathcal{O}(\Delta t)$.

B.4. Isothermal Laminar Flow: 2D Blasius Boundary Layers

The Blasius test case incorporates a two-dimensional laminar boundary layer that develops if there is steady flow with free stream velocity u_∞ parallel to the x -axis across a flat plate.

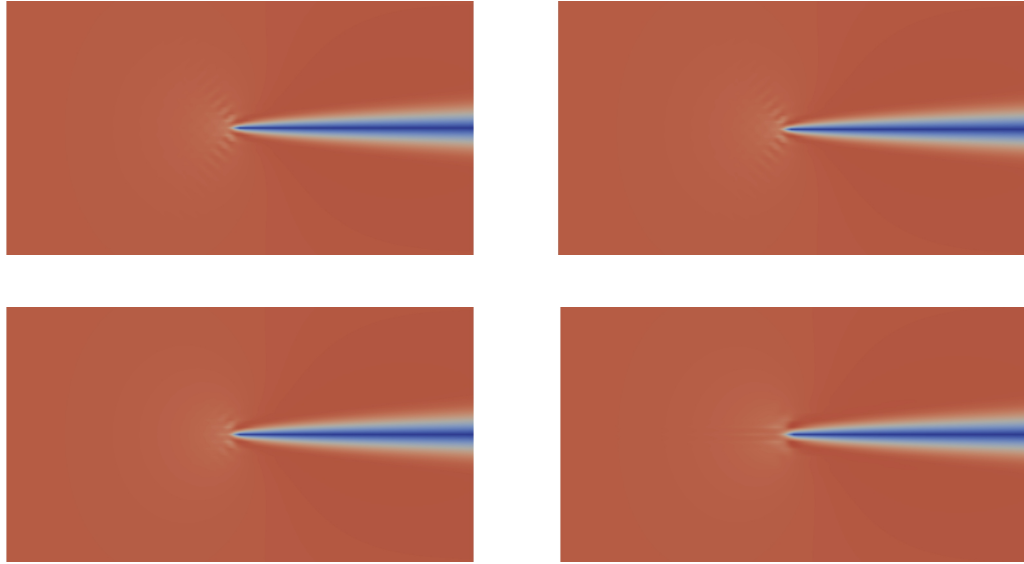


Figure B.9.: Blasius flow with $\nu = 10^{-3}$ for $\gamma_M = 1$ and different choices of the stabilization parameter τ_M^u with $(\mathbb{Q}_2^+/\mathbb{Q}_1) \wedge \mathbb{Q}_1$ elements: $\tau_M^u = 0$ (top left), $\tau_M^u = h^2/\|\mathbf{u}_h\|_{\infty,M}^2$ (top right), $\tau_M^u = h/\|\mathbf{u}_h\|_{\infty,M}^2$ (bottom left), $\tau_M^u = 1/\|\mathbf{u}_h\|_{\infty,M}^2$ (bottom right).

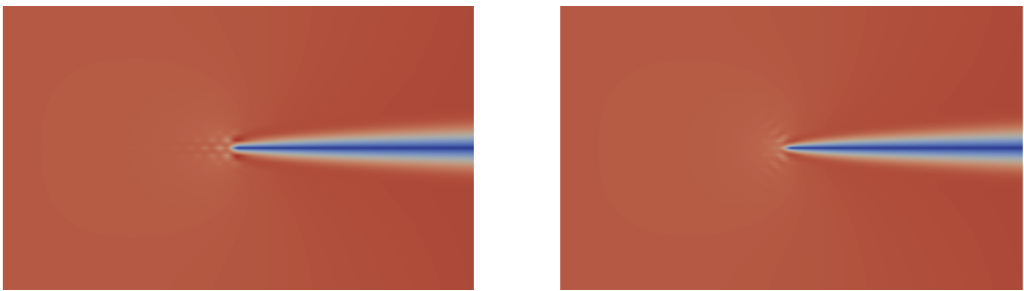


Figure B.10.: Blasius flow with $\nu = 10^{-3}$ for $\gamma_M = 1$, $\tau_M^u = \frac{1}{2}h/\|\mathbf{u}_h\|_{\infty,M}$ in combination with $(\mathbb{Q}_2/\mathbb{Q}_1) \wedge \mathbb{Q}_1$ (left), $(\mathbb{Q}_2^+/\mathbb{Q}_1) \wedge \mathbb{Q}_1$ elements (right).

In addition to grad-div, a LPS SU parameter $\tau_M^u = 1/\|\mathbf{u}_h\|_{\infty,M}^2$ can damp out the oscillations in front of the plate. This holds if $(\mathbb{Q}_2/\mathbb{Q}_1) \wedge \mathbb{Q}_1$ or $(\mathbb{Q}_2^+/\mathbb{Q}_1) \wedge \mathbb{Q}_1$ elements are used (see Figure B.9). Parameters τ_M^u of order $\mathcal{O}(h^2)$ do not remove the wiggles. $\tau_M^u \sim \mathcal{O}(h)$ already yields an improvement but does not provide as much damping as the choice of order

$\mathcal{O}(1)$. Figure B.10 illustrates that $\tau_M^u = \frac{1}{2}h/\|\mathbf{u}_h\|_{\infty,M}$ in conjunction with $(\mathbb{Q}_2/\mathbb{Q}_1) \wedge \mathbb{Q}_1$ elements and with enriched $(\mathbb{Q}_2^+/\mathbb{Q}_1) \wedge \mathbb{Q}_1$ elements is comparable to $\tau_M^u = h/\|\mathbf{u}_h\|_{\infty,M}^2$.

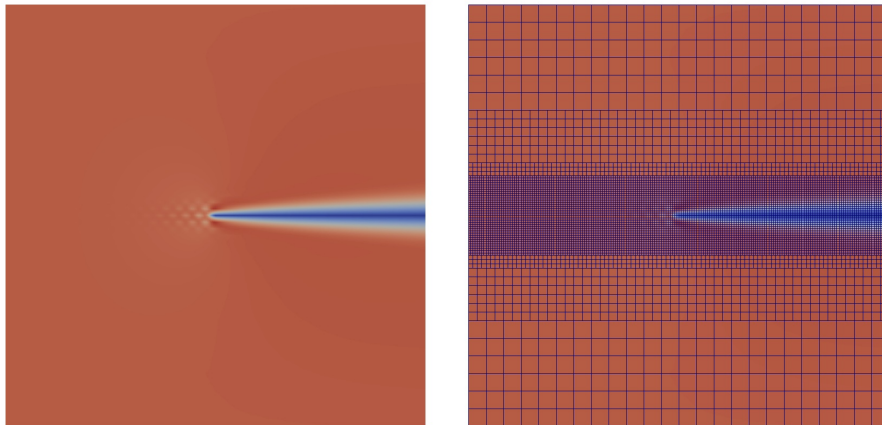


Figure B.11.: Refine cells with midpoint (x, y) if $|y| < \delta$, $\nu = 10^{-3}$, $\gamma_M = 1$: Velocity magnitude (left) and mesh (right).

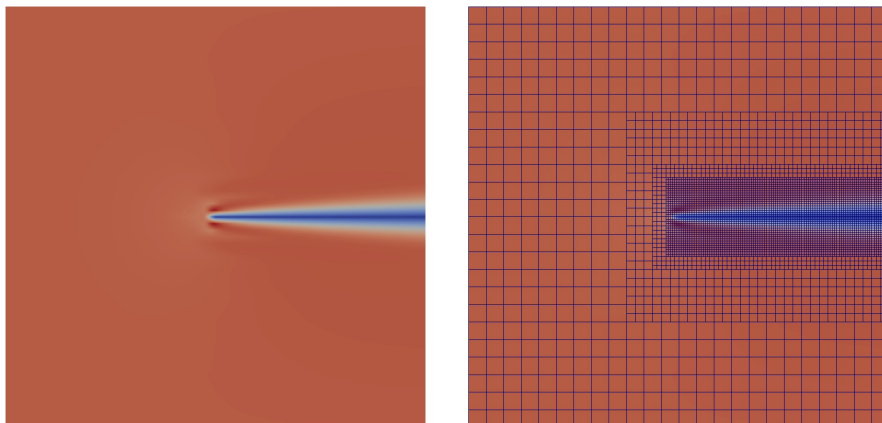


Figure B.12.: Refine in the boundary layer, $\nu = 10^{-3}$, $\gamma_M = 1$: Velocity magnitude (left) and mesh (right).

In Figures B.11, B.12 and B.13, we study refinement strategies near the plate in order to improve the numerical solution. We use $\nu = 10^{-3}$ and grad-div stabilization alone with $\gamma_M = 1$. The meshes are always shown on the right; the resulting velocity magnitude in case of grad-div stabilization $\gamma_M = 1$ on the left. The mesh in Figure B.11 is constructed by refinement of cells where the midpoint (x, y) satisfies $|y| < \delta$. The fine mesh in front of the plate is not suited to damp the oscillations. However, if only the boundary layer, i.e., the region at the plate, is resolved (Figure B.12), the coarser mesh in front of the plate provides mesh diffusion. A refinement criterion based on diminishing the total variation

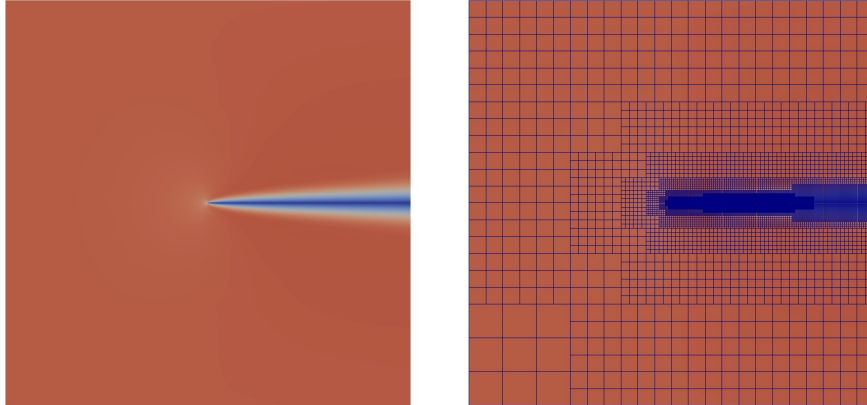


Figure B.13.: TGV based refinement criterion, $\nu = 10^{-3}$, $\gamma_M = 1$: Velocity magnitude (left) and mesh (right).

(TVD), in order to control the velocity difference within a cell, is considered in Figure B.13. It is constructed such that

$$tol_T := \sum_{i=1}^d \left(\max_{\mathbf{x} \in T} |u_i(\mathbf{x})| - \min_{\mathbf{x} \in T} |u_i(\mathbf{x})| \right) \approx 0.1$$

holds on each element $T \in \mathcal{T}_h$ for $\mathbf{u}_h = (u_1, \dots, u_d)^T$ in d dimensions.

B.5. Non-Isothermal Laminar Flow: 2D Heated Cavity

In this example, we consider laminar, non-isothermal flow in a cavity. The left vertical wall of the two-dimensional domain $\Omega = (0, 1)^2$ is heated, the right one is cooled. The flow is driven by this difference.

The mesh is shown in Figure B.14. It is adapted to resolve the boundary layer and is distorted randomly by 1%. The equidistant grid points are transformed by mappings $T_{ab}: [0, 1]^2 \rightarrow [0, 1]^2$ of the form

$$(x, y)^T \mapsto T_{ab}((x, y)^T) := \left(x - \frac{1}{2\pi}(1-a)\sin(2\pi x), y - \frac{1}{2\pi}(1-b)\sin(2\pi y) \right)^T$$

with parameters $0 < a, b < 1$ chosen as $a \approx Nu^{-1}$ and $b \approx Nu^{-1/3}$.

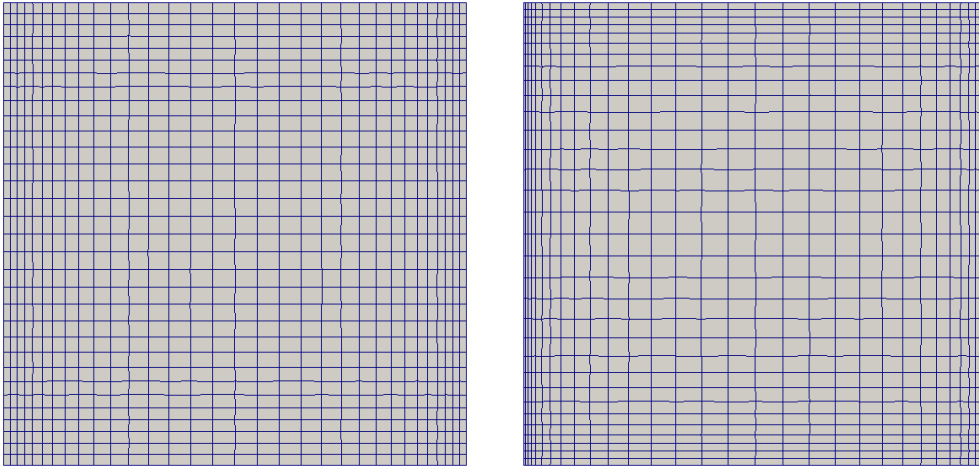


Figure B.14.: Anisotropic, randomly distorted mesh for heated cavity, $Ra = 10^4$ (left) and $Ra = 10^6$ (right), $N = 32^2$.

The steady states of the numerical solutions (\mathbf{u}_h, θ_h) for different Rayleigh numbers $Ra \in \{10^4, 10^5, 10^6, 10^7\}$, resulting in laminar flow, are presented in Figure B.15. No stabilization and $N = 64^2$ cells are used.

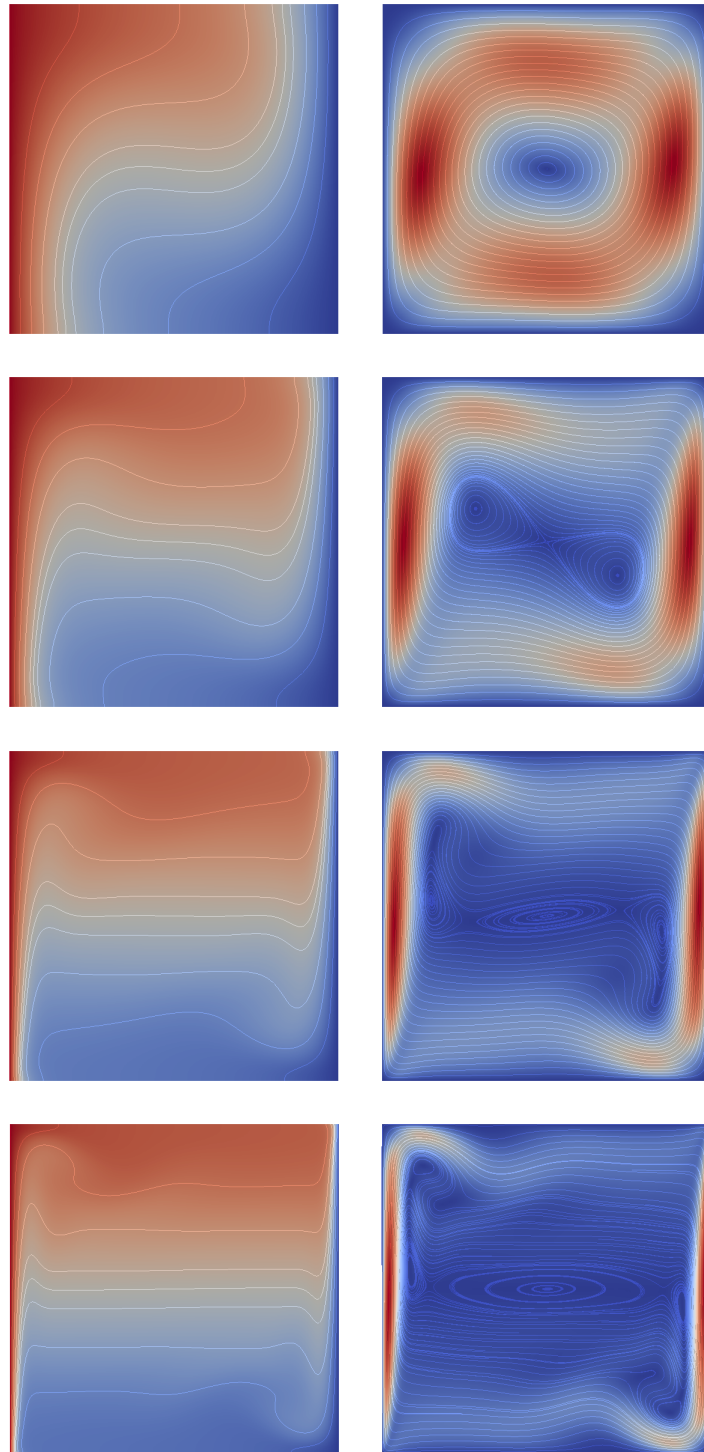


Figure B.15.: Heated cavity, temperature (left) and velocity magnitude (right) with streamlines, without stabilization, $Pr = 0.71$, $Ra \in \{10^4, 10^5, 10^6, 10^7\}$, $N = 64^2$.

B.6. Isothermal Turbulent Flow: 3D Taylor-Green Vortex

The Taylor-Green vortex is an example for isotropic turbulence. We study the adequacy of grad-div and LPS SU stabilization as an implicit LES subgrid model. In Figure B.16, the energy spectra with grad-div stabilization $\gamma_M = 1$, grad-div combined with LPS SU $\gamma_M = 1, \tau_M^u = 1$ and the classical Smagorinsky model are presented for a mesh width $h = \pi/16$. In case of $\gamma_M = 1$, the smallest resolved scales carry too much energy. Additional LPS SU stabilization provides more dissipation. The stabilization with $\gamma_M = 1, \tau_M^u = 1$ works as a turbulence model that has a dissipative effect similar to the classical Smagorinsky model. We remark that in the simulation, we choose the Smagorinsky parameter c_{smag} such that the best results with respect to the $-5/3$ -law are obtained.

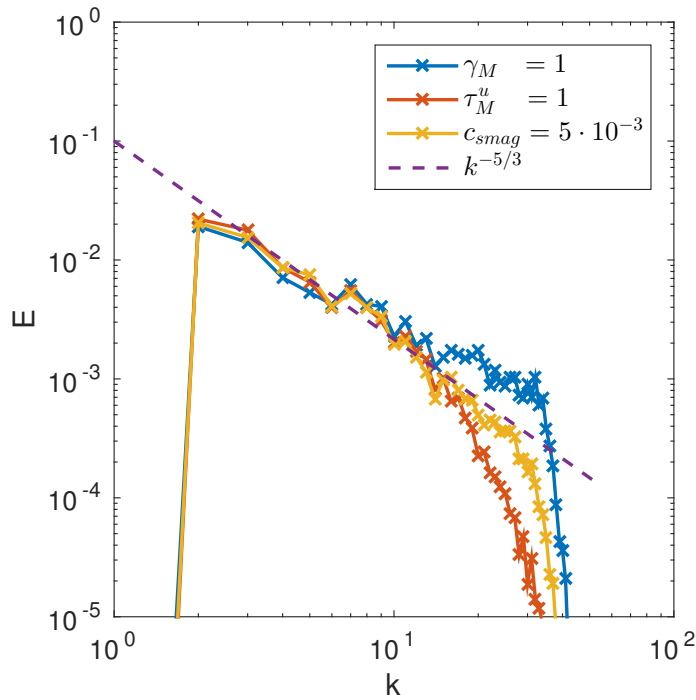


Figure B.16.: Energy spectra at $t = 9$, comparison between grad-div stabilization, grad-div stabilization with LPS SU and use of the Smagorinsky model, $\{a = 2\pi, b = 1\}$, $h = \pi/16$.

B.7. Non-Isothermal Flow: 3D Rayleigh–Bénard Convection

In the Rayleigh–Bénard example, the flow is driven by a temperature gradient between a heated bottom plate and a cooled top plate.

A snapshot of temperature iso-surfaces as well as streamlines of the associated velocity are shown in Figure B.17 for Rayleigh numbers $Ra \in \{10^5, 10^9\}$. $N = 10 \cdot 16^3$ cells, grad-div stabilization with $\gamma_M = 0.1$ and $\mathbb{Q}_2 \wedge \mathbb{Q}_1 \wedge \mathbb{Q}_2$ elements are used. The large scale behavior consists of one large convection cell, i.e., upflow of warm fluid and descent of cold fluid. The velocity streamlines indicate that indeed, material transport occurs.

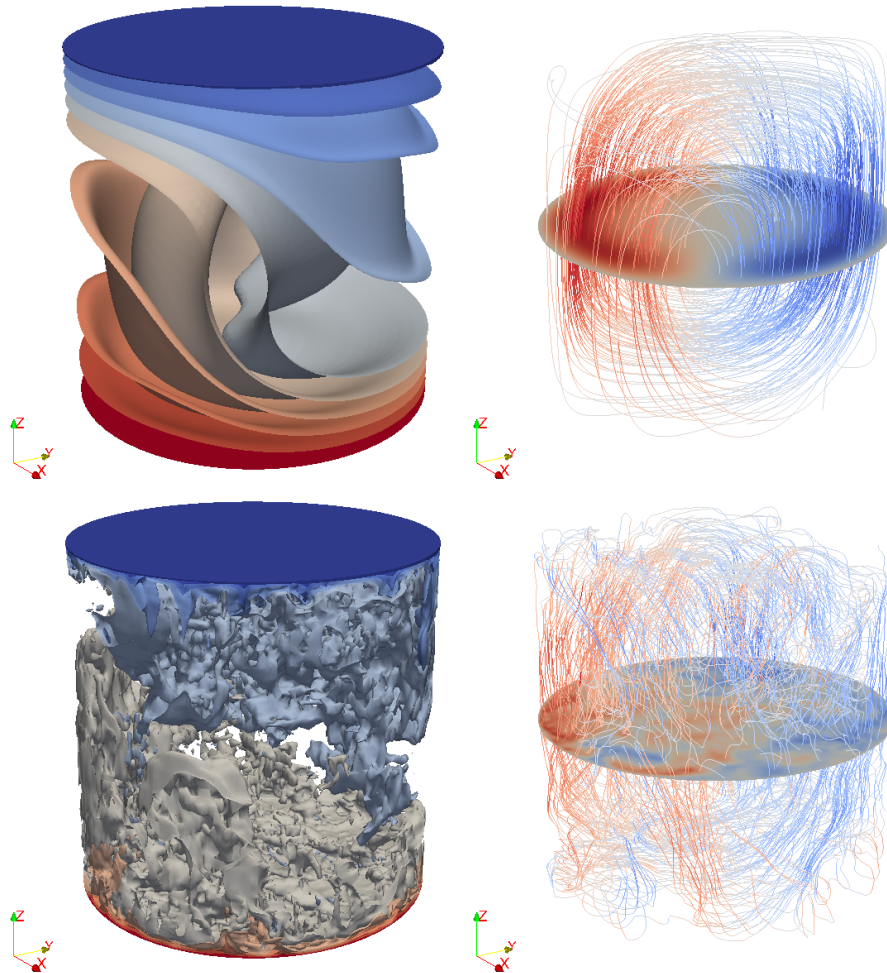


Figure B.17.: Temperature iso-surfaces (left) and streamlines of the associated velocities (right) at $T = 1000$ for $Pr = 0.786$, $Ra = 10^5$ (top) and $Ra = 10^9$ (bottom), $N = 10 \cdot 16^3$, $\gamma_M = 0.1$. Red colored streamlines indicate a positive z -component u_z , blue ones negative u_z .

In Table B.1, we examine the influence of different grad-div and LPS SU parameters with $(\mathbb{Q}_2/\mathbb{Q}_1) \wedge \mathbb{Q}_1 \wedge (\mathbb{Q}_2/\mathbb{Q}_1)$ finite elements. For $Ra = 10^9$, we apply a grid with $N = 10 \cdot 8^3$ cells that is transformed by T_{xyz} . Any LPS SU parameter does not improve the benchmark quantities and yields even worse results than grad-div stabilization alone. The upper bounds from the semi-discrete analysis of Chapter 3 as $\tau_M^u \sim \|\mathbf{u}_h\|_{\infty, M}^{-2}$, $\tau_L^\theta \sim \|\mathbf{u}_h\|_{\infty, L}^{-2}$ (or a combination of both) lead to big deviations σ and poor Nusselt numbers.

Ra	γ_M	τ_M^u	τ_L^θ	Nu^{avg}	σ	Nu^{ref}
10^9	0	0	0	118.7932	137.5588	63.1
	1	0	0	48.1509	2.2666	
	1	1	0	44.7787	1.6884	
	1	hu1	0	46.1522	1.9443	
	1	u2	0	37.2566	1.0368	
	1	0	1	46.1629	0.8950	
	1	0	hu1	47.2953	1.6829	
	1	0	u2	53.7836	17.9261	
	1	1	1	43.6124	2.2634	
	1	hu1	hu1	45.7747	2.1888	
	1	u2	u2	37.4286	2.3599	
	0.01	0	0	55.5231	1.3464	
	0.01	1	0	52.7697	1.4125	
	0.01	hu1	0	53.8371	1.4130	
	0.01	0	1	51.3556	4.0768	
	0.01	0	hu1	52.4530	3.4847	
	0.01	0	u2	67.5182	21.8258	
	0.01	1	1	50.0199	3.5080	
	0.01	hu1	hu1	51.8141	3.4344	
	0.001	0	0	82.1364	5.3807	
	0.001	hu1	0	71.6067	3.5743	
	0.001	hu1	hu1	66.8327	5.3091	
	0.001	0	hu1	72.1467	5.1825	

Table B.1.: Averaged Nusselt numbers and maximal deviations σ for different choices of stabilization, $Ra = 10^9$, averaged over time $t \in [150, 1000]$, $N = 10 \cdot 8^3$. The notation hu1 indicates that $\tau_{M/L}^{u/\theta} = \frac{1}{2}h/\|\mathbf{u}_h\|_{\infty, M/L}$ and u2 that $\tau_{M/L}^{u/\theta} = \|\mathbf{u}_h\|_{\infty, M/L}^{-2}$.

Bibliography

- [ACF⁺11] M. Augustin, A. Caiazzo, A. Fiebach, J. Fuhrmann, V. John, A. Linke, and R. Umla, *An assessment of discretizations for convection-dominated convection–diffusion equations*, Computer Methods in Applied Mechanics and Engineering **200** (2011), no. 47, 3395–3409.
- [AD15] D. Arndt and H. Dallmann, *Error estimates for the fully discretized incompressible Navier-Stokes problem with LPS stabilization*, Tech. report, Institute of Numerical and Applied Mathematics, Georg-August-University of Göttingen, 2015.
- [ADL15] D. Arndt, H. Dallmann, and G. Lube, *Local projection FEM stabilization for the time-dependent incompressible Navier–Stokes problem*, Numerical Methods for Partial Differential Equations **31** (2015), no. 4, 1224–1250.
- [AGL09] G. Ahlers, S. Grossmann, and D. Lohse, *Heat transfer and large scale dynamics in turbulent Rayleigh–Bénard convection*, Reviews of Modern Physics **81** (2009), no. 2, 503.
- [Alt02] H. Alt, *Lineare Funktionalanalysis: Eine anwendungsorientierte Einführung*, Springer, 2002.
- [Ape99] T. Apel, *Anisotropic finite elements: Local estimates and applications*, Advances in Numerical Mathematics, Teubner, Stuttgart, 1999.
- [Bab73] I. Babuška, *The finite element method with Lagrangian multipliers*, Numerische Mathematik **20** (1973), no. 3, 179–192.
- [Bad06] S. Badia, *Stabilized pressure segregation methods and their application to fluid-structure interaction problems*.
- [BB06] M. Braack and E. Burman, *Local projection stabilization for the Oseen problem and its interpretation as a variational multiscale method*, SIAM Journal on Numerical Analysis **43** (2006), no. 6, 2544–2566.
- [BBJL07] M. Braack, E. Burman, V. John, and G. Lube, *Stabilized finite element methods for the generalized Oseen problem*, Computer Methods in Applied Mechanics and Engineering **196** (2007), no. 4, 853–866.

- [BC07] S. Badia and R. Codina, *Convergence analysis of the FEM approximation of the first order projection method for incompressible flows with and without the inf-sup condition*, Numerische Mathematik **107** (2007), no. 4, 533–557.
- [BCES10] J. Bailon-Cuba, M.S. Emran, and J. Schumacher, *Aspect ratio dependence of heat transfer and large-scale flow in turbulent convection*, Journal of Fluid Mechanics **655** (2010), 152–173.
- [BF07] E. Burman and M.A. Fernández, *Continuous interior penalty finite element method for the time-dependent Navier–Stokes equations: space discretization and convergence*, Numerische Mathematik **107** (2007), no. 1, 39–77.
- [BH82] A.N. Brooks and T.J.R. Hughes, *Streamline upwind/Petrov-Galerkin formulations for convection dominated flows with particular emphasis on the incompressible Navier-Stokes equations*, Computer Methods in Applied Mechanics and Engineering **32** (1982), no. 1, 199–259.
- [BH04] E. Burman and P. Hansbo, *Edge stabilization for Galerkin approximations of convection–diffusion–reaction problems*, Computer Methods in Applied Mechanics and Engineering **193** (2004), no. 15, 1437–1453.
- [BHH⁺15] W. Bangerth, T. Heister, L. Heltai, G. Kanschat, M. Kronbichler, M. Maier, B. Turcksin, and T. D. Young, *The deal.II library, version 8.2*, Archive of Numerical Software **3** (2015).
- [BHK07] W. Bangerth, R. Hartmann, and G. Kanschat, *deal.II – a general purpose object oriented finite element library*, ACM Transactions on Mathematical Software **33** (2007), no. 4, 24/1–24/27.
- [BIL05] L. Berselli, T. Iliescu, and W.J. Layton, *Mathematics of large eddy simulation of turbulent flows*, Springer Science & Business Media, 2005.
- [BJK13] G.R. Barrenechea, V. John, and P. Knobloch, *A local projection stabilization finite element method with nonlinear crosswind diffusion for convection–diffusion–reaction equations*, ESAIM: Mathematical Modelling and Numerical Analysis **47** (2013), no. 05, 1335–1366.
- [BL09] M. Braack and G. Lube, *Finite elements with local projection stabilization for incompressible flow problems*, Journal of Computational Mathematics **27** (2009), no. 2-3, 116–147.
- [BMO⁺83] M.E. Brachet, D.I. Meiron, S.A. Orszag, B.G. Nickel, R.H. Morf, and U. Frisch, *Small-scale structure of the Taylor–Green vortex*, Journal of Fluid Mechanics **130** (1983), 411–452.

- [BMZ14] M. Braack, P.B. Mucha, and W.M. Zajackowski, *Directional do-nothing condition for the Navier-Stokes equations*, Journal of Computational Mathematics **32** (2014), no. 5, 507–521.
- [BP79] M. Bercovier and O. Pironneau, *Error estimates for finite element method solution of the Stokes problem in the primitive variables*, Numerische Mathematik **33** (1979), no. 2, 211–224.
- [BPA00] E. Bodenschatz, W. Pesch, and G. Ahlers, *Recent developments in Rayleigh-Bénard convection*, Annual Review of Fluid Mechanics **32** (2000), no. 1, 709–778.
- [BR94] F. Brezzi and A. Russo, *Choosing bubbles for advection-diffusion problems*, Mathematical Models and Methods in Applied Sciences **4** (1994), no. 04, 571–587.
- [Bra07] D. Braess, *Finite elements: Theory, fast solvers, and applications in solid mechanics*, Cambridge University Press, 2007.
- [Bre74] F. Brezzi, *On the existence, uniqueness and approximation of saddle-point problems arising from Lagrangian multipliers*, Revue française d’automatique, informatique, recherche opérationnelle. Analyse numérique **8** (1974), no. 2, 129–151.
- [BS08] S.C. Brenner and L.R. Scott, *The mathematical theory of finite element methods*, vol. 15, Springer Science & Business Media, 2008.
- [CBCP15] O. Colomés, S. Badia, R. Codina, and J. Principe, *Assessment of variational multiscale models for the large eddy simulation of turbulent incompressible flows*, Computer Methods in Applied Mechanics and Engineering **285** (2015), 32–63.
- [CELR11] M.A. Case, V.J. Ervin, A. Linke, and L.G. Rebholz, *A connection between Scott-Vogelius and grad-div stabilized Taylor-Hood FE approximations of the Navier-Stokes equations*, SIAM Journal on Numerical Analysis **49** (2011), no. 4, 1461–1481.
- [Cho69] A.J. Chorin, *On the convergence of discrete approximations to the Navier-Stokes equations*, Mathematics of Computation **23** (1969), no. 106, 341–353.
- [Cia02] P.G. Ciarlet, *The finite element method for elliptic problems*, vol. 40, Siam, 2002.

- [CKS04] B. Cockburn, G. Kanschat, and D. Schötzau, *The local discontinuous Galerkin method for the Oseen equations*, *Mathematics of Computation* **73** (2004), no. 246, 569–593.
- [Cou95] W. Couzy, *Spectral element discretization of the unsteady Navier-Stokes Equations and its Iterative solution on parallel computers*, Ph.D. thesis, EPFL Lausanne, 1995.
- [DAL15] H. Dallmann, D. Arndt, and G. Lube, *Local projection stabilization for the Oseen problem*, *IMA Journal of Numerical Analysis* (2015).
- [DD76] J. Douglas and T. Dupont, *Interior penalty procedures for elliptic and parabolic Galerkin methods*, *Computing Methods in Applied Sciences*, Springer, 1976, pp. 207–216.
- [dFGAJN15] J. de Frutos, B. García-Archilla, V. John, and J. Novo, *Grad-div stabilization for the evolutionary Oseen problem with inf-sup stable finite elements*, *Journal of Scientific Computing* (2015), 1–34.
- [Dzi10] G. Dziuk, *Theorie und Numerik partieller Differentialgleichungen*, Walter de Gruyter, 2010.
- [ESW14] H.C. Elman, D.J. Silvester, and A.J. Wathen, *Finite elements and fast iterative solvers: With applications in incompressible fluid dynamics*, Oxford University Press, 2014.
- [FN09a] E. Feireisl and A. Novotný, *Singular limits in thermodynamics of viscous fluids*, Springer Science & Business Media, 2009.
- [FN09b] ———, *The Oberbeck–Boussinesq approximation as a singular limit of the full Navier–Stokes–Fourier system*, *Journal of Mathematical Fluid Mechanics* **11** (2009), no. 2, 274–302.
- [FNS98] L.P. Franca, A. Nesliturk, and M. Stynes, *On the stability of residual-free bubbles for convection-diffusion problems and their approximation by a two-level finite element method*, *Computer Methods in Applied Mechanics and Engineering* **166** (1998), no. 1, 35–49.
- [GL00] S. Grossmann and D. Lohse, *Scaling in thermal convection: a unifying theory*, *Journal of Fluid Mechanics* **407** (2000), 27–56.
- [GLOS05] T. Gelhard, G. Lube, M.A. Olshanskii, and J.-H. Starcke, *Stabilized finite element schemes with LBB-stable elements for incompressible flows*, *Journal of Computational and Applied Mathematics* **177** (2005), no. 2, 243–267.

- [GMS06] J.-L. Guermond, P. Mineev, and J. Shen, *An overview of projection methods for incompressible flows*, Computer Methods in Applied Mechanics and Engineering **195** (2006), no. 44, 6011–6045.
- [GR12] V. Girault and P.-A. Raviart, *Finite element methods for Navier-Stokes equations: Theory and algorithms*, vol. 5, Springer Science & Business Media, 2012.
- [Gre91] P.M. Gresho, *Some current CFD issues relevant to the incompressible Navier-Stokes equations*, Computer Methods in Applied Mechanics and Engineering **87** (1991), no. 2, 201–252.
- [GS03] V. Girault and L.R. Scott, *A quasi-local interpolation operator preserving the discrete divergence*, Calcolo **40** (2003), no. 1, 1–19.
- [GS04] J.-L. Guermond and J. Shen, *On the error estimates for the rotational pressure-correction projection methods*, Mathematics of Computation **73** (2004), no. 248, 1719–1737.
- [GT10] S. Ganesan and L. Tobiska, *Stabilization by local projection for convection–diffusion and incompressible flow problems*, Journal of Scientific Computing **43** (2010), no. 3, 326–342.
- [Gue96] J.-L. Guermond, *Some implementations of projection methods for Navier-Stokes equations*, RAIRO-Modélisation mathématique et analyse numérique **30** (1996), no. 5, 637–667.
- [Gue99] ———, *Un résultat de convergence d’ordre deux en temps pour l’approximation des équations de Navier–Stokes par une technique de projection incrémentale*, ESAIM: Mathematical Modelling and Numerical Analysis **33** (1999), no. 01, 169–189.
- [HFB86] T.J.R. Hughes, L.P. Franca, and M. Balestra, *A new finite element formulation for computational fluid dynamics: V. Circumventing the Babuška-Brezzi condition: A stable Petrov-Galerkin formulation of the Stokes problem accommodating equal-order interpolations*, Computer Methods in Applied Mechanics and Engineering **59** (1986), no. 1, 85–99.
- [HKW06] H. Hyun Kim and O.B. Widlund, *Two-level Schwarz algorithms with overlapping subregions for mortar finite elements*, SIAM Journal on Numerical Analysis **44** (2006), no. 4, 1514–1534.

- [HMJ00] T.J.R. Hughes, L. Mazzei, and K.E. Jansen, *Large eddy simulation and the variational multiscale method*, Computing and Visualization in Science **3** (2000), no. 1-2, 47–59.
- [HNW93] E. Hairer, S.P. Nørsett, and G. Wanner, *Solving ordinary differential equations I: Nonstiff problems*, Springer-Verlag, Berlin, Germany (1993).
- [How38] L. Howarth, *On the solution of the laminar boundary layer equations*, Proceedings of the Royal Society of London A: Mathematical, Physical and Engineering Sciences, vol. 164, The Royal Society, 1938, pp. 547–579.
- [HR82] J.G. Heywood and R. Rannacher, *Finite element approximation of the non-stationary Navier-Stokes problem. I. Regularity of solutions and second-order error estimates for spatial discretization*, SIAM Journal on Numerical Analysis **19** (1982), no. 2, 275–311.
- [HSW11] S. Horn, O. Shishkina, and C. Wagner, *Non-Oberbeck-Boussinesq effects in three-dimensional Rayleigh-Bénard convection*, Direct and Large-Eddy Simulation VIII, Springer, 2011, pp. 377–382.
- [JJLR13] E. Jenkins, V. John, A. Linke, and L.G. Rebholz, *On the parameter choice in grad-div stabilization for incompressible flow problems*, Advances in Computational Mathematics (2013).
- [JK07] V. John and P. Knobloch, *On spurious oscillations at layers diminishing (SOLD) methods for convection–diffusion equations: Part I—A review*, Computer Methods in Applied Mechanics and Engineering **196** (2007), no. 17, 2197–2215.
- [JK08] ———, *On spurious oscillations at layers diminishing (SOLD) methods for convection–diffusion equations: Part II—Analysis for P1 and Q1 finite elements*, Computer Methods in Applied Mechanics and Engineering **197** (2008), no. 21, 1997–2014.
- [Joh12] V. John, *Large eddy simulation of turbulent incompressible flows: Analytical and numerical results for a class of LES models*, vol. 34, Springer Science & Business Media, 2012.
- [JS86] C. Johnson and J. Saranen, *Streamline diffusion methods for the incompressible Euler and Navier-Stokes equations*, Mathematics of Computation **47** (1986), no. 175, 1–18.

- [KL09] P. Knobloch and G. Lube, *Local projection stabilization for advection–diffusion–reaction problems: One-level vs. two-level approach*, Applied numerical mathematics **59** (2009), no. 12, 2891–2907.
- [KLR02] T. Knopp, G. Lube, and G. Rapin, *Stabilized finite element methods with shock capturing for advection–diffusion problems*, Computer Methods in Applied Mechanics and Engineering **191** (2002), no. 27, 2997–3013.
- [KT13] P. Knobloch and L. Tobiska, *Improved stability and error analysis for a class of local projection stabilizations applied to the Oseen problem*, Numerical Methods for Partial Differential Equations **29** (2013), no. 1, 206–225.
- [Lil67] D.K. Lilly, *The representation of small scale turbulence in numerical simulation experiments*, Proc. IBM sci. comp. symp. on environmental sciences **320** (1967), 195–210.
- [Lin09] A. Linke, *Collision in a cross-shaped domain—A steady 2d Navier–Stokes example demonstrating the importance of mass conservation in CFD*, Computer Methods in Applied Mechanics and Engineering **198** (2009), no. 41, 3278–3286.
- [Lin14] ———, *On the role of the Helmholtz decomposition in mixed methods for incompressible flows and a new variational crime*, Computer Methods in Applied Mechanics and Engineering **268** (2014), 782–800.
- [LL12] J. Loewe and G. Lube, *A projection-based variational multiscale method for large-eddy simulation with application to non-isothermal free convection problems*, Mathematical Models and Methods in Applied Sciences **22** (2012), no. 02.
- [Löw11] J. Löwe, *Eine Finite-Elemente-Methode für nicht-isotherme inkompressible Strömungsprobleme*, Ph.D. thesis, Niedersächsische Staats- und Universitätsbibliothek Göttingen, 2011.
- [LQ91] P. Le Quéré, *Accurate solutions to the square thermally driven cavity at high Rayleigh number*, Computers & Fluids **20** (1991), no. 1, 29–41.
- [LQB98] P. Le Quéré and M. Behnia, *From onset of unsteadiness to chaos in a differentially heated square cavity*, Journal of Fluid Mechanics **359** (1998), 81–107.
- [LR06a] G. Lube and G. Rapin, *Residual-based stabilized higher-order FEM for a generalized Oseen problem*, Mathematical Models and Methods in Applied Sciences **16** (2006), no. 07, 949–966.

- [LR06b] ———, *Residual-based stabilized higher-order FEM for advection-dominated problems*, *Computer Methods in Applied Mechanics and Engineering* **195** (2006), no. 33, 4124–4138.
- [LRL08] G. Lube, G. Rapin, and J. Löwe, *Local projection stabilization for incompressible flows: Equal-order vs. inf-sup stable interpolation*, *Electronic Transactions on Numerical Analysis* **32** (2008), 106–122.
- [MH96] T. Muneer and B. Han, *Simplified analysis for free convection in enclosures — Application to an industrial problem*, *Energy Conversion and Management* **37** (1996), no. 9, 1463–1467.
- [MST07] G. Matthies, P. Skrzypacz, and L. Tobiska, *A unified convergence analysis for local projection stabilisations applied to the Oseen problem*, *ESAIM-Mathematical Modelling and Numerical Analysis* **41** (2007), no. 4, 713–742.
- [MT14] G. Matthies and L. Tobiska, *Local projection type stabilization applied to inf-sup stable discretizations of the Oseen problem*, *IMA Journal of Numerical Analysis* (2014).
- [NTC⁺11] F. Nicoud, H.B. Toda, O. Cabrit, S. Bose, and J. Lee, *Using singular values to build a subgrid-scale model for large eddy simulations*, *Physics of Fluids* **23** (2011), no. 8, 085106.
- [Obe79] A. Oberbeck, *Über die Wärmeleitung der Flüssigkeiten bei Berücksichtigung der Strömungen infolge von Temperaturdifferenzen*, *Annalen der Physik* **243** (1879), no. 6, 271–292.
- [OLHL09] M. Olshanskii, G. Lube, T. Heister, and J. Löwe, *Grad-div stabilization and subgrid pressure models for the incompressible Navier–Stokes equations*, *Computer Methods in Applied Mechanics and Engineering* **198** (2009), no. 49, 3975–3988.
- [Pop00] S. Pope, *Turbulent flows*, Cambridge University Press, 2000.
- [QV08] A. Quarteroni and A. Valli, *Numerical approximation of partial differential equations*, vol. 23, Springer Science & Business Media, 2008.
- [RL10] L. Röhe and G. Lube, *Analysis of a variational multiscale method for Large-Eddy Simulation and its application to homogeneous isotropic turbulence*, *Computer Methods in Applied Mechanics and Engineering* **199** (2010), no. 37, 2331–2342.

- [RST08] H.-G. Roos, M. Stynes, and L. Tobiska, *Robust numerical methods for singularly perturbed differential equations: Convection-diffusion-reaction and flow problems*, vol. 24, Springer Science & Business Media, 2008.
- [Sag06] P. Sagaut, *Large eddy simulation for incompressible flows: An introduction*, Springer Science & Business Media, 2006.
- [SG00] H. Schlichting and K. Gersten, *Boundary-layer theory*, Springer Science & Business Media, 2000.
- [She92] J. Shen, *On error estimates of some higher order projection and penalty-projection methods for Navier-Stokes equations*, *Numerische Mathematik* **62** (1992), no. 1, 49–73.
- [She96] ———, *On error estimates of the projection methods for the Navier-Stokes equations: second-order schemes*, *Mathematics of Computation of the American Mathematical Society* **65** (1996), no. 215, 1039–1065.
- [SZ90] L.R. Scott and S. Zhang, *Finite element interpolation of nonsmooth functions satisfying boundary conditions*, *Mathematics of Computation* **54** (1990), no. 190, 483–493.
- [Tem69] R. Temam, *Sur l'approximation de la solution des équations de Navier-Stokes par la méthode des pas fractionnaires (II)*, *Archive for Rational Mechanics and Analysis* **33** (1969), no. 5, 377–385.
- [Tem95] ———, *Navier-Stokes equations and nonlinear functional analysis*, vol. 66, Siam, 1995.
- [TMVDV96] L.J.P. Timmermans, P.D. Mineev, and F.N. Van De Vosse, *An approximate projection scheme for incompressible flow using spectral elements*, *International journal for numerical methods in fluids* **22** (1996), no. 7, 673–688.
- [WSW12] S. Wagner, O. Shishkina, and C. Wagner, *Boundary layers and wind in cylindrical Rayleigh–Bénard cells*, *Journal of Fluid Mechanics* **697** (2012), 336–366.
- [Zei86] E. Zeidler, *Nonlinear functional analysis and its applications*, Springer-Verlag, 1986.

Acknowledgments

First of all, I would like to thank Prof. Dr. Gert Lube for supervising this thesis and his support during the preparation. From the beginning of my Master's programme, he encouraged my interest in the field of computational fluid dynamics. He always took time for helpful discussions, hints and suggestions in the course of my PHD programme. In addition, I express my gratitude to Prof. Dr. Gerlind Plonka-Hoch, who accompanied me as co-advisor, and to Prof. Dr. Malte Braack for being the co-referee of my thesis.

My thanks go to Daniel Arndt for a productive collaboration and very insightful discussions. A variety of conversations, not only on the topic of this work, created a good working environment. I am also thankful for his proof-reading of parts of this document. Furthermore, Florian Boßmann deserves acknowledgment not only for proof-reading this thesis but also for lifting my spirits, especially in the final phase of my studies.

I would also like to thank the “Research Training Group 1023: Identification in Mathematical Models” and the Institute for Numerical and Applied Mathematics at the University of Göttingen for the financial support.

Last but not least, I am grateful to my family and friends for giving me support and constant appreciation. Marie Krähling and Hedda Pietsch, who accepted the dare to proof-read parts of this thesis, deserve great credit.

Curriculum Vitae

Persönliche Daten

Name	Helene Dallmann
Geburtsdatum	08.11.1988
Geburtsort	Göttingen
Staatsangehörigkeit	Deutsch

Bildungsweg

07/2012 - heute	Promotion im GAUSS-Programm der Georg-August-Universität Göttingen
07/2012 - 06/2014	Mitglied des Graduiertenkolleg 1023 der DFG “Identifikation in mathematischen Modellen”
10/2010 - 06/2012	Master of Science Mathematik, Georg-August-Universität Göttingen, Abschluss M.Sc.
10/2008 - 09/2010	Bachelor of Science Mathematik, Georg-August-Universität Göttingen, Abschluss B.Sc.
10/2007 - 09/2008	2-Fächer Bachelor Mathematik und Physik, Georg-August-Universität Göttingen, kein Abschluss
07/2001 - 06/2007	Gymnasium Corvinianum Northeim, Abitur